

# FINAL REPORT

Behavioural Ecology of Cetaceans: The Relationship of Body Condition with Behavior and Reproductive Status

SERDP Project RC-2337

DECEMBER 2018

Patrick Miller  
Ailsa Hall  
University of St Andrews

*Distribution Statement A*

*This document has been cleared for public release*



*Page Intentionally Left Blank*

This report was prepared under contract to the Department of Defense Strategic Environmental Research and Development Program (SERDP). The publication of this report does not indicate endorsement by the Department of Defense, nor should the contents be construed as reflecting the official policy or position of the Department of Defense. Reference herein to any specific commercial product, process, or service by trade name, trademark, manufacturer, or otherwise, does not necessarily constitute or imply its endorsement, recommendation, or favoring by the Department of Defense.

*Page Intentionally Left Blank*

<b>REPORT DOCUMENTATION PAGE</b>			<i>Form Approved</i> OMB No. 0704-0188		
Public reporting burden for this collection of information is estimated to average 1 hour per response, including the time for reviewing instructions, searching existing data sources, gathering and maintaining the data needed, and completing and reviewing this collection of information. Send comments regarding this burden estimate or any other aspect of this collection of information, including suggestions for reducing this burden to Department of Defense, Washington Headquarters Services, Directorate for Information Operations and Reports (0704-0188), 1215 Jefferson Davis Highway, Suite 1204, Arlington, VA 22202-4302. Respondents should be aware that notwithstanding any other provision of law, no person shall be subject to any penalty for failing to comply with a collection of information if it does not display a currently valid OMB control number. <b>PLEASE DO NOT RETURN YOUR FORM TO THE ABOVE ADDRESS.</b>					
<b>1. REPORT DATE (DD-MM-YYYY)</b> 20-12-2018		<b>2. REPORT TYPE</b> Final SERDP Report		<b>3. DATES COVERED (From - To)</b> May 2013 to Nov 2018	
<b>4. TITLE AND SUBTITLE</b> Behavioral Ecology of Cetaceans: The Relationship of Body Condition and Reproductive Status  Final Report RC-2337				<b>5a. CONTRACT NUMBER</b> W912HQ-13-C-0063	
				<b>5b. GRANT NUMBER</b>	
				<b>5c. PROGRAM ELEMENT NUMBER</b>	
<b>6. AUTHOR(S)</b>  Miller, Patrick J. O Hall, Ailsa J.				<b>5d. PROJECT NUMBER</b> RC-2337	
				<b>5e. TASK NUMBER</b>	
				<b>5f. WORK UNIT NUMBER</b>	
<b>7. PERFORMING ORGANIZATION NAME(S) AND ADDRESS(ES)</b>  UNIVERSITY OF ST ANDREWS 79 NORTH STREET ST ANDREWS KY16 9RJ UNITED KINGDOM				<b>8. PERFORMING ORGANIZATION REPORT NUMBER</b>  RC-2337	
<b>9. SPONSORING / MONITORING AGENCY NAME(S) AND ADDRESS(ES)</b> SERDP/ESTCP Resource Conservation and Climate Change OASD (EI&E) 4800 Mark Center Drive, Suite 17D03 Alexandria, VA				<b>10. SPONSOR/MONITOR'S ACRONYM(S)</b> SERDP	
				<b>11. SPONSOR/MONITOR'S REPORT NUMBER(S)</b> RC-2337	
<b>12. DISTRIBUTION / AVAILABILITY STATEMENT</b> Approved for public release; distribution is unlimited.					
<b>13. SUPPLEMENTARY NOTES</b>					
<b>14. ABSTRACT</b> In this study, we developed and cross-validated a novel, non-invasive method to quantify total body lipid-stores of free-ranging cetaceans based upon their tissue body density. Fieldwork was conducted with a beaked whale (northern bottlenose whale) and a mysticete (humpback whale), using suction cup attached tags, measurement of body shape, and remote biopsy sample collection. Tissue densities for bottlenose whales over 21 tag deployments in the Gully and Jan Mayen (1028.4 to 1033.9 kg m <sup>-3</sup> ) covered a narrow range compared to humpback whales (1027.8 to 1050.8 kg m <sup>-3</sup> ) over 59 tag deployments in Canada and Norway, confirming the role of lipid store cycling in capital breeding baleen whales. Tissue body density of humpback whales decreased by 0.03 kg m <sup>-3</sup> per day (2.7 kg m <sup>-3</sup> over 90 days) over the feeding season. A similar seasonal trend was found for the body shape width to length ratios, which correlated as predicted with tissue body density across adult humpback whales (r <sup>2</sup> =29.9%, N=18), though neither of those measures correlated with cortisol concentrations in blubber samples. Humpback whales with higher body density (lower lipid store) fed more intensely, as predicted, whereas the opposite effect was found for bottlenose whales. By advancing methods to measure body condition of free-ranging cetaceans, this study enables fuller evaluation of the possible biologically-significant effects of anthropogenic disturbance on cetaceans.					
<b>15. SUBJECT TERMS</b> Body condition, density, cortisol, photogrammetry, cetacean, health, disturbance, steroid hormones, body density, gliding, drag, buoyancy, blubber, body shape					
<b>16. SECURITY CLASSIFICATION OF:</b>			<b>17. LIMITATION OF ABSTRACT</b>	<b>18. NUMBER OF</b>	<b>19a. NAME OF RESPONSIBLE PERSON</b>
<b>a. REPORT</b>	<b>b. ABSTRACT</b>	<b>c. THIS PAGE</b>			UU
U	U	U			<b>19b. TELEPHONE NUMBER</b> (include area code) +441334463554

*Page Intentionally Left Blank*

## Contents

1	ABSTRACT.....	1
1.1	Objective .....	1
1.2	Technical Approach .....	1
1.3	Results .....	2
1.4	Benefits.....	3
2	OVERALL INTRODUCTION.....	5
2.1	Background .....	5
2.2	Background to the specific aims of our study .....	8
2.3	Choice of study species .....	11
2.4	Objectives.....	12
3	DEVELOPMENT AND EVALUATION OF THREE INDEPENDENT METHODS TO ESTIMATE BODY CONDITION .....	13
3.1	Tissue indicators of body condition .....	13
3.1.2	Biomarker method development preface .....	16
3.1.3	Detailed methods, results and discussion.....	28
3.1.4	Adipocyte size as a biomarker discussion .....	41
3.1.5	Progesterone results and discussion.....	42
3.1.6	Cortisol results and discussion.....	44
3.1.7	Proteomics result and discussion .....	58
3.2	Use of body shape indicators to study body condition in free ranging cetaceans.....	61
3.2.1	Evaluation of a method to measure body shape using a 3D scanning sonar .....	61
3.2.2	Aerial photogrammetry using UAV drones.....	71
3.3	Body tissue density indicator .....	81
3.3.1	Tissue body density as an indicator of body condition in free-ranging cetaceans..	81
3.3.2	General methods to estimate tissue body density .....	81
3.3.3	Tissue body density of northern bottlenose whales ( <i>Hyperoodon ampullatus</i> ).....	85
3.3.4	Tissue body density of long-finned pilot whales ( <i>Globicephala melas</i> ) .....	88
3.3.5	Measuring Tissue Density of Humpback Whales ( <i>Megaptera novaeangliae</i> ).....	90
3.3.6	Variation of humpback whale tissue density with season and reproductive status	93
3.3.7	Use of humpback whale shape data to improve estimates of body density.....	101
4	CROSS-COMPARISON OF THREE BODY CONDITION INDICATORS.....	107
4.1	Materials and methods .....	108

4.2	Results and discussion.....	109
4.2.1	The relationship of tissue density with cortisol concentration.....	109
5	PATTERNS OF BEHAVIOUR IN RELATION TO BODY CONDITION IN CETACEANS	
5.1	Introduction .....	113
5.2	Northern bottlenose whale body condition and the starvation-predation trade-off .....	114
5.2.1	Materials and Methods.....	115
5.2.2	Estimating anti-predation parameters .....	116
5.2.3	Composite indices of foraging and anti-predation behaviour.....	118
5.2.4	Results and Discussion .....	119
5.2.5	Tissue density variation with anti-predation and foraging behaviour .....	121
5.3	Foraging effort in relation to body in condition in humpback whales .....	122
5.3.1	Materials and Methods.....	122
5.3.2	Results and discussion .....	124
6	CONCLUSIONS AND IMPLICATIONS FOR FUTURE RESEARCH / IMPLEMENTATION.....	127
7	LITERATURE CITED .....	133

8	APPENDICES .....	150
8.1	Inter-Assay CVs .....	152
9	Total Protein Extraction Method Development.....	157
9.1	Sample Collection and Preparation .....	157
9.1.1	Total Protein Extraction Methods.....	158
9.1.2	Quality Assurance / Quality Control.....	161
10	Adipocyte Metrics.....	166
10.1	Method Development using Stranded Animal Samples.....	166
10.2	Histological processing and measurements .....	166
10.3	Image and Statistical Analysis.....	167
10.4	Relationship Between Different Adipocyte Metrics .....	167
10.5	Relationship between Condition Index and Adipocyte size.....	168
10.6	Adipocyte Count.....	169
10.7	Predicting Condition from Adipocyte Metrics .....	170
11	PROTEOMICS .....	172
11.1	Method Development using Stranded Animal Samples.....	172
11.2	Sample Analysis .....	173
11.2.1	Total Protein Extraction and quantification.....	173
11.2.2	Protein Identification using nLC-ESI MS/MS.....	176
11.2.3	Statistical Analysis of SDS-PAGE Protein Bands Data .....	177
11.3	Blubber Protein Identification Initial Investigations Results and Discussion .....	178
11.3.1	Blubber Proteins Identification Results .....	178
11.4	Blubber Proteins as Potential Biomarkers Discussion .....	182
11.4.1	Proteins Identified.....	182
11.4.2	Tissue Specific and Circulatory Proteins.....	183
11.5	1D SDS-PAGE Exploratory Band Group Analysis Results and Discussion .....	185
11.5.1	Stranded Animal Samples Results and Discussion.....	185
11.5.2	Biopsies from Live Animals Results and Discussion.....	187

## LIST OF TABLES

Table 3-1. Summary of the mysticete and odontocete individuals used for full depth blubber samples.....	17
Table 3-2. Summary table of the harbour porpoise and mysticete individuals used for analysis with the data available for each one.....	21
Table 3-3. Summary of the 103 blubber biopsy samples from northern bottlenose whales (n = 21) and humpback whales.....	22
Table 3-4. Summary of each harbour porpoise and balaenopterid sample subset used for different models.....	25
Table 3-5. Results of GLM model selection cortisol concentrations measured in humpback whale biopsies.....	27
Table 3-6. Summary table of the generalized linear model results investigating the effects of various covariates on blubber lipid content.....	30
Table 3-7. Results of GLM model selection for outer layer blubber cortisol concentrations for harbour porpoises.....	46
Table 3-8. All ground truth measurements taken from the two female killer whales.....	63
Table 3-9. Average and % error of measurements (with ~40 scans per sequence) for four of the ‘best’ sequences.....	69
Table 3-10. Parameter values used to produce the ‘best’ estimates for each body dimension.....	69
Table 3-11. Coefficient estimates for the simplest model in the set of models.....	78
Table 3-12. Significant model-averaged effects.....	78
Table 3-13. Details of parameters estimates from the lowest DIC Bayesian model.....	99
Table 3-14. Estimates of body density and drag term for both simple drag term model and combined drag term model.....	105
Table 4-1. Analysis of deviance table for body density versus cortisol concentration.....	110
Table 4-2. Analysis of deviance table for body density versus LSSAI.....	111
Table 4-3. Analysis of deviance table for cortisol concentration versus LSSAI.....	112
Table 5-1. Candidate anti-predation behaviours and the measures representing each behaviour.....	117
Table 5-2. Deployment estimates including: number of 5s glide segments, estimated tissue density, $\rho_{\text{tissue}}$ (mean $\pm$ 95% posterior credible interval in $\text{kg m}^{-3}$ ); composite foraging index ( $\text{CI}_F$ ); composite anti-predation index ( $\text{CI}_{AP}$ ) and the ratio of composite anti-predation to foraging indices ( $\text{CI}_{AP} / \text{CI}_F$ ).....	120
Table 5-3. Fit of general linear models to data of the proportion of time spent in feeding of tagged humpback whales by AIC. ....	127

## LIST OF FIGURES

Figure 2-1. A conceptual framework to link responses to extrinsic stressors to vital rates.....	5
Figure 2-2. Two different suction-cup-attached tags used in the study.....	9
Figure 3-1. Separation of the full depth blubber samples > 30mm thick into five layers of approximately equal thickness prior to lipid extraction.....	18
Figure 3-2. Histogram of blubber progesterone concentrations measured in 130 humpback whale biopsies .....	26
Figure 3-3 Barplots of mean blubber lipid content ( $\pm$ standard error) through blubber depth for each species group .....	29
Figure 3-4. Boxplots of blubber lipid content across blubber layers between COD categories for the three cetacean families.....	31
Figure 3-5. Lipid content in the middle blubber layer plotted against the morphometric body condition estimate for each species group .....	33
Figure 3-6. Body condition histograms for the three species groups using morphometric data ..	34
Figure 3-7. Theoretical schematic demonstrating the relative importance of different blubber functions across three cetacean families.....	40
Figure 3-8. Blubber progesterone concentrations across different reproductive states of the female humpback whales.....	42
Figure 3-9. Blubber progesterone concentrations in 15 Northern Bottlenose Whales .....	43
Figure 3-10. Final GLMM outputs for cortisol concentrations across the body and through the blubber layer for the harbour porpoises.....	45
Figure 3-11. Partial termplots for the covariates retained in the final two best fitting GLMs.....	47
Figure 3-12. Final GLMM output for cortisol concentrations through the blubber depth for the balaenopterids .....	48
Figure 3-13. Partial termplots for the covariates retained in the final best fitting GLM .....	49
Figure 3-14. Typical time line for the total ‘disturbance time’ spent interacting with humpback whales .....	54
Figure 3-15. Blubber cortisol concentrations are not correlated with disturbance time.....	54
Figure 3-16. Predicted relationships between blubber cortisol concentration and Julian day across both study sites from the GLM model averaging results.....	56
Figure 3-17. Cortisol (a-c) concentrations in the blubber of Northern bottlenose whales by age, sex and year.....	57
Figure 3-18. 1D SDS-PAGE gel image to show the grouping of individual bands into band groups .....	60
Figure 3-19. Echoscope mounted on starboard side of the research vessel.....	64
Figure 3-20, left. The sequence of analytical steps used to extract animal dimensions from the scanning sonar cloud data .....	65
Figure 3-21, below. Killer whale data points plotted from the Icelandic field trials.....	65
Figure 3-22. Example 3D reconstructed model of a dolphin.....	66
Figure 3-23. An example of the basic skeleton used for total length .....	66
Figure 3-24. Boxplots showing the median and interquartile ranges of the body dimensions.....	68
Figure 3-25. Map of the fieldwork in the Gulf of St Lawrence.....	72
Figure 3-26. Map of the fieldwork in Norwegian Sea.....	73
Figure 3-27. Examples of images extracted from the video sequences recorded with the UAV drone .....	74
Figure 3-28. Analysis components used to estimate body condition from overhead images.....	75

Figure 3-29. The LSSAI of all 55 imaged humpback whales in the study, plotted as a function of Julian date .....	77
Figure 3-30. Boxplots of body condition (LSSAIx1000) by age and reproductive class, location and season .....	79
Figure 3-31. Examples of data records showing depth (top) and pitch (bottom) versus time of day .....	86
Figure 3-32. The difference in percent time gliding in ascent versus descent phases .....	87
Figure 3-33. Examples of data records of deep dives.....	90
Figure 3-34. The precision of estimates of tissue density.....	92
Figure 3-35. Tissue density of humpback whales tagged in Antarctica and the Gulf of St Lawrence .....	93
Figure 3-36. Relationship between gliding patterns and tissue body density.....	100
Figure 3-37. Body density of humpback whales in the study as a function of Julian date.....	101
Figure 3-38. Empirically-measured calibration of the number of pixel per m vs UAV height..	103
Figure 3-39. The 95% credible interval related with no. of glides .....	106
Figure 4-1. Illustration of the fieldwork efforts undertaken for RC-2337 to enable a contrast of three independent indicators of lipid-store body condition .....	107
Figure 4-2. Body density versus blubber cortisol concentration in humpback whales .....	109
Figure 4-3 . Body density versus LSSAI in humpback whales .....	110
Figure 4-4. Blubber cortisol concentration versus LSSAI in humpback whales.....	111
Figure 5-1. A conceptual framework to link responses to extrinsic stressors to vital rates of individuals and populations .....	113
Figure 5-2. Composite anti-predation index (CI <sub>AP</sub> ) as a function of composite foraging index (CI <sub>F</sub> ) .....	121
Figure 5-3. Ratio of composite foraging to anti-predation indices.....	121
Figure 5-4. Examples of humpback whale tag records.....	125
Figure 5-5. Time budget of tagged humpback whales for Norway in the late feeding season and for Canada.....	126
Figure 6-1. Interlocking objectives of project RC-2337 .....	127

## LIST OF ACRONYMS

3S: An international research collaboration to study effects of sonar on cetaceans. ONR is a co-sponsor of the research with Miller as PI  
ARTS: Aerial Rocket Tag System  
DoD: Department of Defense  
MICS: Mingan Island Cetacean Survey  
MOCHA: A research project funded by ONR, and based in St Andrews, to undertake statistical analyses of data generated by behavioural response studies  
ONR: Office of Naval Research  
PCAD: Population Consequences of Acoustic Disturbance  
VHF: Very High Frequency  
DTAG: Miniature sound and movement tags for marine mammals  
UAV: Unmanned aerial vehicle  
DNA: Deoxyribonucleic Acid  
SMASS : Scottish Marine Animal Stranding Scheme  
COD: Cause of Death  
R: Open source statistical software program  
GLMM: Generalized linear mixed effects model  
GLM: Generalized linear model  
AIC: Akaike's An Information Criterion  
ELISA: Enzyme linked immunosorbent assay  
ECDF: Empirical cumulative distribution function  
ANOVA: Analysis of variance  
HSD1: Hydroxysteroid dehydrogenase type 1  
HPA: Hypothalamus pituitary axis  
SDS-PAGE: Sodium dodecyl sulfate–polyacrylamide gel electrophoresis  
nLC-ESI MS/MS: Nano-HPLC electrospray ionization multistage tandem mass spectrometry  
GPS: Global positioning system  
RHIB: Rigid hull inflatable boat  
ID: Identification  
LSSAI: Length-standardized surface area index  
NK: Not known  
AF: Adult female  
DIC: Deviance information criterion  
CI: Confidence interval/Credible interval  
SD: Standard deviation

## KEYWORDS

Body condition, density, cortisol, photogrammetry, cetacean, health, disturbance, steroid hormones, body density, gliding, drag, buoyancy, blubber, body shape

## ACKNOWLEDGEMENTS

Several parties contributed to the preparation and writing of this report, including Joanna Kershaw, Kagari Aoki, Saana Isojunno, Charlotte Bellot, Eilidh Siegal, Robin Rousseau, Richard Bates.

All of the contributors would like to thank all of the ships' crews and field staff which helped make this project a success. Also thanks to technical staff back in the laboratory. Particular thanks go to our many collaborators, including (but not limited to) Katsufumi Sato, Tomoko Narazaki, Christian Ramp, Martin Biuw, Sophie Smout, Rene Swift, Ricardo Antunes, Volker Deecke, Patrick Pomeroy, Lars Kleivane, Rune Hansen, Takashi Iwata, and Paul Wensveen.

# 1 ABSTRACT

## 1.1 Objective

This study RC-2337 responded to SERDP's request for proposals SISON-11-02 'Behavioral Ecology of Cetaceans'. The risk of harm to cetaceans from underwater noise is an important environmental and regulatory issue faced by the DoD. Long-term consequences of disturbance are particularly difficult to quantify. Noise may reduce foraging rates and thereby health of individual animals which could then negatively impact survival and reproduction ultimately affecting vital rates of populations. Lipid-store body condition, defined here as the quantity of lipid store carried by an animal, is a measure of individual health which has been shown to be a good predictor of offspring survival and reproductive success in seals. Body condition is thought to influence how animals broadly trade-off foraging and anti-predator behaviors, and modulates responses to natural and anthropogenic disturbance. Unfortunately, for free-ranging cetaceans that cannot be captured for study, it is not possible to use the 'gold-standard' method to measure lipid store in mammals (isotope dilution), though indicators of body condition have been developed using visual observation, measurement of body shape from photogrammetry, and analysis of remotely collected biopsy samples of blubber.

In this study, we develop and cross-validate a novel, state-of-the-art non-invasive method to measure total body lipid-stores of free-ranging cetaceans based upon their tissue body density. Tissue body density measures from individual animals are compared to two independent indicators of body condition: body shape and lipid and steroid hormonal markers in blubber. We describe how these three measures of body condition vary with reproductive status, location, and timing in relation to feeding and fasting cycles. Finally, we explore how body condition of individuals relates to behavioral time budgets, focusing on foraging effort versus resting and/or anti-predator behaviors.

## 1.2 Technical Approach

Fieldwork efforts were conducted with two key species: the beaked whale *Hyperoodon ampullatus* (northern bottlenose whale) and mysticete whale *Megaptera novaeangliae* (humpback whale), after we demonstrated that it was possible to calculate body tissue density from those species. A beaked whale was selected based upon their sensitivity to naval sonar signals, and a mysticete whale based upon their known cycling of lipid fat stores across annual fasting and feeding seasons. Measurement of body density was conducted via analysis of gliding performance from data collected by an external tag attached to the body using non-invasive suction cups. Body density determines the overall buoyancy of cetaceans in seawater, which affects speed changes during glides in the ascent and descent phases of cetacean dives. State-of-the-art Bayesian statistical techniques simultaneously account for the effects of diving air volume and body drag on gliding performance, providing a rich set of physiological measurements. The same animal-attached tag records high-resolution behavioral data used for classification of functional feeding and anti-predator behaviors, enabling exploration of how body condition relates to foraging time budgets.

In addition to concurrent attachment of suction cup tags, fieldwork efforts focused on collection of measurements of body shape and remote biopsy sample collection including external blubber layers. Following evaluation of an approach to measure body shape using a 3-dimensional

scanning sonar, we systematically used digital photography from Unmanned Aerial Vehicles (UAV) to collect body shape images of humpback whales. Analysis of photogrammetry images entailed calculation of body width versus length, which we quantified using a length-standardized surface area index (LSSAI). Collection of biopsy samples from tagged animals enables both estimation of female reproductive status and estimation of lipid-store body condition based upon blubber lipid content or hormone concentrations. Hormonal and potential proteomic approaches to quantify body condition were tested and refined based upon analysis of tissue samples obtained from stranded or by-caught cetacean carcasses. Blubber cortisol concentration was found to correlate with body condition based upon morphometric condition indices of stranded cetaceans, so was used as the primary hormonal indicator of body condition in this study. Proteins in blubber using a ‘shotgun’ proteomic approach were also explored in relation to body condition.

### 1.3 Results

During project RC-2337, we successfully conducted multiple field efforts with 3 excursions to study northern bottlenose whales off Jan Mayen, Norway (June 2014-2016) and 7 excursions early and later in the feeding season for humpback whales in the Gulf of St Lawrence, Canada (3 during June-September 2016-2017) and northern Norway (4 during May-January 2014, 2016-2018). Additional tag data for these species were obtained during Limited Scope fieldwork in the Gully and Gulf of St Lawrence funded by SERDP prior to commencement of this full project, and from collaborating partners. Calculation of tissue body density was successfully accomplished for the two target species, and another deep-diving delphinidae *Globicephala melas*, the long-finned pilot whale. In all species studied, tissue body density modulated swimming patterns during ascent and descent phases of dives, with more gliding in the direction aided by buoyancy. Northern bottlenose whales were found to have individual differences in tissue body density, but the range of observed densities (1028.4 to 1033.9 kg m<sup>-3</sup>) over 21 tag deployments in the Gully and Jan Mayen was narrow compared to what we measured for humpback whales (1027.8 to 1050.8 kg m<sup>-3</sup>.) over 59 tag deployments in Canada and Norway, indicating that unlike humpback whales that cycle lipid fat stores seasonally, free-ranging bottlenose whales maintain an allostatic body condition, probably by continuous feeding. Interestingly, bottlenose whales tagged off Jan Mayen had a consistently lower tissue body density, indicating larger lipid stores, than whales tagged off Nova Scotia, Canada. Greater deviations away from neutral buoyancy observed in the Gully animals may entail higher dive transit swimming costs, indicating greater metabolic requirements than occur for bottlenose whales off Jan Mayen.

As predicted for humpback whales, tissue body density was higher (indicating smaller lipid stores) early in the feeding season and lower (indicating greater lipid stores) later in the feeding season. Statistical analysis indicated that across both Norway and Canada, tissue body density of whales decreased by 0.03 kg m<sup>-3</sup> per day, or 2.7 kg m<sup>-3</sup> over 90 days of the feeding period. A similar seasonal trend was found for the body shape measure LSSAI of 55 humpback whales for which photogrammetry images were taken using a drone UAV, indicating whales were wider per unit length later in the feeding season. Reproductive status also influenced tissue body shape with lactating females being thinner per unit length than other adult females, as expected. We found a strong statistical correlation between LSSAI and tissue body density with wider adult humpback whales having a lower body density, as predicted (N = 18). In contrast, cortisol concentrations of 73 blubber samples of humpback whales did not vary with season and did not correlate with tissue body density or LSSAI across the 33 tagged animals for which biopsy samples were also collected.

However, we found a strong trend between body density and cortisol across 9 pregnant females, those with lower tissue density (hence greater lipid stores) had higher cortisol concentrations. Whilst blubber cortisol concentrations *per se* were not a useful quantitative indicator of condition, our validation studies (and recently additional published studies in cetaceans) indicate they provide information on the metabolic state of the tissue at the time of sampling, where high concentrations are seen in animals mobilizing fat and lower concentrations are seen when fat is being deposited. Thus, overall, the strongest and statistically significant correlation was found between tissue body density and LSSAI for adult humpback whales ( $R^2=29.9\%$ ,  $N=18$ ).

As expected for whales tagged during the feeding season, production of echolocation click buzzes by northern bottlenose whales and performance of underwater lunges by humpback whales indicated active feeding by animals tagged in our study. Humpback whales spent relatively large amount of time in foraging in both the early ( $68 \pm 19\%$ , range, 17-92%,  $n = 17$  whales) and middle season ( $61 \pm 38\%$ , range, 7-93%,  $n = 4$  whales) in Canada. Tagged whales in Norway spent relatively little time foraging in the late season ( $18 \pm 24\%$ , range, 0-62%,  $n = 10$  whales) compared with the early season ( $42 \pm 31\%$ , range, 17-92%,  $n = 14$  whales). Indeed, time spent feeding substantially decreased with decreasing tissue body density. The result suggests lipid store body condition affects feeding behavior and that relatively fat humpback whales might be less motivated to feed, as predicted by starvation-predation tradeoff theory. Intriguingly, the opposite trend was observed across the 15 northern bottlenose whales tagged off Jan Mayen. Contrary to predictions of starvation-predation tradeoff theory, lower tissue body density (indicating a greater lipid store) was found to predict more foraging time and less anti-predator behavior, indicating that lipid-store body condition may be the consequence, rather than the driver, of foraging effort over the narrow ranges of body condition observed for northern bottlenose whales.

#### 1.4 Benefits

This study has made several fundamental advances in methods to estimate body condition of free-ranging cetaceans, and our understanding of the factors that can influence it. The method of analysing gliding performance to estimate tissue body density has now been applied to several cetacean species, including a DoD priority beaked whale and a relatively shallower-diving baleen whale. This confirms that the tissue body density method can be a widely-applicable tool, enabling routine measurement of body condition of free-ranging cetaceans. As a tag-based method, it has the potential to enable longitudinal measurement of body condition changes in the same individual animal. Long-term monitoring of the body condition of individuals can be a powerful tool to measure health changes that might arise from disturbance associated with DoD activities. Transition of this technology and its incorporation into a longer-duration tag, with onboard calculation of body density and satellite telemetry of the results, has been started under ONR funding.

Our study has also confirmed that the camera-mounted UAV approach to measure body condition via photogrammetry is effective and correlates well with the body density approach to estimate full body lipid stores in humpback whales. As a low-cost method that is even less invasive than suction-cup tagging, we expect that UAV approaches to measure body shape will also become more widely used to study body condition of free-ranging cetaceans. Our study also showed that use of remotely collected biopsy samples to estimate body condition requires care as simple measures like lipid content are not reliable. Hormones such as the glucocorticoids that are

upregulated in response to local tissue metabolic state and particularly when measured in combination with other regulatory proteins and peptides, have the potential to add valuable information on the energetic status of the animals at the time of sampling.

These approaches have advanced our ability to measure body condition of this group of animals. By quantifying how natural factors of season and reproductive status affect body condition, this study enables fuller evaluation of the possible biologically-significant effects of disturbance on cetaceans, including by DoD activities.

## 2 OVERALL INTRODUCTION

### 2.1 Background

This project was conducted under the SERDP program SISON-11-02 ‘Behavioral Ecology of Cetaceans’. Many published effects of sonar on cetaceans include changes to biologically important behavior such as foraging (De Ruiter et al., 2013; Isojunno and Miller, 2015), social acoustic communication, and energy expenditure (Williams et al., 2017). The clear documentation of the short-term effects of sonar disturbance, due to acute exposures at sea, has led to concern that chronic exposure to disturbance might impact the longer-term health of individuals and populations of marine mammals (Southall et al., 2016). One of the important predicted impacts is that disturbed animals will be unable to feed effectively (Miller et al., 2009), and may expend more energy to find food due to relocation or avoidance responses (Miller et al., 2012c). To lead to a population-level impact, such effects have to lead to detrimental impacts on individual health, which then lead to effects on reproductive and survival rates (NRC, 2016).

For marine mammals, the quantity of the lipid energy store is an intermediate health parameter that integrates such impacts with the foraging efforts of individuals (Figure 2-1), and ultimately should also be a good predictor of the fitness and reproductive health of populations. For example, in phocid grey seals (*Halichoerus grypus*), Hall et al., (2001) demonstrated that fat stores from the mother were an important predictor of the chances of first-year survival in her offspring. Because cetacean mothers also face extensive gestation and lactation demands, body energy stores are expected to be closely tied to reproductive cycles and ultimately to the reproductive success and survival of both mother and offspring.

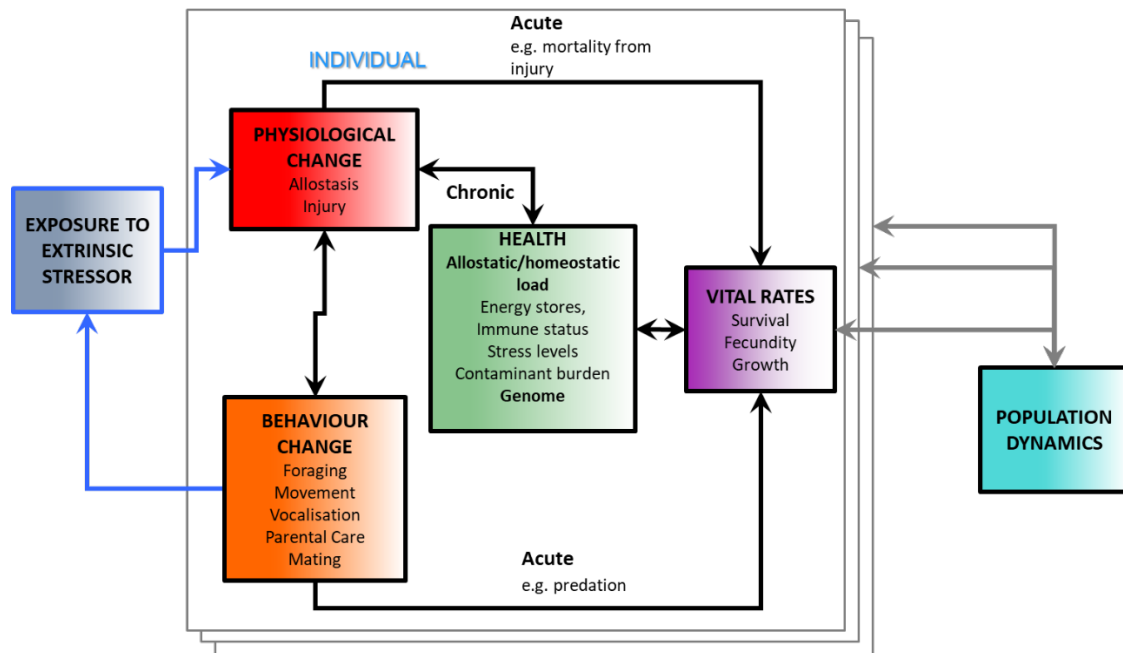


Figure 2-1. A conceptual framework to link responses to extrinsic stressors to vital rates of individuals and populations. Energy store status is one core aspect of the central feature ‘Health’ that links the physiology of individuals to their ability to survive, grow, and reproduce. Image from NRC, 2016.

Indeed, body condition has been demonstrated to be a predictor of fitness in many ways in addition to survival and reproductive success (Bradford et al., 2012; Moya-Larano et al., 2008), such as immune fitness (Eraud et al., 2005). Body condition can be defined in numerous ways, but is usually measured as nutritive condition, specifically the quantity of energy stores carried in the fat (lipid) stores (which in marine mammals is all stored as subcutaneous blubber) of an individual. The size of the lipid stores reflects an integration of metabolic costs and foraging success, but also reflects the reproductive needs of the individual in their life cycle (Miller et al., 2011). For example, for seals that breed on land, researchers have been able to quantify the resources required to produce offspring and the consequences of variation in resources on future survival and reproductive success (McMahon et al., 2000; Pomeroy et al., 1999). “Capital-breeding” seals, such as the grey seal, fast while breeding, and female fat stores transferred to the offspring predict first-year survival and therefore reproductive success (Hall et al., 2001).

The linkage between lipid-store body condition and vital rates of marine mammals has been the focus of recent research in the ONR-funded project: The ‘Population Consequences of Disturbance (PCoD) Working Group.’ That research established a modeling framework to connect disturbance events to effects on vital rates of populations, a key challenge to quantify the biological significance of noise (Figure 2-1, (NRC, 2005, 2016) and our project fits with this approach in addressing the key link between the exposure and response, through finding reliable ways of assessing health and energetic status in cetaceans. Evolutionary theory suggests that fitness of individuals can be optimized if organisms vary responses to their environment dependent on their status or condition (Rands et al., 2004). Animals in poorer nutritive condition should increase their foraging efforts, including increasing the risk of being predated upon, in order to increase their foraging success (Frid and Dill, 2002). Human disturbance may result in worsened body condition of affected individuals (New et al., 2013a), but little is known how effectively those individuals might be able to compensate for such effects by increasing their foraging effort.

The state of the art method to measure lipid stores in mammals is isotope dilution (Reilly and Fedak, 1990), which requires injection of isotopic water, and subsequent extraction after dilution. This method is clearly only feasible for animals that can be held for several hours. Amongst marine mammals, this method has been used most widely with pinnipeds (e.g. Biuw et al., 2003) that are available for research when they haul-out on land. However, such measurements cannot be made for cetaceans that cannot be temporarily captured for study, or indeed for pinnipeds during the long periods of time they are away from land.

Because lipids are less dense than other animal tissues, a consequence of changes in lipid stores is a change in overall body density; and measurement of body density is the state-of-the-art approach to measure fat content in humans (Fields et al., 2005). A critical tool for the study of body condition in elephant seals (*Mirounga leonina*) is that lipid store body condition can be estimated during drift dives (Biuw et al., 2003), in which the seal is passive in the water and its vertical drift rate is a consequence of its buoyancy in relation to body drag. Drift dives are known to be performed by only a few species (Aoki et al., 2011b), whereas gliding during descent and ascent phases of dives is a common behavior that increases when movement is aided by buoyancy (Miller et al., 2004a; Williams et al., 2000). Gliding periods can be identified unequivocally using accelerometers deployed on animals and sampled at more than twice the stroke frequency, which register animal thrusting movements (Sato et al., 2003). Sato et al. (2003) showed that percentage of time gliding, and ascent and descent rates of diving Weddell seals (*Leptonychotes weddelli*) were strongly

correlated to girth/length fatness ratios. Speed and acceleration of gliding bodies are a predictable outcome of identified forces (drag, buoyancy) acting upon them. Miller et al. (2004) used Dtags to measure acceleration in sperm whales (*Physeter microcephalus*) during ascent and descent glides and Watanabe et al., (2006) showed how body density can be measured from prolonged glides in seals.

To date, three different methods have been demonstrated to estimate body density of divers from analysis of hydrodynamic performance during glides. The drift dive method (Biuw et al., 2003) requires animals to drift motionless at depth – a behavior limited to a few species. The all-glide method makes use of all available glides to fit a 3-term model of drag, air buoyancy, and tissue buoyancy and has been successfully used with Dtags on sperm whales (see Equation 1 in Methods below; Miller et al., 2004). The prolonged glide model (Watanabe et al., 2006) estimates body density from the terminal descent gliding velocity of a diving seal. Recent research in the Miller lab has validated these three methods with translocated Northern elephant seals (*Mirounga angustirostris*) whose fat content was measured using the isotope dilution method (see Biuw et al., 2003). Three elephant seals were outfitted with Little Leonardo 3MPD3GT tags, a weight and float. The weight and float together were neutrally buoyant. All three methods gave a good correlation ( $r^2$  0.95-0.99) with density estimated from fat content derived from isotope dilution measurements (see Figure 3 in Aoki et al., 2011). Thus, in seals which can be more easily captured for blood measurements, the method to determine body condition from buoyancy-based methods has been tested against the ‘gold-standard’ method of isotope dilution (Reilly and Fedak, 1990).

With large cetaceans that cannot be captured for isotope-dilution, alternative methods of estimating body condition have been developed and used in various studies (Nowacek et al., 2016). Measurement of blubber-thickness in the Northern right whale (*Eubalaena glacialis*) indicated that that blubber stores vary with reproductive status (Miller et al., 2011). Visual-assessment of body condition appears to be effective for certain species (Bradford et al., 2012). Overhead photogrammetry has been used successfully to measure shape changes of cetaceans in relation to reproductive status (Miller et al., 2012a; Perryman and Lynn, 2002). However, until recently this was achieved using fixed wing plans and helicopters. Recently, the capability of small UAV (drone) systems to make such photographic measurements of cetaceans has been demonstrated (Durban, 2015; Fearnbach et al., 2011). Measurements of shape changes over the fasting season of humpback whales have demonstrated the potential of UAV systems to track lipid-store body condition changes (Christiansen et al., 2016).

Remote biopsy samples are often collected from large, free-living cetaceans, largely for genetic studies, for which only the skin is used. Thus recent investigations have demonstrated that the underlying blubber can be used for analysis of lipophilic hormones, particularly the steroids (Hunt et al., 2013). This resource could therefore also provide information on the nutritional or energetic status of the animals. For example, an alternative approach to estimate body condition from blubber samples, which has been explored is the analysis of its lipid content, which has been demonstrated to be a potential useful predictor of total energy stores (Aguilar and Borrell, 1990) particularly when coupled with other body measurements. As predicted from other mammalian species, blubber lipid content should be highly correlated with total body fat stores and may therefore provide a further, independent validation method for the body density estimates. However, this has only been explored in a limited number of species and results have been equivocal (Ackman et al., 1975a; Dunkin et al., 2005). Therefore, further research into the

reproducibility and robustness of this approach needs to be established if the widely available biopsy tissue samples are to be useful for determining nutritional status in free-living cetaceans.

In addition, the upregulation of the ‘adipocytokine’ and glucocorticoid hormones or other important peptides and proteins involved in fat metabolism could be investigated. The adipocytokines are related to long-term energy balance in a wide variety of mammalian species (Ahima, 2006). These hormones are secreted in combination by adipocytes and are the means by which animals judge their long term energy stores (Collins et al., 1996; Guerre-Millo, 2004) and are likely to have similar paracrine actions and functional roles in cetaceans.

## 2.2 Background to the specific aims of our study

Despite positive progress to measure body condition of cetaceans using diverse methods, there is no existing method to measure total-body lipid store body condition of cetaceans in a quantitative and replicable fashion. Therefore, we aimed to establish, cross-validate, and implement the glide method as a relatively non-invasive method to quantitatively measure lipid-store body condition of free-ranging cetaceans.

A centerpiece of the project was to refine the method of estimating body density from swimming performance data recorded using animal-attached tags (Figure 2-2) using advanced statistical techniques, and to apply the method to cetacean species. The process model describing how body density alters the pattern of acceleration observed during glides (Equation 1) includes influences of body drag and gas-volume. Before the start of this study, methods used non-linear least-squares regression to estimate the unknown parameters in the model (Aoki et al., 2011a). This has been effective in some cases, but has some weaknesses. It does not allow us to apply prior knowledge about the likely range of the parameters, for most of which we have good information. Also, it does not allow the consideration of how measurement errors might influence the parameter estimates. Therefore, we will establish a Bayesian analysis procedure for estimating the parameters. Prior ranges for the parameters will be based upon literature reports or logical analysis. An observation model will include the measurement accuracy of the parameters which are obtained using the tag devices.



Figure 2-2. Two different suction-cup-attached tags used in the study. Left: The 3MPD3GT tag produced by Little Leonardo, Tokyo, Japan. Right: The Dtag produced by the Woods Hole Oceanographic Institution, USA. Both devices sense high-rate acceleration data which enables identification of glides, and pressure to measure animal depth during glides. The 3MPD3GT device has a flywheel speed sensor to measure speed changes during glides, while for the Dtag speed is measured using the change of depth divided by  $\sin(\text{pitch})$  which works well for relatively vertical transit during descent and ascent phases of dives (Miller et al., 2004).

Equation 1: The hydrodynamic process model. The sum of drag, tissue and gas buoyancy forces determine the acceleration experienced by a gliding body. The effects of hydrostatic pressure on gas volumes and density of tissues are explicitly included in the model.  $C_d$  is the drag coefficient,  $A$  is the relevant surface area ( $\text{m}^2$ ),  $m$  is the mass of the whale (kg),  $\rho_{sw}$  is the density of the surrounding seawater ( $\text{kg m}^{-3}$ ),  $\rho_{tissue}$  is the density of the non-gas component of the whale body ( $\text{kg m}^{-3}$ ),  $g$  is acceleration due to gravity ( $9.8 \text{ m s}^{-2}$ ),  $p$  is animal pitch (rad) with negative values indicating a downward orientation,  $V_{air}$  is the volume of air carried from the sea surface (ml),  $\rho_{air}$  is the density of air ( $\text{kg m}^{-3}$ ),  $d$  is glide depth (m) and  $r$  is compressibility of the animal tissue or the fractional change in volume per unit increase in hydrostatic pressure. The value 101,325 converts pressure in atmospheres to pressure in Pa, so that the units of body tissue compressibility are  $\text{proportion} \times 10^{-9}$  per Pa. The equivalent compressibility value for  $0^\circ\text{C}$  water of salinity 35 ppm is  $0.447 \times 10^{-9} \text{ Pa}^{-1}$ .

$$a = -0.5 \times \frac{C_d \times A}{m} \times \rho_{sw} \times v^2 + \left( \frac{\rho_{sw}}{\rho_{tissue}(d)} - 1 \right) \times g \times \sin(p) + \frac{V_{air}}{m} \times g \times \sin(p) \times \frac{\rho_{sw} - \rho_{air} \times (1 + 0.1 \times d)}{(1 + 0.1 \times d)},$$

$$\rho_{tissue}(d) = \frac{\rho_{tissue}(0)}{1 - r \times (1 + 0.1 \times d) \times 101,325 \times 10^{-9}}.$$

Unfortunately, it remains infeasible to attempt to determine the true state of lipid-stores of free-ranging cetaceans using the gold standard method of isotope dilution. Therefore we sought to validate the body density method to estimate energy store by comparing body density values of

individuals with measures from biopsy samples and body dimensions. Thus fieldwork efforts including tagging using suction cups, remote collection of an external biopsy sample, and measurement of body shape of the same individual whale, ideally during the same encounter. Core efforts in this project focused on testing and evaluation of specific ways to refine these methods, with the joint goal of being feasible to collect during fieldwork efforts, and to provide a measure expected to reflect body condition. For tissue indicators, we evaluated hormone and lipid concentrations as candidate indicators of body condition using tissues obtained from stranded or bycaught animals. For body shape measurements, we first evaluated use of a 3D underwater scanning sonar, and later developed methods to use an UAV drone to collect photogrammetry images of the shape of tagged whales. After refining each of the methods independently, we then compared the results of the measures across different sampled whales. We predicted that animals with large energy stores will have low body density, large girth/width to length shapes, and high levels of lipid or variously high or low hormonal indicators in their blubber.

Little is known the patterns of variability of lipid store body condition in cetaceans, though we predict that animals should gain lipids over the feeding season, and that pregnant animals have higher lipid stores to provide for energy required during lactation. We will explore patterns of variability in body density, tissue indicators, and body dimensions against animal sex, location and date of tagging. Sex can be determined from DNA analysis of part of the skin collected with the biopsy sample (Rosel, 2003). Reproductive status will be classified as pregnant, lactating or resting. Pregnancy will be determined based upon progesterone concentrations in blubber biopsy samples (Trego et al., 2013). The state of “lactation” will be assessed by observation of calf presence at sea.

The determination of pregnancy status using blubber samples was first investigated in minke whales (*Balaenoptera acutorostrata*) by the determination of progesterone (the major hormone necessary to maintain pregnancy) in samples collected following a Norwegian whale hunt (Mansour et al. 2002). Pregnancy status was therefore confirmed at post-mortem. Hormones were extracted from the blubber using various solvents before measurement by immunoassay. Progesterone concentrations were significantly higher in pregnant females than in non-pregnant females and males (mean  $\pm$  SE 133  $\pm$  23 ng/g blubber of pregnant compared with 1.95  $\pm$  0.3 ng/g in non-pregnant females,  $p < 0.0001$ ). This approach was also confirmed by Kellar et al. (2006) in which 110 blubber samples from three delphinid species (*Delphinus delphis*, *Lissodelphis borealis* and *Lagenorhynchus obliquidens*) by-caught in fisheries were analysed for progesterone (and testosterone). Blubber progesterone was again significantly higher in pregnant females (132-415 ng/g) than non-pregnant and immature animals (0.92-48.2 ng/g) for all three species. In the limited-scope study, using the same methods we found high blubber levels were detectable in biopsy samples from pregnant humpback whales that were subsequently seen with a calf.

Finally, we examine how body condition relates to foraging effort of the cetaceans tagged in this study. In addition to potentially being a good indicator of the reproductive health of populations, body condition may be an important predictor of behavior patterns in cetaceans. Body condition influences how individuals trade-off foraging and anti-predator behaviors (Hilton et al., 1999; McNamara and Houston, 1990), with poor condition foragers taking greater risks in order to increase foraging rates. This leads to two important predictions. The first is that cetaceans should have some ability to adjust their foraging effort to recover their desired body condition, or to maintain “allostasis” (McEwen and Wingfield, 2003). Thus, individuals whose body condition is

poor, including any that might have been negatively affected by human disturbance, are predicted to have some capacity to compensate for those effects, but the effort of compensation could have its own costs, such as increased predation risk or delayed reproduction. The second prediction is that animals in poor body condition should be more tolerant of disturbance sources than animals in good body condition, a prediction which has been tested in birds (Beale and Monaghan, 2004). Unrecognized variability in body condition could lead to increased variation in behavioral responsiveness to human disturbance, complicating attempts to derive effective dose-response relationships.

### 2.3 Choice of study species

Our goal in the choice of target species for this study was to cover some of the diversity among cetacea, both in relation to breeding life history and diving behavior. Some cetacea are known to be capital breeders that fast during breeding seasons by utilizing energy stores amassed during feeding periods. Capital breeders are expected to undergo annual cycling of fat stores, whereas income-breeders that feed throughout the year, are expected to have less strong variations in lipid-store body condition. A secondary consideration was to attempt to apply the body density methodology to a relatively shallower-diving cetacean, as to date the method has been applied solely with deep-divers. Gas spaces become more strongly compressed at depth, which simplifies the calculation of body density for deep divers (Biuw et al., 2003; Miller et al., 2004).

As a Ziphiid, the Northern bottlenose whale (*Hyperoodon ampullatus*) is a deep-diving species within a key taxonomic group of priority interest to DoD. Among the Ziphiids, Northern bottlenose whales are relatively well-studied, particularly the initially proposed study population in the Gully, Canada. As one of the few Ziphiid species to have been whaled commercially, relevant information on seasonality of calving and body length of pregnant females is available (Benjaminsen, 1972). Researchers have successfully worked in the Gully to tag, photo-identify, biopsy sample, and observe Northern bottlenose whales in dozens of research trials over the past 20 years (Dalebout et al., 2001; Gowans et al., 2000; Hooker and Baird, 1999b; Hooker et al., 2002; Whitehead and Wimmer, 2005; Whitehead et al., 1997a; Whitehead et al., 1997b; Wimmer and Whitehead, 2004). In our limited-scope pilot study of 2011, we were able to tag three different whales in just three days of workable weather in the Gully and use those data to calculate the body density of individual *Hyperoodon*. In 2013, the 3S collaborative research program identified a large population of bottlenose whales off Jan Mayen, Norway and found them to be sensitive to disturbance from sonar signals (Miller et al., 2015b). We shifted our efforts from the Gully to Jan Mayen to study this species of beaked whale, aided by matched funding from ONR to study the sensitivity of the species to sonar signals.

The mysticete humpback whale (*Megaptera novaeangliae*) is one of the better studied baleen whales, with numerous studies of their life-history and behavior (Clapham, 2000). Humpbacks undertake an annual fasting cycle as part of their migration to breeding grounds. Thus, as for phocid seals, deposition and utilization of lipids are expected to occur on an annual cycle, and the amount of lipid stored during the feeding season should be an important factor in shaping their behavior and reproductive success. Humpback whales display site fidelity to their feeding grounds (Stevick et al., 2006), so individual animals can be resighted over successive years. Adult and calf survival has been estimated in some populations for this species (Barlow and Clapham, 1997; Ramp et al., 2010). Humpback whales are relatively shallower-divers, so our ability to measure body density in this species was confirmed (Narazaki et al., 2018) during the project. Unlike the

ziphiid bottlenose whales which are very difficult to follow and resight at sea, humpback whales are also a more feasible species for conducting the multiple sampling efforts (tagging, biopsy sample, photogrammetry) of each individual whale that was required for this study.

## 2.4 Objectives

The overall objective of the study was to develop, validate and apply a novel, non-invasive, tag-based technique to measure the body condition of free-ranging cetaceans. Specific objectives are to:

- 1.) Measure the body density of individual Northern bottlenose whale (*Hyperoodon ampullatus*) and humpback whale (*Megaptera novaeangliae*), using biomechanical and hydrodynamic data recorded using high-resolution tags attached with suction cups. We will develop a Bayesian state-space statistical modeling framework to estimate body density and relative lipid stores using the balance-of-forces equation as a process model for hydrodynamic performance during glides. An observation model accounting for measurement error will be established, and used for measurement of body density from diverse tag types, including the 3MPD3GT tag and the Dtag.
- 2.) Validate body density as a metric of body condition using two independent methods. For each individual tagged with a 3MPD3GT tag or Dtag, we will collect biopsy samples and photogrammetric data to determine independent validation metrics of body condition. The specific metrics will be lipid and glucocorticoid (cortisol) content of blubber biopsy samples and body dimensions. We will inspect the relationship between these three independent approaches to measure lipid-store body condition, with a prediction that fatter animals will have a combination of lower body density, higher lipid levels in blubber, lower glucocorticoid levels and greater girth/length ratios. When possible, individual animals identified with photographs will be repeatedly measured in order to track within-animal changes in lipid-store body condition.
- 3.) Identify patterns of lipid store body condition for individuals based upon their sex, reproductive status, location, and time of year. Humpback whales of both sexes are predicted to increase fat stores throughout the foraging period, while Northern bottlenose whales are predicted to maintain a more narrow range of body density. However, females of both species are predicted to deposit larger lipid stores when pregnant and reduce stores during nursing periods. For female subjects, we will determine the subject's reproductive status as either pregnant, lactating, or resting. Pregnancy status will be assessed using progesterone concentrations in biopsy samples. Lactation status will be assessed by observation of calf presence at sea, and estimates of calf size.
- 4.) Use the high-resolution tag data to quantify how individuals might vary foraging effort and anti-predator behavioral responses in relation to body condition. Behavioral ecology theory predicts that body condition should influence these behaviors, with high-density (lean) animals tending to forage more intensely and be less responsive to predation risk than low-density (fat) animals.

### 3 DEVELOPMENT AND EVALUATION OF THREE INDEPENDENT METHODS TO ESTIMATE BODY CONDITION

#### 3.1 Tissue indicators of body condition

##### 3.1.1.1 Blubber Progesterone as an Indicator of Pregnancy

Historically, the pregnancy status of cetaceans was assessed by examining carcasses taken in commercial whale hunts. More recently, biochemical techniques have been developed to detect pregnancy using non-lethal methods by measuring progesterone concentrations in the blubber of individuals through biopsy sampling. Progesterone is a lipophilic steroid hormone that is produced by the corpus luteum, and is the primary regulator of oestrous cycling and pregnancy in mammals (Pineda, 2003). Concentrations of this hormone increase during pregnancy to maintain the uterus lining, and its lipophilic properties mean that this increase in circulating concentrations is measurable in the blubber. The collection and analysis of biopsy samples of skin and blubber are therefore a readily obtainable and non-lethal way of assigning pregnancy in free-ranging cetaceans.

Previous work in a range of cetacean species, both mysticetes (Kellar et al., 2013; Mansour et al., 2002) and various species of smaller odontocetes (Kellar et al., 2006; Perez et al., 2011; Trego et al., 2013) have shown that blubber progesterone concentrations are indicative of pregnancy as confirmed by physical examination of the carcasses and recording the number of corpora, corpus lutea and size and/or length of the fetus if present. Since the validation of blubber progesterone as a marker of reproductive state, this method has been used to investigate pregnancy rates in free-ranging bottlenose dolphins (*Tursiops truncatus*) (Perez et al., 2011), long-finned pilot whales (*Globicephala melas*) (Perez et al., 2011) and humpback whales (Clark et al., 2016; Pallin et al., 2018). The same methods will be applied here to assess the pregnancy status of the female humpback whales and northern bottlenose whales sampled for this work.

##### 3.1.1.2 Blubber Lipid Content as an Indicator of Body Energy Stores

The high energy yield of fats, specifically triacylglycerols (esters made up of a glycerol and three fatty acids), relative to carbohydrates or proteins make them the favoured energy storage form in mammals (Coleman and Lee, 2004; Young, 1976). A proper capacity for triacylglycerol storage in adipocytes is important for normal metabolic regulation (Wang et al., 2015). Adipose tissue lipid content has therefore been linked with total fatness in a range of mammalian species (Beck et al., 1993; Shier and Schemmel, 1975; Stirling et al., 2008), such that when coupled with demographic and ecological data, using lipid content as a body condition index can be a biologically relevant, relatively inexpensive and rapidly assessed marker (McKinney et al., 2014). Lipids in cetacean blubber are mobilized in times of energetic need and nutritional stress, and then deposited when food is in excess. Recent evidence suggests that cetaceans have evolved an enhanced capacity for inhibiting unrestricted lipolysis and are able to finely control the lipid content of their blubber through the positive selection of certain lipolysis-related genes (Wang et al., 2015).

Similarly to other mammal species, the direct quantification of blubber lipid content has been used as a metric of overall energy stores and body condition in mysticetes (Ackman et al., 1975b; Aguilar and Borrell, 1990; Konishi, 2006; Lockyer, 1986), and to a lesser extent, in odontocetes (Evans et al., 2003; Gómez-Campos et al., 2011; Montie et al., 2008b; Read, 1990). Variation in overall body condition and lipid content tend to be more extreme in mysticetes because their

seasonality in feeding and reproduction is stronger than in odontocetes (Boness et al., 2002). Here we investigate how blubber lipid content can be used as an indicator of body condition and overall fat stores as it is important to appreciate the degree of variability in blubber lipid content both within and between individuals in order to correctly interpret the results from blubber samples collected by biopsy dart from live animals.

### 3.1.1.3 Adipocyte Metrics as an Indicator of Body Energy Stores

Blubber is primarily composed of lipid filled adipocyte cells surrounded by a matrix of collagen and elastic structural fibers (Pabst et al., 1999). Given that mammalian adipocytes typically shrink and swell in response to fasting and fattening, as opposed to increase and decrease in number in a given depot (Pond, 1998), measuring the size of adipocytes may act as an alternative means of measuring blubber adiposity and thus body condition.

Previous research has investigated the occurrence of adipocyte shrinkage in two cetacean species: harbour porpoises (Koopman et al., 2002) and humpback whales (Castrillon, Huston, & Bengtson Nash, 2017). A change in both size and number of adipocytes was observed in the blubber of stranded harbor porpoises in response to a decline in body condition (Koopman et al., 2002). Analysis of necropsied blubber samples revealed starved harbour porpoises had fewer, smaller adipocytes in the middle layer thorax blubber than their healthy counterparts, suggesting both a decrease in adipocyte size and number occurs in response to nutritional stress. Interestingly, a similar pattern in adipocyte size was observed in migrating humpback whales (Castrillon et al., 2017), where “migration cohort” of animals travelling to or from feeding grounds was used as a proxy for fasting state. Analysis of blubber samples revealed fasted animals had smaller adipocytes than those returning from feeding grounds, suggesting adipocytes shrink in response to nutritional stress. Furthermore, adipocyte area had a greater probability of predicting migration cohort in comparison to blubber lipid content, suggesting adipocyte area may prove a viable, and indeed potentially more informative alternative biomarker of blubber adiposity in wild cetaceans.

We therefore further investigated the use of adipocyte metrics as an informative biomarker for body condition in cetaceans. However, due to blubber biopsy sample mass limitation, it was not possible to apply this method to the samples collected from the free-living cetaceans. Therefore further details about the methods and findings regarding adipocyte metrics are given in the Supplementary Material, with a summary presented in Section 3.4.

### 3.1.1.4 Blubber Cortisol as an Indicator of Physiological State

As well as their involvement in the stress response, glucocorticoids have also been proposed as long-term regulators of both energy intake and storage (Strack et al., 1995). Glucocorticoids, including cortisol, are metabolic hormones that increase in circulation in response to energetic needs, and their concentrations can be interpreted as indicators of allostatic load (Bonier et al., 2009). Cortisol is of particular interest in the regulation of whole body energy stores as it is involved in maintaining the balance between fat storage where triglycerides are deposited, and fat depletion where they are catabolised and released into circulation (McMahon et al., 1988) (Peckett et al., 2011). Overall, cortisol is known to play an active role in lipolysis in subcutaneous adipose tissue (Divertie et al., 1991; Djurhuus et al., 2004; Samra et al., 1998), stimulate gluconeogenesis, mobilise amino acids, and increase circulating concentrations of plasma proteins (Bergendahl et al., 1996; Exton et al., 1972). Thus, overall, cortisol is a catabolic hormone, and together these processes act to increase the availability of all fuel substrates by mobilisation of glucose, free fatty-

acids and amino acids from endogenous stores (Dinneen et al., 1993; Djurhuus et al., 2002). Cortisol concentrations could therefore be used as indicators of overall physiological state.

To date, investigation of this hormone in marine mammal energy regulation and fasting metabolism has focused on pinnipeds (Bennett et al., 2012; Gardiner and Hall, 1997; Guinet et al., 2004; Kershaw and Hall, 2016; Ortiz et al., 2003; Riviere et al., 1977). Specifically, similar to terrestrial mammals, there is an increase in plasma cortisol concentrations with prolonged fasting events in subantarctic fur seals (*Arctocephalus tropicalis*) and northern elephant seals (*Mirounga angustirostris*) (Guinet et al., 2004; Ortiz et al., 2001). It has been hypothesised that these higher circulating cortisol concentrations may contribute to significantly increased fat oxidation during the fast, and may also serve as a cue to terminate fasting and initiate feeding (Ortiz et al., 2001). Blubber cortisol concentrations were not correlated with handling time in wild caught harbour seals (*Phoca vitulina*), indicating that the concentrations are not reflective of an acute stress response to the capture and handling event (Kershaw and Hall, 2016). Blubber cortisol concentrations were shown to vary by sex, with females having higher concentrations than males, and importantly for this work, concentrations were significantly higher during natural fasting periods of the life cycle, during the breeding season, and especially during the moult (Kershaw and Hall, 2016). Finally, blubber cortisol concentrations decreased inversely with proportion blubber lipid content in California sea lions (*Zalophus californianus*) (Beaulieu-McCoy et al., 2017), further suggesting that this hormone could be used to monitor long-term nutritional status. Here, blubber cortisol concentration will be investigated as a potential endocrine marker of overall physiological state rather than an acute stress response.

#### 3.1.1.5 Protein Components of Blubber as Markers of Health and Condition?

Since the 1980s, mammalian adipose tissue, or fat tissue, is increasingly being recognized as an endocrine organ involved in the regulation of a number of metabolic processes and pathways. It responds to signals from different hormone systems and the central nervous system, and expresses a variety of protein factors with important paracrine and endocrine functions (Ahima, 2006; Galic et al., 2010; Kershaw and Flier, 2004; Siiteri, 1987). As such, adipose tissue is integrally involved in coordinating a variety of biological processes including the regulation of appetite and energy balance, immune system function, insulin sensitivity, angiogenesis, inflammation and the acute-phase response, blood pressure, nutrient transport and lipid metabolism and haemostasis (Trayhurn and Wood, 2004). These processes enable the organism to adapt to a wide range of different metabolic challenges including starvation, stress, infection and periods of energy excess (Frühbeck et al., 2001). The presence and concentrations of certain proteins and their metabolites in adipose tissue, as well as circulating concentrations in the blood stream can therefore provide information on various physiological processes and metabolic challenges experienced by individuals at the time of sampling. More generally, protein screening and identification are commonly used as diagnostic markers in medicine to detect disease and perturbations to metabolic pathways (Steffen et al., 2016).

The protein components of adipose tissue are therefore of interest to understand whole tissue function, the regulation of whole body metabolism and overall systemic health. Here, we aim to investigate whether cetacean blubber could show equivalent pleiotropic functions to the adipose tissue in terrestrial animals by starting to identify some of the main protein components in the tissue. The separation and identification of proteins in blubber tissue from different species are important steps in establishing a database of baseline, identifiable proteins and subsequently

applying a proteomic approach to using various proteins as biomarkers of health and condition in these animals with otherwise limited sampling opportunities from live individuals.

However, as with the adipocyte size metrics, the amount of tissue available from the biopsy sampled animals was limited. Therefore, this approach was not used in the final cross-validation. All the details of the methods and results are therefore given in the Supplementary Material with a summary of those findings and further recommendations give in Section 3.1.4.

### 3.1.2 Biomarker method development preface

The majority of the work for the tissue analysis part of the project has been to investigate and validate the use of novel biomarkers of health and condition in blubber samples. This was done by using full depth blubber samples from a combination of stranded cetaceans and biopsy samples collected from individuals that were not collected specifically for the RC-2337 project. Full depth blubber samples were collected from dead animals of various cetacean species by the Scottish Marine Animal Standings Scheme (SMASS). These full depth dorsal samples were collected with accompanying information on the individual including sex, age class, cause of death and various morphometric measurements. These accompanying data on the individual that was sampled were vital to put the results of the blubber sample analysis into context, and thus assess the applicability of different blubber biomarkers.

A small number of full depth blubber samples were also collected from dead animals sampled opportunistically by the Mingan Island Cetacean Study, referred to from now on as MICS, during their summer field seasons in the Gulf of St Lawrence, Quebec, Canada. These were from both minke and humpback whales, but because of logistical constraints, accompanying morphometric and cause of death information was not recorded for this handful of animals. Finally, a number of blubber biopsy samples taken by the MICS between 2004 and 2013, again from both minke whales and humpback whales were also used to assess the applicability of the methods on remotely obtained, shallow depth samples from different species, and to put the results from the RC-2337 sampled animals into context.

The methods that are described in the rest of this section are therefore based on these samples used for method development, or, where the methods were assessed to be robust and warranted further investigation, are split into these method development samples followed by the application of the methods to the biopsy samples from live animals.

#### 3.1.2.1 Lipids

##### 3.1.2.1.1 Method Development using Stranded Animal Samples

A total of 27 individuals, from three cetacean families, were sampled and are summarised in Table 3-1. These were delphinids (n = 10) - white beaked dolphins (*Lagenorhynchus albirostris*); ziphiids (n = 8) - Cuvier's beaked whales (*Ziphius cavirostris*), Sowerby's beaked whales (*Mesoplodon bidens*) and Northern bottlenose whales (*Hyperoodon ampullatus*); and balaenopterids (n = 9) - minke whales (*Balaenoptera acutorostrata*) and humpback whales (*Megaptera novaeangliae*). These were freshly dead individuals that showed minimal signs of decomposition, 25 of which were sampled and assessed by the SMASS between 2013 and 2015. For these animals, the cause of death (COD) was determined either by necropsy, or based on visual observations of the carcass showing signs of trauma, disease or emaciation. Two COD categories were generated. 'Acute' cases were individuals that died of an acute trauma (bycatch, acute

entanglement, storm damage, and predatory attacks). ‘Chronic’ cases were individuals that died of general debilitation and a prolonged decline in their health either through infectious disease (parasitic, bacterial, viral, or mycotic infections), starvation (severely emaciated animals that died of starvation/hypothermia) or chronic injuries (e.g. chronic entanglement). Measurements of mass, length, girth and blubber thickness proximal to the dorsal fin along the dorsal axis were taken (Kuiken and Hartmann, 1991). Due to the logistical constraints presented by their larger body size, mass was not recorded for the ziphiids or the balaenopterids. Individuals were classed as adults or juveniles using the lengths at sexual maturity for each species based on published data (Galatius et al., 2013; Hauksson et al., 2011; Heyning, 2002; Hooker and Baird, 1999b; Mead, 1989; Whitehead et al., 1997b). The final 2 individuals were an adult female minke whale and an adult female humpback whale that dead stranded in the Gulf of St Lawrence, Canada, and were opportunistically sampled by the MICS during their 2013 and 2010 summer field seasons respectively. No cause of death was confirmed for these animals and morphometric measurements were not taken.

*Table 3-1. Summary of the mysticete and odontocete individuals used for full depth blubber samples across three different families. \*SMASS (Scottish Marine Animal Strandings Scheme). \*\*MICS (Mingan Island Cetacean Study).*

Suborder	Family	Species	Number	Source
Mysticete	Balaenopteridae	Minke whale <i>(Balenoptera acutorostrata)</i>	6	SMASS* MICS**
		Humpback whale <i>(Megaptera novaeangliae)</i>	3	SMASS MICS
		Sowerby’s beaked whale <i>(Mesoplodon bidens)</i>	4	SMASS
Odontocete	Ziphiidae	Cuvier’s beaked whale <i>(Ziphius cavirostris)</i>	2	SMASS
		Northern bottlenose whale <i>(Hyperodon ampullatus)</i>	2	SMASS
		Delphinidae	White beaked dolphin <i>(Lagenorhynchus albirostris)</i>	10

Approximately 2.5cm<sup>2</sup> to 5cm<sup>2</sup> blocks of full depth blubber were collected from the dorsal area immediately caudal to the dorsal fin. This area was chosen to emulate the standard biopsy site from live animals. The entire blubber layer was sampled for all animals to include both the epidermis and some underlying muscle so as to recognize the orientation of the sample. The samples were

wrapped in aluminum foil, placed individually in plastic containers, and frozen at  $-20^{\circ}\text{C}$  before further analysis.

### 3.1.2.1.2 Sample Analysis

The thickness of the fresh blubber samples was measured to the nearest millimetre by measuring the length from the interface between the skin and the blubber, down to the interface between the blubber and the muscle (Figure 3-1). Any freezer burnt edges with a dark yellowish color were removed and discarded. To reduce the loss of lipid while the samples were being prepared, the blubber was subsampled while still partially frozen. A full depth subsample of the original block was cut, and the epidermis and muscle tissue removed. While visible layering was apparent in the blubber of some samples, others did not show visible differences through the blubber depth. For this reason, the blubber was not divided according to visually discernible characteristics, but was subdivided into layers of approximately equal thickness. For balaenopterid and ziphiid samples over 30mm in depth, the blubber thickness was sufficient to allow its subdivision into five layers of equal thickness (Figure 3-1). The inner layer (adjacent to the muscle), the middle layer, and the outer layer (adjacent to the epidermis) were used for lipid extraction while the two transitional layers were discarded (Figure 3-1). The white beaked dolphin samples were not of sufficient thickness to follow this same protocol, and for this reason, they were divided into thirds and each layer was used for lipid extraction. Duplicate subsamples, each weighing between 0.15g and 0.3g were taken from the full blubber depth as well as the inner, middle and outer layers, and lipid was independently extracted from each of the blubber samples using a modified version of a previously published protocol (Folch et al., 1957).

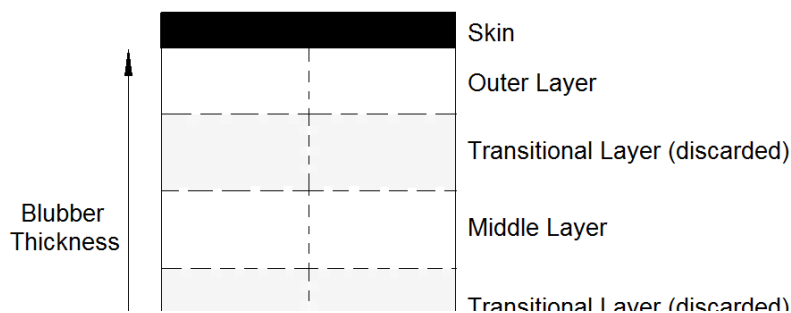


*Figure 3-1. Separation of the full depth blubber samples > 30mm thick into five layers of approximately equal thickness prior to lipid extraction. The vertical dashed line shows where the blubber was divided in half to generate duplicate subsamples. The horizontal dashed lines show where the blubber was divided such that the outer, middle and inner layers were retained for analysis while the two transitional layers were discarded.*

### 3.1.2.1.3 Statistical Analysis

The data from the white beaked dolphins, ziphiids and balaenopterids were modelled separately. Two different statistical approaches were used to firstly investigate differences in the distribution of lipids through blubber depth, and secondly, to investigate what other factors may be affecting blubber lipid content including blubber thickness sex, species, age class, cause of death and body condition. For the white beaked dolphins, mass/length<sup>2</sup> was used as the most appropriate morphometric index of body condition (Kershaw et al., 2017), and girth/length was used for the ziphiids and the balaenopterids as mass data were lacking for the larger animals.

All statistical analyses were performed using the statistical programme, R, version 3.1.2 (R Core Development Team, 2014). The main challenges for analysing these data were that multiple lipid content measurements came from the same individuals, and these were not normally distributed. The modelling approach used here takes advantage of the statistical structure of generalized linear mixed effect models (GLMMs). GLMMs combine the properties of two statistical frameworks, linear mixed models, which are able to incorporate both fixed and random effects, and generalised linear models which are typically used for non-normal data (Bolker et al., 2008). Random effects can encompass variation among individuals when multiple responses are measured per individual. GLMMs are thus the best tool for analysing non-normal data that involve random effects (Bolker et al., 2008). For this reason, GLMMs were used here first, to investigate lipid content through the blubber depth whilst accounting for the repeated measurements from the same individuals. A GLMM (*glmer* function in the package ‘*lme4*’) with a gamma distribution, a log link function and each individual treated as a random effect was used to investigate the effect of blubber layer (full, outer, middle, inner) on the lipid content of the samples from each species group.

Generalised Linear Models (GLMs) were then used to investigate the effects of cause of death (COD), blubber thickness, body condition (either mass/length<sup>2</sup> or girth/length), sex, species (for the balaenopterid and the ziphiid data that were made up of multiple species) and age class on the blubber lipid content of the *full depth* samples from each individual. GLMs with a gamma distribution and a log link function were used to better model the non-normal distribution of lipid content. All sampled individuals were used for the white beaked dolphins (n = 10) and for the ziphiids (n = 8). However, for the balaenopterids, the 2 individuals sampled by the MICS, an adult humpback whale and an adult minke whale, for which COD and morphometric data were not available, were not included in this second part of the analysis (n = 7).

For each species group, the largest GLM was generated to include the effects of all explanatory variables. To ensure that the explanatory variables were not correlated, and thus to avoid multicollinearity in the final model, variables were selected for inclusion based on variance inflation factors (VIFs). The covariate with the highest VIF value was removed from the model in a stepwise fashion until the VIF values for all covariates were below three (Zuur et al., 2010). Then, the ‘*dredge*’ model selection function (*MuMIn* package) was used to identify from this subset of uncorrelated variables, which ones best explain the variation in blubber lipid content data, and should be included in the final model. The goodness of fit of each model was assessed using the AICc (Second-order Akaike Information Criterion which uses a correction for finite sample sizes). The models were ranked by their AICc and the model with the lowest AICc value was used for further interpretation. Summary statistics of the model coefficients were used to assess the effect of each covariate on blubber lipid content.

### 3.1.2.2 Steroids (progesterone and cortisol)

#### 3.1.2.2.1 Method Development using Stranded Animal Samples

Harbour Porpoises: Full depth skin, blubber and underlying muscle samples were collected from 20 dead harbour porpoise by the SMASS between 2013 and 2015. Only freshly dead animals, classified as those that originally stranded alive or had only recently died and thus showed no evidence of bloating, and the meat is considered to be edible (Kuiken and Hartmann, 1991), were sampled for this work in order to prevent erroneous hormone concentration measurements as a result of tissue decomposition after death. The following morphometric measurements were taken; mass, length (tip of rostrum to fluke notch) and girth (immediately anterior of the dorsal fin).

Samples were collected from the dorsal, lateral and ventral axes around the girth of the animal, immediately caudal to the dorsal fin. Blubber depth was recorded at each sampling site. Tissue samples were individually wrapped in aluminium foil and stored at  $-20^{\circ}\text{C}$  in plastic vials before hormone analysis. These individuals were both adults ( $n = 13$ ) and juveniles ( $n = 7$ ), and males ( $n = 11$ ) and females ( $n = 9$ ). The cause of death (COD) was determined as described above, following post-mortem examination, and classified, as either an acute case ( $n = 13$ ) or a chronic case ( $n = 7$ ). Individual details are shown in Table 3-2.

Balaenopterids: Full depth, dorsal blubber samples were collected from 9 stranded balaenopterids (3 humpback whales and 6 minke whales). Samples were collected by the SMASS (2013-2015), and by the MICS (2010 and 2013) from the dorsal area immediately caudal of the dorsal fin. For the samples collected by the SMASS, information on the COD was used to classify each individual as an 'acute' or 'chronic' case. Morphometric measurements including girth (immediately anterior of the dorsal fin), length (tip of rostrum to fluke notch) and blubber thickness were also collected from the SMASS animals only, and lipid content data were available for all samples from previous analyses (Table 3-2).

Table 3-2. Summary table of the harbour porpoise and mysticete individuals used for analysis with the data available for each one. ID codes starting with an ‘M’ were collected by the SMASS, while codes starting with a ‘GSL’ were collected by the MICS. Blubber lipid content values taken from previously described analyses. \* Body Condition Index: Mass/Length<sup>2</sup> for harbour porpoises and Girth/Length for the balaenopterids.

Species Group	Species	ID	Age Class	Sex	COD Class	Body Condition Index*	Blubber Lipid Content
Harbour Porpoise	Harbour Porpoise	M018/13	Adult	Male	Chronic	✓	
		M020/15	Adult	Female	Acute	✓	
		M028/14	Juvenile	Male	Acute	✓	
		M055/14	Adult	Male	Acute	✓	
		M060/13	Adult	Male	Acute	✓	
		M072/13	Juvenile	Male	Chronic	✓	
		M134/14	Adult	Female	Acute	✓	
		M147/14	Adult	Female	Acute	✓	
		M265/13	Adult	Female	Chronic	✓	
		M307/14	Adult	Male	Acute	✓	
		M315/13	Adult	Female	Acute	✓	
		M319/14	Adult	Male	Chronic	✓	
		M343/13	Juvenile	Female	Acute	✓	
		M373/13	Juvenile	Female	Acute	✓	
		M377/13	Adult	Male	Chronic	✓	
		M38.2/14	Juvenile	Male	Acute	✓	
		M396/13	Adult	Female	Acute	✓	
M040/14	Juvenile	Male	Chronic	✓			
M061/15	Juvenile	Female	Chronic	✓			
M068/14	Juvenile	Female	Chronic	✓			
Balaenopterid	Humpback	M159/14	Juvenile	Male	Acute	✓	✓
	Humpback	M163/15	Juvenile	Female	Acute	✓	✓
	Humpback	GSL-2010	Adult	Female			✓
	Minke	M292/13	Juvenile	Female	Acute	✓	✓
	Minke	M297/14	Juvenile	Male	Chronic	✓	✓
	Minke	M180/15	Juvenile	Male	Acute	✓	✓
	Minke	M319/15	Juvenile	Male	Chronic	✓	✓
	Minke	M396/15	Juvenile	Female	Acute	✓	✓
Minke	GSL-2013	Adult	Female			✓	

### 3.1.2.2.2 Application to Biopsies from Live Animals

Northern bottlenose whales: A total of 21 biopsies were collected from Northern bottlenose whales in the waters around Jan Mayen, Norway, during the summer field seasons of 2014 and 2016. Fifteen of these biopsies were from females and six were from males. Of these 21 individuals, 4 were tagged with DTags – 2 in 2014 and 2 in 2016. All samples were extracted for cortisol quantification, and progesterone was also quantified in all the female samples (Table 3-3).

Humpback whales: Humpback whale biopsy samples were taken from two study sites, one in Quebec, Canada, and a second in Norway. A total of 43 samples were collected in Norway between 2011 – 2017 and 39 were collected in Canada over the same time period. Of these 82 samples, 64 were from tagged animals (DTags and Little Leonardo tags), 32 were males and 50 were females. All samples were extracted for cortisol quantification, and progesterone was also quantified in all the female samples (Table 3-3). An additional sample set of 72 humpback whale biopsies collected by the MICS between 2004 and 2009 from known females was included in the progesterone analysis to better interpret the individual hormone concentrations and establish a threshold concentration indicative of pregnancy.

*Table 3-3. Summary of the 103 blubber biopsy samples from northern bottlenose whales (n = 21) and humpback whales (n = 82) collected during tagging fieldwork and processed to measure cortisol and progesterone concentrations.*

Species	Area	Samples Analysed		
		Year	Cortisol	Progesterone
Northern Bottlenose Whales	Jan Mayen	2014	12	7
		2016	9	8
Humpback Whales	Coastal Norway	2011	3	2
		2012	13	8
		2013	6	3
		2014	6	4
		2016	9	5
		2017	6	4
	Quebec, Canada	2011	9	3
		2012	2	2
		2013	1	1
		2016	7	5
2017		20	13	

### 3.1.2.2.3 Sample Analysis

#### 3.1.2.2.3.1 Cortisol and Progesterone Extraction:

Given the similarities in the structure and physical properties of the steroid hormones, the same method has been used for the extraction of progesterone and cortisol from human adipose tissue (Newton et al., 1986). For this reason, a previously developed extraction method for reproductive hormones from cetacean blubber samples (Kellar et al., 2006) was used here to extract both progesterone and cortisol from the SMASS full depth blubber samples as well as the remotely obtained, frozen, blubber biopsy samples from northern bottlenose whales and humpback whales. The protocol involves tissue homogenisation followed by tissue debris removal in a series of solvent rinses with recovery of the supernatant each time. The resulting residues are washed to remove any remaining lipid, and the final extract dried down for resuspension and assaying.

Briefly, between 0.15-0.2 g of the blubber tissue are accurately weighed and homogenized in ethanol. Homogenates are then centrifuged and the supernatants collected. These are then evaporated under compressed air while incubating at 25°C. Ethanol and acetone (4:1) are added to the residue and after the same vortexing and centrifugation steps, the solution is again evaporated to leave a new residue. Diethyl ether, acetonitrile and hexane are used to further clean up the extract, with the final residue re-dissolved in phosphate buffered saline before assaying.

#### 3.1.2.2.3.2 Cortisol Concentration Measurements:

A commercially available Enzyme Linked Immunosorbent Assay (ELISA) (DRG International Inc. Cortisol ELISA EIA-1887) is used for the quantification of cortisol in all sample extracts. This kit has been used to quantify cortisol in blubber biopsies from harbour seals (Kershaw and Hall, 2016). The concentrations are measured according to the ELISA kit instructions with a standard curve ranging between 0 and 800 ng/ml with a sensitivity of 2.5 ng/ml. The hormone concentrations in the samples are determined using a 4 parameter log-logistic model based on the standard curve. Any samples with a concentration higher than the highest standard (> 800 ng/ml) are diluted with the 0ng/ml standard and re-assayed to bring the concentration down onto the standard curve. All samples are assayed in duplicate and the mean hormone concentration reported as cortisol per wet weight of the blubber samples in ng/g. From the live biopsy samples, extracts of varying concentrations, high, medium and low (n=3), were used to calculate inter-assay (between different plates) and intra-assay (within a plate) coefficients of variation (CV), with mean percentage CVs of <20 % and <10 % set as the acceptable limits respectively (Andreasson et al., 2015). Inter- and intra- assay CVs were all below these acceptable thresholds for both species and are given in the Supplementary Material. Standard parallelism, matrix effect and extraction efficiency checks were carried out to ensure that the ELISA kit was performing adequately and is compatible with cetacean cortisol in these tissue extracts (see Supplementary Material).

#### 3.1.2.2.3.3 Progesterone Concentration Measurements:

A commercially available ELISA (DRG International Inc. Progesterone ELISA EIA-1561) is used for the quantification of progesterone in all sample extracts from the live biopsies samples from females only. The concentrations are measured as for the cortisol, according to the ELISA kit instructions with a standard curve ranging between 0 and 40ng/ml with a sensitivity of 0.045 ng/ml. The northern bottlenose whale females were all assayed on the same plate, with the exception of a single female with very high concentrations that was assayed twice. Inter- and intra-assay CVs were all below these acceptable thresholds for both species and are given in the Supplementary Material. Again, standard parallelism, matrix effect and extraction efficiency checks were carried out to ensure that the ELISA kit was performing adequately and is compatible with cetacean progesterone in these tissue extracts (see Supplementary Material).

#### 3.1.2.2.3.4 Cortisol and Progesterone Concentration Calculations:

The extraction efficiency of the method, together with the effect of sample mass on the hormone concentrations were assessed by measuring the cortisol recovery from spiked samples (see Supplementary Material). These extraction efficiencies and sample mass corrections were then used to correct the measured cortisol and progesterone concentrations in each sample to give a final cortisol concentration used for statistical analysis (see Supplementary Material).

#### 3.1.2.2.4 Stranded Animal Samples

Harbour Porpoises: Two different modelling approaches were used to assess firstly, the effects of both sampling site and sampling depth on blubber cortisol concentration and, secondly, the effects of other explanatory covariates (age class, sex, COD and body condition). A summary of each set of subsamples used for the various models is given in Table 3-4.

*Body Location and Blubber Layer:* Generalised Linear Mixed Effect Models (GLMMs) were used to investigate cortisol concentrations both across body locations and through the blubber depth whilst accounting for the repeated measurements from the same individuals that are considered as random effects (Bolker et al., 2008). Two GLMMs (*glmer* function in the R package *lme4*) with a gamma distribution to better model the right skew in the cortisol concentration data, a log link function, and each individual treated as a random effect were used to investigate firstly, the effect of body location on cortisol concentration in full depth subsamples (n = 20 individuals with 3 samples each), and secondly, the effect of body location *and* blubber layer (n = 6 individuals consisting of 3 females and 3 males, 4 acute cases and 2 chronic cases with 12 samples each Table 3-4). An interaction between body condition (mass/length<sup>2</sup>) and location, as well as between body condition and layer were also included. The model with the lowest AICc value was used for further interpretation.

*Individual Covariate Analysis:* Generalised Linear Models (GLMs) were used to assess the effects of other variables on the cortisol concentrations measured in the outer layer of the dorsal samples as those that are representative of biopsies taken from live animals (n = 20, Table 3-4). GLMs were used to better model the right skew in hormone concentrations using a gamma distribution and a log link function. The largest GLM including all the explanatory variables (age class, sex, COD category as either acute or chronic, and body condition) was generated.

Balaenopterids: Again two different modelling approaches were used to assess firstly, the effect of sampling depth on blubber cortisol concentration and, secondly, the effects of other explanatory covariates (sex, COD, body condition and lipid content). A summary of each set of subsamples used for the various models is given in Table 3-4.

*Blubber Layer:* As with the harbour porpoise data, GLMMs were used to investigate cortisol concentrations through blubber depth whilst accounting for the repeated measurements from the same individuals. Firstly, a GLMM with a gamma distribution to better model the right skew in the concentration data, a log link function, and each individual treated as a random effect was used to investigate variation in cortisol concentration by blubber depth (n = 9 individuals with 3 samples each, (Table 3-4). An interaction between body condition (girth/length) and layer was also included to consider the possibility that animals in varying condition may show differences in their cortisol distribution though the blubber depth.

*Individual Covariate Analysis:* The cortisol concentrations in the outer blubber layer were modelled using a GLM including sex, body condition (girth/length), outer blubber lipid content (as cortisol concentrations were measured in this part of the tissue) and COD as other explanatory variables. For this second model, only the samples collected by the SMASS where COD and girth/length had been recorded were used, thus reducing the sample size down to just 7 animals (Table 3-4.). As previously described, the largest model was built first, and backwards model selection using the *dredge* function was used to identify the variables that best explain the variation in hormone concentrations, and thus to include in the final model based on the smallest AICc.

Table 3-4. Summary of each harbour porpoise and balaenopterid sample subset used for different models to assess cortisol variation by body location, blubber layer and other individual covariates. \*GLMM: Generalised Linear Mixed Effect Model. \*\*GLM: Generalised Linear Model.

Species Group	No. of Individuals	Body Location	Blubber Layer	Model
Harbour porpoises	20	Dorsal, Lateral, Ventral	Full	GLMM* of Body Location
	6	Dorsal, Lateral, Ventral	Full, Outer, Middle, Inner	GLMM of Body Location and Layer together
	20	Dorsal	Full, Outer	GLM** of Individual Covariates
Balaenopterids	9	Dorsal	Outer, Middle, Inner	GLMM of Blubber Layer
	7	Dorsal	Outer	GLM of Individual Covariates

### 3.1.2.2.5 Biopsies from Live Animals

**Progesterone:** Progesterone was extracted from and measured in 130 blubber biopsy samples from humpback whales. These were a mixture of samples from collected by the MICS between 2004 and 2009 ( $n = 72$ ) and the samples collected for the RC-2337 project ( $n = 58$ ). Of these samples, 6 were from confirmed pregnant females as these were well-known, photo-identified females sampled by the MICS that were seen the following year with a calf. Another 31 of these samples were extracted and assayed as controls as these were confirmed non-pregnant animals that were a mixture of males and immature females and calves. The range in measured progesterone concentrations is shown in Figure 3-2. Using these two datasets of progesterone values from individuals of known pregnancy status, an empirical cumulative distribution function (ECDF) modelling approach was taken to estimate empirical probabilities (proportion of observations) that a certain progesterone value is above or below those of the confirmed pregnant or non-pregnant animals.

An ECDF is a probability model for data. It is a non-parametric estimator of the underlying cumulative distribution function of a random variable, here blubber progesterone concentration. It assigns a probability of  $1/n$  (where  $n$  is the sample size) to each data point, orders the data from smallest to largest in value, and calculates the sum of the assigned probabilities up to and including each data point. The ECDF can then give the fraction of sample observations less than or equal to a particular value of  $x$ . Here, two ECDFs were modelled for the progesterone concentrations in the confirmed pregnant and non-pregnant animals, and a probability of being pregnant and non-pregnant was then assigned to all of the unknown animals using the *stat\_ecdf* function in the *ggplot2* package in R. If the probability of being pregnant was  $> 0.05$ , the individual was classified

as pregnant, and if the probability of being not-pregnant was  $> 0.05$ , the individual was classified as not pregnant. If any individuals were assigned an intermediate probability of either being pregnant or not pregnant, these animals would be classified as ‘undetermined’. For the SERDP RC-2337 sampled animals, all were assigned a clear pregnancy status.

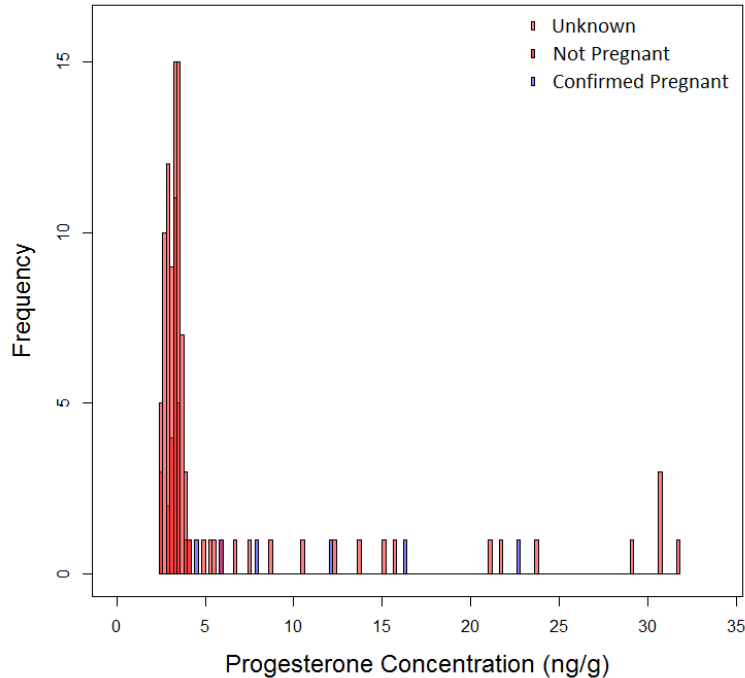


Figure 3-2. Histogram of blubber progesterone concentrations measured in 130 humpback whale biopsies collected by the MICS and the RC-2337 project. The concentrations measured in the confirmed pregnant females are shown in blue.

Cortisol: The cortisol concentrations measured in the humpback whale biopsies were modelled using a GLM with a gamma distribution to better model the right skew in the concentration data, and a log link function. Sex, area (Norway or Canada), reproductive status (mature male, resting female, pregnant, lactating, immature or unknown), Julian day (samples taken at the beginning of January were added on to the end of the year rather than starting again at Julian day 1), an interaction between Julian day and reproductive status and an interaction between Julian day and area were included in a global model in order to consider a potential changing relationship across the feeding season between the two study areas and reproductive classes. Backwards model selection showed that 4 models were of equal fit to the data as they all showed an AICc within two units of each other (Table 3-5). This subset of models was then used for model averaging using the *model.avg* function in the *MuMIn* package in R. Model averaging is used to average regression coefficients across multiple models in order to capture the overall effects of the different variables (Banner and Higgs, 2017). Model averaging is particularly useful when there is little to differentiate between a set of models, and avoids the justification of a single, final model. Interpretations of the averaged model coefficients were used to assess the effects of each covariate.

*Table 3-5. Results of GLM model selection cortisol concentrations measured in humpback whale biopsies showing the 4 best-fitting models with the lowest AICc values that are of equivalent fit to the data and were subsequently used for model averaging.*

Model	Covariates Retained	df	AICc	$\Delta$ AICc	weight
1	Cortisol ~ Area + Sex	4	651.3	0.00	0.265
2	Cortisol ~ Area + Sex + Day	5	651.6	0.31	0.226
3	Cortisol ~ Sex	3	651.8	0.48	0.208
4	Cortisol ~ Area + Sex + Day + Day*Area	6	653.2	1.90	0.102

### 3.1.3 Detailed methods, results and discussion

#### 3.1.3.1 Lipid results and discussion

##### **Blubber Lipids: Highlights**

- Blubber lipid content of remotely obtained, shallow biopsy samples provides little information about the body condition of these species sampled. The investigation of other blubber biomarkers should be prioritised.
- Compared to the delphinids and the balaenopterids, the ziphiids showed very little variation in blubber lipid content. Beaked whale blubber may play a fundamentally different role compared to other cetacean species that consistently mobilise and deposit blubber fat stores.
- One potential reason for this lack of variation could be that Ziphiid blubber is known to consist primarily of wax esters that are less easily metabolised, but are less dense than triacylglycerols. Deep diving species may benefit from stores of these low density wax esters to remain closer to neutral buoyancy at depth. These species likely have to prioritise maintaining consistent blubber hydrodynamic, thermal and buoyancy parameters which comes at the expense of having variable fat deposits for energy storage.

##### *3.1.3.1.1 Variation through blubber depth results*

Each species group showed a different pattern in the lipid content through blubber depth. The balaenopterids showed the most variation in blubber lipid content both within and between individuals (full dataset range from  $2.40 \pm 0.3\%$  to  $77.55 \pm 0.2\%$ ), followed by the white beaked dolphins (full dataset range from  $29.3 \pm 8.5\%$  to  $74.2 \pm 5.0\%$ ), while the ziphiids showed the least variation (full dataset range from  $51.30 \pm 0.4\%$  to  $84.06 \pm 1.1\%$ ). For the white beaked dolphins, the outer layer and the full depth samples both had a higher lipid content than the inner and middle layers ( $p$  values both 0.01) that were not significantly different to each other (Figure 3-3). For the ziphiids, there were no differences in lipid content between layers (Figure 3-3). Finally, there were significant differences between all layers in the balaenopterids (Figure 3-3). The outer layer had the highest lipid content and the inner layer had the lowest (Figure 3-3). The lipid content was significantly higher in the full depth samples compared to both the middle and the inner layers ( $p$  values  $< 0.005$ ).

There was no overall increase or decrease in the extraction variability, quantified as the measurement standard error between duplicate samples extracted in tandem, with increasing lipid content (linear model: Adjusted  $R^2 = 0.01$ ,  $p = 0.15$ ), confirming that this lipid extraction method is appropriate for the range of sample masses analyzed here. There were also no differences in the measurement error between the different blubber layers (ANOVA;  $df = 3$ ,  $F = 1.786$ ,  $p = 0.154$ ). There was significantly higher variation in the measurement standard error as well as a higher overall measurement standard error in the white beaked dolphin samples compared to both the balaenopterids and the ziphiids (ANOVA;  $df = 2$ ,  $F = 34.23$ ,  $p < 0.0001$ ). This could be because the full depth white beaked dolphin samples were thinner (mean blubber depth of  $17.4 \pm 1.28\text{mm}$ ) than the samples taken from the other two species groups that had a much thicker dorsal blubber

layer (means of  $53.25 \pm 7.56\text{mm}$  and  $37.0 \pm 5.57\text{mm}$  for the ziphiids and the balaenopterids respectively). As such, by subsampling a thicker blubber layer, the likelihood of subsampling a more homogenous part of the tissue is higher than when sampling from the thinner layer where the tissue properties may change within the piece that is sampled. As the species that are typically sampled through remote dart biopsy, including ziphiids and balaenopterids, are much larger than white beaked dolphins, the samples obtained will probably be more homogeneous than from smaller species, so differences between duplicate samples are less likely, and this extraction method is robust for such species.

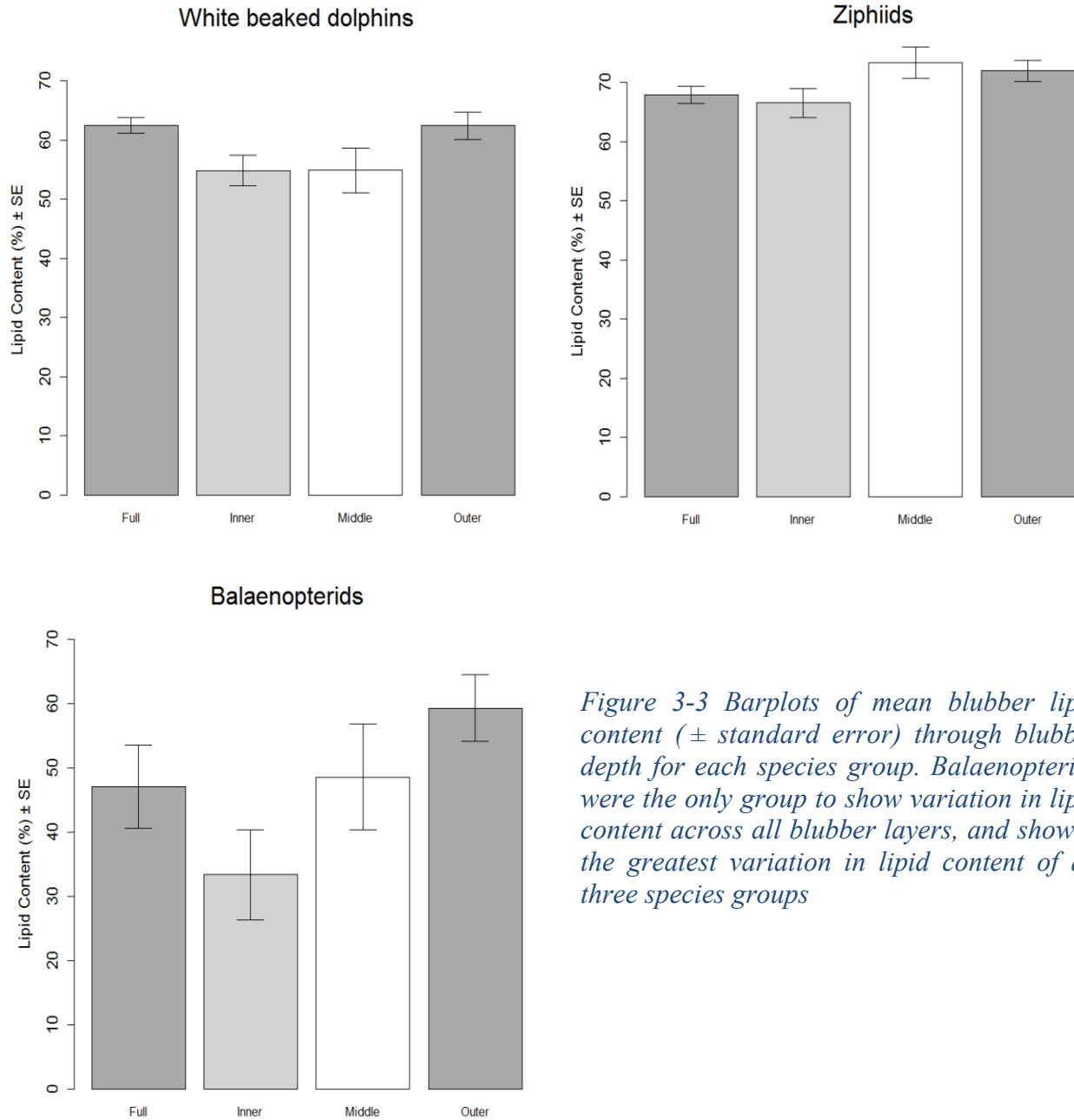


*Figure 3-3 Barplots of mean blubber lipid content ( $\pm$  standard error) through blubber depth for each species group. Balaenopterids were the only group to show variation in lipid content across all blubber layers, and showed the greatest variation in lipid content of all three species groups*

3.1.3.1.2 *Variation with other covariates results*

The lipid content in the full blubber depth samples was not correlated with blubber thickness for any of the three species groups. No covariates were retained following generalized linear model selection for the white beaked dolphins or the ziphiids, indicating that sex, age class, cause of death and body condition did not contribute to the explanation of the variability in the blubber lipid content of these full depth, dorsal samples (Table 3-6). The best fitting GLM for the balaenopterid data included only COD as an important explanatory variable with a significantly lower lipid content in the chronic cases compared to the acute cases ( $p = 0.004$ ) (GLM:  $df = 3$ , weight = 0.87,  $\Delta AICc$  of 4.18 to the next best fitting model) (Table 3-6). In fact, individuals that died as a result of an acute trauma had significantly higher blubber lipid content across all blubber layers than those with a chronic cause of death (ANOVA;  $F = 44.71$ ,  $df = 1$ ,  $p < 0.0001$ , Figure 3-4).

*Table 3-6. Summary table of the generalized linear model results investigating the effects of various covariates on blubber lipid content for the three species groups. \*VIFs: variance inflation factors measure collinearity between predictor variables. These predictor variables with high VIFs were excluded from the analysis.*

Species	Sample Size	Covariates Discarded Based on VIFs*	Covariates Retained following GLM model selection
Delphinids	10	Sex, Age Class	
Ziphiids	8	Sex, Age Class	
Balaenopterids	7	Girth / Length	COD

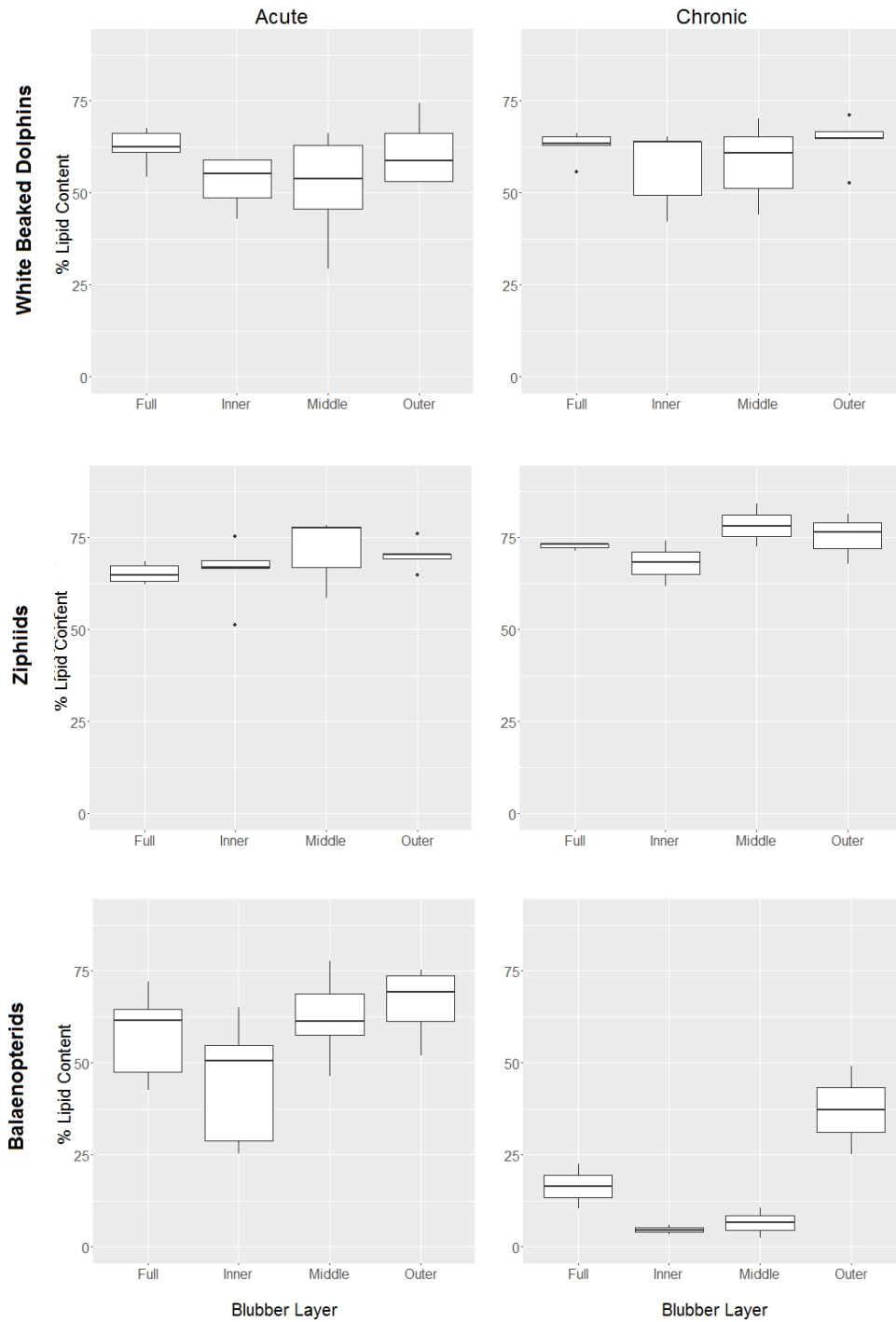


Figure 3-4. Boxplots of blubber lipid content across blubber layers between COD categories for the three cetacean families. The balaenopterids were the only group to show significant differences in blubber lipid content between acute and chronic cases. Blubber lipid content was significantly lower across all blubber layers in the chronic compared to the acute cases (ANOVA;  $F = 44.71$ ,  $df = 1$ ,  $p < 0.0001$ ).

The effect of body condition, either as mass/length<sup>2</sup> for the white beaked dolphins, or as girth/length for the ziphiids and the balaenopterids, was not retained as an important explanatory variable in the full blubber depth lipid content models for any of the three species groups. The relationship between the lipid content of each layer and body condition was then assessed separately. For the balaenopterids, there was a significant positive correlation between lipid content and girth/length in the middle blubber layer alone (linear model;  $p = 0.035$ , Adjusted  $R^2 = 0.4$ ), which was not seen in the other two groups (Figure 3-5). Variation in this layer therefore likely drives the differences in full blubber depth lipid content that are associated with different causes of death.

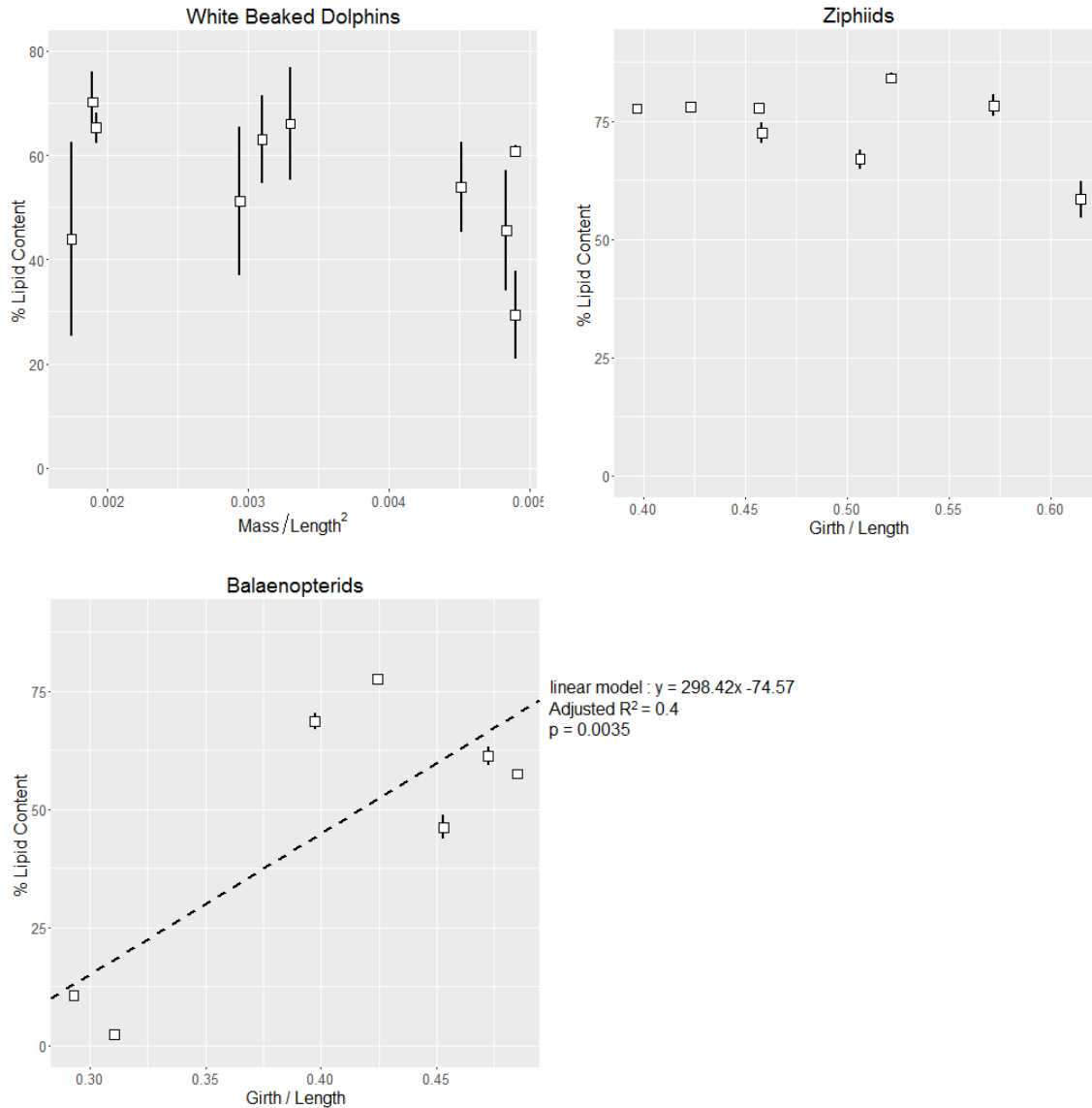


Figure 3-5. Lipid content in the middle blubber layer plotted against the morphometric body condition estimate for each species group. There was a significant correlation between the lipid content in the middle layer and body condition in the balaenopterids alone ( $p = 0.035$ , Adjusted  $R^2 = 0.4$ ).

The lack of correlation between lipid content and body condition in the white beaked dolphins and the ziphiids could have been a result of the small sample size of individuals. It is possible that only a small number of animals in either good or poor condition has been sampled here. To investigate this possibility, the range in individual condition estimates for each species group was assessed using morphometric data collected by the SMASS for these species between 1991 and 2015. These data were from 51 balaenopterids from 4 species (minke, humpback, fin (*Balaenoptera physalus*) and sei whales (*Balaenoptera borealis*)), 42 ziphiids from 4 species (Northern bottlenose whales, Sowerby's, Cuvier's and Blainville's beaked whales (*Mesoplodon densirostris*)) and 90 white beaked dolphins. The range in condition estimates varied between each group. There was a four-

fold difference between the white beaked dolphins in the thinnest and the fattest condition (mass/length<sup>2</sup> range between 0.0012 – 0.0049), and a huge ten-fold difference in the balaenopterids (girth/length range between 0.064 – 0.67). For the ziphiids however, there was less than a factor of two difference between the individuals in the thinnest and the fattest condition (girth/length range between 0.37 – 0.63), indicating a very narrow range in body condition in these species. The individuals sampled for lipid extraction covered a large part of these ranges for the white beaked dolphins and the ziphiids (Figure 3-6). Thus the absence of any correlations between blubber lipid content and condition is likely not a result of the sample size, or a bias in the sampled individuals. The balaenopterids sampled were from only a small range of the potential variation (Figure 3-6), yet there was still a positive correlation between girth/length and the lipid content in the middle layer, as well as differences in the animals with acute or chronic causes of death.

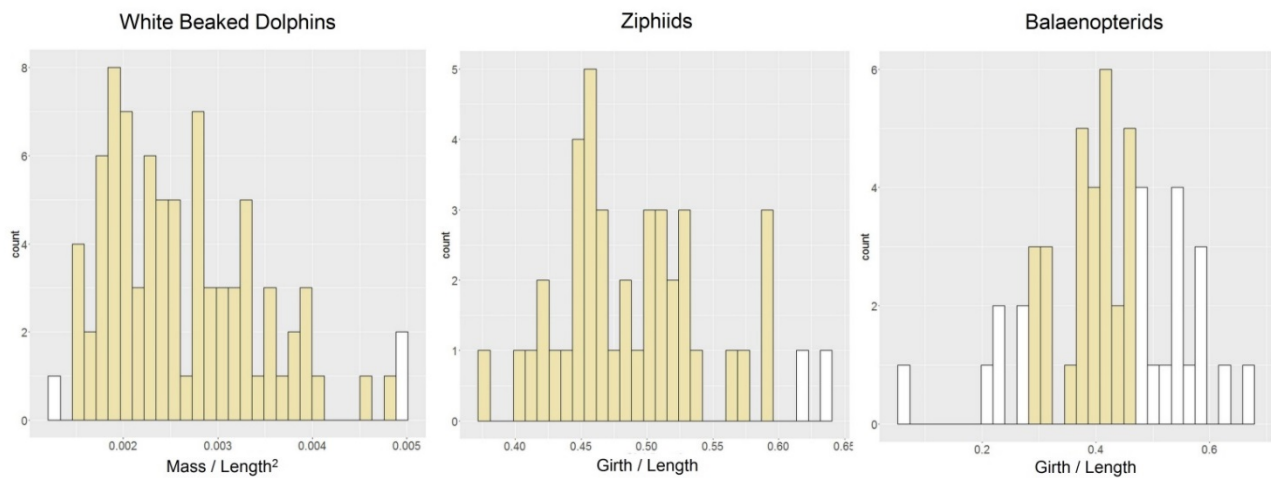


Figure 3-6. Body condition histograms for the three species groups using morphometric data collected by the SMASS. a) Mass/length<sup>2</sup> histogram for the white beaked dolphins (n = 90). b) Girth/length histogram for ziphiids (n = 42). c) Girth/length histogram for balaenopterids (n = 51). The shaded bars indicate the range in condition indices of the individuals sampled for blubber lipid extraction.

### 3.1.3.1.3 Lipid content as a biomarker discussion

#### 3.1.3.1.3.1 Lipid content stratification through blubber depth?

Stratification of lipid content through blubber depth was seen in both the white beaked dolphins and the balaenopterids. In both of these groups, the middle and inner layers had a lower lipid content than the outer layer closest to the skin, and the inner layer of the balaenopterids had the lowest lipid content overall. The stratification observed here is likely the result of differential metabolism of fatty acids, and thus deposition and mobilisation of lipid stores through the blubber depth (Lockyer et al., 1984; Samuel and Worthy, 2004; Smith and Worthy, 2006). Long-chain polyunsaturated fatty acids of dietary origin are present in higher concentrations in the inner layer compared to the outer layer, and these are preferentially metabolised due to their proximity to the body core (Koopman et al., 1996; Krahn et al., 2004; Lockyer et al., 1984). This makes the inner and middle layers more metabolically active in terms of lipolysis and lipogenesis compared to the outermost layer which is made up primarily of short chain monosaturated fatty acids and has a

more structural, and possibly thermoregulatory role with a more stable composition over time as it is more metabolically inert (Olsen and Grahl-Nielsen, 2003; Ruchonnet et al., 2006; Samuel and Worthy, 2004). Koopman and colleagues (2002) found that the outermost layer of the blubber in starved harbour porpoises (*Phocoena phocoena*) was virtually indistinguishable from normal animals, but throughout the rest of the blubber, the adipocytes shrank and ‘disappeared’ during starvation.

Here, only the lipid content of the middle layer of the balaenopterids was significantly correlated with condition. This is consistent with previous reports that the middle layer of fin and sei whale blubber consisted of loose, fatty tissue, and was the most variable in thickness compared to the other two layers (Lockyer et al., 1985). The lowest lipid content seen in the inner layers of both the delphinids and the balaenopterids is consistent with the findings in other species whereby the inner layer contained proportionally more fibrous tissue than the other two layers. (Ackman et al., 1975a; Krahn et al., 2004; Lockyer et al., 1984). Thus, had shallow biopsy samples been taken from these animals, they would provide inflated estimates of blubber lipid content as the outermost layer did not reflect the lipid available for mobilisation in the middle layers. In addition, a number of studies have now shown that the lipid content measured in a biopsy sample is not reflective of that of the tissue when sampled at necropsy (Krahn et al., 2004; McKinney et al., 2014; Ryan et al., 2012). The discrepancies are thought to be a result of lipid loss during dart retrieval as the adipocytes burst upon dart impact.

In contrast to the other two families, the ziphiids showed no variation in lipid content through depth. The blubber of ziphiids has been shown to display stratification of fatty acids and wax esters through blubber depth, but the overall lipid content appears to be uniform (Koopman, 2007; Litchfield et al., 1976; Singleton et al., 2017). Ziphiid blubber therefore does not show the same stratified characteristics as seen in other cetacean species in terms of layers of lipid deposition and mobilisation. This suggests that the tissue is not being used in the same way for the same energy storage functions as other cetacean species. Blubber lipids in ziphiids have been shown to be dominated by wax esters (Koopman, 2007; Litchfield et al., 1976; Singleton et al., 2017), and this different composition of the tissue likely affects the patterns of lipid deposition and mobilisation, as well as tissue function, which will be discussed in detail below.

#### 3.1.3.1.3.2 Lipid content variation as an indicator of condition?

The huge variation in lipid content both within and between the balaenopterid samples compared to the other two species groups is likely a result of the life-history strategies of these species whereby they cycle their energy stores during seasonal migrations that link temporally and spatially separated breeding and feeding seasons (Koopman, 2007). As they are adapted to cycle their fat stores, the range in blubber lipid content is likely to vary much more than for species that do not undertake prolonged fasting periods, and thus live within much narrower limits of stored energy reserves. This was highlighted in the larger dataset of morphometric measures from the SMASS with the 10 fold difference between the girth / length index of individuals in the thinnest and fattest condition. Cause of death was retained following model selection, showing that individuals that died as a result of acute trauma had a higher lipid content across the full blubber depth compared to chronically debilitated animals. This is to be expected as chronically debilitated animals have depleted their fat reserves following a more gradual decline in health and perhaps reduced foraging opportunities compared to individuals that died as a result of an acute trauma event. These results from dorsal blubber samples are consistent with previous work on fin and sei

whales where the dorsal posterior area of the body has been shown to be a major site for lipid storage in both the blubber and the muscle, so it was suggested that this area may be useful as an indicator of overall body fat condition (Lockyer et al., 1985). While the full blubber depth samples could be used to differentiate between gross differences as a result of different cause of death categories, only the lipid content measured in the middle layer was an appropriate metric to detect more subtle differences in condition between the balaenopterid individuals. Neither sex nor age class were retained as important explanatory variables which was surprising given previous evidence of variation in fat stores across sex and reproductive classes in balaenopterids (Aguilar and Borrell, 1990; Lockyer et al., 1985). These data were dominated by juvenile minke whales, and for this reason little can be inferred about the effect of age class on blubber lipid content. Similarly, as the animals had likely not reached sexual maturity, the lack of differences between the sexes could be indicative that sex differences only appear once animals start to deposit and mobilise fat stores associated with the costs of reproduction.

Model selection for the delphinid and the ziphiid data retained no covariates as important explanatory variables. When plotted individually, there were no significant correlations between the lipid content in any blubber layer and body condition. One explanation for the lack of variation here could be a consequence of the dorsal site of the blubber sample. Dorsal blubber samples were taken immediately caudal to the dorsal fin in all species in order to investigate the potential use of lipid content as measured in remotely obtained biopsy samples which target this area. However, in small odontocetes, the blubber in the thoracic-abdominal region is hypothesized to play an important role in insulation and energy storage, whereas the region posterior to the dorsal fin is thought to primarily act to maintain hydrodynamic and locomotory functions and is metabolically inert (Gomez-Campos et al., 2015; Koopman, 1998; Koopman et al., 2002; Tornero et al., 2004). Specifically, harbour porpoises and common dolphins (*Delphinus delphis*) showed the highest blubber lipid content in the anterior-ventral region (Koopman et al., 2002; Tornero et al., 2004), and the patterns of lipid distribution in starved harbour porpoises showed that they are mobilized from their ventral girth region but not from other areas of the body (Koopman, 1998). It was hypothesized that altering the structure of the posterior blubber by mobilizing lipids could have serious effects on the locomotory efficiency of the animal as this region of the blubber acts to reduce the costs of locomotion by acting as a biological spring (Koopman et al., 2002). This pattern of lipid deposition and mobilization may extend to other odontocete species as well, such as the white beaked dolphins and the ziphiids sampled here, which could explain why lipid content in this dorsal sampling site did not correlate with the condition or cause of death of the individuals. Thus, there are apparent differences in the function of the blubber as an energy store across the bodies of the larger cetaceans, the balaenopterids, and the smaller odontocetes studied to date. These differences are likely due to a combination of the different hydrodynamic body shapes and maneuverability of the species, as well as their life histories and reproductive strategies that determine their reliance on endogenous energy stores. Some areas of the body are therefore more important for energy storage than others, and this variation is not necessarily captured in the dorsal sampling site of biopsy samples for some species.

#### *Implications of the dominance of wax esters in ziphiids?*

The apparent absence of variation in lipid content both within and between the ziphiids sampled here could be a result of the different lipid-type composition of the tissue. Ziphiid blubber is made up of between 80% and 100% and wax esters (Hooker et al., 2001; Koopman, 2007; Litchfield et al., 1976), and their relative contribution to the tissue changes with different age and reproductive

classes (Singleton et al., 2017). It is possible that beaked whale blubber lipid storage properties differ from other species because wax esters have different chemical properties to the triacylglycerols that are more rapidly metabolized and more efficiently hydrolysed (Place, 1992; Pond, 1998). As most mammals are incapable of metabolizing wax esters and thus eliminate them in their feces (Hansen and Mead, 1965), the proportion of the lipid stored in the blubber that is available for mobilization to provide energy during times of reduced foraging may therefore be much smaller in beaked whales than species of a similar size that preferentially store triacylglycerols. The dominance of wax esters, a less easily metabolized lipid-class, in the blubber of these species is a further indication that the tissue is not being used as an energy store in the same way as other cetacean species.

Recent studies on the composition of fresh undigested forestomach and colon contents of minke whale and right whale (*Eubalaena glacialis*) feces suggested that they may have evolved an unusual metabolic capability, such as specialized enzymes or a particular gut symbiont, which, unlike other mammals, enables them to utilize most of the wax esters in their diet (Nordøy, 1995; Swaim et al., 2009). Baleen whales that rely on a wax ester-rich diet from their copepod prey thus seem to have overcome the digestive limitations of most terrestrial mammals. Interestingly, however, the ingestion of wax esters does not necessarily mean that these compounds will be stored in their adipose tissue. Even though baleenopterids consume large quantities of wax esters, and are apparently able to metabolize them, their blubber is composed almost entirely of triacylglycerols. Given the importance of these lipids in beaked whale blubber, it is likely that these species have also evolved this metabolic capability. For example, as beaked whales and sperm whales (*Physeter macrocephalus*) approach adult size, the blubber is increasingly made up of wax esters (Koopman, 2007; Singleton et al., 2017), suggesting that wax ester storage is minimal at birth, and they then develop the ability to synthesize and deposit it. The mechanisms by which they are able to utilize the wax ester components of their fat storage remain unclear however, as are the roles of wax esters as an energy store for cetaceans in general.

The differences in the basic structure and common constituents of wax esters and triacylglycerols give them distinct physical properties. Specifically, wax esters have lower densities (specific gravities) than triacylglycerols, such that a unit volume of wax esters will provide more positive buoyancy than the same unit volume of triacylglycerols in sea water (Sargent, 1978). Wax esters are the dominant lipid storage class of calanoid copepods (Sargent et al., 1977), deep water and vertically migrating fishes (Nevenzel, 1970) as well as beaked whales, *Kogia* species and sperm whales (Koopman, 2007; Litchfield et al., 1975). It has therefore been suggested that lipids are preferentially stored as wax esters in many marine organisms as they provide greater buoyancy (Sargent, 1978). This may be especially the case for beaked whale species that are particularly deep divers (Tyack et al., 2006a), and may use the positive buoyancy provided by wax esters to maintain an overall body status close to neutral buoyancy as gas stores compress with depth (Miller et al., 2004a; Miller et al., 2016c). Neutral buoyancy is thought to minimize locomotion costs both for vertical transits (Adachi et al., 2014; Miller et al., 2012b) and for horizontal swimming (Sato et al., 2013).

Wax esters in the blubber have also been suggested to play a potentially important role in thermoregulation (Bagge et al., 2012; Singleton et al., 2017). The blubber of deep diving species with a higher wax ester content, but with the same overall lipid content as shallower divers, has been shown to be a superior insulating material (Bagge et al., 2012). Deep divers can experience

large variations in ambient temperatures during the course of a single dive, and it has been suggested that this increased insulative capacity of the blubber may facilitate deeper, longer dives in these species (Bagge et al., 2012). It was concluded that the function of blubber as an insulator is highly complex and is likely affected by a number of factors including lipid class, stratified composition and dynamic heat storage capabilities as well as currently unmeasured characteristics such as vascularization, collagen content or water content (Bagge et al., 2012).

Finally, blubber with a high wax ester content has a significantly higher nitrogen solubility than blubber composed of triacylglycerols (Koopman and Westgate, 2012; Lonati et al., 2015). Having blubber stores with higher nitrogen solubility could result in greater storage of nitrogen while submerged, and lead to an increased release of nitrogen upon surfacing, thus putting these species at a greater risk of decompression sickness. However, models of decompression sickness risk suggest that risks are highest during repetitive, shallow dives and when animals are in water shallower than the depth of alveolar collapse (Ridgway and Howard, 1979; Zimmer and Tyack, 2007). So, in theory, it is possible that as deeper divers spend comparatively little time performing repetitive shallow dives, they are able to store wax esters and hence have high nitrogen solubility in their blubber (the physiological functions of which remain to be established) (Koopman and Westgate, 2012). Shallower divers cannot, as this puts them more at risk of decompression sickness, and this difference could have contributed to the evolution of different lipid storage classes between deep and shallow divers (Koopman and Westgate, 2012). However, it is thought that deviations from the normal diving patterns of beaked whales interrupts gas dynamics and cause decompression-related injuries (Tyack et al., 2006; Zimmer and Tyack, 2007). These beaked whale results highlighting the lack of variation in lipid content add to a body of work aiming to understand the potential physiological functions of, and the selective pressures leading to the presence of wax esters in the blubber of odontocetes.

Currently, there is no evidence to suggest that any of the beaked whale species experience substantial or predictable fasting cycles, or periods of food shortage when lipid reserves might be drawn upon (MacLeod, 2018). Species that rely on blubber lipids during fasting may be constrained to storing only triacylglycerols, as this lipid source can be reliably and rapidly mobilized. By extension, perhaps as beaked whales do not experience prolonged fasting periods, they are preferentially able to store blubber lipids that provide some element of physiological or mechanical advantage during diving instead of energy storage. For these reasons, the role of beaked whale blubber in diving physiology may determine the extent to which it can change in lipid composition as the structural and mechanical properties of the tissue are prioritized at the expense of available energy stores. The very narrow range in the girth / length condition estimates using the larger morphometric dataset from the SMASS further supports the possibility that these species survive within very narrow physiological limits.

#### *Much more than just an energy store*

Here, there was no relationship between blubber thickness and blubber lipid content for any of the individuals sampled, regardless of species group. Results of this study therefore support the idea that blubber thickness alone is an inadequate index of fat stores as the lipid content of the tissue varies independently of its thickness (Ackman et al., 1975a; Aguilar et al., 2007; Dunkin et al., 2005; Evans et al., 2003). There are two possible reasons for this lack of a relationship: either the small sample size of this dataset prevented the detection of any correlations between lipid content and blubber thickness, or, the other functional roles of the blubber not involved in energy storage

also affect blubber thickness. This is a small sample size of only 27 individuals, and it is possible that the lack of correlation between lipid content and blubber thickness here could be because there was not a great enough range in blubber thicknesses or lipid content within each species group. However, as the individuals sampled, with the exception of the balaenopterids, covered the range of potential morphometric body condition estimates from the larger SMASS dataset, this is likely not the case.

Various other studies have also shown similar results where blubber thickness was determined to be a poor index of nutritive condition as it was not correlated with changes in overall body fat reserves (Aguilar et al., 2007; Caon et al., 2007; Evans et al., 2003; Gomez-Campos et al., 2015; Koopman, 2007; Read, 1990; Ruchonnet et al., 2006). This is because the extent to which blubber lipids can be mobilised is limited by thermoregulatory and hydrodynamic considerations, and is not simply a function of its energy reserves. It is well recognised that in addition to its role as a depot of energy, cetacean blubber also serves important functions as an insulator, it is involved in active thermoregulation, it streamlines the body, facilitates hydrodynamic locomotion, contributes to water balance, and provides buoyancy (Iverson, 2009). For this reason, attempts should be made to move away from using blubber thickness as an indicator of condition, and alternative methods should be investigated across all species, not just beaked whales. There are likely very complex relationships between body size, thermal habitat, lipid stratification, blubber thickness, and metabolism that warrant further investigation. With the results of this comparative study, together with previous studies we hypothesise that ziphiids cannot tolerate large variations in blubber thickness or blubber lipid content. Variations would affect their thermal regulation, their hydrodynamic shape required for capture of fast-swimming prey, and importantly, their neutral buoyancy which enables them to forage efficiently at depth. As such, the maintenance of structural and hydrodynamic properties of the blubber are prioritised over its use as an energy storage organ (Figure 3-7). Thus, if the ecology and hence physiology of a species requires stability to be maintained in one blubber function, this will therefore influence the variability possible in others.

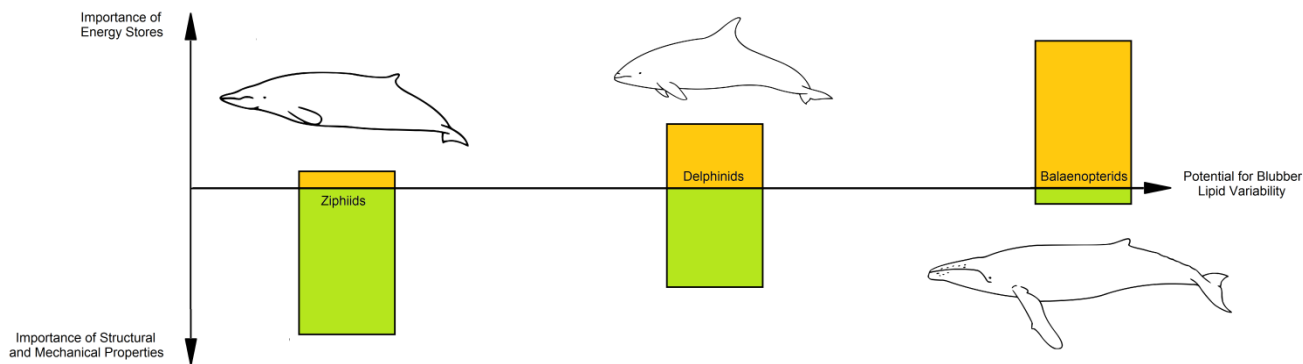


Figure 3-6. Theoretical schematic demonstrating the relative importance of different blubber functions across three cetacean families with respect to the extent to which the tissue can vary in total lipid content. It is hypothesised that ziphiids prioritise the preservation of a constant blubber structure and lipid content to maintain the hydrodynamic, insulative and buoyant properties of the tissue. Balaenopterids however, show huge amounts of variability in blubber lipid content both within and between individuals, likely because they rely on blubber lipid stores during prolonged fasting periods of their life-cycles.

### 3.1.3.2 Conclusions

Cetaceans have evolved very specialized adipose tissues to meet the challenges of their aquatic environment. Varying habitats and life history strategies have shaped different typical blubber functions and composition such that the blubber may serve a fundamentally different purpose across different species. Here, the lipid content of the middle layer in the balaenopterids was correlated with body condition, in-keeping with previous work suggesting that this layer is the most important in terms of lipid deposition and mobilisation. However, it still remains unclear for most cetacean species whether changes in lipid content and blubber thickness in this part of the tissue occur as a result of adipocyte hyperplasia or hypertrophy, or a combination of both. The lipid content measured in the outer part of the tissue for these species, available through remote dart biopsy, thus gives little information on an individual's condition, as it provides no information on the layers that are involved in lipid deposition and mobilisation.

There was a lack of stratification of total lipid through the blubber depth of the ziphiid samples, as well as a lack of variability between individuals. The lack of variability here together with the known high wax ester content of the blubber suggests that its other roles in diving physiology for example, may be of greater importance than its role as an energy depot. The blubber in these species may therefore not be optimized as an energy store as it is in many other cetacean species. The relationship between blubber lipid content and overall energy stores is not straightforward in these animals of different body sizes, life history strategies, foraging ecologies and physiological capabilities. Using the proportions of different saturated / unsaturated fatty acids or the proportion of triacylglycerols to wax esters, for example, might be a more reliable indicator of condition. Thus, because of the inherent variability in the structure and composition of blubber, among families, species, individuals, and even within individuals, extreme caution should be used when making inferences and generalizations based on the lipid content of only a small portion of this extremely complex tissue. Further work should prioritise measuring other components of blubber biopsies as potential markers of condition.

### 3.1.4 Adipocyte size as a biomarker discussion

#### **Adipocyte size: Highlights**

- Adipocyte size (count or area) from blubber biopsy samples may be a useful additional independent measure of body condition in large cetaceans. However, a larger sample size, both from dead stranded animals and live biopsy samples with independent estimates of nutritional condition, is needed to further validate the initial findings reported here.
- The ability of adipocyte metrics to predict condition (girth/length) was investigated. The best model given the data included adipocyte area and count but not sex and age (accounting for cetacean group).

#### 3.1.4.1 Adipocyte size (area)

This initial exploratory analysis of adipocyte size shows some promise as predictors of body condition (see Supplementary Material and also (Castrillon et al., 2017). Here, a significant relationship was observed between adipocyte area, morphometric condition (girth/length) and dorsal blubber thickness, accounting for age and sex differences, consistent across four cetacean groups. Adults were found to have larger adipocytes than juveniles and this finding is in accordance with previous research that found adipocyte size increased with age in bottlenose dolphins (Struntz et al., 2004). A good model fit with significant prediction power included just the two main size metrics accounting for cetacean group. Discriminating between animals in different nutritional states by combining adipocyte size with the other blubber biomarkers being developed in this study (such as cortisol and the protein biomarkers) will assist in our ability to assess the processes that are occurring at the cellular level, and indeed whether animals are undergoing lipolysis (are utilizing fat stores for energy) or lipogenesis (are storing excess fat) at the time of sampling. Indeed Castrillon et al., (2017) also concluded in a study investigating adiposity measures (including adipocyte area) from blubber biopsies in humpback whales, that a wider set of biomarkers is necessary to accurately determine energetic health.

### 3.1.5 Progesterone results and discussion

#### Blubber Progesterone: Highlights

- Blubber progesterone concentrations were used to distinguish between pregnant and non-pregnant females.
- One female sampled in Norway was simultaneously both pregnant and lactating. This has been recorded in an increasing humpback population in the South Atlantic, likely in response to favourable environmental conditions.

#### 3.1.5.1 Progesterone Concentrations Across Reproductive States

Progesterone concentrations measured across the different reproductive states of females are shown in Figure 3-8. Interestingly, one female sampled in Norway was both lactating and also pregnant which was been reported in Southern Ocean humpbacks sampled on the feeding grounds in the Antarctic (Pallin et al., 2018). For the whales sampled in Canada, ~ 24% were pregnant (5/21) while a slightly larger proportion were pregnant in Norway with ~35% (9/26). Finally, there was no relationship between progesterone concentration and Julian Day in the pregnant females, suggesting that there is not an increase in blubber progesterone as gestation progresses across the feeding season (linear model: Adjusted  $R^2 = 0.08$ ,  $p = 0.91$ ). Interestingly, for the northern bottlenose whales, only one of the females had elevated concentrations of progesterone indicating pregnancy. All the other samples were collected from non-pregnant females (Figure 3-9).

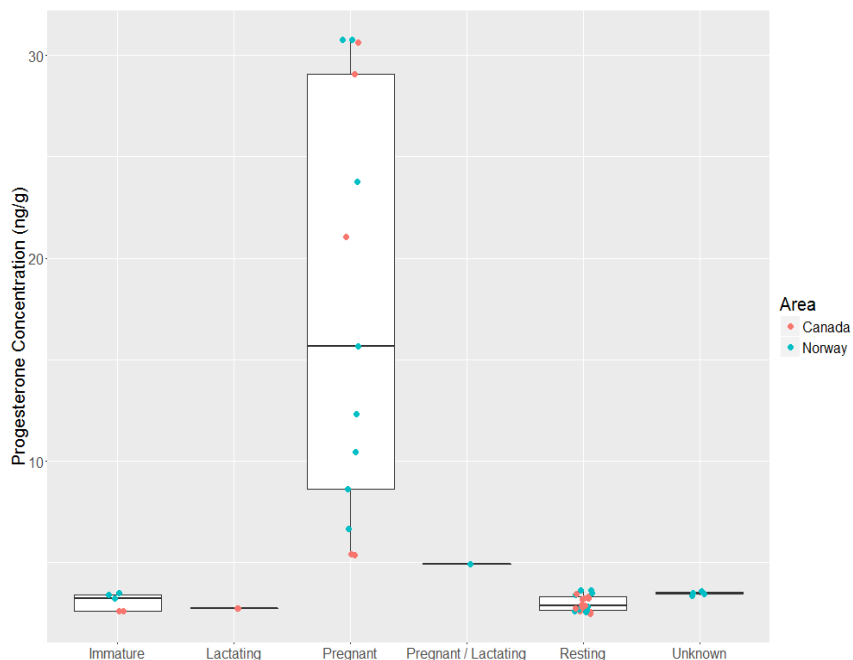
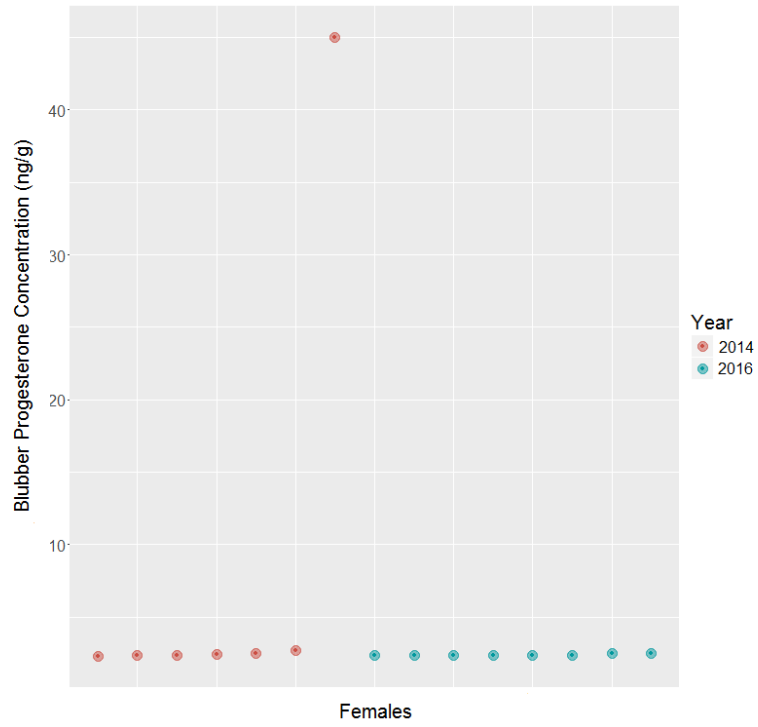


Figure 3-7. Blubber progesterone concentrations across different reproductive states of the 47 female humpback whales sampled for the SERDP RC-2337 project. The unknown females are those where age class was not recorded.



*Figure 3-9. Blubber progesterone concentrations in 15 Northern Bottlenose Whales*

### 3.1.6 Cortisol results and discussion

#### **Blubber Cortisol: Highlights**

- Cortisol is the main glucocorticoid hormone involved in the regulation of lipolysis and overall energy balance in mammals.
- There was significant vertical stratification of cortisol concentrations through the blubber depth in harbour porpoises, but not in the balaenopterids. In both species groups, concentrations in the dorsal, outermost layer were representative of concentrations through the full blubber depth.
- Cortisol concentrations in the outer blubber layer in both species groups were negatively correlated with body condition. Higher blubber cortisol concentrations measured in animals in poorer condition that are likely metabolising fat stores, rather than depositing them, therefore appear to be consistent in both non-fast adapted and fast-adapted species.
- Cortisol concentrations in the dorsal, outermost blubber layer could potentially be used as a biomarker of condition in free-ranging cetaceans.
- Biopsy samples were collected from free-ranging humpback whales in Norway and Canada (n=82). Sex-specific differences were identified, with males showing significantly higher concentrations than females. Overall, whales sampled in Canada showed higher concentrations than those sampled in Norway, and there was an overall increase in concentrations across the feeding season in Norway alone although these trends were not statistically significant.
- The variability in the cortisol concentrations suggests different physiological states in terms of animals either going through lipolysis or lipolysis. Depending on how long the animals have been on the feeding ground, and how successful their foraging has been, their state will likely change.

#### 3.1.6.1 Method Development Using Stranded Animal Samples Results and Discussion

##### *3.1.6.1.1 Harbour Porpoise Results*

Body Location and Blubber Layer: Blubber cortisol concentrations ranged between 3.65 - 759.51ng/g. The final GLMMs following variable selection did not retain either body location or the interaction with body location and body condition as significant explanatory variables. Mean concentrations of  $69.09 \pm 31.30\text{ng/g}$ ,  $90.48 \pm 52.22\text{ng/g}$  and  $83.22 \pm 59.95\text{ng/g}$  were measured in the full depth dorsal, lateral and ventral samples respectively. Thus, there are no significant differences in blubber cortisol concentrations across these three different sampling locations (Figure 3-10). When blubber layer was considered together with body location and condition, the final GLMM following variable selection retained only blubber layer as an important explanatory variable. This suggests that the pattern of cortisol distribution through blubber depth does not

change with sampling site, or animal condition. The highest concentrations were measured in the inner and middle layers (means of  $180.02 \pm 177.06\text{ng/g}$  and  $156.28 \pm 167.02\text{ng/g}$  respectively) ( $p$  values  $< 0.01$  Figure 3-10), and there was no significant difference between the concentrations in the full depth samples compared to the outer layer alone (means of  $88.65 \pm 68.38\text{ng/g}$  and  $77.84 \pm 48.32\text{ng/g}$  respectively) (Figure 3-10).

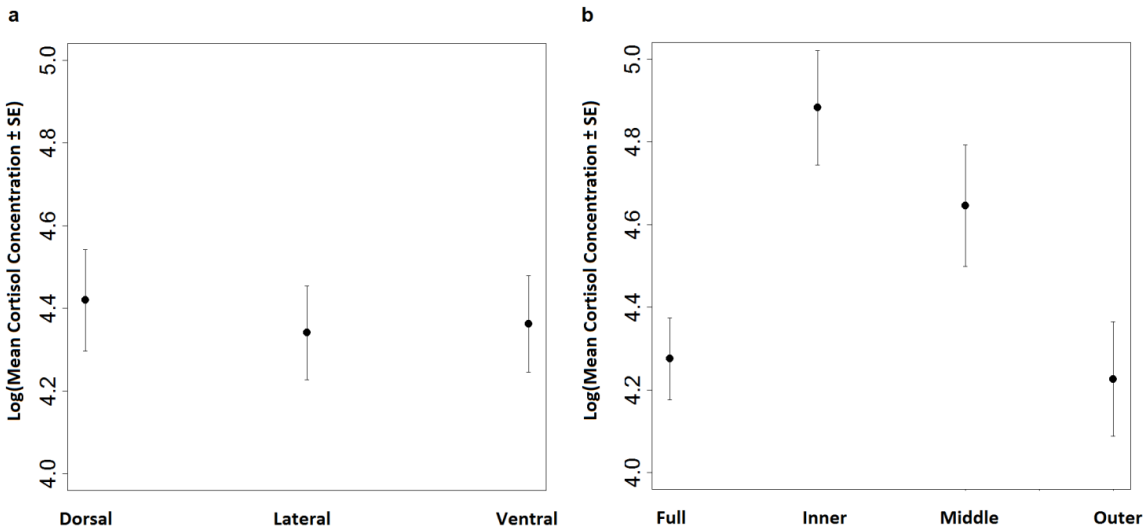


Figure 3-10. Final GLMM outputs for cortisol concentrations across the body and through the blubber layer for the harbour porpoises. a) GLMM output for blubber cortisol concentrations around the girth. There were no significant differences in cortisol concentration in full depth blubber samples from three different sampling locations. b) GLMM output following variable selection for blubber cortisol concentrations with both location and blubber depth. The inner and middle layers had significantly higher cortisol concentrations than the full depth and outer layers ( $p$  values  $< 0.01$ ), while the outer layer was not significantly different to the full depth sample overall.

Individual Covariates: Variable selection for the GLM of cortisol concentration in the dorsal, outer layer samples revealed that there were less than two points difference in the AICc between the two best fitting models, indicating that they were of equivalent fit to the data (Table 3-7). These models retained both age class and sex, and body condition and sex as important explanatory variables (Table 3-7). Juveniles had higher cortisol concentrations than adults ( $p = 0.05$ ), and there was a weakly significant negative relationship between mass/length<sup>2</sup> and cortisol concentration ( $p = 0.1$ ). Overall, females had significantly higher cortisol concentrations than males with means of  $111.37 \pm 59.86\text{ng/g}$  compared to  $66.77 \pm 29.73\text{ng/g}$  ( $p = 0.02$ ) (Figure 3-11). This could be as a result of the cross-reactivity of the ELISA kit with progesterone ( $< 9\%$ ). However, one adult female that died as a result of dystocia (classed here as an acute case) did not have an elevated blubber cortisol concentration ( $53.90\text{ng/g}$ ) as would be expected if there were high levels of blubber progesterone associated with pregnancy (Trego *et al.* 2013). Nonetheless, to investigate the potential confounding effect of this cross-reactivity, the male and female data were modelled separately with the same covariates and model selection process. For the male dataset, again, the final model selection showed that there was less than a two point difference in the AICc between the two best

fitting models including both age class and mass/length<sup>2</sup> although neither was individually significant. For the female dataset, variable selection excluded all covariates, and these results are likely a result of the small sample size used for analysis when the data are split by sex. COD was not retained in the final model likely because it is tightly linked to the condition of the individuals as the acute cases were generally in better condition, and showed a smaller range in mass/length<sup>2</sup> than the chronic cases with mean mass/length<sup>2</sup> values of  $0.0022 \pm 0.0035$  and  $0.0018 \pm 0.00050$  for each group respectively. The body condition of the animals therefore explained more of the variation in the data than the COD.

*Table 3-7. Results of GLM model selection for outer layer blubber cortisol concentrations for harbour porpoises (n=20) and balaenopterids (n = 7) showing the 3 best-fitting models with the lowest AICc values. Harbour porpoise models 1 and 2 are of equivalent fit to the data.*

Species	Model	Covariates Retained	df	AICc	ΔAICc	weight
Harbour Porpoises	1	Cortisol ~ Sex + Age Class	4	209.4	0.0	0.29
	2	Cortisol ~ Sex + Mass/Length <sup>2</sup>	4	210.9	1.5	0.14
	3	Cortisol ~Age class	3	211.9	2.5	0.08
Balaenopterids	1	Cortisol ~ Girth/Length + Sex	4	190.4	0.0	0.36
	2	Cortisol ~ Girth/Length + Sex + Lipid	5	192.6	2.2	0.12
	3	Cortisol ~ Girth/Length + Sex + COD	5	193.9	3.5	0.06

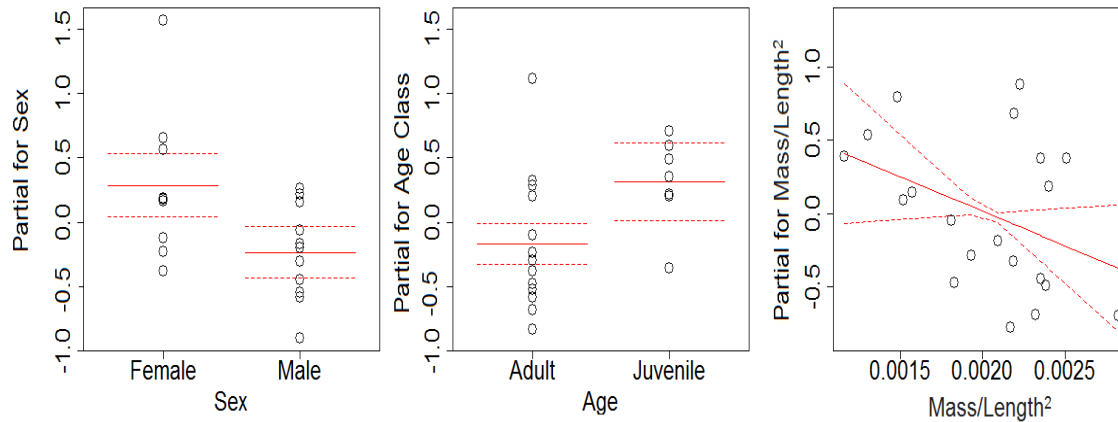
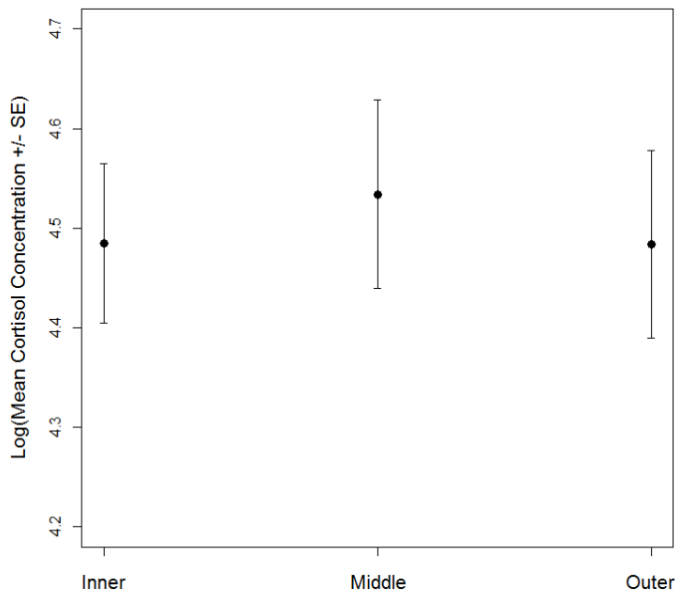


Figure 3-11. Partial termplots for the covariates retained in the final two best fitting GLMs following variable selection for the harbour porpoise data:  $\text{glm}(\text{Outer.Cort} \sim \text{Sex} + \text{Age.Class}, \text{family}=\text{Gamma}(\text{link}=\text{"log"}))$  and  $\text{glm}(\text{Outer.Cort} \sim \text{Sex} + \text{Mass/Length}^2, \text{family}=\text{Gamma}(\text{link}=\text{"log"}))$  ( $n=20$ ). Termplots plot regression terms against their predictors with the associated standard errors, while holding other predictors at their mean values. Significantly higher cortisol concentrations were measured in females than males ( $p = 0.02$ ), and in juveniles than adults ( $p=0.05$ ). There was a weakly significant negative relationship between mass/length<sup>2</sup> and blubber cortisol concentration ( $p = 0.1$ ).

### 3.1.6.1.2 Balaenopterid Results

Blubber Layer: Cortisol concentrations showed less variation in the balaenopterids than in the harbour porpoises with a range of between 53.89 – 154.95 ng/g. Model selection for the GLMM which investigated variation in cortisol concentration through blubber depth showed that there were no significant differences in cortisol concentration between the inner, middle and outer layers (means of  $93.7 \pm 10.0\text{ng/g}$ ,  $98.3 \pm 5.3\text{ng/g}$  and  $89.5 \pm 9.9\text{ng/g}$ , respectively, Figure 3-12). The interaction between body condition and blubber layer was not retained in the final model either.



*Figure 3-12. Final GLMM output for cortisol concentrations through the blubber depth for the balaenopterids. Model selection did not retain layer as an important explanatory variable as there were no significant differences in cortisol concentration between the inner, middle and outer layers.*

Individual Covariates: Variable selection for the GLM which investigated other factors contributing to the variation in measured cortisol concentrations in the outermost layer of the balaenopterid samples retained girth/length and sex as important explanatory variables (Table 3-7). There was a strong negative correlation with girth/length ( $p < 0.001$ ), such that individuals in poor condition had higher blubber cortisol concentrations than those in better condition (Figure 3-13). As with the harbour porpoises, females had a higher blubber cortisol concentration than males ( $p = 0.002$ ) with mean concentrations in their outer layer of  $91.4 \pm 8.86\text{ng/g}$  and  $87.9 \pm 15.88\text{ng/g}$  respectively, although the highest concentration was measured in a male. There was no difference in cortisol concentrations between animals with acute or chronic CODs. Finally, lipid content was not retained following model selection either. In fact, cortisol concentrations were not correlated with lipid content across any of the samples collected from all 9 individuals.

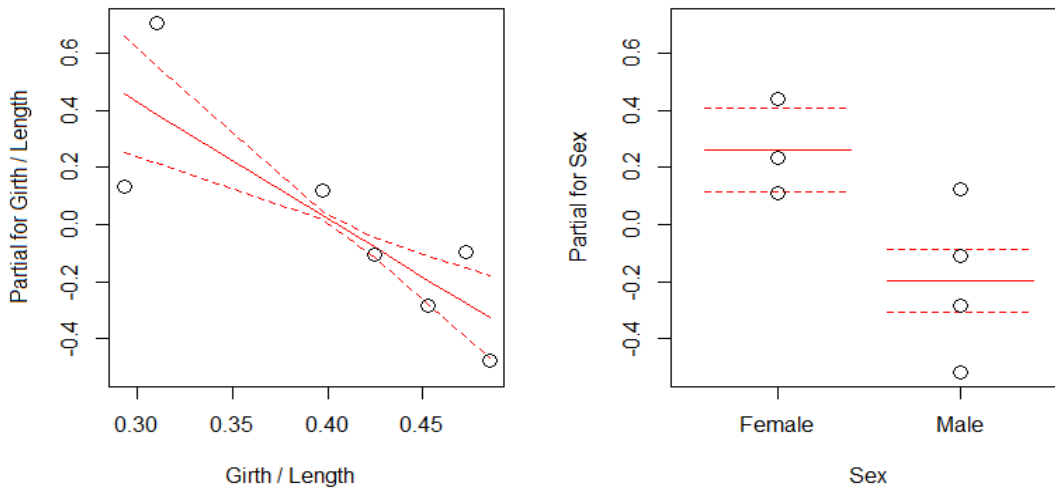


Figure 3-13. Partial termplots for the covariates retained in the final best fitting GLM following variable selection for the balaenopterid data:  $glm(Outer.Cort \sim Girth/Length + Sex, family=Gamma(link="log"))$  ( $n=7$ ). There was a significant negative relationship between girth/length and blubber cortisol concentration ( $p < 0.001$ ), and significantly higher cortisol concentrations were measured in females than males ( $p = 0.002$ ).

### 3.1.6.2 Blubber Cortisol as a Biomarker Discussion

#### 3.1.6.2.1 Blubber cortisol concentrations across sampling sites and through blubber depth

Here, no significant variation in blubber cortisol concentrations were seen across the three different sampling locations on harbour porpoises. Dorsal sampling through the collection of remote biopsies could therefore provide information on typical blubber cortisol concentrations across this area of the body. These results are consistent with the notion that while harbour porpoises and other small odontocetes may selectively mobilise lipids unevenly across different areas (Koopman et al., 2002; Tornero et al., 2004), blubber composition remains relatively consistent across the body (Koopman et al., 2002).

Evidence of stratification in cortisol concentration was seen through the blubber depth in harbour porpoises with highest concentrations measured in the middle and inner layers. Overall, the highest concentrations were measured in the inner layer which was also found in belugas (Trana et al., 2015). This is perhaps because the inner layers are more highly vascularised in shallow diving odontocetes compared to the superficial blubber layers closer to the skin (McClelland et al., 2012). This stratification in cortisol concentration is unsurprising given that cetacean blubber is stratified into three layers that can be differentiated visually, histologically and biochemically in many cetacean species (Olsen and Grahl-Nielsen, 2003; Smith and Worthy, 2006). In harbour porpoises specifically, the inner and middle blubber layers are more dynamic, and are likely used for lipid deposition and mobilization at a much faster rate than the outermost layer next to the skin (Koopman et al., 1996). Given the differences in the rate of turnover of the tissue, the cortisol concentrations measured in the full depth blubber samples represent the integration of the hormone through the tissue over a longer time period than either the middle or inner layers alone. There

were no significant differences in the concentrations measured in full depth blubber samples compared to the outer layer. Thus, these superficial samples could be representative of the longer term presence of cortisol in the blubber that is not subject to strong fluctuations as a result of short term changes in the blood flow through the tissue to the skin during thermoregulation (Barbieri et al., 2010; Noren et al., 2009). Cortisol concentrations in the outer blubber layer available through remote dart biopsy could thus be used as a potential indicator of longer-term physiological changes.

The cortisol concentrations measured in the balaenopterid samples were both lower, on average, and showed less variation than those measured in the harbour porpoises. Concentrations in the outer layer are representative of concentrations measured through the full blubber depth as there was no variation in cortisol concentrations through the blubber in these balaenopterid samples. This was surprising given previous findings of stratification of this hormone through the blubber depth in belugas (Trana et al., 2015), and the variation in concentrations measured in harbour porpoises here. It is also surprising given the documented differences in tissue structure, lipid content and fatty acid signatures of the different blubber layers in balaenopterids (Ackman et al., 1975a; Lockyer et al., 1984, 1985) which demonstrate the different potential functions of the layers in terms of nutrient transport, lipid storage and mobilisation, and structural support. It seems logical therefore, that hormone concentrations would also show similar variation.

Currently, the only published data on steroid hormone concentrations in balaenopterid blubber are progesterone concentrations measured in minke whales and bowhead whales (*Balaena mysticetus*) (Kellar et al., 2013; Mansour et al., 2002). There was no stratification in progesterone concentrations through blubber depth in minke whales (Mansour et al., 2002), and concentrations through the blubber depth were indicative of pregnancy status. In the second study, stratification through blubber depth was not investigated in the bowhead whale samples, but concentrations measured in the superficial blubber tissue next to the epidermis were able to distinguish between pregnant and non-pregnant females (Kellar et al., 2013). The lack of stratification in cortisol concentrations seen here could be comparable to the lack of stratification recorded for progesterone in these species.

#### 3.1.6.2.2 *Cortisol concentrations as a potential marker of condition*

Covariate analyses revealed that, even with a small sample size of just 20 individuals for the harbour porpoises, and 7 individuals for the balaenopterids, as well as high levels of individual variation, cortisol concentrations in dorsal, outer layer samples were negatively correlated with body condition, and females showed higher concentrations than males. In terrestrial mammals (Castellini and Rea, 1992), humans (Bergendahl et al., 1996) and pinnipeds (Champagne et al., 2012; Champagne et al., 2006; Guinet et al., 2004) extended periods of food restriction are associated with an increase in the circulating concentrations of cortisol. During these periods of reduced food intake or fasting, cortisol increases lipolysis to provide energy (Bergendahl et al., 1996), and is involved in the maintenance of circulating glucose concentrations through increased gluconeogenesis (Exton et al., 1972). It is likely that the same principles apply to cetaceans. Interestingly, the COD category was not retained as an important explanatory variable following model selection for either species group, demonstrating that the body condition of individuals explained more variation than the way in which an animal died. The small sample size here of just 7 balaenopterid individuals with accompanying morphometric data and cause of death information was confounded by both species (dominated here by minke whales) and age class (all individuals

were juveniles), and for these reasons, it was not possible to assess age-class variation or potential species-specific differences in blubber cortisol concentrations. Further investigations should prioritize a larger sample size of individuals to confirm these results.

#### *3.1.6.2.3 Next Steps: Turnover Time Scales?*

The greatest challenge for proper interpretation of cortisol concentrations in this ‘new’ matrix, is how to quantify the time frame captured by this single hormone measurement. The time frame over which steroid hormones, like cortisol, and their metabolites are distributed around the body in the blood and are then excreted in the feces, or sequestered in the blubber for example, will vary greatly. As such, there is little known about how they may be stored and mobilized in the blubber, and at what rates. Currently, there is still conflicting evidence as to the time scales over which circulating steroid hormones are thought to be reflected in the blubber. For example, no significant relationship was seen between serum and blubber progesterone concentrations in non-pregnant harvested bowhead whales (Kellar et al., 2013). It was therefore suggested that progesterone concentrations are mirrored in these two sample types over longer periods (e.g. over weeks to months, the time frame of reproductive changes) but not shorter periods (e.g. over hours to days, the time frame of daily fluctuations). In addition, in wild caught harbour seals, blubber cortisol concentrations were shown not to be significantly affected by capture time, and thus were likely not driven by a stress response to the capture event, but were indicative of longer term physiological changes (Kershaw and Hall, 2016). In bottlenose dolphins however, blubber cortisol was found to qualitatively reflect circulating cortisol concentrations after oral administration of hydrocortisone (Champagne et al., 2017). As a result, there remains some disagreement of the interpretation of cortisol concentrations in this tissue as an indicator of a shorter term stress response, or a longer term indicator of overall physiological state, uncoupled from short term fluctuations in the circulating concentrations of the hormone.

While the turnover of cortisol in the blubber of marine mammals remains unknown, steroids are known to diffuse passively from the blood into human adipose tissue (Deslypere et al., 1985), but the turnover of these hormones in adipose tissue is slow (Hughes et al., 2010). Here, there was no relationship between blubber lipid content and cortisol concentration in the balaenopterid samples, suggesting that the presence of cortisol in the tissue is not just a function of the lipophilic nature of the hormone. Blubber cortisol concentrations thus probably provide information on both the stress response of an individual, and a physiological response to energetic requirements, but these are most likely over longer term time scales than those apparent in circulation. As the blubber of shallow diving cetaceans has been shown to be more highly vascularised than the adipose tissue typical of terrestrial species (McClelland et al., 2012), a greater perfusion of the tissue could result in the high concentrations of cortisol measured in both species groups here, but it is still unknown to what extent steroid hormones are in dynamic equilibrium between the blubber and the circulatory system. As such, further work is urgently needed to establish the relationships between hormone levels in different tissues and excreta, how these concentrations relate to each other, and what this means in terms of the physiology of the animal, the stimulation of the HPA axis and the overall impact on the individual.

#### *3.1.6.2.4 Next Steps: Localised Cortisol Production?*

Adipose tissue in mammals is known to be a major site for the metabolism of glucocorticoids and other steroids as it has been shown to express a range of enzymes involved in the activation, interconversion and inactivation of both the steroid sex hormones, and the glucocorticoids

(Bélanger et al., 2002; Meseguer et al., 2002; Seckl and Walker, 2001; Stulnig and Waldhäusl, 2004). The metabolism of glucocorticoids in adipose tissue is thought to be mediated primarily by one enzyme, 11 $\beta$ -hydroxysteroid dehydrogenase type 1 (11  $\beta$ -HSD1), which catalyses the conversion of hormonally inactive precursors (cortisone and dehydrocorticosterone) to their hormonally active metabolites (cortisol and corticosterone) (Seckl and Walker, 2001; Stimson et al., 2009; Stulnig and Waldhäusl, 2004). Therefore, in terrestrial mammals, as well as its release following the activation of the HPA axis, cortisol is also produced within the adipose tissue and the liver from its inert precursor, cortisone. However, while 11  $\beta$ -HSD1 amplifies local concentrations of glucocorticoids in the adipose tissue, it does not contribute significantly to systemic glucocorticoid concentrations, as has been shown with transgenic mice (Masuzaki et al., 2001). Specifically, overexpression of 11  $\beta$ -HSD1 in the adipocytes of transgenic mice results in normal serum concentrations of glucocorticoids and normal HPA axis function, but highly elevated levels of glucocorticoids locally in adipose tissue (Masuzaki et al., 2001).

*In vitro* studies have recently shown that bottlenose dolphin blubber microsomes exhibit the ability to metabolize cortisol to cortisone, and potentially the reverse reaction as well, cortisone to cortisol, presumably through the activity of 11 $\beta$ HSD (Galligan et al., 2018). As such, the blubber may act as an important site for both the metabolism and production of sex steroids and glucocorticoids, and it is possible that blubber could act as an independent endocrine organ, and is not merely a storage tissue reflective of the past or present circulating concentrations of glucocorticoid hormones. While it is unknown how much of the cortisol pool in cetacean blubber may be derived from local production, the cortisol concentrations measured in the blubber here may therefore reflect a combination of both circulating concentrations of this hormone through passive diffusion from the blood, and the local production of the hormone in the tissue itself. For these reasons, care should therefore be taken when interpreting glucocorticoid hormone levels in blubber biopsies and associating them with a response to chronic stress.

Blubber cortisol concentrations should therefore be interpreted with the multi-functional roles of cortisol in the regulation of the distribution of fat deposits, adipogenesis and adipose metabolic and endocrine function in mind (Lee et al., 2014), rather than as a passive hormonal store with no metabolic effect on the tissue itself. Given the mass of adipose tissue as blubber in marine mammals, it is possible that the relative contribution of the blubber to an individual's steroid hormone metabolism is quite significant, and the endocrinological functions of blubber in terms of glucocorticoid metabolism should thus be further investigated. Efforts to extract and quantify cortisol's inactive precursor, cortisone, from the tissue, and investigate the equilibrium between the two should be prioritised. The enzyme activity of 11  $\beta$ -HSD1 during periods of fasting and feeding in these species would help us to understand the how much of the cortisol within the blubber tissue originates from the adipocytes themselves during energetically demanding periods.

### 3.1.6.3 Conclusions

While very little is known about how cortisol may be produced, stored and mobilized in marine mammal blubber, and at what rates, the evidence of involvement in the regulation of physiological state and its presence in adipose tissue, make it a good candidate biomarker of condition worth investigation in cetaceans. Determining the dynamics of blubber cortisol throughout the life cycle of these species would be a key step towards understanding the endocrine control of energy regulation in marine mammals. Of key importance now is a better understanding of species specific concentrations in order to establish a baseline library of endocrine information from which we can

compare in future studies. If these results showing a negative correlation between blubber cortisol concentrations and body condition persist across other cetacean species, the analysis of cortisol concentrations in remotely obtained blubber biopsies, the metabolic site of action of this hormone, has the potential to be a valuable tool for studying physiology and body condition particularly in free-ranging cetaceans. More generally, given the importance of cortisol in the regulation of lipolysis, concentrations in the adipose tissue of other mammalian species for which morphometric measurements cannot be obtained could also be of use as an informative condition marker.

### 3.1.6.4 Biopsies from Live Animals Results and Discussion

#### 3.1.6.4.1 Cortisol Concentrations and Disturbance Time

There is evidence that blubber cortisol concentrations in bottlenose dolphins (*Tursiops truncatus*) are correlated with circulating concentrations after oral administration of hydrocortisone to simulate an artificial stress response (Champagne et al., 2017). As such, it was suggested that blubber samples from remote sampling may be useful to detect stress loads in this species at the time of sampling (Champagne et al., 2017). If this is the case in larger cetaceans as well, the interactions of whales with the research vessels that follow and approach them for tagging and biopsy sampling could result in a stress response that is then measured in the blubber. This potential stress response would be similar to that seen when animal handling cannot be avoided for the collection of physiological samples. Increases in circulating cortisol concentrations are characteristic of a stress response to such handling and physical restraint procedures in pinnipeds (Champagne et al., 2012; Engelhard et al., 2002; Harcourt et al., 2010) and in small cetaceans (Schwacke et al., 2014). It is therefore very important to appreciate the magnitude and duration of this potential stress response to the tagging and sampling events as it may compromise the specific aims of the study by masking any underlying variation in hormone concentrations.

In order to investigate this possibility in remotely obtained biopsy samples for humpback whales, the total ‘disturbance time’ was recorded for whales tagged and biopsied in the 2016 and 2017 field seasons in Canada (n = 27). The disturbance time was taken as the time from which tagging approaches were started on either a group of animals or an individual, to when the biopsy sample was taken (Figure 3-14). This time ranged from between just 16 minutes (an individual that was approached only for biopsy sampling as it had been tagged on a previous day), to 4 hours and 48 minutes (an individual that was tagged, followed for drone footage and then biopsied on the same day). This time therefore encompasses the entire duration of the potential stressor event from initial approach by the research vessel to sampling, and is taken as a proxy for the magnitude of the potential stress response. If this stress response is captured in the blubber cortisol concentration measurement, we would expect a correlation between disturbance time and cortisol concentration, but this was not the case in these animals (Figure 3-15). We are confident that blubber cortisol in this species, over this time period, doesn’t appear to reflect circulating concentrations and we are therefore not measuring an acute stress response to our approaches on the animals by measuring blubber cortisol. Instead we are measuring a longer-term integration of the hormone into the tissue that is more representative of overall physiological state rather than an acute stress response.

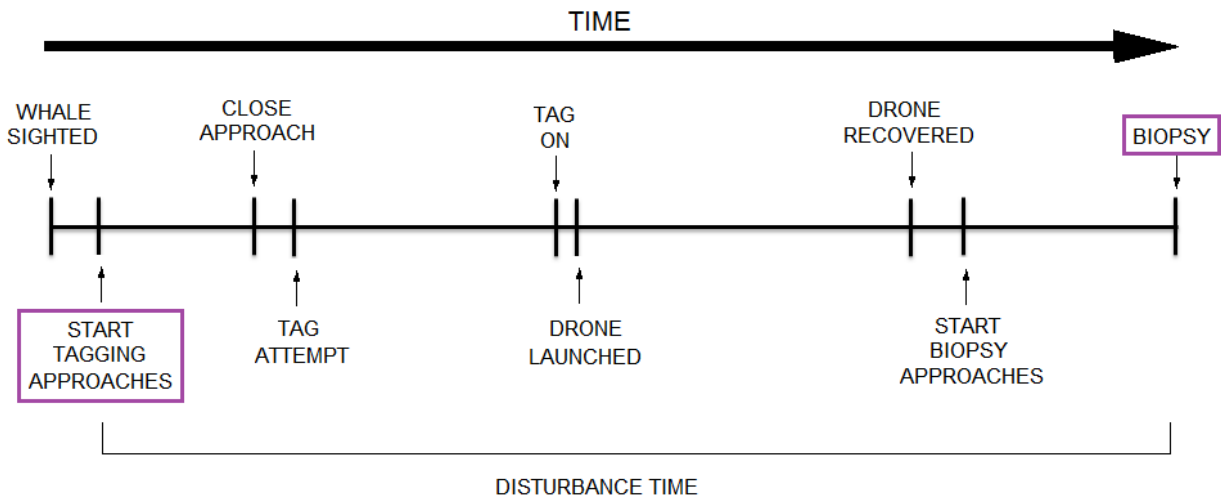


Figure 3-9. Typical time line for the total ‘disturbance time’ spent interacting with humpback whales during fieldwork with the MICS. This varied by individual however depending on the weather conditions (suitable / unsuitable for flying the drone) or their behaviour making them easier / harder to approach which shortened or lengthened the total disturbance time.

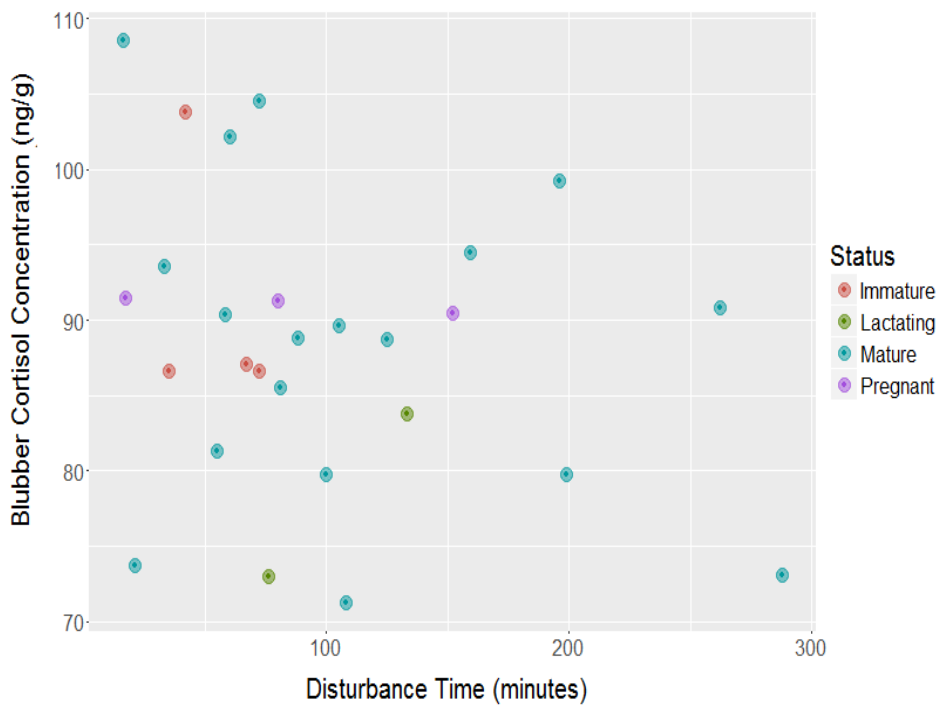


Figure 3-8. Blubber cortisol concentrations are not correlated with disturbance time in humpback whales. The disturbance time was recorded for 27 whales tagged and sampled in Quebec, Canada, in 2016 and 2017.

#### 3.1.6.4.2 *Variation in Cortisol Concentrations in Humpback Whales*

There was considerable variation seen in cortisol concentrations across both field sites. Reproductive state (mature male, resting female, pregnant, lactating, immature and unknown status) was retained following initial variable selection, but it was seen that the animals of ‘unknown’ reproductive status from Norway were largely driving this relationship. When these 13 animals were removed from the analysis, reproductive state was no longer retained as an important explanatory variable. The variability in the cortisol concentrations could therefore not be explained by differences between the reproductive states of the animals sampled here.

Results from the model averaging of the four best-fitting GLMs showed that unlike for the much smaller SMASS dataset of balaenopterids, males had significantly higher blubber cortisol concentrations than females ( $p = 0.02$ ) (Figure 3-16). Overall, while area was retained as an important explanatory variable, it was not individually significant but showed higher blubber cortisol concentrations in the whales sampled in Canada compared to in Norway. Finally, Julian day, as well as an interaction between Julian day and area were retained in the final models, but again, were not individually significant. Model averaging results showed that there was an overall increase in blubber cortisol concentrations with Julian day in Norway, but no change in Canada (Figure 3-16). It appears that there are different patterns in the data with considerably more variability in the cortisol concentrations measured in the individuals in Norway.

The individuals were sampled over a longer feeding season between June and January compared to the individuals sampled in Canada between just June and September (Figure 3-16). The feeding season appears to be much longer in Norway as some whales continue to feed on schooling herring

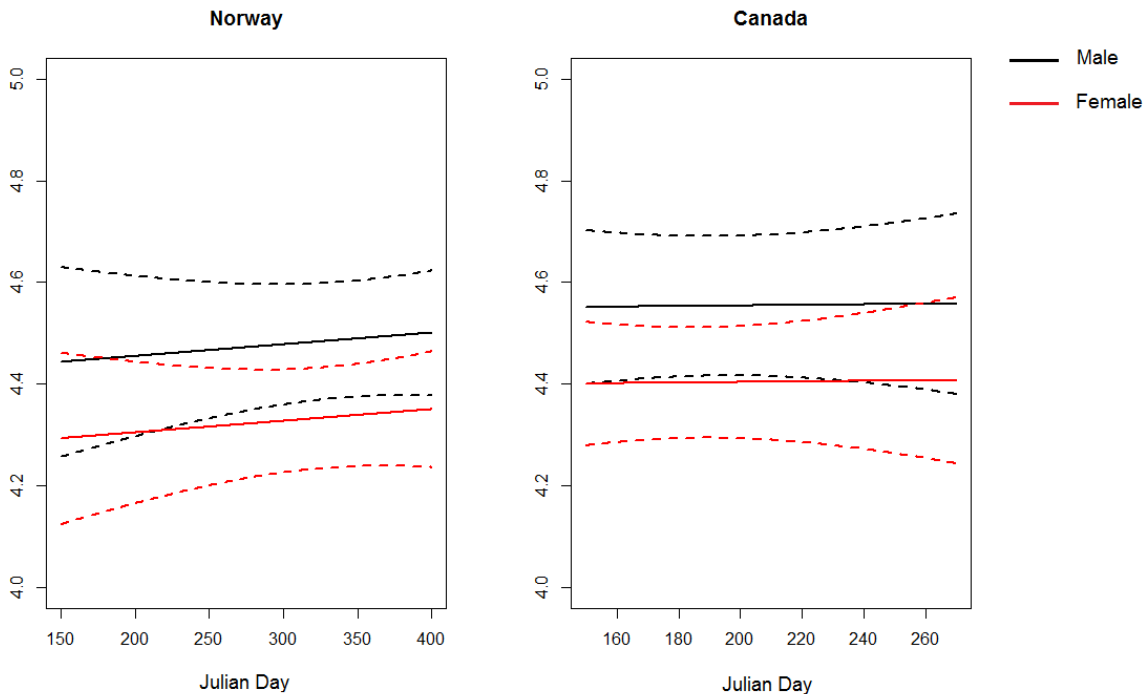


*Figure 3-10. Predicted relationships between blubber cortisol concentration and Julian day across both study sites from the GLM model averaging results. Overall, slightly higher concentrations were measured in Canada compared to Norway, and while there was an increase in concentrations across the feeding season in Norway, this was not seen in the Canadian samples. Males had significantly higher concentrations than females at both study sites ( $p = 0.02$ ).*

that move into the northerly most fjords between November and February. The difference in the apparent change in cortisol concentrations across the feeding season in both areas could be the result of different timings and durations of the migrations of these two populations in the North Atlantic as they move between the feeding grounds in the northern latitudes, to the breeding grounds close to the equator. It could also be the result of different durations of the feeding season in each area. For example, the individuals sampled between November - January in Norway could be 'left behind' late in the feeding season if these animals will not migrate if they haven't accumulated enough fat reserves. The variability in the cortisol concentrations suggests different physiological states in terms of animals either going through lipolysis or lipolysis. Depending on how long the animals have been on the feeding ground, and how successful their foraging has been, their state will likely change.

### 3.1.6.4.3 Cortisol Concentrations in Northern Bottlenose Whales

Cortisol concentrations in the blubber biopsy samples from the Northern bottlenose whales showed no variation with either age, sex (although males had lower concentrations than females, this difference was not statistically significant) or by year (Figure 3-17, a-c). This likely indicates that the animals were all in similar energetic states when they were sampled.

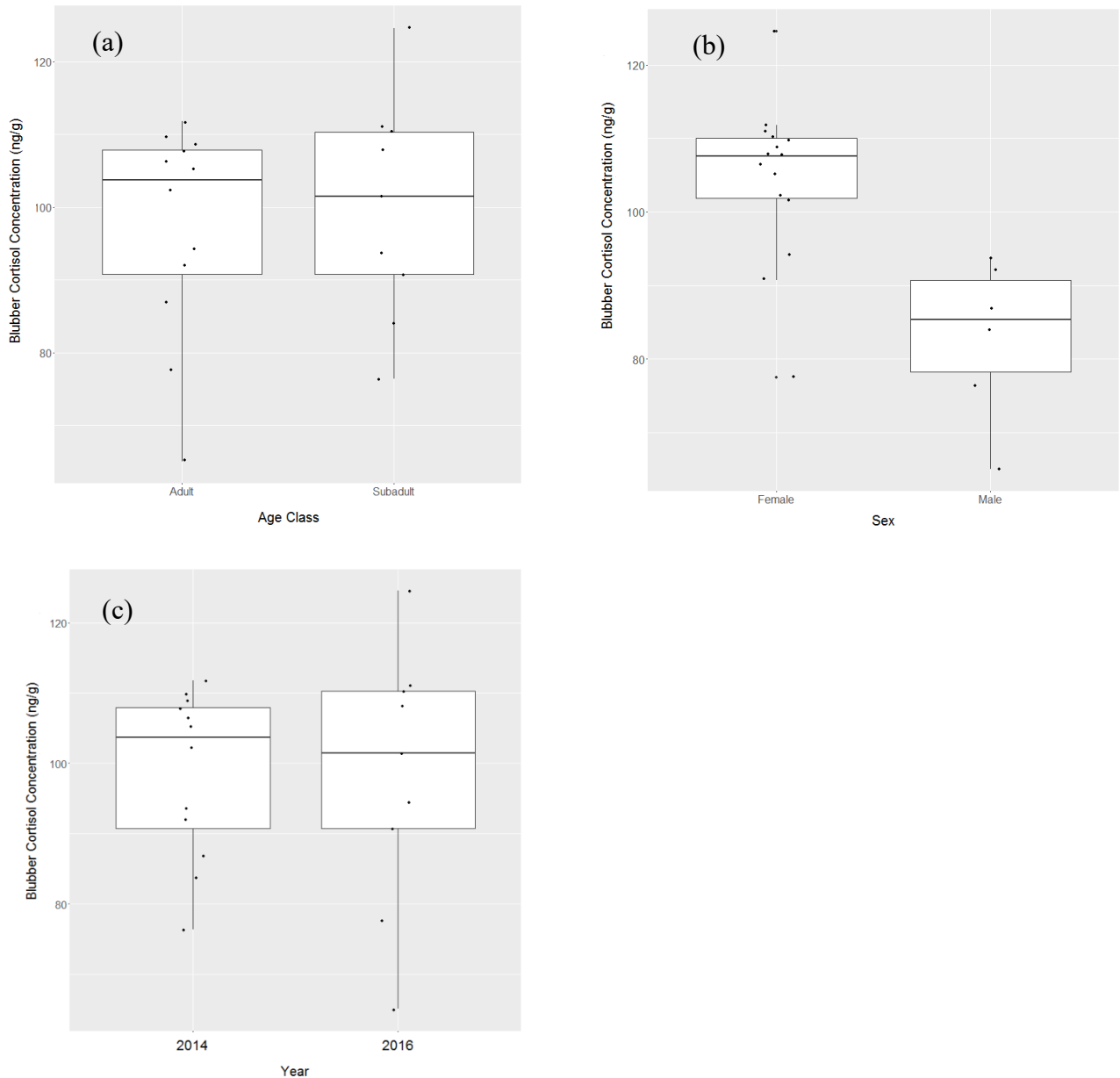


Figure 3-17. Cortisol (a-c) concentrations in the blubber of Northern bottlenose whales by age, sex and year.

### 3.1.7 Proteomics result and discussion

#### **Blubber Proteins: Highlights**

- A range of blubber proteins were identified across two cetacean species (n=409), and classed into ten functional groups, the most abundant of which were involved in cell function and metabolism, immune response and inflammation and lipid metabolism.
- These proteins likely originate both from the various cell types within the blubber tissue itself, and from the circulation. They therefore have the potential to capture information on the cellular and physiological stresses experienced by individuals at the time of sampling.
- Despite the range of proteins identified here, separation and visualisation of different protein bands using 1D SDS-PAGE was not at a fine enough resolution to be able to identify patterns of specific protein bands that correlated with the condition of individuals or different reproductive states.
- A finer scale approach, using 2D SDS-PAGE, for example, could lead to the development of a suite of biomarkers to better monitor the physiological state and health of live individuals though remote blubber biopsy sampling.

#### 3.1.7.1 Potential for Biomarker Development

While there were over 400 different proteins identified in the extracts from the two species, overall, the relative abundance of the proteins across the functional groups were very similar. Moving forward, the identification and quantification of different hormones and proteins involved in various metabolic pathways within blubber tissue could lead to the development of potential new protein markers of interest that can be quantified to provide information on a range of physiological processes and life history states. Explaining and quantifying the natural variability in these protein markers in the context of different life histories or causes of death, for example, is the next step in developing this approach.

Such indicator proteins may be produced directly by the blubber itself, secreted either by the adipocytes, the stromovascular cells, or a combination of both, or may have accumulated in the tissue from the circulation in a manner dependent on the individual's metabolic state. They therefore have the potential to capture information on a range of different metabolic processes and provide insight into the physiological stresses experienced by individuals. Of particular interest to assess energy stores and body condition would be the adipocytokines such as adiponectin, detected here, as well as various protein factors involved in lipid metabolism. In addition, the range of immune proteins identified suggests that the blubber could be a valuable tissue for assessing immune system function and inflammatory responses. Overall, proteomic studies have the potential to identify key metabolic processes and pathways and therefore assign novel functional roles to marine mammal blubber tissue.

One potential reason for the lack of any relationships in the band group profiles and the qualitative variables of interest used here is that these data are not of fine enough resolution to detect subtle changes in individual protein presence and abundance. The nLC-ESI MS/MS protein identification

results from the harbour porpoise and the minke whale samples showed that each protein band is a mixture of proteins of the same size, not a single protein. This is because the total protein extracts from the blubber are a complex mixture of proteins of different sizes from different cell types. Then, for analysis purposes, the band groups are made up of a number of individual protein bands. This means that a band group can potentially contain a huge variety of different proteins with different functions (Figure 3-18). Thus, these band group pattern analyses are a summation of many different proteins, so subtle changes in certain proteins of interest that are likely lost through this coarse analysis.

#### 3.1.7.2 Future Recommendations

An important next step in the identification of different proteins and / or combinations of different proteins that can act as biomarkers of overall health and condition in cetacean blubber is to use 2 dimensional PAGE to separate the proteins in blubber extracts. 2D-PAGE separates complex mixtures of proteins using two different properties of the proteins. In the first dimension, proteins are separated by their charge called the isoelectric point, and in the second dimension they are separated by their relative molecular weight (Saraswathy and Ramalingam, 2011). 2D PAGE can thus separate several thousand different individual proteins in one gel. In addition, significant improvements have been made in 2D PAGE technology with the development of two-dimensional fluorescence difference gel electrophoresis, which can be used to reduce gel-to-gel variations (Saraswathy and Ramalingam, 2011) Differentially expressed proteins can be visualised by investigating different protein spot patterns and can then be subsequently identified by mass spectrometric methods as with the 1D PAGE used here.

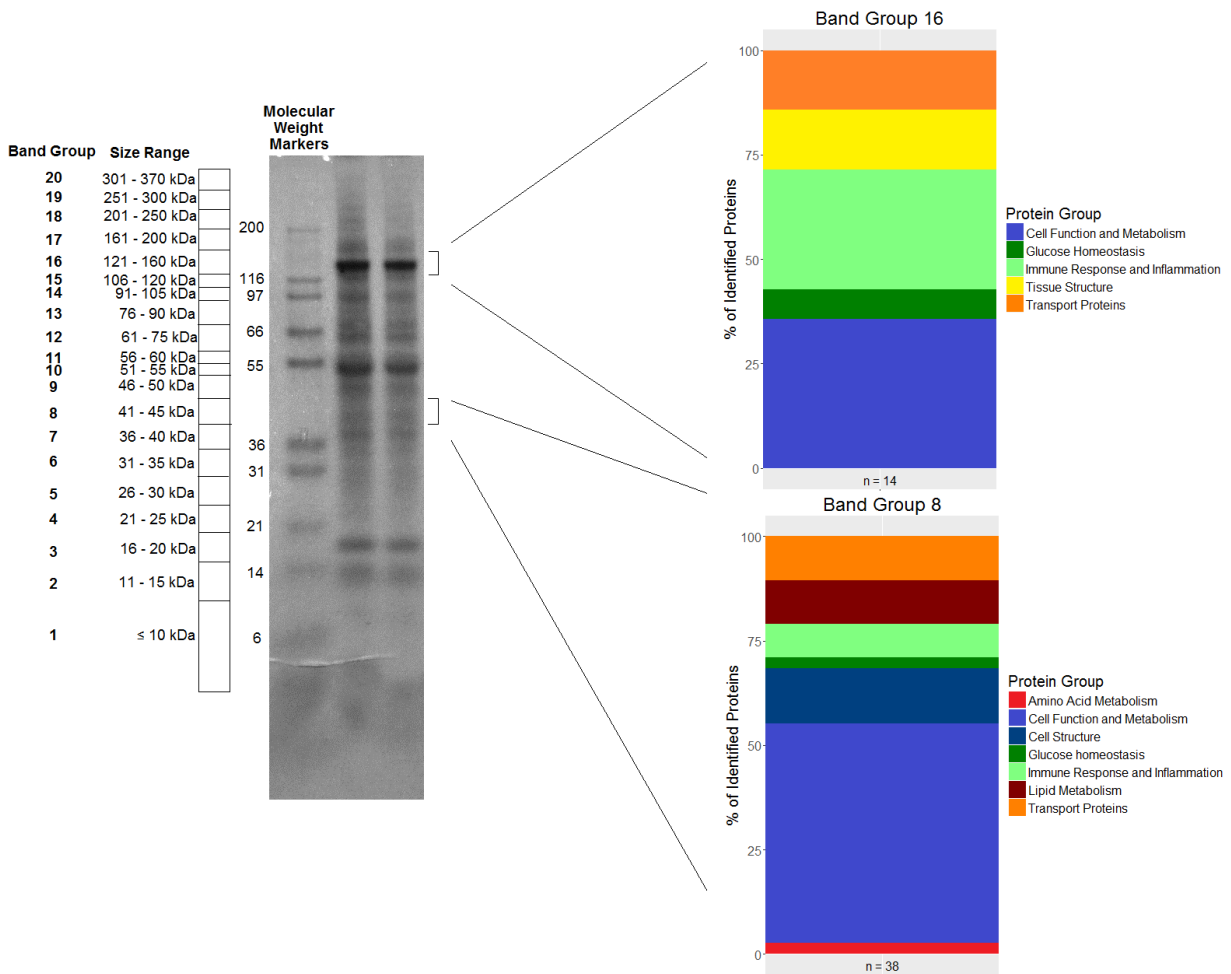


Figure 3-11. 1D SDS-PAGE gel image to show the grouping of individual bands into band groups numbered 1 to 20 used for NDMS analysis with protein identification results examples for band group 8 and 16. A total of 38 and 14 different proteins were identified in band groups 8 and 16 respectively from harbour porpoise and minke whale blubber extracts analysed through nLC-ESI MS/MS. The contribution of different proteins that make up various functional groups are indicated.

### 3.2 Use of body shape indicators to study body condition in free ranging cetaceans

The goal of the scope of work reported in this Subsection (3.2) was to test and implement a method to measure body-shape of cetaceans, as an independent method to estimate their lipid-store body condition for comparison with the tissue based methods (subsection 3.1) and the tag-based tissue body density method (Subsection 3.3) for estimating body condition. Girth / length ratios are a standard way of estimating body condition in cetacean carcasses (Read, 1990; Víkingsson, 1995), given the primary location of lipid stores within external blubber layers of cetaceans. We predict that animals with greater lipid stores will be wider in girth per unit length than animals with less lipid store.

In studies prior to the start of RC-2337, overhead photogrammetry had been used successfully to measure shape changes of cetaceans in relation to reproductive status (Perryman and Lynn, 2002; Miller et al., 2012). However, at that time, overhead photogrammetry was accomplished using fixed wing planes and helicopters, which was beyond the scope of the project. Therefore, at the start of project RC-2337, we evaluated use of an underwater 3D scanning sonar (Echoscope 3D underwater sonar; CodaOctopus Inc.) deployed from a follow-vessel to measure girth and length of free-ranging cetaceans. Following a test trial evaluating the method with killer whales in a captive setting and in near-shore coastal waters of Iceland, the sonar-based method was stopped for the project following a NO-GO decision. In the meantime, the capability of small UAV (drone) systems to make such photographic measurements of cetaceans had been demonstrated (Fearnbach et al., 2011; Durban et al., 2015), so our efforts to measure body shape of tagged whales changed to use of a UAV drone system to take overhead photogrammetry images.

In the first part of this subsection, we report the outcome of the evaluations of the use of the Echoscope 3D scanning sonar. In the second part of this subsection, we detail results using the UAV drone to measure body dimensions of humpback whales in the study.

#### 3.2.1 Evaluation of a method to measure body shape using a 3D scanning sonar

Herein, we report on two aspects of the effectiveness of using a scanning sonar evaluated in two different efforts: one to measure the precision of computer processing methods for the measurement of body dimensions of killer whales (*Orcinus orca*) from 3D scans acquired with a high-frequency underwater 3D sonar; and the second to determine the feasibility of routinely using the scanning sonar to make measurements of free-ranging cetaceans.

To assess the accuracy of the scanning-sonar technique, sonar results were compared to ground-truth whale measurements acquired at Loro Parque (Tenerife) in August 2014 from two captive killer whales of known body dimensions. Data for the captive whales was acquired over a 6 day period. The sonar equipment was slowly introduced in order to fully assess any potential reaction to the sonar. No adverse reactions were noted, and a number of different types of deployment were achieved over the testing period. The sonar results were compared to the ground truth measurements made on the whales.

To assess the feasibility of making routine measurements of free-ranging cetaceans, wild killer whales were approached and imaged using the 3D sonar in Iceland in February 2014. Data for the free-ranging whales was acquired over a 5 day period with over 10 separate encounters. As with the captive study, a phased approach was tested in order to determine reactions of the whales.

### 3.2.1.1 Data Collection

An Echoscope 3D underwater sonar (CodaOctopus Inc.) was used for this evaluation. The sonar has an operational frequency range between 375 kHz and 610 kHz depending on the ping rate and volume of ensonification. The sonar generates 16,384 beams per acoustic transmission with a frame rate of over 10 scans per second. The ensonified cone or angular coverage is user defined from 50°x50° to 25°x25° with beam spacing of 0.39° to 0.19°. In low frequency mode, the sonar has a maximum range of 120 meters and a range resolution of 3cm.

The sonar operates by sending an acoustic pulse or transmission that bounces off the target and is received with up to 16,384 beams. Each echo signal received by the Echoscope is separately evaluated to generate a 'point cloud'. The most general definition of a point cloud is: *a set of data points within some coordinate system*. Here, a point cloud is the data in three dimensional coordinates recorded by the Echoscope from a single scan. These coordinates are the sum of the global position of the sonar (measured with a GPS interfaced with the system), and the relative position of each point cloud with the sonar as the origin. These point clouds are used for analysis. Each Echoscope point cloud can be treated as a separate volume similar to each picture in a photo-ID database, however, because the Echoscope produces up to 10 transmissions per second these can also be combined to give more statistical weight to the object that is being studied when that object does not move or change shape. For this project where scanning whales was the objective, this criteria is only met for very short periods of time and thus combining more than 2-3 transmissions can lead to data degradation rather than enhancement. The project aimed to develop a method for reconstructing the shape of whales from the point clouds from which body dimensions could be estimated. Further, a methodology was developed to investigate the validity of combining data from multiple point cloud data sets in order to automatically process and analyse the sonar data for whale surveys.

Data Collection in Captivity: In order to obtain the 'ground truth' data with which to assess the usefulness of the Echoscope as a tool to accurately measure the lengths and girths of cetaceans, three adult killer whales at Loro Parque (Tenerife) were used in a series of captive experiments. All the experiments were done in a roughly circular pool with a diameter of approximately 30m. The sonar head was mounted on a pole attached to a weighted cart on wheels which allowed the sonar head to be moved easily around the side of the pool. A rope was attached to the sonar head which allowed it to be lowered into, and lifted out of the water. The initial exposures of the killer whales to the sonar were progressive and carefully monitored, and no visible reaction to the sonar was observed when it was in the pool but turned off, at low power, or at full power. When the sonar was being used for data collection, the whales were instructed by trainers to swim slowly from one side of the pool to the other such that their track, perpendicular to the sonar, was recorded by the Echoscope.

The ground-truth measurements of whale dimensions were made by hand using a measuring tape when the whales were lifted out of the water onto a platform or at the water surface. The total length was measured from the rostrum tip to the origin of the fluke. The girth was measured at up to 5 places along the body, but of interest here were the girth measurements immediately anterior and immediately posterior to the dorsal fin. Finally, the dimensions of the dorsal fin and the pectoral fins were also measured. The full set of these measurements was only taken for two of the three whales as the male had a bent over dorsal fin. For this reason, full comparisons between the ground-truth values and the 3D sonar values could only be made for the two female whales,

Kohana and Skyla. One set of measurements was made during the sonar survey and a second set made following the survey in order to determine the variability in taking measurements by hand (Table 3-8).

*Table 3-8. All ground truth measurements taken from the two female killer whales at Loro Parque on two different dates, the 17<sup>th</sup> of September and the 29<sup>th</sup> of November 2014.*

<b>Name</b>	<b>Total Length (m)</b>	<b>Half Length (m)</b>	<b>Dorsal Height (m)</b>	<b>Dorsal Width (m)</b>	<b>Pectoral Length (m)</b>	<b>Pectoral Width (m)</b>	<b>Anterior Girth (m)</b>	<b>Posterior Girth (m)</b>	
Kohana	5.34	2.70	0.51	0.49	0.63	0.46	3.00	2.89	
	5.20	"	0.54	0.56	0.61	0.45	3.07	2.75	
	<b>Average</b>	<b>5.27</b>	<b>2.70</b>	<b>0.53</b>	<b>0.53</b>	<b>0.62</b>	<b>0.46</b>	<b>3.04</b>	<b>2.82</b>
	SD	0.07	0.00	0.02	0.04	0.01	0.01	0.03	0.07
	SE	0.05	0.00	0.01	0.02	0.01	0.00	0.02	0.05
Skyla	5.35	2.65	0.47	0.51	0.58	0.42	3.09	2.80	
	5.37	""	0.54	0.60	0.55	0.42	""	2.81	
	<b>Average</b>	<b>5.36</b>	<b>2.65</b>	<b>0.51</b>	<b>0.56</b>	<b>0.57</b>	<b>0.42</b>	<b>3.09</b>	<b>2.81</b>
	SD	0.01	0.00	0.04	0.05	0.02	0.00	0.00	0.01
	SE	0.01	0.00	0.02	0.03	0.01	0.00	0.00	0.00

**Data Collection in the Wild:** A survey of killer whales in Iceland was conducted in January 2014 using the Echoscope, and recorded data on a number of individual whales over several deployments. A small rigid-hull inflatable boat (RHIB) was used for the deployment with the sonar dry side protected by a custom-made splash-proof cover (Figure 3-19). The most critical aspect of the deployment system was a firm mounting bracket that allowed the pole arrangement to be lifted clear of the water during transit to survey sites but which allowed easy but rigid deployment once at the site.

Weather conditions varied during the deployments with survey effort discontinued in winds greater than force 4, and a sea state greater than moderate to rough. During the sonar survey, individual whales were photographed for photo-ID purposes and tagging efforts were also made from the same vessel. Photogrammetry images were also taken to estimate the lengths and widths of the dorsal fins using calibrated lasers. Thus, a number of individual killer whales were photographed and identified and could be cross-correlated with individuals on the sonar records.

A phased approach was used for deployment of the sonar that included the following stages, each with an extensive observation period to determine the reactions of the animals:

1. Deploying with no power
2. Deploying with “listen-only” mode
3. Deploying with “listen and transmit”
4. Listen, transmit at full power and follow the animals

No reaction in terms of avoidance, changes in respiration patterns or surface behavior was discernible for the stages above from behavior observed when following whales using the same RHIB without the sonar deployed.

### 3.2.1.2 Data Analysis

Preliminary data evaluation can be conducted using the acquisition software. This allows the user to observe, in real time, the quality of transmissions and the saturation of echo bounces from individual animals. This is important for quality control as it is the aim of surveying to maximise



*Figure 3-12. Echoscope mounted on starboard side of the research vessel.*

the number of points on an animal to give the best sonar data returns for that individual. Replay using the acquisition software can also be used subsequently to pick the best sections of data where this criterion is met. In subsequent processing, the user can then make the decision to use only the best quality data. Alternatively, the user can choose to use all of the data with an automated processing regime. In this project an automated processing regime was designed in order to reduce the subjectivity and necessity of making decisions on “what is the best data” to process. The automated data analysis was conducted using the processing outlined below (Figure 3-20). Following this, analysis of the data was made to determine goodness of fit to the ground truth measurements.

**Data Processing:** To facilitate automated processing of the point cloud data, a series of analytical steps were developed and performed in various software packages (*Underwater Survey Explorer* by CodaOctopus, *CloudCompare* by Telecom ParisTech / EDF, *Meshlab* by ISTI-CNR and *MatLab*). The main purpose of the processing was to increase the signal to noise ratio of the data and to remove the subjectivity from analysis for body dimensions of individual whales. The series of analytical steps followed a progression specifically developed for this project to include cloud registration, noise removal, filtering, segmentation, normal estimation and surface rendition of the main body (Figure 3-20). At each step, several algorithms were implemented and compared to find the most appropriate one for this analysis to produce a 3D model of the individual using extrapolation with left-right symmetry (Figure 3-21). For each set of data (a set being defined as one swim pass of an animal past the sonar), it was possible to process the echo returns using a number of different parameters. The parameters were defined as the variables associated with individual transmissions to include in each “summed” point cloud. The sums are then calculated

as a running value along each set of data or data track as the animal swims past the sonar. A sum of between three and five transmissions was typical for the test data.

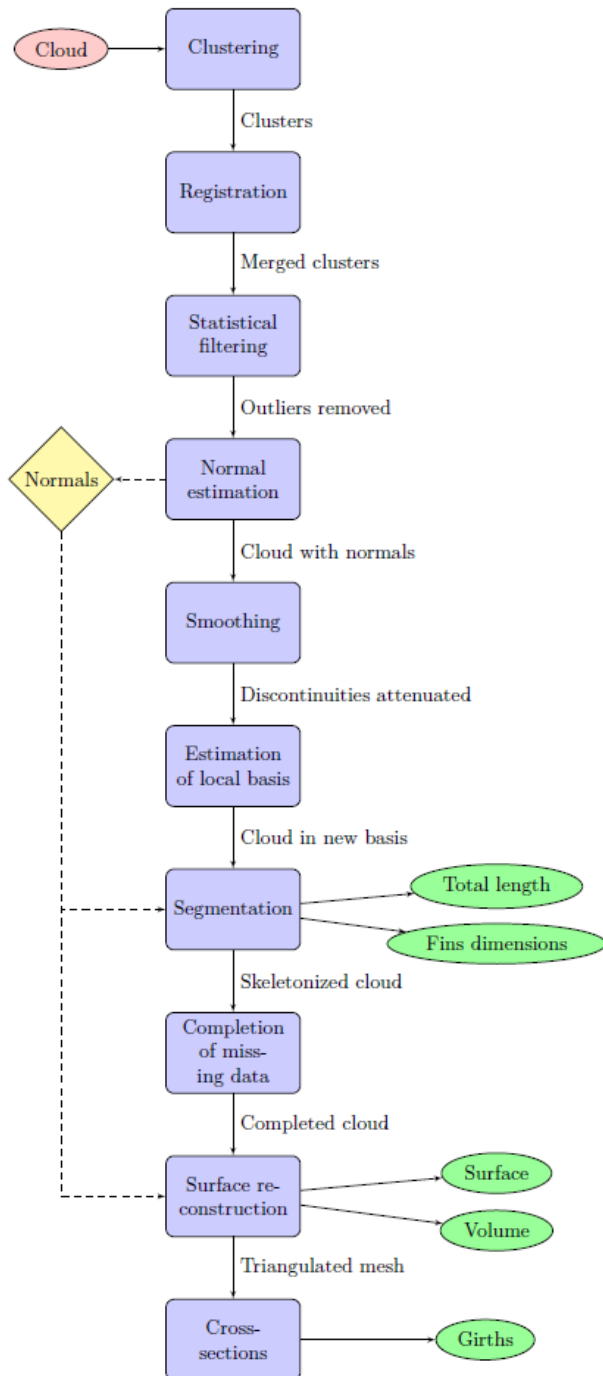
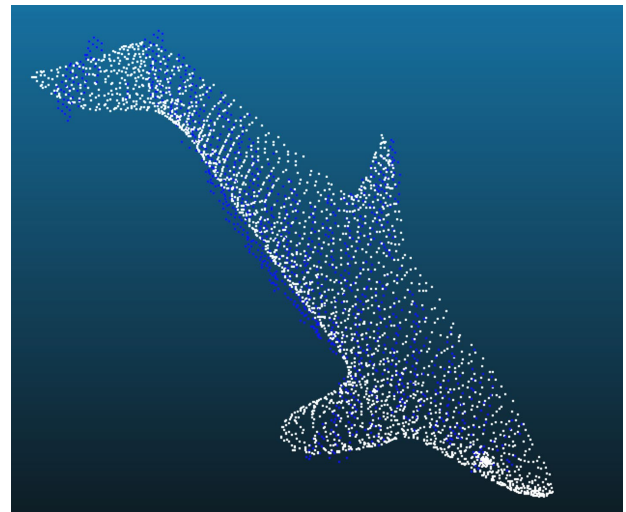


Figure 3-20, left. The sequence of analytical steps used to extract animal dimensions from the scanning sonar cloud data.

Figure 3-21, below. Killer whale data points plotted from the Icelandic field trials shown in dark blue, with the corresponding half of the 3D model generated shown in white.



Comparison with Ground Truth Data: Data from both the captive and the wild killer whales were processed to reconstruct 3D models of the animals, but only data from the captive animals were

then used to make measurements from the sonar data to ground-truth the method against hand measurements of whale dimensions. To measure the total body length, the first approach took the peak-to-peak distance along the  $X_{loc}$  axis (Figure 3-22.). However, this only works if the animal is fully extended, which is often not the case when swimming. Consequently, its curved shape was approximated with segments, defining the edges of a basic skeleton. This skeleton contained 6 nodes defined as the average of portions of the cloud centered at specific values of  $X$  (Figure 3-23.). The dimensions of the fins were calculated using the width as the 3D distance between the two extremal points along  $X_{loc}$  axis, the length of the dorsal fin was the 3D distance between the two extremal points along  $Y_{loc}$  axis, and the length of the near pectoral fin was the 3D distance between the two extremal points along  $Z_{loc}$  axis. Finally, girth was calculated at two points along the body; at the anterior dorsal node, and at the posterior dorsal node (Figure 3-23.). The girth was calculated as the sum of the length of smaller segments that make up the ‘mesh’ of the reconstructed 3D model. These measurements from the reconstruction of the sonar data were then compared to the ‘ground-truth’ measurements of the captive whales.

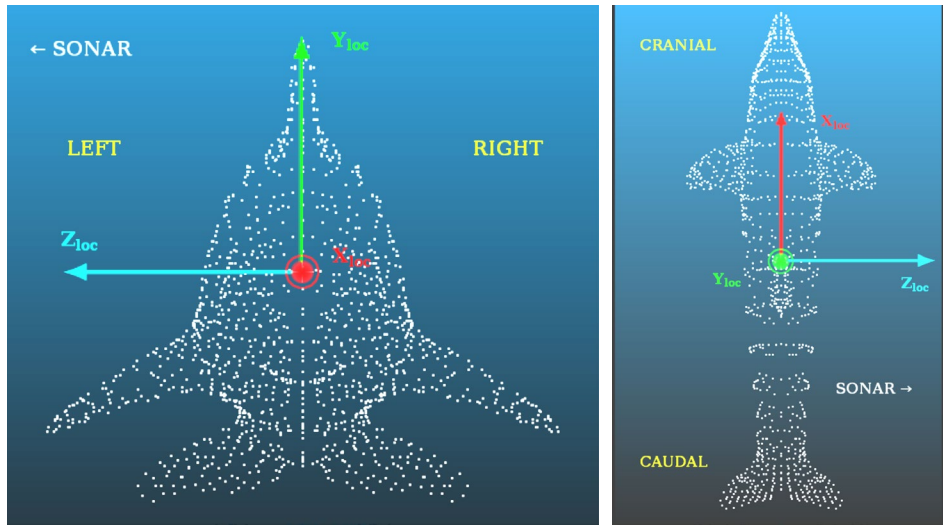


Figure 3-13. Example 3D reconstructed model of a dolphin showing the three axes,  $X_{loc}$ ,  $Y_{loc}$  and  $Z_{loc}$ .

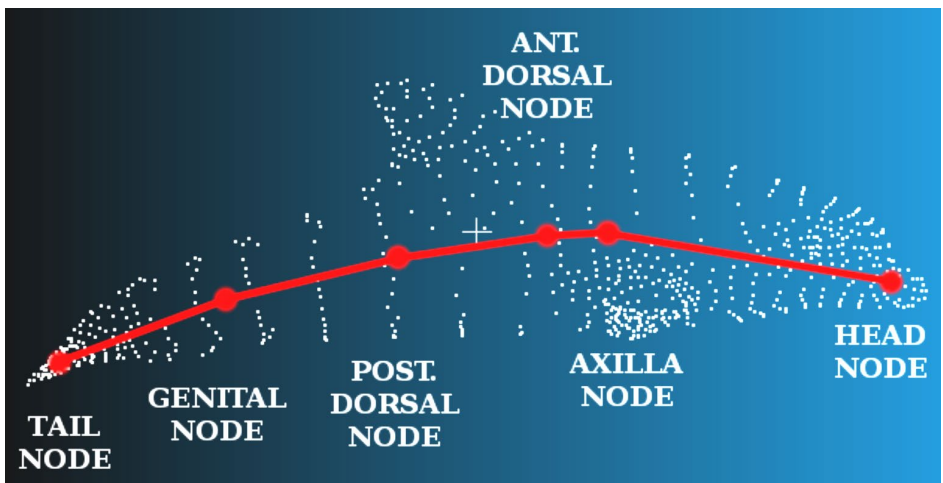


Figure 3-14. An example of the basic skeleton used for total length measurement from the reconstructed 3D models.

### 3.2.1.3 Results and Discussion

### **3D Scanning sonar to measure body shape – highlights**

Trials in a captive facility derived measurements of a number of critical lengths (full body length, half body length, girth at key sections, dorsal fin length) on two different animals were made. Lengths (total and half) were determined with less accuracy than girths as a result of more movement at the tip of the animal from vertical oscillations of the fluke while swimming resulting in a more mobile and smaller target.

To investigate the potential to automate the processing of data, a large number of algorithm parameters were tested. It was noted that the parameters that provided the best estimates of length and those that provided the best estimate of girth were different, and thus at this stage, manual interrogation/filtering of the data is still necessary to achieve a target accuracy of <10%. Testing of the “best parameters” necessitates further study, which is why we recommended a NO-GO decision for use of this tool in the RC-2337 project.

The ability to make measurements on free-ranging animals was achieved and demonstrated from these initial trials on killer whales in Iceland.

#### *3.2.1.3.1 Can we measure body length and girth in captive cetaceans?*

Two methods of analysis are possible with the type of data collected. Either, the user can decide to use all of the data with no pre-filtering, or, the user can either decide to analyse a sub-set of the best data. Using the second approach, the user decides which of the scans are most appropriate for analysis and chooses only these scans based on experience in use of the sonar. While this approach, akin to taking the best of a photographic record of an individual animal for photo-identification, is likely to give the best results, it was decided to test all of the data in order to avoid unintentional bias in the results and subjectivity in data analysis. All of the following results are therefore based on the analysis of *all* the data collected along individual “swims” of each animal past the sonar in the captive facility.

Using this automated approach a range of values were considered for the five main parameter variables in the algorithms: number of merged scans (1, 3 or 5), smoothness factor (2, 3 or 4), search range multiplier (2, 3 or 4), angular threshold (10, 20 or 30) and residual threshold (1, 2 or 3). The result of varying all these parameters was a large variation in the estimates for the body dimensions of the whales (Figure 3-24). Together, only 7.69 % of the estimated lengths and 1.05 % of estimated half lengths had a <10 % error for both whales, which was the target for our evaluation. 34.7 % of the estimated anterior girths and 19.8 % of the estimated posterior girths had a <10 % error for both whales. It is therefore concluded that a specific set of parameters is required for processing as the algorithms are highly sensitive to picking the most appropriate parameters for analysis.

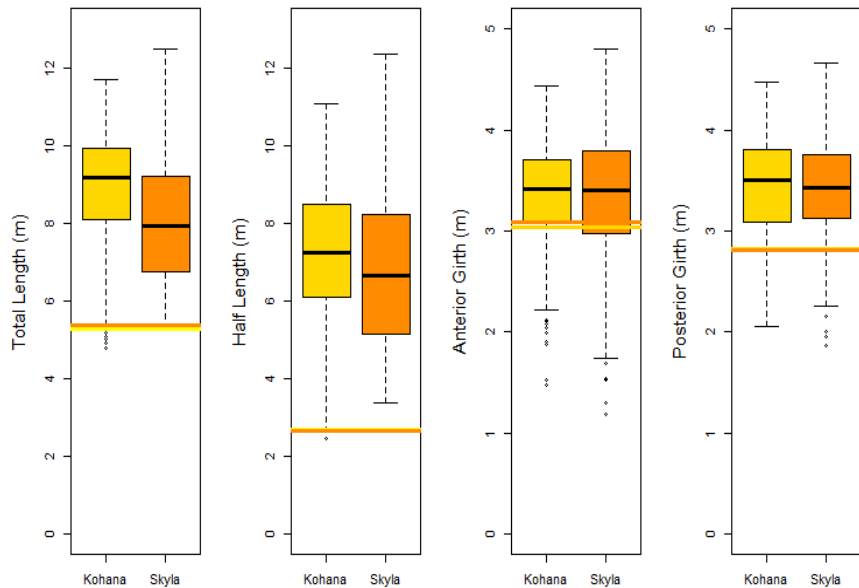


*Figure 3-15. Boxplots showing the median and interquartile ranges of the body dimensions estimated by the sonar data for the two captive, female killer whales. The same colored horizontal lines indicate the true measurements taken by hand. Overall, the sonar data tended to overestimate the body dimensions of the whales.*

It should be noted here however that there was also variability in the hand-measured ground truth data (Table 3-8). For example, the average total lengths for Kohana and Skyla based on two measurements were  $5.27 \pm 0.05\text{m}$  and  $5.36 \pm 0.01\text{m}$  respectively. The anterior and posterior girths for Kohana were  $3.04 \pm 0.02\text{m}$  and  $2.82 \pm 0.05\text{m}$  respectively, but the girth measurements for Skyla were identical. This variation was possibly a result of observer differences, changes in the exact point of measurement on the animal, and the change of shape of the animals as they were lifted to different extents out of the water. Thus, the variability in the sonar results has to be viewed along with this.

As there was such variation in the sonar estimates of body dimensions when a range of parameters were tested, we evaluated which set of parameter values used in the algorithms would yield the most accurate results. A subset of the best sequences of scans that produced errors similar to those of the ground truth measurements were identified (Table 3-9). The estimates for each of the four measurements (total length, half length, anterior girth and posterior girth) with errors  $<10\%$  were used for further analysis to establish which set of parameters produces these ‘best’ estimates. The parameters are listed in Table 3-10.

Table 3-9. Average and % error of measurements (with ~40 scans per sequence) for four of the 'best' sequences. These sequences had the lowest percentage errors from the hand measurements of length and girth shown in blue.

Sequence	Total length (m)	Half length (m)	Dorsal height (m)	Dorsal width (m)	Pectoral length (m)	Pectoral width (m)	Anterior Girth (m)	Posterior Girth (m)
K 1	5.08	2.82	0.49	0.53	1.29	0.49	4.42	4.47
%	0.03	0.04	0.07	0.02	1.07	0.08	0.46	0.57
S 1	5.46	3.49	0.49	0.56	1.51	0.44	4.00	3.89
%	0.02	0.32	0.03	0.01	1.63	0.04	0.29	0.39
S 2	5.56	3.81	0.40	0.54	1.66	0.44	3.71	3.79
%	0.04	0.44	0.21	0.03	1.89	0.05	0.20	0.35
K 3	10.40	9.50	0.85	2.62	1.11	2.82	3.05	2.49
%	0.96	2.52	0.63	4.28	0.78	5.15	0.01	0.11

Table 3-10. Parameter values used to produce the 'best' estimates for each body dimension with errors of <10%.

Parameter	Parameter Values			
	Length	Half Length	Anterior Girth	Posterior Girth
Number of Merged Scans	1	1	1	1
MLS: Smoothness Factor	2	2	3	3
RG: Search Range Multiplier	2	2	4	4
RG: Angular Threshold	10	10	30	30
RG: Residual Threshold	1	1	3	3

From the data analysed to date it can be concluded that for some parameters, the automatic filtering and processing regime can produce measurements that are to <10% of the true values. Where results are not <10% it is likely due to inappropriate parameters being used in the analysis and also the large amount of backscatter noise that results from trying to make measurements in a confined tank.

### 3.2.1.3.2 *Can we collect measurements from wild animals?*

The sonar was easily deployed in the field. During transit to the site it was kept inboard the vessel and lowered into the water when in the presence of the whales. Reliable data was recorded when the whales were close to the sonar at a distance (20-80m) for other activities such as photo-ID and tagging. Thus, the method was found to be complementary to those field operations. With the sonar in the water, boat manoeuvrability was not impaired and the whales were approached with ease and without showing any adverse reactions to the sonar. During each approach it was possible to obtain a number of usable sonar passes for analysis.

The Coda Echoscope provides real-time data at two different frequencies, namely 375 kHz and 610kHz for low and high resolution imaging. While the high frequency mode is desirable for greater resolution it also has less water penetration and a smaller window of insonification. During the initial survey both were tested. However, due to the speed of movement of the killer whales moving in and out of the smaller survey window, only the low resolution mode (375 kHz) was successful.

The Echoscope provides data in real-world coordinates and thus for each whale surveyed, it was possible to extract from the records reflection points in UTM coordinates for x,y, depth and amplitude of return. Typical ping rates achieved for the survey were 4-6 per second so extensive data for any one individual was recorded. Data processing in the field included:

- Isolation of point cloud data on a ping-by-ping basis for individual animals;
- Noise cleaning of information from the data scene to isolate the individual (noise includes water column noise, sea floor noise, surface scatter noise);
- Measurements of dimensions from the resulting point cloud data;
- Model building of surfaces for additional measurements of dimensions;
- Comparison of dimensions taken manually from point cloud data with those taken from the simultaneous photogrammetry survey using laser dots. These measurements demonstrated for the dorsal fin showed an agreement to better than 10%.

Thus, the ability to make measurements on free-ranging animals has been achieved and demonstrated from these initial trials on killer whales. The experience with the killer whales showed the challenges associated with working with such a fast moving species. The main challenge was to follow the animals and to manoeuvre the boat to keep track of them without a pan-and-tilt head. In the field trials it was originally hoped to be able to use a mechanical aided pan-and-tilt head to the Echoscope and thus to have the ability to track the killer whales with more precision as they were swimming alongside the vessel. This was not achieved because the pan-and-tilt mechanism broke prior to deployment and there was not sufficient time to ship a new one to the field site. Tracking was thus achieved using a manually adjustable survey setup.

Thus, it is anticipated that more consistent results could be achieved with both a more rugged head assembly, and when possible with animals whose movement is more consistent in one direction through the water.

### 3.2.1.3.3 *Conclusions and recommendations for future research efforts*

Ultimately, we recommended a No-Go decision for continued use of the scanning sonar in the project. Data were effectively collected from killer whales in the field, and there was no indication

of behavioural response by killer whales to the sonar in either captive or field tests of the scanning sonar system. With appropriate mounting designs, we are confident that the system could be deployed off platforms that could operate with the study target species, northern bottlenose (*Hyperoodon ampullatus*) and humpback whales (*Megaptera novaeangliae*). However, there remains some risk that behavioural response to the sonar, or response to tagging while sonar scans are underway may differ in our target species compared to those observed with free-ranging killer whales. Thus, there remains some risk that it will be more difficult to effectively collect data from the target species than we determined for killer whales.

Though the system has potential for using in the field with free-ranging cetaceans, processing the sonar signals returns posed several challenges and we could not conclusively demonstrate our ability to measure body dimensions within 10% of their true value in the captive studies. Analysis of the sonar returns depends upon a set of algorithm parameters, and it is clear that the results are sensitive to the parameters chosen (Figure 3-24). Though we were able to identify a set of parameter value combinations that appear to have the potential to provide precise and accurate measurements of length and girth, we were not able to test whether or not those parameters would be effective with an independently collected test data set.

Additional data analysis steps and data collection could further inform the utility of the system to make accurate measurements of whale dimensions by addressing the following questions:

1. Does the range of analysis parameter values that yield acceptable results increase if a smaller, higher-quality, subset of the data were used? If pre-filtering based upon detailed data inspection were applied to the data and only the ‘best’ echo return data used for processing, would a greater number of parameters give more values with <10% error more consistently?
2. With pre-filtering using only the best data, do the best parameters give consistent results on all data collected and/or would they give consistently good results on any independent test data collected as an independent test of application of the parameters?

### 3.2.2 Aerial photogrammetry using UAV drones

The purpose of this component of the RC-2337 study was to collect overhead photogrammetry images to estimate the body shape of humpback whales. Images were then processed to quantify length-standardized surface areas, analogous to width-length ratios, of whales as an index of their body condition. Width-length ratios have been previously shown to reflect body shape changes expected with changes in condition (Miller et al., 2012a), and do not require measurement of absolute dimensions of the target whales. Photogrammetry using the UAV was not attempted with the other study species, the northern bottlenose whale, due to the difficulty following a target group and their short surfacing times. In this section, we detail patterns of body shape of humpback whales in relation to reproductive status and time within the feeding season. In section 4.1, we compare the three measures of body condition (body density, tissue indicators, and body shape) made on the same whale.

#### 3.2.2.1 Data Collection

To obtain overhead photogrammetry images of humpback whales, we used a DJI Phantom 4 UAV flown above the individuals, provided the wind speed was under 15 km hr<sup>-1</sup> and the sea state was

less than 3. The DJI Phantom is outfitted with bottom-side landing gear which were used as handles for safe launch and recovery from a boat at sea (inset in Figure 3-25). The Phantom 4 is flown using the DJI GO App as the interface through an android tablet. By communicating with the controller, this provides a live feed from the camera and details of the status and settings of the Phantom 4 as well as its location on a map. As photos of the whales surfacing took some time to be captured, we saw that this led to lost opportunities, so video footage at a 4K resolution was recorded instead. This ensured that the whole surfacing sequence of a whale was captured, and the ‘best’ position of the whale at the surface when the body is fully extended and the tag is clearly visible can be extracted. The video recording was made continuously when the UAV was airborne.

The UAV flew at a target elevation of 16-20m above sea level during flights while the research vessel followed the targeted individual at a low speed (less than 5 knots) roughly 200m away. Target whales were carefully observed throughout all UAV flights, and no response (i.e. startle, sudden avoidance, or surface display) was observed during any of the flights. Typically, UAV flights were only made after a suction-cup tag had been attached to a study animal (for calculation of tissue body density - see section 3.3), and that animal was the primary target for imaging. Once the UAV was airborne, any animal in the same group as the tagged, target individual was also followed for imaging. For the tagged whale, the research team also sought to obtain a biopsy sample following termination of the UAV flight (for tissue analyses of reproductive state and body condition - see section 3.1).

Data were collected on North Atlantic humpback whales in two different feeding grounds (1) Gulf of St Lawrence, Quebec, Canada near Cap-aux-Os (48°50'N, 64°19'W) and Godbout (49°32'N, 67°59'W) from June to September 2016 and 2017; (2) Polar waters of Northern Norway: near Vengsøy (69°50'N, 18°30'E) and Skjervøy (69°59'N, 21°40'E) in mid-January 2017 and 2018 (Figure 3-25 & Figure 3-26). These are two major summer feeding grounds for North Atlantic humpback whales.

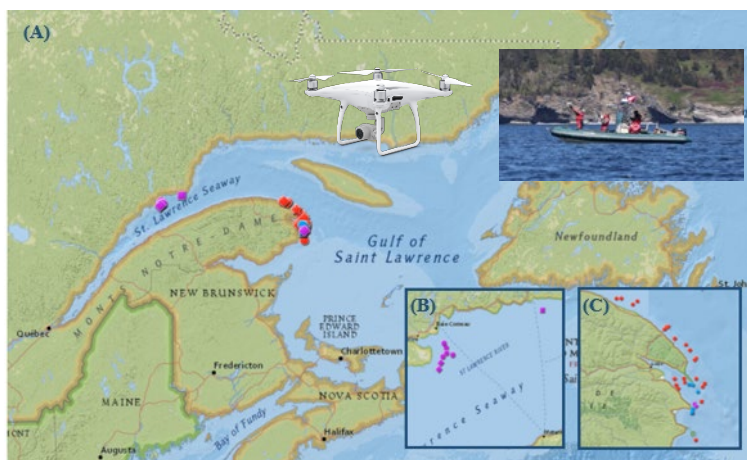


*Figure 3-25. Map of the fieldwork in the Gulf of St Lawrence. (A) Overview of samples location from 2016 to 2017. Inset shows the DJI Phantom UAV and vessel used to deploy the system. (B) Zoom on sample locations August-September 2016 (purple dots) (C) Zoom on sample locations June-July 2016 (blue dots) and 2017 (red dots). Circles = females, diamonds = males and squares = unknown sex.*

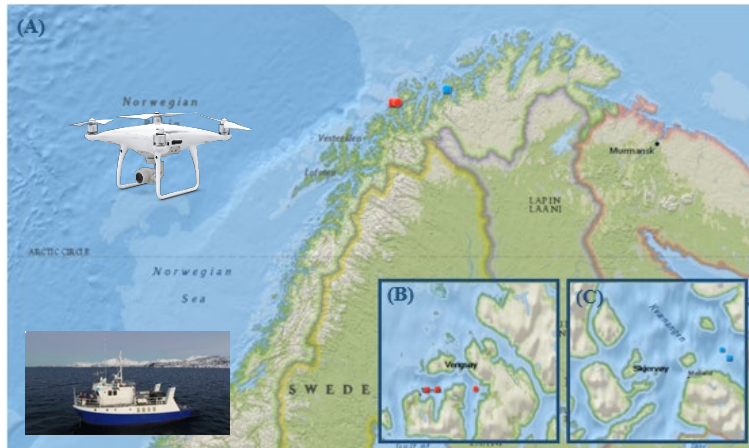


*Figure 3-26. Map of the fieldwork in Norwegian Sea. (A) Overview of samples location from 2017 to 2018. Inset shows the DJI Phantom UAV and vessel used to deploy the system. (B) Zoom on sample locations January 2017 (C) Zoom on sample locations January 2018.*

A total of 10h 57min 36s of footage were collected (mean flight duration = 13min 09s). Images were collected from a total of 55 individuals, 31 of which were tagged, and 26 of which had a biopsy sample collected. Based upon their hormonal status and visual observations, we determined the data consist of 7 lactating females, 6 pregnant females, 10 non-breeding females, 6 mature males, 14 mature unsexed individuals, 5 immature unsexed individuals, and 5 calves judged based upon their size to be <1yr of age.

### 3.2.2.2 Data Extraction and Analysis

Video footage was edited using VLC media player 3.0.2. Only sequences of interest were kept, that is, footage with whales at or near the surface (see section 3.2.1). From the remaining footage, individual frames were extracted using Free Video to JPG Converter 5.0.101.201. From the data extracted, the best quality frames were selected relying on the following predetermined criteria: (1) the depth and the angle of the individual relative to the UAV's position, (2) the visibility and the angle of the tag relative to the individual's body axis, (3) the posture of the individual, (4) the elevation of the drone and (5) the brightness of the image (see Figure 3-27 for illustration).

Frames judged to be of usable quality to measure relative body dimensions were measured in detail using a script in R studio 1.1.447 initially provided by Christiansen et al. (2016), and modified for use in this study. Initially, the analyst marks the position of the tip of the rostrum and the notch in the flukes, considered to be the length of the whale (in pixels). The software then automatically calculates the body axis and creates lines perpendicular to the body axis, dividing the length (from the rostrum tip to the fluke notch), into 20 equal sections (Figure 3-28, left).



Figure 3-27. Examples of images extracted from the video sequences recorded with the UAV drone. Left: undesirable images. From top to bottom: curved posture of the whale; elevation of the UAV; poor light conditions from glare. Right: images of sufficient quality to be usable in the analysis.

The analyst next marks the external boundary of the whale along each line, to create an outline of the whale's body shape enabling measurement of the width of the whale (in pixels) at that location (Figure 3-28, middle). The software was modified to enable detailed zoom to mark the edge of the whale, other anatomical features, and the tag attached to the body when applicable.

*The Length-Standardized Surface Area Index (LSSAI) of body condition*

Given the top-down view provided by aerial photogrammetry, we expect that animals with larger lipid stores should be wider, for a given body length, than animals with smaller lipid stores (Miller et al., 2012). To quantify this expected body-shape effect, we used the outline measurements of each whale to calculate a length-standardized surface area index (LSSAI). The length-standardized surface area of the 20 regions of each whale's body was calculated using the trigonometric equation for area of a trapezoid (inset in Figure 3-28) as:

$$A = (B/L + b/L) * (\frac{h}{L})/2$$

Where B and b are the widths of the top and bottom of each region of the whale's body in pixels, h is the height of each region in pixels. To standardize the area by length, each dimension is divided by total length (L), also in pixels.

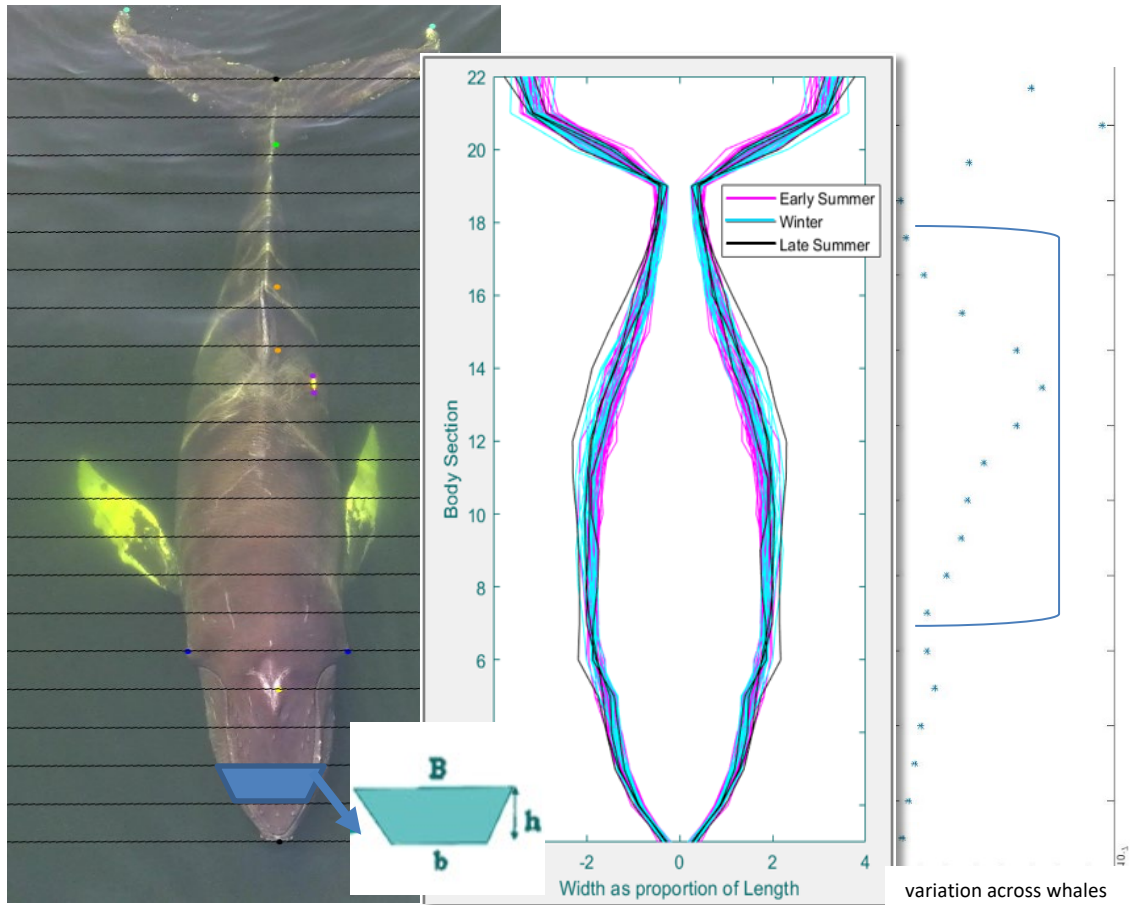


Figure 3-28. Analysis components used to estimate body condition from overhead images. Left: images of the whale selected for analysis. Black dots mark the tip of the rostrum and fluke notch representing total length. The software divides the whale into 20 equal length sections (horizontal black lines). Each section of the whale's body can be represented as a trapezoid for calculation of surface area (inset). Middle: the length-standardized width of different whales in the study. Note the variation across different seasons. Right: Variation in width across whales. The blue bracket captures the central regions of the whales' bodies with high inter-individual variability, which were the body sections used for calculation of the LSSAI as a metric of body condition.

We then summed A over all of the regions most likely to reflect body condition of individual whales (Figure 3-28, right). These regions were specified as those with the most variability in width across animals, excluding areas near the rostrum and flukes that are not likely to hold many lipid stores (Figure 3-28, right). Our results indicated these to be the body sections between lines 7 and 17, representing 10 body sections near the middle of the body.

#### Statistical methodology

To test seasonal and individual variation in body condition, LSSAI was specified as a response variable in a generalized linear model (GLM) with age class, sex, reproductive status, and season as explanatory variables. As LSSAI is continuous and positive valued, it was assumed to follow a Gamma distribution. An identity link function was chosen in order to fit linear relationships.

Age and sex were included in the models as three factor covariates, Age\_Class (Calf, Juvenile, Adult, NK [not known]), Age\_Class\_2 (Immature, Adult, NK), and Sex (Male, Female, NK). Including “NK” as a level in the factor covariates allowed the inclusion of the whole dataset for each condition metric.

The reproductive status of mature females (Pregnant, Lactating, Resting) was coded as two presence-absence covariates, with an indicator variable (presence-absence of adult female [AF]) that made sure the effect was not applied to other animals in the dataset that were either not mature females, or were of unknown sex and age class. The presence-absence coding allowed the female to be both pregnant and lactating at the same time (N=1 in the dataset).

Seasonality was included in the models as an interaction between the tagging location (Norway vs. Canada) and Julian date (an integer number). Three-way interactions were included to allow the seasonal effect to vary between Age\_Class2, Sex and female reproductive status. To allow for more flexible (non-linear responses), season was also included as a factor main effect with three levels (early:  $\leq 190$ , mid: 191-300, late:  $>300$  days).

We conducted global (all combinations) model selection (R package MuMIn version 1.15.6, function dredge). Multi-model inference was carried out based on a “confidence set” of models that were within 2 AIC units of the lowest AIC model. We calculated the “importance” of each covariate, which reflects both its prevalence in the confidence set of models, and its influence on the likelihood of the model it was included in. We also report model-averaged coefficients and plot model-averaged predictions from the confidence set (functions model.avg and predict in package MuMIn). The model coefficients were calculated based on “full average”, which sets the coefficients of absent variables to zero, rather than excluding them from the average (“conditional average”). The full average ensures that the presence of variables does not bias the model-averaged estimate away from zero.

### 3.2.2.3 Results and Discussion

#### **Aerial photogrammetry using UAV drones to measure body shape – highlights**

We measured body dimensions of 55 humpback whales using images taken from an Unmanned Aerial Vehicle (UAV), concurrent with other field activities with the subject whales. Body condition was quantified using a length-standardized surface area index (LSSAI), a relative index of whale width to body length.

Humpback whales varied in their body dimensions (LSSAI) as a function of their age-sex class and reproductive status. Adult females were found to have wider bodies per unit length (greater LSSAI values) than other age-sex classes likely reflecting fat deposition to prepare for lactation. Lactating females had narrower bodies per unit length (lower LSSAI values) than other females, likely reflecting the energetic demand required for lactation.

The LSSAI of humpback whales also increased as expected across the feeding season, with higher values in the mid-feeding season in Canada than the early season. Whales in Norway were sampled latest in the feeding season, and tended to have LSSAI values similar to those measured later in the feeding season in Canada.

For convenience, LSSAI is reported with multiplier of x 1000. A wide range of LSSAI values were found in the data, with important variations observed based upon age-sex class, reproductive status, and timing in the feeding season represented as Julian date (Figure 3-29).

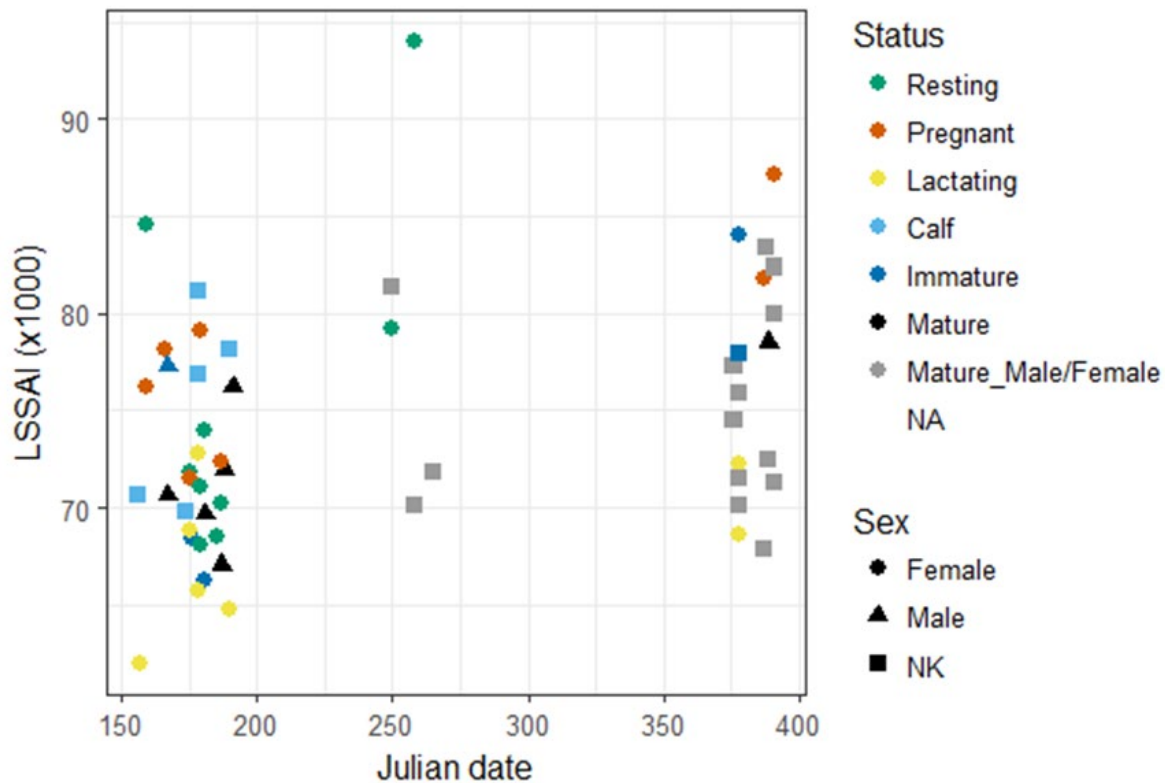


Figure 3-29. The LSSAI of all 55 imaged humpback whales in the study, plotted as a function of Julian date. Note that animals studied in Norway latest in the feeding season (January) have Julian dates >365 for visualization. Symbol shapes indicate animal sex, while color indicates reproductive status and/or age.

The confidence set of models included 10 models. Every model in the confidence set (delta AIC < 2) included the following covariates: AF, Season, AF:Lactating. This indicates that we can have a high degree of confidence that LSSAI was statistically different for adult females, lactating females, and that these values changed across the feeding season as animals gained lipid stores, as predicted.

The simplest model in the set was: AF + Age\_Class2\_ + Location + Season + AF:Lactating. This model explained 43.7% (R<sup>2</sup>) of the LSSAI response data (Table 3-11). Most of these retained parameters were the same as those that were in all models in the confidence set (Table 3-12) or that occurred in some of the models in the confidence set: Age\_Class2, Location, Age\_Class, Sex, AF:Pregnant.

Table 3-11. Coefficient estimates for the simplest model in the set of models. Positive estimate values indicate factors that led to higher LSSAI values, while negative estimate values are factors that led to lower LSSAI values. 'NK' indicates not-known.

	<b>Estimate</b>	<b>Std. Error</b>	<b>t value</b>	<b>Pr(&gt; t )</b>
(Intercept)	68.48	1.67	41.1	0.000
AF	6.22	1.91	3.3	0.002
Age_Class2_Immature	5.17	2.16	2.4	0.020
Age_Class2_NK	7.98	3.96	2.0	0.050
LocationNorway	6.96	1.73	4.0	0.000
SeasonMid	8.02	2.50	3.2	0.002
AF:Lactating	-8.72	2.14	-4.1	0.000

Table 3-12. Significant model-averaged effects (i.e., the coefficient estimates that were not zero and therefore different from the intercept) at the 5% level. Positive estimate values indicate factors that led to higher LSSAI values, while negative estimate values are factors that led to lower LSSAI values.

	<b>Estimate</b>	<b>Std. Error</b>	<b>Adjusted SE</b>	<b>z value</b>	<b>Pr(&gt; z )</b>
(Intercept)	67.33	3.29	3.33	20.3	0.000
AF	7.16	3.43	3.47	2.1	0.039
SeasonMid	8.29	2.53	2.60	3.2	0.001
AF:Lactating	-8.59	2.21	2.27	3.8	0.000

Variations by reproductive status largely matched predictions, with lactating females have the lowest range of LSSAI values, both in Canada and Norway (Figure 3-30). Pregnant females tended to have higher LSSAI values than most other age-sex classes, but some resting females in the mid-feeding season in Canada were also found to have notably high LSSAI values.

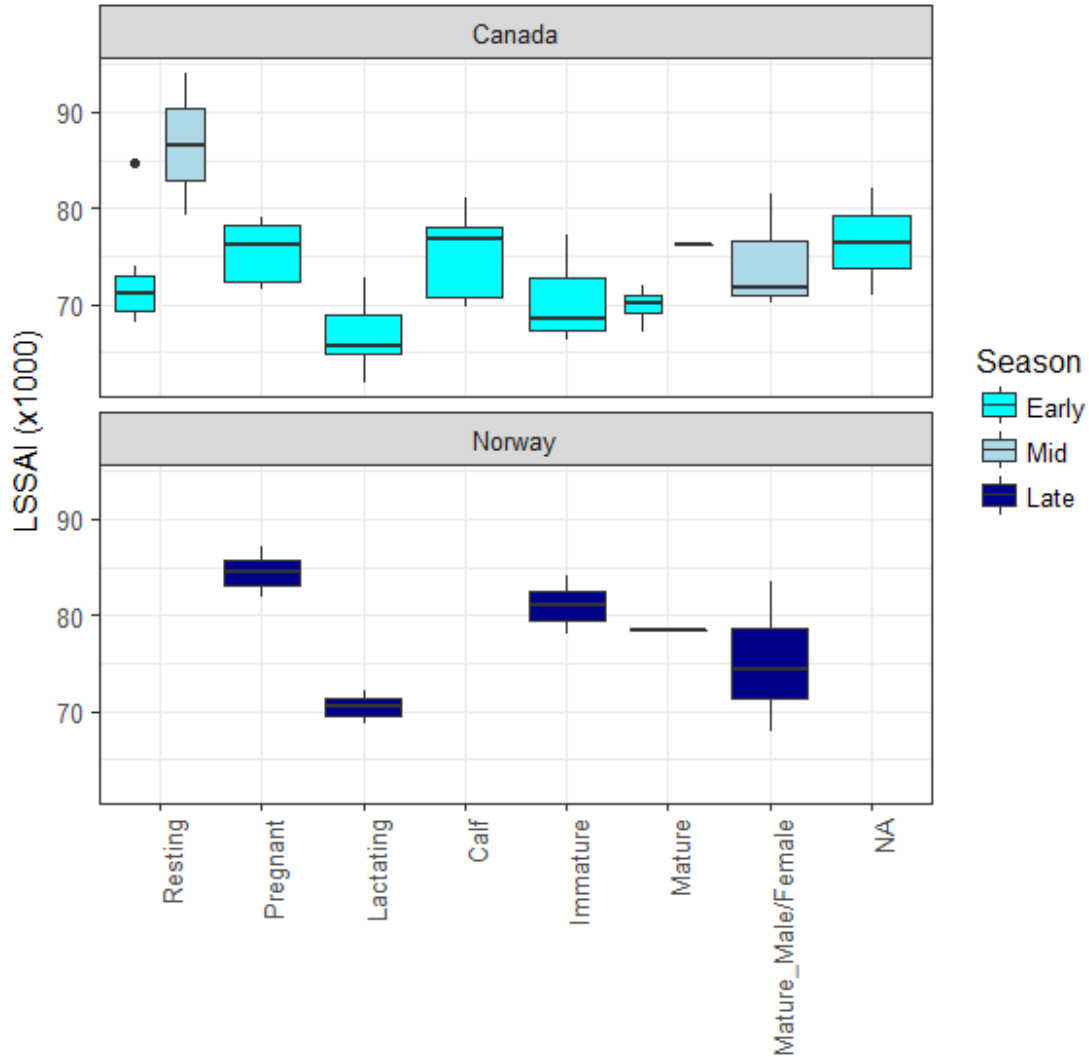


Figure 3-30. Boxplots of body condition (LSSAIx1000) by age and reproductive class, location and season

Reproduction is likely to have direct and indirect physiological costs for individuals. Direct costs for females are in terms of physiological demands such as lactation and gestation. Indirect costs are due to trade-offs that individuals have to engage in to save energy which can then be allocated to reproduction or competing functions (e.g. foraging, migrating). Indirect costs are especially relevant in challenging environments where resources are limited ((Calow, 1979; Gittleman, 1988). The factors we identified to describe patterns in body shape reflect direct costs, assessed in terms of changes in fat content across individuals' reproductive status. We found evidence that reproductive status explained 38% of body condition variations in individuals. Lactating was the most costly reproductive event as females accompanied by calves were significantly thinner compared to non-breeding females. Lactation costs play an important role in depleting energy reserves in many species (e.g. marine mammals: (Bowen et al., 2001; Nowacek et al., 2016) monkeys: (Barrett et al., 2006)). However other factors and indirect costs likely drive the variability observed in our measurements of the body condition of humpback whales.

Overall, the approach to use UAVs to measure body shape of humpback whales was highly effective. The method was feasible for use in tandem with other field operations with free-ranging cetaceans, and the results largely matched predictions of how we expect body condition to vary in cetaceans. For future research, it will be helpful to extend the sample effort to breeding grounds for females arriving after their southern migration but before the parturition to better understand how females allocate their energy during late pregnancy stages. One prediction is that late pregnant females will have more fat stored than other females if they tried to maximise their fat store prior to parturition. If repeat sampling of the same individuals were possible, it would be interesting to monitor females throughout their pregnancy to address questions such as the duration of their migration between feeding and breeding area, the exact duration and physical changes of a pregnancy, or the variation of different body sections during pregnancy. Another set of questions relates to how females compare to males in terms of energetic expenditure. Here, it could be interesting to compare adult males with non-breeding females to understand how sex relates to energy expenditure during migration and mating behaviour, and how males allocate their fat stores to prepare their migration.

### 3.3 Body tissue density indicator

#### 3.3.1 Tissue body density as an indicator of body condition in free-ranging cetaceans

A central feature of the work in RC-2337 has been to develop, refine and cross-validate a novel, state-of-the-art non-invasive method to measure total body lipid-stores of free-ranging cetaceans based upon their tissue body density.

In this subsection, we describe outcome of our efforts to refine and apply this specific method to various species of cetaceans. In 3.3.1, we describe the methods to estimate tissue body density from high-resolution animal-attached sensor data. The results of this method as applied to three cetacean species in work published during the project is then summarized. In 3.3.2, we apply the method to data collected during the project with humpback whales in the Gulf of St Lawrence, Canada and northern Norway, particularly relating body density to timing in the feeding season and reproductive status of the tagged individuals.

#### 3.3.2 General methods to estimate tissue body density

The overall approach to calculate tissue body density from animal-attached tag data relies on the analysis of speed performance during glide periods of ascent and descent transit phases of dives. Gliding during transit phases of dives is a common behavior among cetaceans, with more gliding occurring in the movement direction aided by net buoyancy (Williams et al., 2000; Miller et al., 2004). As no thrust is produced by the animal while gliding, the speed and acceleration of the gliding body is a predictable outcome of identified external forces (drag, buoyancy) acting upon it at that time. Well-established hydrodynamic equations predict how drag and buoyancy forces influence speed performance during glides, which enabled quantification of body density of divers using analysis of short-duration glides (Miller et al., 2004) or longer-duration terminal velocity glides (Watanabe et al., 2006) prior to this study. Aoki et al. (2011, Table 2 therein) found strong correspondence in body density of diving elephant seals estimated using either vertical rates during drift dives, terminal velocity during prolonged glides, or change in speed during short glides.

##### 3.3.2.1 Animal-borne recorders

Two types of animal-borne recorders were used in RC-2337: acceleration and speed data-loggers 3MPD3GT (Little Leonardo Co., Tokyo, Japan) and sound and movement recording DTAGs (Woods Hole Oceanographic Institution, MA, USA). The 3M PD3GT logger recorded depth, water temperature, and speed from a flywheel at 1-s intervals and 3-axis acceleration at 32 Hz. DTAGs measured pressure, water temperature, and 3-axis acceleration at 50 Hz, which was later downsampled to 5 Hz.

##### 3.3.2.2 Tag Data analyses

Diving data were analyzed using software IGOR Pro (Wave-Metrics Inc., Lake Oswego, OR, USA) and MATLAB (MathWorks Inc., Natick, MA, USA). Pressure data recorded by the archival loggers were converted to absolute values of pressure using calibration values. Propeller rotations on the 3MPD3GT were converted to speed through the water using a calibration line for each tag deployment (Sato et al., 2003): a linear regression of rotation rate against swim speed that was calculated from mean vertical depth change divided by mean sine of the pitch at 5s intervals during steep periods of ascent or descent. Tags were attached to whales at random orientations, so the tag-frame 3-axis acceleration data recorded by the loggers was converted to whale frame using

established methods (Johnson and Tyack, 2003; Miller et al., 2004a). Animal pitch from  $-90^\circ$  to  $+90^\circ$  was calculated as the arcsine of the dorsal-ventral axis of the animal-frame accelerometer. The DTAG lacks a speed sensor, so speed during glides was estimated using the rate of change of depth divided by the sine of pitch (Miller et al., 2004).

All dives (maximum depth:  $\geq 5$  m) were divided into three phases: (1) the descent phase (from the start of the dive to the time when whale's pitch first exceeded  $0^\circ$  (i.e., when it was no longer oriented downward); (2) the ascent phase (from the last time when an animal's pitch was downward ( $<0^\circ$ ) to the end of the dive); and (3) the bottom phase (the time between the end of the descent phase and the beginning of the ascent phase). Dive depth was defined as the maximum depth of the dive.

Acceleration in the tri-axis (longitudinal, lateral, and dorso-ventral axes) directions can be divided into components related to the body orientation of the animal with respect to gravity (gravity-based components) and propulsive activities imposed by fluke thrust (specific components; Sato et al., 2003). Lower frequency (mostly gravity-based) acceleration of the longitudinal axis was used to calculate the pitch of a whale (Sato et al., 2003). Higher-frequency specific acceleration of the dorso-ventral and/or longitudinal axis was used to identify stroking (i.e., fluking movements; Sato et al., 2003, for details see also Aoki et al., 2017). According to the power spectral density of each axis, stroking was determined when oscillation on the dorso-ventral and/or longitudinal axis of the accelerometer exceeded a threshold that was set manually for each deployment.

Gliding data were extracted for 5s-duration segments. Glides longer than 5s were broken into 5s segments and every other 5s segment within those longer glides was excluded from analysis to reduce autocorrelation. Acceleration during each glide ( $a$ ) was measured by regressing speed versus time over the 5s segments. The variance of the measurement was quantified as the root-mean square sum of residuals from the fit of speed versus time (acceleration). Mean speed ( $v$ ), depth ( $d$ ) and pitch angle ( $p$ ) were calculated for each 5s glide segment. Water density ( $\rho_{sw}$ ) for each glide segment was calculated from the CTD cast that was closest in time to each tag record, but was updated with sea water temperature measurements from temperature- only casts or recordings on the 3MPD3GT logger deployments on whales. To avoid the influence of animal manoeuvring on speed performance during a glide, only stable glides (circular variance of roll  $< 0.1$ ) were included.

### 3.3.2.3 Hydrodynamic performance model

We modified the equation presented by Miller et al. (2004) where acceleration ( $\text{ms}^{-2}$ ) along the swimming path is determined by drag force (the first term) and buoyancy forces derived from body tissue (the second term) and gasses carried by each whale (the third term):

$$\text{acceleration} = -0.5 \cdot \frac{C_D \cdot A}{m} \cdot \rho_w \cdot v^2 + \left( \frac{\rho_{sw}}{\rho_{tissue}(d)} - 1 \right) \cdot g \cdot \sin(p) + \frac{V_{air}}{m} \cdot g \cdot \sin(p) \cdot \frac{\rho_{sw} + \rho_{air} \cdot (1 + 0.1 \cdot d)}{(1 + 0.1 \cdot d)}$$

$$\text{where } \rho_{tissue}(d) = \frac{\rho_{tissue}(0)}{1 - r \cdot (1 + 0.1 \cdot d) \cdot 101325 \cdot 10^{-9}}$$

In the above equation,  $C_D$  is the drag coefficient,  $A$  is the relevant surface area ( $m^2$ ),  $m$  is the mass of the whale (kg),  $\rho_{sw}$  is the density of the surrounding seawater ( $kg\ m^{-3}$ ),  $\rho_{tissue}$  is the density of the non-gas component of the whale body ( $kg\ m^{-3}$ ),  $g$  is  $9.8ms^{-2}$ ,  $p$  is animal pitch (radians),  $V_{air}$  is the volume of air inspired at the surface (ml),  $\rho_{air}$  is the density of air ( $kg\ m^{-3}$ ),  $d$  is glide depth (m), and  $r$  is compressibility for animal tissue or the fractional change in volume per unit increase in pressure. The value 101325 converts pressure in atmospheres to pressure in pascals and expresses body tissue compressibility as proportion per Pascal  $\times 10^{-9}$ . The equivalent compressibility value for 0° water of salinity 35 ppm is  $0.447 \times 10^{-9}$  Pascal $^{-1}$ .

Note that effects of lift and associated induced drag (if present) are ignored in this equation (see Aoki et al., 2011). However, the question of lift-related drag is addressed explicitly in section 3.3.1.3 (Narazaki et al., 2018).

Thus, the model consists of three terms which represent external forces acting on the gliding body: drag, density of tissue relative to surrounding seawater, and air volume. The first term quantifies the effect of drag on the speed of the whale during a glide, which always acts against the direction of movement of the body. The effect of drag is primarily a function of speed and unknown terms  $CdA\ m^{-1}$  which are treated together in this paper with unit  $m^2\ kg^{-1}$ .

The second and third terms relate to the weight of the body (net-buoyancy) in water, and can either act with or against the direction of movement of the body. Total body density is the total mass of both tissue and gas components divided by their volumes. Because net buoyancy operates vertically, the component along the movement axis of the whale is obtained by multiplication by sine of pitch ( $p$ ).

The second term quantifies the influence of unknown non-gas tissue density ( $\rho_{tissue}$ ) on speed during a glide. This is the key term that reflects lipid store body condition. While the temperature of the whale body is not expected to follow ambient conditions, the whale will experience local pressure effects, and though the tissue compartment of the body should be relatively incompressible compared to gas compartments, some compression is expected at the extreme pressures experienced by these divers. Previous studies have assumed this compressibility factor to be similar to that of seawater (Miller et al., 2004). However, our model in the present study explicitly accounts for tissue compressibility by multiplying the tissue density by the whale tissue compressibility factor ( $r$ ).

The third term quantifies the influence of the unknown volume of gas per unit mass carried in the dive ( $V_{air}\ m^{-1}$ ) on the net buoyancy of the diver. Gas compartments of cetaceans are largely unprotected from ambient pressure conditions. Thus, the volume and density of gas carried by the animal was modelled to change with hydrostatic pressure following Boyle's law.

#### *Bayesian parameter estimation procedure*

Data extracted for each 5s glide segment were used to estimate unknown parameters ( $CdA\ m^{-1}$ ,  $\rho_{tissue}$ ,  $r$ ,  $V_{air}\ m^{-1}$ ) in the hydrodynamic performance model using Bayesian Gibbs sampling in freely available software JAGS within r (coda package: (Plummer, 2015) and *R2jags* package: (Su and Yajima, 2012)). The Bayesian estimation assumes that parameters are random variables with a “prior” distribution (our a-priori expectation of what the parameter distribution should be), as opposed to traditional frequentist estimation that assumes parameters are unknown and fixed. The

Gibbs sampling algorithm seeks to estimate the posterior distribution, which is the best estimate of the true parameter distribution after the prior expectation of this distribution has been updated with data (Lunn et al., 2012).

We chose the Bayesian over frequentist methods to allow for more flexibility in the statistical model development. A key innovation of the statistical procedure was the inclusion of nested (hierarchical) parameters to contrast within and across-individual variability, which was more straightforward to implement using the MCMC algorithm. The Bayesian estimation framework also allowed us to implement models with informative priors so that we could include information from other studies and a-priori reasoning to support the model-fitting process. We compared the results to fits using uninformative priors to determine the sensitivity of the process to assumptions about the priors. Finally, instead of using traditional regression analysis where the sum of squared errors is minimized, we were able to implement observation error for the measured acceleration values. This weighted the high-quality over low-quality acceleration data in the estimation.

There were four unknown terms in the equation, each of which was set a Bayesian prior range specific to the species studied, and separately detailed in each subsection below.

A set of models were evaluated in order to explore variability in body density, the drag term, and diving lung volume. For each of these quantities, we considered models in which the quantity remained constant across all tag records and dives within them (global estimates). With global parameters, the estimation routine was able to borrow strength across the tag records and different dives to estimate the individual and dive-by-dive parameters in a hierarchical model structure. The global distribution also has a meaningful interpretation as the population distribution for that parameter. For tissue density for example, the global distribution is the expected distribution of tissue densities in the population of whales from which the tagged whales were a sample.

We evaluated models with individual-specific estimates estimated for each tag record as is predicted for tissue density and drag values that are expected to be constant within one tag deployment, but to vary across individual animals. For diving lung volume, we also considered a dive-specific as opposed to individual-specific model. Finally, we also fitted hierarchical models with a global parameter included. In these hierarchical models, each individual or dive-by-dive estimate was considered to be a sample from a global or ‘population’ distribution with an estimated global mean, and an estimated variance across the dives and individuals. Thus, this model structure assumed a central tendency (a shared mean and variance) to the distribution of dive-specific and individual specific values.

Model selection was based upon the deviance information criterion (DIC), with lower values indicating better model fit relative to model complexity. All models were sampled in three independent chains, with 24,000 iterations each. The first 12,000 samples were discarded for burn-in, and the remaining posterior samples were down-sampled by a factor of 36. Convergence was assessed for each parameter, using trace history and Brooks-Gelman-Rubin diagnostic plots (BGR: (Brooks, 1998).

### 3.3.3 Tissue body density of northern bottlenose whales (*Hyperoodon ampullatus*)

#### **Tissue body density of northern bottlenose whales – highlights**

We estimated values for all unknown terms in the hydrodynamic performance model, including the combined drag, tissue density, compressibility of tissues, and diving gas volume term, enabling the first estimates of tissue body density and diving gas volume in a beaked whale.

Estimated tissue densities of individuals covered a narrow range 1028.4-1033.9 kg m<sup>-3</sup>, indicating slightly negative tissue buoyancy in seawater. Body density estimates were highly precise with ±95% CI ranging from 0.1 to 0.4 kg m<sup>-3</sup>, which would equate to a precision of <0.5% of lipid content based upon extrapolation from the elephant seal.

Six whales tagged near Jan Mayen (Norway, 71°N) had lower body density and were closer to neutral buoyancy than six whales tagged in the Gully (Nova Scotia, Canada, 44°N), a difference that was consistent with the amount of gliding observed during ascent versus descent phases in these animals. This indicates that net buoyancy of bottlenose whales tagged in the Gully deviated more from neutral buoyancy, which could indicate greater energetic swimming costs (Sato et al., 2003) than experienced by animals tagged off Jan Mayen.

This section summarizes research published in Miller et al. (Miller et al., 2016c). Additional results on the body density of bottlenose whales off Jan Mayen and their associated behavioural patterns are reported in section 5 of this report.

Field studies were carried out in the Gully Marine Protected Area off Eastern Canada from F/V On A Mission in July 2011 and 2013 (N=6). Field studies were carried out off Jan Mayen, Norway in 2013 from the M/S HU Sverdrup II and in 2014 from the 29m T/S Prolific (N=6). Conductivity-temperature-depth (CTD) casts were made in the Gully on September 04, 2013 at 43° 49.166N, 58° 52.164W. CTD casts were done off Jan Mayen on June 24, 2013 at (70° 47.154' N, 6 ° 0,473'W), and temperature-only casts were done off Jan Mayen in 2014 near each tag location. CTD and temperature cast data were converted to ambient water density following the standard international thermodynamic equation of state for seawater (Millero, 2010).

Each of the four unknown terms in the equation was set a specific prior range. Compressibility ( $r$ ) was set a uniform (non-informative) prior from 0.3 to 0.7 x 10<sup>-9</sup> Pa<sup>-1</sup>. Body tissue density ( $\rho_{\text{tissue}}$ ) was set a uniform prior from 800 to 1200 kg m<sup>-3</sup>. Diving gas volume was set a uniform prior from 5 - 50 ml kg<sup>-1</sup>. For the combined drag coefficient term ( $Cd A m^{-1}$ ) (Biuw et al., 2003), several sources of data were used to set an informative prior. Drag coefficient was estimated to be roughly 0.0030 based upon previous research on similar sized large cetaceans (killer whale (*Orcinus orca*): 0.0029 - (Fish, 1998); fin whale (*Balaenoptera physalus*, Linnaeus 1758): 0.0026 - (Bose, 1989); sperm whale (*Physeter microcephalus*, Linnaeus 1758): 0.0031 - (Miller et al., 2004a). Based upon body length ranges from 5.8-9.8 m, surface area (mean 23.0 m<sup>2</sup>, range 12-36 m<sup>2</sup>) and mass (mean: 6816 kg; range: 3027-12739 kg) were estimated using the equation derived for sperm whales (Miller et al., 2004). This led to an expected value for the northern bottlenose whale for the

combined ( $CdA\ m^{-1}$ ) term of  $10 \times 10^{-6}\ m^2\ kg^{-1}$ , with a range from  $8 \times 10^{-6}$  for large animals to  $12 \times 10^{-6}\ m^2\ kg^{-1}$  for small animals. We captured uncertainty in this mean value by specifying the prior to be a normal distribution with mean of  $10.0 \times 10^{-6}\ m^2\ kg^{-1}$  and standard deviation of  $2.0 \times 10^{-6}\ m^2\ kg^{-1}$ . The distribution for  $CdA\ m^{-1}$  was truncated at  $5.0 \times 10^{-6}$  and  $20.0 \times 10^{-6}\ m^2\ kg^{-1}$  to limit the range of values explored by the Bayesian sampling algorithm.

### Results and Discussion

Gliding periods were successfully identified in all northern bottlenose whale tag records (Figure 3-31). While all whales spent time gliding, there was substantial variation in the proportion of time spent gliding during descent versus ascent across the different tag records (e.g. Figure 3-31).

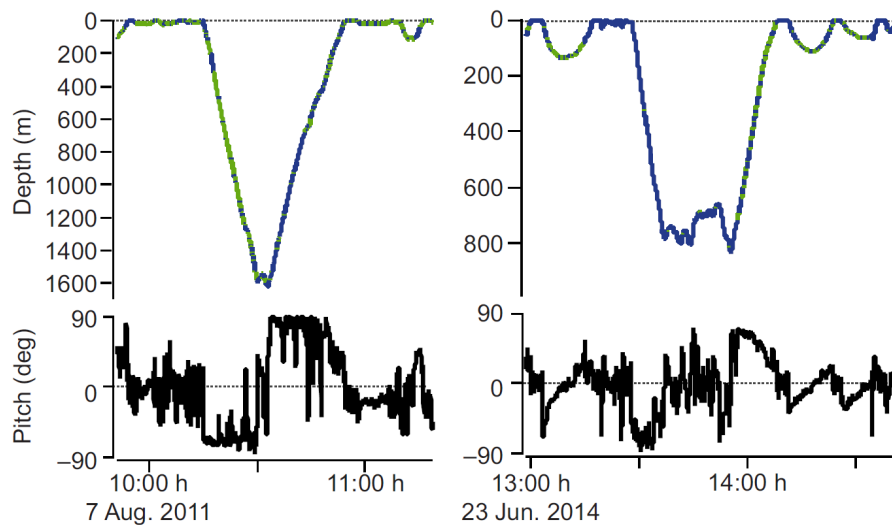


Figure 3-31. Examples of data records showing depth (top) and pitch (bottom) versus time of day. Stroking periods are marked in blue while gliding periods are marked in green.

The best model structure with the lowest DIC included global plus individual variation in body density and drag terms, as predicted, as well as global plus dive-by-dive variability in diving lung volume. The posterior mean of the global drag term ( $CdA\ m^{-1}$ ) was  $12.6 \times 10^{-6}\ m^2\ kg^{-1}$ , overlapping, but slightly greater than the specified prior mean. Most individual posterior means were near  $15 \times 10^{-6}\ m^2\ kg^{-1}$  and ranged overall from  $2-27 \times 10^{-6}\ m^2\ kg^{-1}$ . The mean global diving gas volume was estimated at  $27.4 \pm 4.2$  (95% CI) ml  $kg^{-1}$ . The lowest-DIC model also included dive-by-dive variation in the diving lung volume, but there was no apparent relationship between estimated diving gas volume and dive duration or dive depth.

The global mean tissue density was estimated at  $1031.5 \pm 1.0$  (95% CI)  $kg\ m^{-3}$ . Individual posterior mean values for tissue density ranged from 1028.4 to 1033.9  $kg\ m^{-3}$ , with  $\pm 95\%$  credible intervals of 0.1-0.4  $kg\ m^{-3}$ . Tissue compressibility was estimated as a single global parameter, with a posterior 95% credible interval of 0.37-0.39 (mean of 0.38), indicating only slightly lower compressibility than surrounding seawater (0°C water of salinity 35 ppm).

Whales tagged in Jan Mayen had an overall tendency to be less dense than whales tagged in the Gully. Though several animals from both locations had values in the range of 1030.5-1032.6  $kg\ m^{-3}$ , only whales from Jan Mayen had values lower than that range while only whales from the Gully had values greater than that range. Mean values from the two locations differed by 1.5  $kg\ m^{-3}$ .

m<sup>-3</sup>. This small but consistent difference in body density was clearly reflected in gliding patterns at depths >100m (deep enough to reduce the influence of diving gas volumes; (Biuw et al., 2003), with animals in the Gully gliding substantially more during descent phases and Jan Mayen animals gliding more equally throughout descent and ascent phases (Figure 3-32).

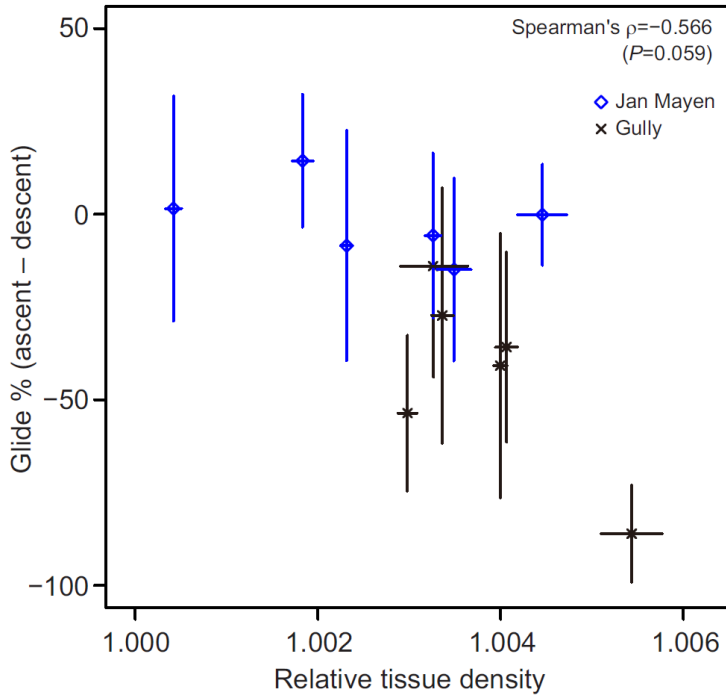


Figure 3-32. The difference in percent time gliding in ascent versus descent phases at depths >100m plotted as a function of the tissue density of tagged northern bottlenose whales relative to ambient seawater density. Greater X-axis values are more dense negatively-buoyant whales, while values close 1.0 are near neutral buoyancy. A negative Y-axis value indicates more gliding during the descent phase, and values near zero indicate equal proportions of gliding during descent and ascent phases.

### 3.3.4 Tissue body density of long-finned pilot whales (*Globicephala melas*)

#### **Tissue body density of long-finned pilot whales – highlights**

Via analysis of glides, this study provided the first estimate of drag coefficient (0.0035), tissue body density ( $1038.8 \pm 1.6 \text{ kg}\cdot\text{m}^{-3}$ ), and diving gas volume ( $34.6 \pm 0.6 \text{ ml}\cdot\text{kg}^{-1}$ ) in this relatively deep-diving delphinid.

Estimated tissue densities of individuals were 1034.6-1044.4  $\text{kg m}^{-3}$ , indicating radically more negative tissue buoyancy in seawater than other species studied. This was consistent with the percent time gliding during descent phases ( $63 \pm 18\%$ ), which greatly exceeded gliding during ascent ( $21 \pm 10\%$ ) as expected for a highly negatively buoyant animal.

High transit speeds compared to similar-sized animals, combined with strong negative buoyancy, indicate that this species has a higher locomotion cost than other deep divers (sperm whales and bottlenose whales), and likely utilizes a “spend-more, gain-more” strategy.

This section summarizes research published in (Aoki, 2017). Field studies were conducted in collaboration with the 3S research program using the 29m research vessel M/S Strønstad in the Vestfjord basin off Lofoten, Norway. This study was conducted during May and June in 2008–2010 and 2013. Tagging was conducted either from a 140 small motor boat Tango (7 m), or from a small boat deployed from M/S Strønstad and 141 R/V H. U. Sverdrup II (55 m, engine driven). We recorded fine-scale underwater movements of 18 long-finned pilot whales and obtained a total of 160.8 h diving data: 16 individuals were tagged with DTAG, and 2 individuals were tagged with the speed data-logger PD3GT.

Each of the four unknown terms in the equation was set a specific prior range. Compressibility ( $r$ ) was specified as  $0.38 \times 10^{-9} \text{ Pa}^{-1}$ , as was determined for bottlenose whales (Miller et al., 2016c). Body tissue density ( $\rho_{\text{tissue}}$ ) was set a uniform prior from 800 to 1200  $\text{kg m}^{-3}$ . Diving gas volume was set a uniform prior from 5 - 80  $\text{ml kg}^{-1}$ . The prior for the combined drag coefficient term ( $Cd A m^{-1}$ ) was specified using measurements of speed changes during horizontal glides, a novel advance in this methodology. The prior was set to be a normal distribution with mean  $24.0 \times 10^{-6} \text{ m}^2 \text{ kg}^{-1}$  with a standard deviation of  $3.0 \times 10^{-6}$ , truncated within the range of  $5\text{-}50 \times 10^{-6} \text{ m}^2 \text{ kg}^{-1}$ .

#### *Results and Discussion*

The 18 tagged whales spent  $16 \pm 15\%$  of their time in deep dives that exceeded a maximum depth of 250 m (Figure 3-33). Dive duration and dive depth of deep dives ( $> 250 \text{ m}$ ) was  $536 \pm 90 \text{ s}$  and  $444 \pm 85 \text{ m}$ , respectively ( $n = 140$  dives). The maximum dive duration and depth were 821 s and 617 m, respectively. During deep dives (maximum dive depth,  $>250 \text{ m}$ ), tagged pilot whales predominantly employed stroking during ascent ( $20 \pm 10\%$  of descent time was spent gliding,  $n = 140$  dives), and the mean swim speed during ascent phases was  $2.7 \pm 0.3 \text{ m} \cdot \text{s}^{-1}$  (pitch,  $69 \pm 8^\circ$ ,  $n = 135$  dives). In contrast, they employed prolonged glides or stroke-and-glide throughout descent phases ( $63 \pm 18\%$  of ascent time was spent gliding,  $n = 140$  dives), and the average speed was  $2.9 \pm 0.4 \text{ m} \cdot \text{s}^{-1}$  (pitch,  $-59 \pm 8^\circ$ ,  $n = 123$  dives). Drag coefficient was estimated as  $0.0037 \pm 0.0009$ ,

using data from two whales tagged with the speed data logger PD3GT (median  $C_d = 0.0035$ , range =  $0.0022$ – $0.0070$ ,  $n = 31$  glides). We estimated  $C_d$  over a wide range of swim speeds ( $0.7$ – $3.1$   $\text{m}\cdot\text{s}^{-1}$ ). The estimated  $C_d$  was consistent with that of other cetacean species reported to date.

A total of 2018 vertical gliding periods were successfully identified at depths ranging from 1 m to 553 m, with a wide range of swim speed  $0.5$ – $5.7$   $\text{m}\cdot\text{s}^{-1}$ . Most individual tag records had more than 50 glides (range, 26–374). The most parsimonious Bayesian model with the lowest DIC evaluated global plus individual variations in tissue body density and drag terms, as well as global plus dive-by-dive variability in diving lung volume. This is the same model structure identified in the study on northern bottlenose whales (Miller et al., 2016).

The mean global diving gas volume was estimated at  $34.6 \pm 0.6$   $\text{ml}\cdot\text{kg}^{-1}$ , indicating somewhat larger gas volume than that of sperm whales ( $26.4$   $\text{ml}\cdot\text{kg}^{-1}$ ; Miller et al., 2004a) and northern bottlenose whales ( $27.4$   $\text{ml}\cdot\text{kg}^{-1}$ ; Miller et al., 2016). Individual mean of the dive-by-dive estimates ranged between  $27.4$ – $38.9$   $\text{ml}\cdot\text{kg}^{-1}$ . The posterior mean of the global drag term was  $22 \times 10^{-6}$   $\text{m}^2 \text{kg}^{-1}$ , very close to the mean of the prior, indicating that the novel approach of estimating the drag term from horizontal glides might be an effective approach to solve that nuisance term for estimating tissue density.

The global species mean tissue density was estimated at  $1038.8 \pm 1.6$  ( $\pm 95\%$  credible interval)  $\text{kg m}^{-3}$ . Individual posterior mean values for tissue density ranged from  $1034.6$  to  $1044.4$   $\text{kg m}^{-3}$ , with  $\pm 95\%$  credible interval widths of  $0.3$ – $1.6$   $\text{kg m}^{-3}$ . The credible intervals were wider than estimated for northern bottlenose whales, indicating a lower precision and less resolution to measure tissue density changes than in the deeper-diving northern bottlenose whales. Estimated tissue densities of all tagged animals were higher than any of the values recorded for northern bottlenose whales, indicating a very different allostatic strategy as related to overall buoyancy in seawater.

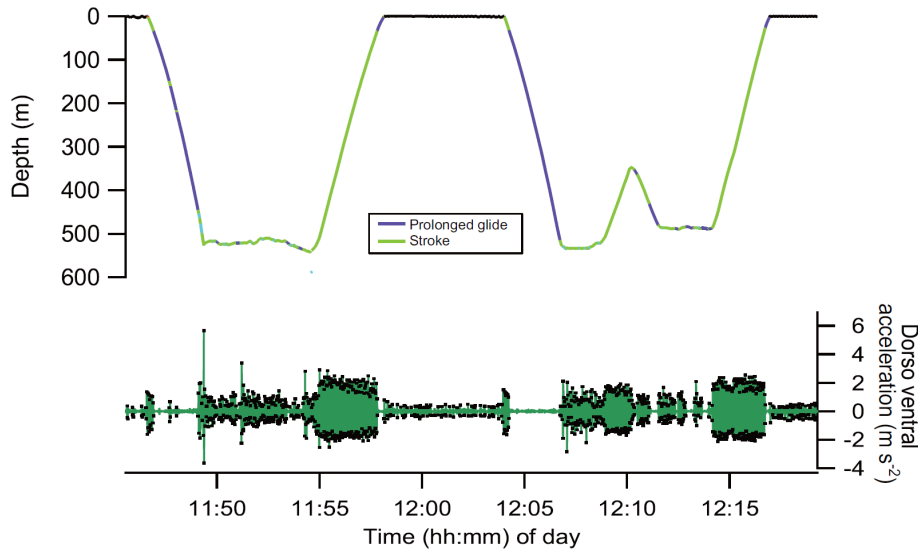


Figure 3-33. Examples of data records of deep dives. Stroking periods during dives (marked in green, top) had lower dorsal-ventral acceleration levels (bottom) than thrusting phases. Note gliding during descent vs stroking during ascent.

### 3.3.5 Measuring Tissue Density of Humpback Whales (*Megaptera novaeangliae*)

In this sub-section we summarize research published in Narazaki et al. (2018), which demonstrated that it is possible to estimate the tissue density of humpback whales using data from Gulf of St Lawrence Canada and Antarctica. In section 3.3.6, we report how humpback whale tissue density varied with respect to season and reproductive status using data from the Gulf of St Lawrence Canada and Norway.

#### Measuring tissue density of humpback whales – highlights

Humpback whale tissue density overall averaged  $1031.6 \pm 2.1 \text{ kg m}^{-3}$ , similar to mean values for northern bottlenose whales, but substantially less dense than was found for long-finned pilot whales. Whales tagged off Antarctica tended to have lower tissue density than whales tagged in the Gulf of St Lawrence, Canada.

Estimated tissue densities of individuals ranged  $1025.2\text{-}1043.1 \text{ kg m}^{-3}$ , much wider than had been measured for northern bottlenose whales or long-finned pilot whales. The precision ( $\pm 95\%$  CI range) of estimates of tissue density values of individual whales ranged from  $0.04 - 4.9 \text{ kg m}^{-3}$ , and was found to be strongly related to the number of glides recorded.

This study demonstrated that it was possible to use the glide method, with data recorded both with the Dtag and with the 3MPD3GT loggers, to estimate the tissue density (as an indicator of body condition) of the relatively shallow-diving humpback whale. The wide range of body density was expected given variation in lipid body stores over the annual cycle of humpback whales.

Field studies were carried out at two geographically distinct summer feeding grounds of humpback whales (*Megaptera novaeangliae*). In the Gulf of St Lawrence, archival tags were deployed on 12 whales in the Jacques-Cartier Passage and adjacent waters between July and September 2011. At the Antarctic field-site, 19 whales were tagged over the course of two field seasons that ran between May and June in both 2009 and 2010. Antarctic animals were tagged in Wilhelmina and Andvord Bays along the WAP and inshore waters of the Gerlache Strait. Animals were actively feeding with lunge events clearly visible in the data records. We discarded glides associated with lunge feeding events.

Each of the four unknown terms in the equation was set a specific prior range. Compressibility ( $r$ ) was specified to be  $0.38 \times 10^{-9} \text{ Pa}^{-1}$  as was determined for bottlenose whales (Miller et al., 2016). A non-informative uniform prior from 800 to 1200  $\text{kg m}^{-3}$  was set for body tissue density ( $\rho_{\text{tissue}}$ ). An informative prior was set for the combined drag coefficient term ( $CdAm^{-1}$ ) based on several sources of information: drag coefficient ( $Cd$ ) was estimated to be 0.0026 based on the value estimated for a fin whale (*Balaenoptera physalus*) swimming at 4  $\text{m s}^{-1}$  (Bose and Lien, 1989). Based on body lengths ( $L$ ) ranges from 6 to 15 m, body mass ( $m$ ) was estimated as 20005 kg on average (range  $3253 \pm 48556$  kg) using an equation derived for humpback whales:  $m = 0.016473L^{2.95} \times 1000$  (Lockyer, 1976). Surface area ( $A$ ) was estimated as  $47.4 \text{ m}^2$  (range  $15.3 \pm 89.0 \text{ m}^2$ ) using a prediction equation obtained from bottlenose dolphins (*Tursiops truncatus*):  $A = 0.08m^{0.65}$  (Fish, 1993). Thus, an expected value for the combined drag term ( $CDAm^{-1}$ ) would be  $7 \times 10^{-6} \text{ m}^2 \text{ kg}^{-1}$ , with a range from  $5 \times 10^{-6} \text{ m}^2 \text{ kg}^{-1}$  for large whales to  $12 \times 10^{-6} \text{ m}^2 \text{ kg}^{-1}$  for small whales. In order to capture uncertainty around this expected value, we specify the prior to be a normal distribution with a mean of  $7 \times 10^{-6} \text{ m}^2 \text{ kg}^{-1}$  and standard deviation of  $2 \times 10^{-6} \text{ m}^2 \text{ kg}^{-1}$  that was truncated at  $1\text{-}20 \times 10^{-6} \text{ m}^2 \text{ kg}^{-1}$ . For diving gas volume ( $V_{\text{airm}^{-1}}$ ), a uniform prior from 5 to 80  $\text{ml kg}^{-1}$  was used.

### Results and Discussion

The humpback whales tagged for this study conducted dives to shallower depths than were recorded for northern bottlenose (3.3.3) or long-finned pilot (3.3.4) whales, with an average maximum recorded depth of  $64.0 \pm 67.2$  m. The depth of glides extracted for analysis ranged from 5.1 to 343.2 m with individual mean ranging  $25.2 \pm 10.8$  to  $97.3 \pm 55.4$  m. Mean swim speed throughout dives was  $1.5 \pm 0.4 \text{ m s}^{-1}$  ( $\pm$  SD). Gliding was observed both during descent and ascent phases although the percentage of time spent gliding varied among whales ranging over 1.5 – 45.2% and 2.8 – 60.0% during descent and ascent phases, respectively. Pitch angles during descent and ascent phases were  $-39.8 \pm 20.6^\circ$  and  $30.6 \pm 22.4^\circ$  on average, respectively.

The most parsimonious Bayesian model with the lowest DIC evaluated global plus individual variations in tissue body density and drag terms, as well as global plus dive-by-dive variability in diving lung volume. This is the same model structure identified in the study on northern bottlenose (Miller et al., 2016) and long-finned pilot (Aoki et al., 2017) using this hierarchical Bayesian method. The concordance of this model structure as the ‘best-fit’ model with the lowest DIC across different species and diverse data-sets indicates that it does successfully capture the expected variation in body density and drag terms across individuals, which diving gas volume is indicated to have dive-by-dive variability.

The best-fitting model with the lowest DIC evaluated global plus dive-by-dive variation in diving gas volume. The posterior mean of global diving gas volume was  $27.7 \pm 1.1 \text{ ml kg}^{-1}$  ( $\pm 95\%$  CI). The dive-by-dive estimates of diving gas volume ranged from 0.03 to 129.2  $\text{ml kg}^{-1}$ , but 90% of

the estimates were within 9.2 – 53.5 ml kg<sup>-1</sup>. Diving gas volume was estimated slightly higher for feeding dives with more than 1 lunge (median = 26.3 ml kg<sup>-1</sup>, range = 2.6 – 110.8 ml kg<sup>-1</sup>) than other dives (median = 21.3 ml kg<sup>-1</sup>, range = 0.8 – 97.5 ml kg<sup>-1</sup>; Wilcoxon rank sum test, p = 0.021). This difference might indicate whales carefully manage their diving gas volumes, possibly to finely regulate their overall buoyancy, rather than always diving on full inspiration.

The posterior mean of the global drag term was  $11.8 \times 10^{-6} \pm 1.6 \times 10^{-6} \text{ m}^2 \text{ kg}^{-1}$  ( $\pm 95\%$  CI). The posterior mean was higher and the distribution had little overlap with the prior distribution that had a mean of  $7.0 \times 10^{-6} \text{ m}^2 \text{ kg}^{-1}$ . This finding indicates that observed drag of gliding humpback whales was greater than was predicted based upon published drag coefficients and humpback whale body dimensions. It is possible that the influence of induced drag due to lift generation, which may be particularly important during gliding at shallow pitch angles, may explain the mismatch of the prior expectation of the combined drag term and its posterior estimate from the data. The lift coefficient of a humpback whale flipper is estimated as 0 – 0.9 through wind tunnel measurements (Miklosovic et al., 2004). Based upon literature values for the surface area ( $A_{\text{Flipper}}$ , 12.20 m<sup>2</sup>) and the aspect ratio ( $AR$ , 5.67) of a humpback whale flipper (Woodward et al., 2006),  $A_{\text{Flipper}}C_L^2/(\pi ARm)$  is estimated as 0 – 22  $\times 10^{-5}$  for a 12-m long whale (see Narazaki et al., 2018 for details). Adding this range of values to  $7 \times 10^{-6}$  (i.e. mean of the  $C_DAm^{-1}$  prior), the combined drag term in the parenthesis is expected to range between  $7 \times 10^{-6}$  and  $29 \times 10^{-6} \text{ m}^2 \text{ kg}^{-1}$  which overlaps with the global drag term estimates in this study ( $11.8 \times 10^{-6} \pm 1.6 \times 10^{-6} \text{ m}^2 \text{ kg}^{-1}$ ,  $\pm 95\%$  CI). This suggests that the mismatch between the prior and  $C_DAm^{-1}$  estimates derived from the addition of the induced drag and that lift-related drag forces should not be ignored for this species or possibly any species that uses shallow pitch angles during glides.

The global body tissue density was estimated as  $1031.6 \pm 2.1 \text{ kg m}^{-3}$ . Individual posterior mean values ranged from 1025.2 to 1043.1 with  $\pm 95\%$  CI of 0.04 – 4.8  $\text{kg m}^{-3}$ . The 95% CI range for individual tissue density estimates decreased with increasing number of 5-s sub-glides in the dataset (Figure 3-34). There was no significant relationship between the 95% CI range and the average depth at which the sub-glides occurred (Spearman’s rank test, p = 0.22).

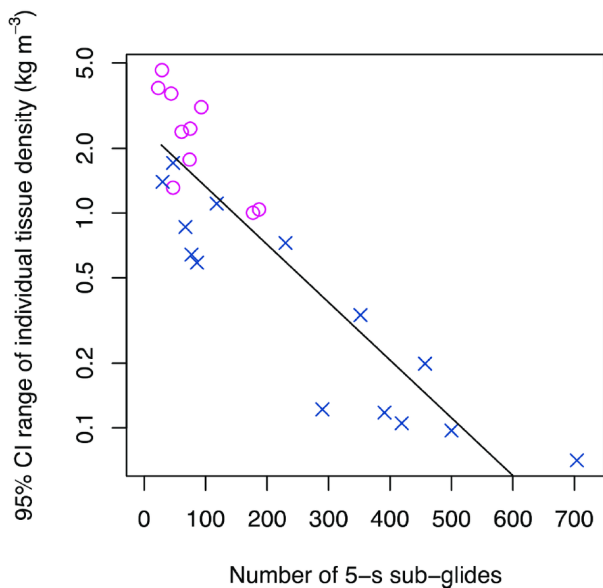


Figure 3-34. The precision of estimates of tissue density (95% CI range of individual estimates) as a function of the number of 5s sub-glides used for analysis.

Whales in the Gulf of St Lawrence had relatively higher tissue density estimates (median = 1034.0  $\text{kg m}^{-3}$ , range = 1026.5 – 1043.1  $\text{kg m}^{-3}$ ) than Antarctic whales (median = 1029.0  $\text{kg m}^{-3}$ , range = 1025.2 – 1040.8  $\text{kg m}^{-3}$ ) although there was high inter-individual variation within each feeding population (Figure 3-35). The posterior mean tissue density of the male Mn11\_H607 that was tagged twice in July and September 2011 in the Gulf of St Lawrence decreased by 5.8

kg m<sup>-3</sup> in 40 days. Tissue densities of two pregnant females were estimated as the lowest (1026.5 ± 0.5 kg m<sup>-3</sup> for Mn11\_H002) and the second lowest (1028.6 ± 0.7 kg m<sup>-3</sup> for Mn11\_H584\_2) among the whales from the Gulf of St Lawrence.

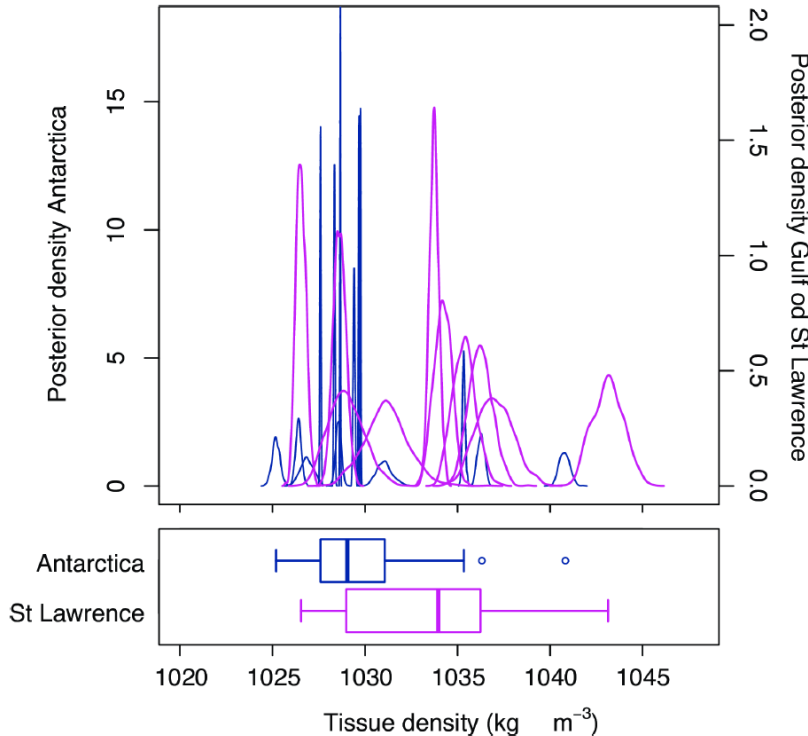


Figure 3-35. Tissue density of humpback whales tagged in Antarctica and the Gulf of St Lawrence, Canada. Note the tendency for whale tissue densities to be higher in the Gulf of St Lawrence. Note also the variation in width of the posterior estimates of body density.

This study represented a test of the capability of the method to estimate tissue density of humpback whales that dive to relatively shallow depths, also at relatively shallow pitch

angles. Both of those factors detract from the method, because gas volumes are more important at shallow depths, and the influence of buoyancy along the axis of movement decreases at shallower pitch angles. It is likely that such factors led to wide 95% CI ranges for some of the tissue density estimates, particularly when there were relatively few glides to use. However the precision of the results was much more fine than the variation across individuals (Figure 3-35). The observed variations in tissue density as a function of feeding location (Antarctica vs Gulf of St Lawrence), timing in the feeding season and reproductive status (especially pregnancy) of individual whales indicate that tissue body density as estimated using the glide method has the potential to be a valuable tool for tracking the lipid-store body condition of relatively shallow diving baleen whales for which annual cycling of lipid stores is a central feature in their physiological ecology.

### 3.3.6 Variation of humpback whale tissue density with season and reproductive status

In this section, we apply the hydrodynamic glide model to estimate body tissue density of humpback whales tagged as part of RC-2337 during early and late feeding seasons in two geographically distinct feeding populations (the Gulf of St Lawrence and Norway). A previous tagging study (Narazaki et al. 2018) showed the hydrodynamic glide model can be applied to shallower diving baleen whales by examining the precision of body density estimates obtained from a narrow depth-range dataset. Thus, this study used similar methods as those demonstrated with cetaceans throughout the project.

During the feeding season, it is essential for humpback whales to accumulate a sufficient amount of energy for survival, growth and/or reproduction. Many studies have investigated seasonal trends in energy storage of several species of baleen whales by means of blubber thickness and morphometric data, reporting that seasonal fattening varies with different sex and age classes, reproductive stages, as well as prey availability (Lockyer et al., 1985; Vikingsson, 1995; Williams et al., 2013). The objective of this study was to examine seasonal differences of body density and how different life history classes vary.

### 3.3.6.1 Materials and Methods - Data collection

Field studies were carried out at two geographically distinct feeding grounds of humpback whales: the Gulf of St Lawrence in Canada and the coastal waters and off the Svalbard Islands of northern Norway. During all fieldwork, in addition to tagging, we sought to collect biopsy samples from tagged individuals, which were analysed to determine the sex and reproductive state of tagged animals. CTD casts were routinely made near the tagging location, and used to calculate ambient seawater density for each glide.

Four types of animal-borne recorders were used: acceleration and speed data-loggers W-3MPD3GT (Little Leonardo Co., Tokyo, Japan), ORI-3MPD3GT (Little Leonardo Co., Tokyo, Japan), ORI-PD3GTC (Little Leonardo Co., Tokyo, Japan) and sound and movement recording DTAGs (Woods Hole Oceanographic Institution, MA, USA). The W-3MPD3GT logger recorded depth, water temperature, 3-axis magnetism and speed from a flywheel at 1-s intervals and 3-axis acceleration at 32 Hz. The ORI-3MPD3GT logger recorded depth, water temperature, speed from a flywheel at 1-s intervals and 3-axis acceleration and 3-axis magnetism at 20 Hz. The ORI-PD3GTC logger recorded depth, water temperature, and speed from a flywheel at 1-s intervals and 3-axis acceleration at 20 Hz. The version-2 DTAGs measured pressure, water temperature, and 3-axis acceleration at 50 Hz, which was later downsampled to 5 or 25 Hz.

#### *Tag Data Analysis*

Diving data were analyzed using software IGOR Pro (Wave-Metrics Inc., Lake Oswego, OR, USA) and MATLAB (MathWorks Inc., Natick, MA, USA). The start and end of dives were defined as the time when the whales descended below and ascended above a depth of 4 m, respectively. All dives (maximum depth:  $\geq 5$  m) were divided into three phases: (1) the descent phase (from the start of the dive to the time when whale's pitch first exceeded  $0^\circ$  (i.e., when it was no longer oriented downward); (2) the ascent phase (from the last time when an animal's pitch was downward ( $<0^\circ$ ) to the end of the dive); and (3) the bottom phase (the time between the end of the descent phase and the beginning of the ascent phase). Dive depth was defined as the maximum depth of the dive. Acceleration in the tri-axis (longitudinal, lateral, and dorso-ventral axes) directions can be divided into components related to the body orientation of the animal with respect to gravity (gravity-based components) and propulsive activities imposed by fluke thrust (specific components; Sato et al., 2003). Lower frequency (mostly gravity-based) acceleration of the longitudinal axis was used to calculate the pitch of a whale (Sato et al., 2003). Higher-frequency specific acceleration of the dorso-ventral and/or longitudinal axis was used to identify stroking (i.e., fluking movements; Sato et al., 2003, for details see also Aoki et al., 2012).

According to power spectral density of each axis, stroking was determined when oscillation on the dorso-ventral and/or longitudinal axis of the accelerometer exceeded a threshold that was set manually for each deployment. Since the accelerometer was not attached exactly parallel to the

axes of the whale, we corrected possible off-axis placement on the body, following Johnson and Tyack (2003). Speed through the water was measured using an external propeller on the Little Leonardo loggers. The propeller rotation count was converted to actual swimming speed ( $\text{m}\cdot\text{s}^{-1}$ ) by using a calibration line obtained from a linear regression of rotation rate against swim speed ( $\text{m}\cdot\text{s}^{-1}$ ), which was calculated from the rate of vertical depth change divided by the sine of the pitch (Sato et al., 2003) when  $\sin|\text{pitch}| \geq 0.7$ . The DTAG lacks a speed sensor; therefore, the speed was estimated using the depth change rate divided by the sine of pitch, when  $|\text{pitch}| \geq 30^\circ$ .

Acceleration during glides was measured using a linear regression line of speed versus time. Observation error measured from variance of acceleration for each 5 s was incorporated in the model by treating acceleration as a normal variable with a precision parameter (1/variance) (Miller et al. 2016). A small increment (0.001) was added to the standard errors to ensure finite values for the precision parameter. Seawater density ( $\rho_{\text{sw}}$ ) for each sub-glide was calculated from a CTD cast that was made close in time and location to each tagged whale. Pitch ( $p$ ), sea water density ( $\rho_{\text{sw}}$ ), and speed ( $U$ ) were averaged during each glide period. Only stable glides (circular variance of roll, pitch, and head  $< 0.1$ ) during descent and ascent phases when absolute pitch was steeper than  $30^\circ$  were included in the analysis. Furthermore, we cut last 15 sec of descent phase and first 15 sec of ascent phases to avoid maneuverability gliding which were possibly caused by feeding.

#### *Statistical Analysis*

The hydrodynamic equation (see equation 1 in section 3.3.1) and Bayesian statistical procedure described in section 3.3.1 which was used successfully used in Miller et al (2016), Aoki et al (2017), and Narazaki et al. (2018) was used for this analysis.

For the Bayesian estimation, a specific prior distribution set set for each unknown parameter. Compressibility ( $r$ ) was specified to be  $0.38 \times 10^{-9} \text{ Pa}^{-1}$  as was determined for bottlenose whales (Miller et al., 2016). A non-informative uniform prior from 800 to 1200  $\text{kg m}^{-3}$  was set for body tissue density ( $\rho_{\text{tissue}}$ ). Following Narazaki et al. (2018), we specify the prior to be a normal distribution with a mean of  $11 \times 10^{-6} \text{ m}^2 \text{ kg}^{-1}$  and standard deviation of  $2 \times 10^{-6} \text{ m}^2 \text{ kg}^{-1}$  that was truncated at  $1 \times 10^{-6} \text{ m}^2 \text{ kg}^{-1}$  and  $29 \times 10^{-6} \text{ m}^2 \text{ kg}^{-1}$  based on information of drag coefficient of other species (0.0026 for a fin whale, Bose 1983; 0.003 for sperm whales, Miller et al. 2004) and possible effect of lift. Estimated body mass ( $m$ ) and surface area ( $A$ ) of tagged animals ( $m = 0.016473L^{2.95} \times 1000$ , Lockyer 1976;  $A = 0.08m^{0.65}$ , Fish 1993). For diving gas volume ( $V_{\text{air}}m^{-1}$ ), a uniform prior from 5 to 80  $\text{ml kg}^{-1}$  was set based on the total lung capacity (65 – 72  $\text{ml kg}^{-1}$ ) estimated for 6 to 15 m long whales using an equation derived from various marine mammals: total lung capacity =  $0.10m^{0.96} \times 1000$  (Kooyman, 1989).

The statistical methodology to examine how seasonal and reproductive status might influence body density was the same as that used for testing LSSAI and cortisol (see sections 3.1.6.4.2 and 3.2.2.2). To test seasonal and individual variation in body condition, body density was specified as a response variable in a generalized linear model (GLM) with age class, sex, reproductive status, and season as explanatory variables. All three metrics were continuous and positive valued, and so were assumed to follow a Gamma distribution. Identity link function was chosen in order to fit linear relationships.

Age and sex were included in the models as three factor covariates, Age\_Class (Calf, Juvenile, Adult, NK [not known]), Age\_Class\_2 (Immature, Adult, NK), and Sex (Male, Female, NK). Including “NK” as a level in the factor covariates allowed the inclusion of the whole dataset for

each condition metric. A significant effect for NK might indicate that the lack of information was biased with respect to individual's age class or sex.

The reproductive status of mature females (Pregnant, Lactating, Resting) was coded as two presence-absence covariates, with an indicator variable (presence-absence of adult female [AF]) that made sure the effect was not applied to other animals in the dataset that were either not mature females, or were of unknown gender and age class. The presence-absence coding allowed the female to be both pregnant and lactating at the same time (N=1 in the dataset).

Seasonality was included in the models as an interaction between the tagging location (Norway vs. Canada) and Julian date (an integer number). Three-way interactions were included to allow the seasonal effect to vary between Age\_Class2, Sex and female reproductive status. We conducted global (all combinations) model selection for each response variable (R package MuMInversion version 1.15.6, function *dredge*).

Multi-model inference was carried out based on a confidence set of models that were within 2 AIC units of the lowest AIC model. We calculated the “importance” of each covariate, which reflects both its prevalence in the confidence set of models, and its influence on the likelihood of the model it was included in. We also report model-averaged coefficients and plot model-averaged predictions from this confidence set (functions *model.avg* and *predict* in package *MuMin*). The model coefficients were calculated based on “full average”, which sets the coefficients of absent variables to zero, rather than excluding them from the average (“conditional average”). The full average ensures that the presence of variables does not bias the model-averaged estimate away from zero.

### 3.3.6.2 Results and discussion

#### **Variation of humpback whale tissue density with season and reproductive status – highlights**

The tissue densities of 59 humpback whales from feeding areas in the Gulf of St Lawrence and northern Norway were successfully estimated using the glide method. The global mean tissue density of the data sample was  $1037.1 \pm 2.6$  ( $\pm 95\%$  credible interval, CI)  $\text{kg m}^{-3}$  and individual posterior mean values for tissue density ranged from 1027.8 to 1050.8  $\text{kg m}^{-3}$ . Denser whales within each study region glided more during the descent phase of dives, as expected.

Statistical analysis indicated that the body density of tagged humpback whales was lower in the late feeding season than that of early feeding season in both areas, with a predicted decrease of  $0.03 \text{ kg m}^{-3}$  per day or  $2.7 \text{ kg m}^{-3}$  per 90 days.

Interestingly, the statistical model did not identify any sex or reproductive status parameters as significant explanatory factors in the model.

We recorded fine-scale underwater movements of 62 humpback whales and obtained a total of 700 hour diving data: 21 individuals tagged with DTAG and 40 individuals tagged with the speed data-logger 3MPD3GT. Maximum dive duration and depth was, 854 sec and 225 m, respectively. A total of 6602 gliding periods were successfully identified at depths ranging from 4 m to 181 m, with a wide range of swim speed  $0.1 - 3.9 \text{ m s}^{-1}$ . Most individual tag records had more than 50 glides (range, 8 – 605; Table 3-13.).

The most parsimonious model with the lowest DIC evaluated global plus individual variation in tissue body density and drag terms, as well as global plus dive-by-dive variability in diving lung volume. The model had a DIC value of 6166, and it decreased from a DIC value of 329973 of the model contained only global values for all three terms. This outcome supports our finding that cetacean body density data varies across individuals, as expected.

From data of 59 whales analyzed, The posterior mean of the global drag term ( $C_D A m^{-1}$ ) was  $11.9 \times 10^{-6} \text{ m}^2 \text{ kg}^{-1}$ , overlapped with the mean of the specified normal prior ( $11 \times 10^{-6} \text{ m}^2 \text{ kg}^{-1}$ ) included the possible effect of induced drag resulted from lift. Relatively large flippers and shallow pitch probably caused large induced drag for this species. Most individual posterior means for the drag term were  $5-25 \times 10^{-6} \text{ m}^2 \text{ kg}^{-1}$  and ranged overall from  $0.3-36.7 \times 10^{-6} \text{ m}^2 \text{ kg}^{-1}$  (Table 2). One tagged whale had a very low posterior mean of the global drag term ( $0.3 \times 10^{-6} \text{ m}^2 \text{ kg}^{-1}$ ) (Table 3-13.). The mean global diving gas volume was estimated at  $37.2 \pm 1.7 \text{ ml kg}^{-1}$ , indicating somewhat larger gas volume than that of sperm whales ( $26.4 \text{ ml kg}^{-1}$ , Miller et al., 2004) and northern bottlenose whales ( $27.4 \text{ ml kg}^{-1}$ , Miller et al., 2016).

The global mean tissue density of the data sample was estimated at  $1037.1 \pm 2.6$  ( $\pm 95\%$  credible interval, CI)  $\text{kg m}^{-3}$  (Figure 3-35). Individual posterior mean values for tissue density ranged from 1027.8 to 1050.6  $\text{kg m}^{-3}$ , with  $\pm 95\%$  credible interval widths of  $0.8-8.3 \text{ kg m}^{-3}$  (Table 3-13.). The tissue body density was higher than that of the ambient sea water ( $1025.3 \pm 2.4 \text{ kg m}^{-3}$ ), indicating that non-gas body tissues are typically denser than seawater. This matches our findings with other cetaceans ( $1030.0 \pm 0.8 \text{ kg m}^{-3}$  for *Physeter microcephalus*, Miller et al. 2004;  $1031.5 \pm 1.0 \text{ kg m}^{-3}$

<sup>3</sup> for *Hyperoodon ampullatus*, Miller et al. 2004;  $1038.8 \pm 1.60 \text{ kg m}^{-3}$  for long finned pilot whales, Aoki et al. 2017). The global mean value for tissue density in this sample was  $1037.1 \pm 2.6$  ( $\pm 95\%$  credible interval), which was higher than the value of  $1031.6 \pm 2.1 \text{ kg m}^{-3}$  reported by Narazaki et al., (2018). This finding indicates a difference in the body densities of the humpback whales in the two analysis datasets. Narazaki's data included whales from Antarctica, which were found to have relatively low tissue density (median =  $1029.0 \text{ kgm}^{-3}$ ). In contrast, this current dataset has substantially more data from early in the feeding season in Norway and the Gulf of St Lawrence, for which animals are expected to have a smaller lipid store and therefore higher body density.

Table 3-13. Details of parameter estimates from the lowest DIC Bayesian model.

Tag ID	No. of Glides	Body density (kg m <sup>-3</sup> )	± 95% CI of body density	CDAM (10 <sup>-6</sup> m <sup>2</sup> ·kg <sup>-1</sup> )	± 95% CI of CDAM
Mn11_H607	39	1037.4	3.1	12.2	2.8
Mn11_H686	75	1036.4	2.5	6.7	4.0
Mn11_H761	43	1030.6	3.9	21.9	14.0
Mn11_H731	60	1035.8	2.5	13.4	4.1
Mn11_H698	61	1033.4	3.0	36.5	15.5
Mn11_H584	46	1028.7	1.4	11.8	3.0
Mn11_H707	98	1043.6	2.9	12.3	3.0
Mn11_H755	181	1032.0	1.0	24.7	1.8
Mn11_H607_sept	29	1032.5	4.7	19.9	23.9
Mn11_H002	184	1027.8	1.2	6.6	6.3
Mn11_H405	89	1033.7	1.6	12.5	1.8
Mn12_H801	9	1036.9	7.1	11.6	15.6
Mn16_023a	14	1035.2	7.8	7.8	21.8
Mn16_177a	32	1049.8	5.2	35.7	7.7
Mn16_178a	10	1042.6	8.4	17.0	11.4
Mn16_248a	424	1040.6	1.7	23.9	4.5
Mn16_250a	27	1036.7	4.9	12.6	4.6
Mn16_258a	45	1028.0	3.3	14.8	6.7
Mn16_Jan19a	89	1038.0	1.9	17.7	5.1
Mn16_Jan25a	400	1037.3	0.7	18.0	1.2
Mn17_022LLa	34	1030.0	1.7	11.5	2.7
Mn17_022LLb	159	1033.1	1.1	16.3	3.5
Mn17_026LLa	21	1033.2	3.4	3.5	6.9
Mn17_165a	414	1032.7	1.4	8.4	3.9
Mn17_184a	151	1038.7	2.4	16.5	3.5
Mn17_186c	150	1033.5	1.8	5.3	3.7
Mn11_157a	77	1039.0	3.3	10.3	12.7
Mn11_158a	295	1041.6	2.1	10.6	3.4
Mn11_160a	313	1043.1	1.7	12.2	2.7
Mn11_165e	278	1034.7	1.6	10.4	3.3
Mn11_176b	87	1036.9	2.9	1.0	3.0
Mn12_158a	605	1038.9	1.2	10.1	1.6
Mn12_164a	152	1042.3	3.1	14.2	13.2
Mn12_164b	24	1039.3	5.8	3.8	10.3
Mn12_170a	157	1036.7	2.3	3.9	6.4
Mn12_170b	153	1037.1	1.9	7.2	3.6
Mn12_180a	85	1046.5	4.0	13.6	7.8
Mn14_121r	85	1039.6	2.4	11.7	4.2
Mn16_175a	88	1032.5	1.5	9.8	4.2
Mn17_158a	83	1030.5	1.8	7.9	4.3
Mn17_174a	177	1033.5	1.5	20.4	4.2
Mn17_180a	133	1036.6	2.1	15.4	3.2
Mn17_180b	92	1043.5	2.9	20.4	3.7
Mn17_186b	101	1038.2	3.0	5.4	4.8
Mn17_186d	68	1031.6	2.2	20.1	4.7
Mn17_190a	277	1035.3	1.7	14.0	2.7
Mn17_191a	111	1032.4	2.2	10.4	5.9
Mn17_178a	208	1034.7	1.4	20.2	2.1
Mn11_165d	80	1035.2	0.8	15.6	1.0
Mn11_165f	58	1039.4	0.7	16.4	1.1
Mn12_161a	8	1037.8	4.8	1.6	5.0
Mn12_171a	197	1039.7	0.7	0.1	0.2
Mn12_171b	142	1042.9	1.4	0.1	0.3
Mn12_178a	118	1048.1	0.9	10.1	1.8
Mn16_021a	42	1035.0	0.8	7.7	1.6
Mn17_018a	125	1042.3	0.4	12.3	0.4
Mn17_026a	99	1038.7	0.8	17.3	1.6

The proportion of time gliding during ascent ( $41 \pm 28 \%$ ,  $n= 4672$  dives) was similar to that of descent ( $42 \pm 30 \%$ ,  $n= 4672$  dives). Changes in tissue density lead to changes in buoyancy that influence swimming patterns of diving animals given strong selection for them to travel efficiently to and from depth (e.g. (Williams et al., 2000)). It is expected that animals with higher density should glide more during descent aided by negative buoyancy whereas less dense positively buoyant animals should employ more glides during ascent. The gliding ratio (ascent minus descent) within both areas tended to decrease with the body density of whales (Figure 3-36), suggesting that the model successfully detected relative differences in individual tissue density.

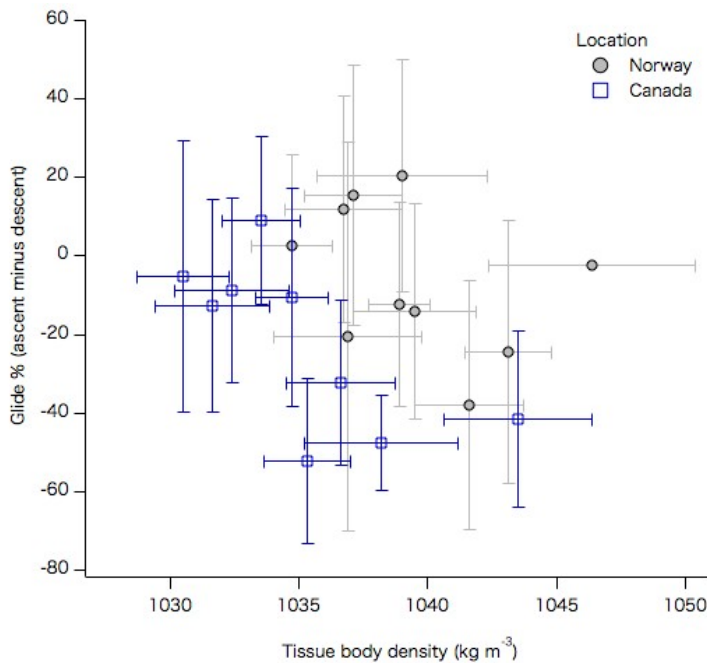


*Figure 3-36. Relationship between gliding patterns and tissue body density. The y-axis indicates differences in the percentage of time spent gliding during ascent and descent phases of relatively deep dives (> 50 m) by each whale. Vertical and horizontal error bars show standard deviation and 95% credible interval range, respectively.*

The body density of tagged humpback whales was lower in the late feeding season than that of early feeding season in both areas (Figure 3-37) as we expected. During the feeding season, it is essential for humpback whales to accumulate a sufficient amount of energy for survival, growth and/or reproduction. The statistical model predicts that the body density decreased by  $0.03 \text{ kg m}^{-3}$  per day in both areas. Norwegian whales started migration from the breeding area and arrived in feeding areas around May-June (Biuw, unpublished data). Some of these whales spend in time in north feeding areas until January. The model predicted body density decreased about  $-5.4 \text{ kg m}^{-3}$  per 180 days. Indeed, mean body density of tagged whales was  $1041.6 \pm 4.2 \text{ kg m}^{-3}$  ( $\pm$ SD,  $n=14$  whales, range  $1035.1 - 1049.6 \text{ kg m}^{-3}$ ) in the early feeding season and  $1035.8 \pm 4.0 \text{ kg m}^{-3}$  ( $\pm$ SD,  $n=13$  whales, range  $1029.1 - 1042.0 \text{ kg m}^{-3}$ ) in the late feeding seasons, respectively. In contrast, Canadian whales arrive on their feeding ground around June to July and stay only until September to October (Ramp et al., 2015). This relative short stay gave a relative small amount of time to accumulate energy. The model predicted body density decreased  $2.7 \text{ kg m}^{-3}$  per 90 days. Mean body density of tagged whales was  $1037.1 \pm 5.1 \text{ kg m}^{-3}$  ( $\pm$ SD,  $n=17$  whales, range  $1030.6 - 1050.6 \text{ kg m}^{-3}$ ) in early feeding season and  $1034.3 \pm 4.6 \text{ kg m}^{-3}$  ( $\pm$ SD,  $n=15$  whales, range  $1027.9 - 1043.5 \text{ kg m}^{-3}$ ) in the middle feeding season, respectively.

Covariates in the confidence set of models included: Season, Location, Julian\_date, Age\_Class\_, Age\_Class2\_, AF, indicating some level of support for those parameters. However, the simplest statistical model only included Julian date and location as a statistically-significant explanatory factor, and this model explained 25 % of the data ( $R^2$ ).

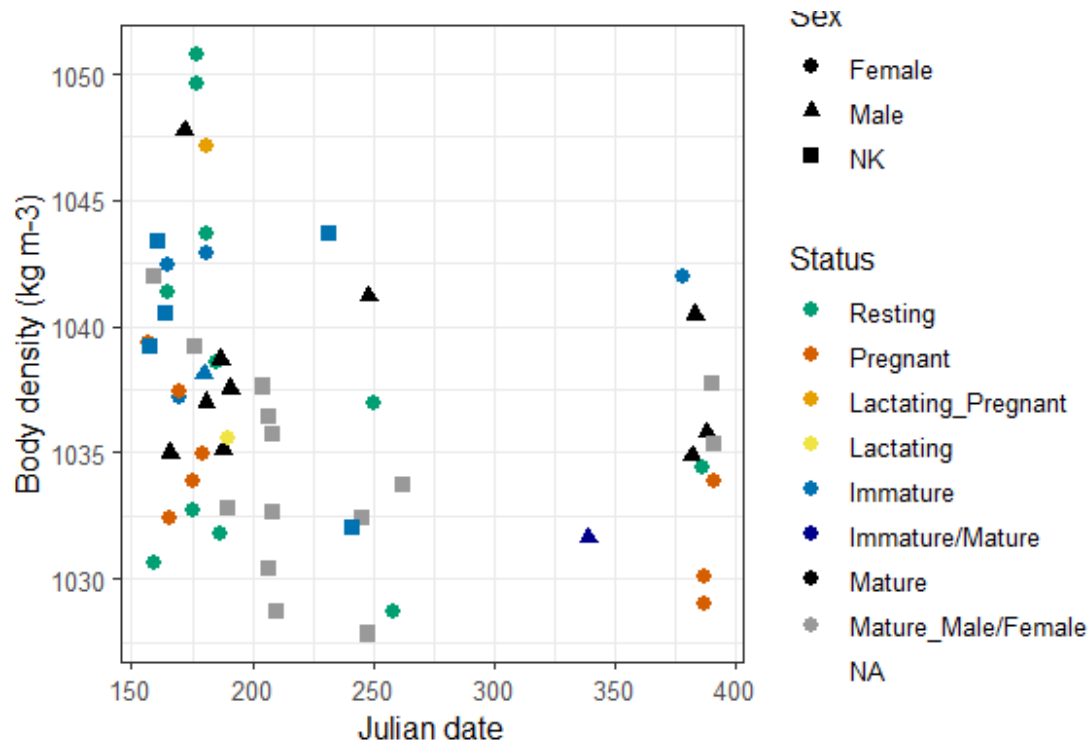


Figure 3-37. Body density of humpback whales in the study as a function of Julian date. The symbol shape indicates the sex of each whale, while the color indicates its reproductive status.

### 3.3.7 Use of humpback whale shape data to improve estimates of body density

In this section, we tested whether the precision of body density estimates increases when an estimate of body dimension (total length) of the tagged whales is available. As detailed in section 3.3.1, the predicted acceleration during each glide is a function of drag and buoyancy forces acting on the body. The amount of acceleration due to drag experienced by a diver depends upon its drag coefficient, surface area, and total mass as the combined drag term  $C_D A m^{-1}$ . Because drag force is a ‘nuisance parameter’ (e.g. see (Biuw et al., 2003)) in the hydrodynamic equation used to derive body density, information which can more finely constrain parameter space of the drag component of total forces operating on the gliding animal is predicted to have some benefit to estimate body density.

We specifically predicted that specification of a narrower prior range for the drag term  $C_D A m^{-1}$  would result in a narrower posterior range, and that the 95% credible intervals (CI) for individual whales would decrease when animal size data were available.

#### Materials and Methods

This analysis made use of a subset of tag data records from northern Norway or the Gulf of St Lawrence for which a total length estimate was available from UAV photogrammetry (section 3.2.2.). Total whale length in pixels was measured from each whale using the number of pixels

measured between the tip of the rostrum and the fluke notch. Length in pixels was converted to length in m using an empirically-measured calibration line (Figure 3-38).

Two different prior distributions were used for the combined drag term, and their outputs compared. A ‘Combined-Drag-Term’ prior matched that used in Narazaki et al. (2018). This prior was a normal distribution with a mean of  $11 \times 10^{-6} \text{ m}^2 \text{ kg}^{-1}$  and standard deviation of  $2 \times 10^{-6} \text{ m}^2 \text{ kg}^{-1}$  that was truncated at  $1 \times 10^{-6} \text{ m}^2 \text{ kg}^{-1}$  and  $20 \times 10^{-6} \text{ m}^2 \text{ kg}^{-1}$  based on information of drag coefficient of other species (0.0026 for a fin whale, Bose 1983; 0.003 for sperm whales, Miller et al. 2004) and possible effect of lift.

The second prior tested was the ‘Simple Drag Term’ model which was based upon information for each parameter, including measurements of the lengths of each whale. An informative prior was set for the drag coefficient ( $C_D$ ) based on several sources of information: drag coefficient ( $C_D$ ) was estimated to be 0.0026 for a fin whale (*Balaenoptera physalus*) swimming at  $4 \text{ m s}^{-1}$  (Bose, 1989), 0.0029 for killer whales (Fish 1998), 0.0026 for bottlenose whale (Fish 1998), 0.003 for sperm whales (Miller et al. 2004) and 0.0035 for long-finned pilot whales (Aoki et al. 2017). To consider uncertainty, we specify the prior to be a normal distribution with a mean of 0.003 and standard deviation of 0.001 that was truncated at 0.0005 and 0.02 for the drag coefficient ( $C_D$ ). Based on body lengths ( $L$ ) measured by drone images from 10.1 to 15.7 m, body mass ( $m$ ) was estimated using an equation derived for humpback whales:  $m = 0.016473L^{2.95} \times 1000$  (Lockyer 1976). Surface area ( $A$ ) was estimated using a prediction equation obtained from bottlenose dolphins (*Tursiops truncatus*):  $A = 0.08m^{0.65}$  (Fish 1993).

A non-informative uniform prior from 800 to  $1200 \text{ kg m}^{-3}$  was set for body tissue density ( $\rho_{\text{tissue}}$ ). For diving gas volume ( $V_{\text{air}} \text{ m}^{-1}$ ), a uniform prior from 5 to  $80 \text{ ml kg}^{-1}$  was set based on the total lung capacity ( $65 - 72 \text{ ml kg}^{-1}$ ) estimated for 6 to 15 m long whales using an equation derived from various marine mammals: total lung capacity =  $0.10m^{0.96} \times 1000$  (Kooyman 1989).

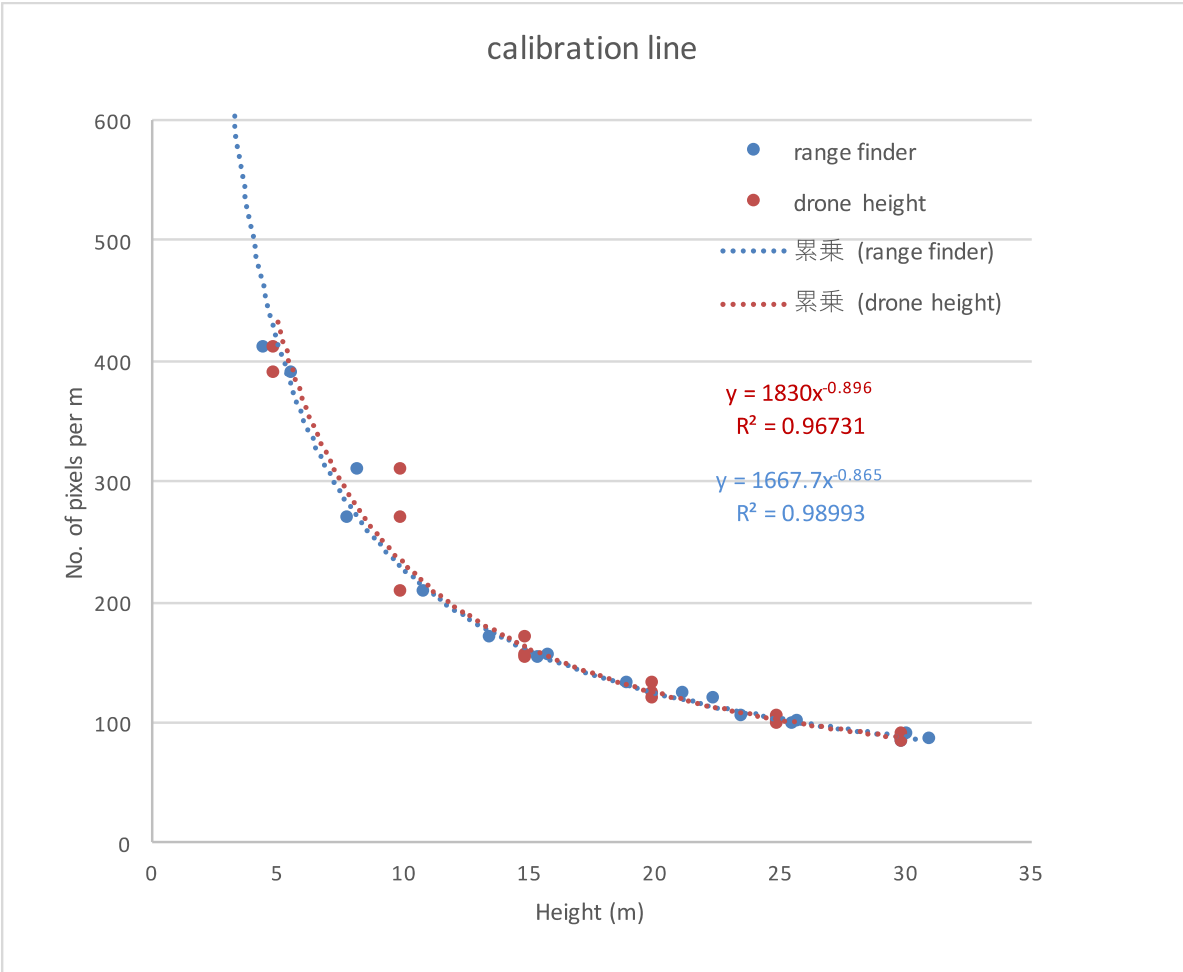


Figure 3-38. Empirically-measured calibration of the number of pixel per m vs UAV height. Note the close correspondence of height estimated by the drone and a laser range-finder.

### 3.3.7.1 Results and discussion

#### **Use of humpback whale shape data to improve estimates of body density – highlights**

The tissue densities of 15 tagged humpback whales estimated from feeding areas in the Gulf of St Lawrence and northern Norway for which the tagged whale length was measured using UAV data (section 3.2). Models were run using standard priors used in previous studies, and compared to results when informed priors using whale measurements were used.

Neither the absolute values of the tissue densities estimates, nor their 95% CI, differed when prior information using whale dimensions was used to create a more informative prior. Other factors such as the number of glides used in the analysis had a larger impact on the magnitude of the 95% CI.

The results of this section indicate that the Bayesian estimation procedure is largely effective at estimating the unknown combined drag term, even without individual whale dimensions. Estimates for  $Cd$  as a specific parameter can be obtained when whale dimensions are available, which would add value to any study using these methodologies.

A total of 2046 glides was obtained from 15 tagged humpback whales. We examined whether the precision of body density estimation increases using absolute body length of tagged animals measured from Drones (simple drag term models) compared with existing models (combined drag term models, Narazaki et al. 2018).

#### *Combined drag term models*

The parsimonious model with the lower DIC evaluated global plus individual variations in tissue body density and drag terms, as well as global plus dive-by-dive variability in diving lung volume (as was found for all other evaluations of this model structure with other species). The model had a DIC value of 4250, and it decreased from a DIC value of 4680 of the model 1 containing only global values (i.e., fixed values) for combined drag terms.

The global mean tissue density was estimated at  $1035.7 \pm 4.7$  ( $\pm 95\%$  credible interval)  $\text{kg}\cdot\text{m}^{-3}$ . Individual posterior mean values for tissue density ranged from 1028.8 to 1044.8  $\text{kg}\cdot\text{m}^{-3}$ , with  $\pm 95\%$  credible interval widths of 0.8–4.9  $\text{kg}\cdot\text{m}^{-3}$  (Table 3-14.).

The posterior mean of the global drag term ( $C_D A \cdot m^{-1}$ ) was  $11.6 \times 10^{-6} \text{ m}^2 \cdot \text{kg}^{-1}$ , overlapping, but slightly higher than the mean of the specified normal prior ( $7.0 \times 10^{-6} \text{ m}^2 \cdot \text{kg}^{-1}$ ). This might be because the effect of induced drag as Narazaki et al. (2018). Suggested. Individual posterior means for the drag term ranged overall from  $4.6 \times 10^{-6} \text{ m}^2 \cdot \text{kg}^{-1}$  to  $21.2 \times 10^{-6} \text{ m}^2 \cdot \text{kg}^{-1}$  (Table 3-14).

#### *Simple drag term models*

The model 12 had a DIC value of 4270, and it decreased from a DIC value of 4720 of the model 1 containing only global values (i.e., fixed values) for the drag term. The global species mean tissue density was estimated at  $1035.7 \pm 4.7$  ( $\pm 95\%$  credible interval)  $\text{kg}\cdot\text{m}^{-3}$ . Individual posterior mean values for tissue density ranged from 1029.0 to 1044.8  $\text{kg}\cdot\text{m}^{-3}$ , with  $\pm 95\%$  credible interval widths of 0.81–4.7  $\text{kg}\cdot\text{m}^{-3}$  (Table 3-14). Thus, there was little difference in the tissue density estimates across the two types of models.

Table 3-14. Estimates of body density and drag term for both simple drag term model and combined drag term model.  $C_D$  was also calculated from the  $C_{DAM}$  term in the combined drag term model.

ID	Body length (m)	No. of glides	Simple drag term model		Combined drag term model		
			Body density (kg m <sup>-3</sup> )	$C_D$	Body density (kg m <sup>-3</sup> )	$C_{DAM}$ (10 <sup>6</sup> m <sup>2</sup> ·kg <sup>-1</sup> )	Calculated $C_D^*$
mn16_250a	13.3	41	1037.3 ± 4.7	0.006 ± 0.002	1037.1 ± 5.0	12.7 ± 4.7	0.006
mn16_258a	13.9	76	1029.0 ± 3.2	0.008 ± 0.003	1028.8 ± 3.4	15.0 ± 7.2	0.008
mn17_026a	11.8	99	1038.7 ± 0.8	0.007 ± 0.001	1038.7 ± 0.8	17.3 ± 1.7	0.007
mn17_026LLa	12.9	21	1033.9 ± 3.6	0.002 ± 0.003	1033.8 ± 3.5	4.6 ± 7.0	0.002
mn17_158a	12.9	84	1030.9 ± 1.8	0.004 ± 0.002	1030.9 ± 1.8	8.5 ± 4.2	0.004
mn17_165a	15.2	444	1033.7 ± 1.6	0.005 ± 0.002	1033.7 ± 1.6	9.5 ± 3.9	0.005
mn17_174a	15.7	181	1034.5 ± 1.6	0.012 ± 0.002	1034.5 ± 1.7	21.2 ± 4.3	0.012
mn17_178a	11.3	211	1035.5 ± 1.5	0.008 ± 0.001	1035.5 ± 1.5	20.8 ± 2.1	0.008
mn17_180a	12.9	145	1037.5 ± 2.3	0.008 ± 0.002	1037.5 ± 2.3	16.4 ± 3.6	0.008
mn17_180b	11.1	99	1044.8 ± 3.4	0.008 ± 0.002	1044.8 ± 3.4	21.1 ± 4.0	0.008
mn17_184a	12.9	152	1039.4 ± 2.3	0.008 ± 0.002	1039.4 ± 2.2	17.3 ± 3.4	0.008
mn17_186b	13.3	108	1039.7 ± 3.2	0.003 ± 0.002	1039.5 ± 3.4	6.9 ± 4.9	0.003
mn17_186c	12.7	152	1034.0 ± 1.9	0.003 ± 0.002	1033.9 ± 1.8	5.9 ± 3.4	0.003
mn17_186d	10.1	68	1032.2 ± 2.3	0.008 ± 0.002	1032.1 ± 2.2	20.8 ± 4.7	0.008
mn17_190a	15.2	278	1036.2 ± 1.8	0.008 ± 0.002	1036.2 ± 1.8	15.1 ± 2.9	0.008

Although the drag coefficient shouldn't be different very much between individuals because of similar morphology of tagged animals, individual posterior means for the drag term varied widely and ranged overall from 0.0022-0.0122 (Table 3-14). This might be caused by induced drag from lift generation by the flippers. According to Narazaki et al. (2018), combined drag term including induced drag is:

$$- 0.5\rho_{sw} \left( \frac{C_D \cdot A}{m} + \frac{A_{Flipper}}{\pi \cdot AR} \cdot \frac{C_L^2}{m} \right) v^2$$

where  $A_{Flipper}$  is flipper surface area (m<sup>2</sup>),  $AR$  is flipper aspect ratio and  $C_L$  is the lift coefficient. Based upon literature values for the surface area of flippers ( $A_{Flipper}$ , 12.20 m<sup>2</sup>) and the aspect ratio ( $AR$ , 5.67), body surface area ( $A$ , 68.2 m<sup>2</sup>) of a humpback whale whose body length 13.5m (Woodward et al., 2006), body surface area ( $A$  m<sup>2</sup>) is approximately 5.6 times of the surface area of flippers ( $A_{Flipper}$  m<sup>2</sup>). Thus, above equation can be changed to:

$$- 0.5\rho_{sw} \left( C_D + \frac{A_{Flipper}}{5.6\pi \cdot AR} \cdot C_L^2 \right) \cdot \frac{A}{m} \cdot v^2.$$

The lift coefficient of a humpback whale flipper is estimated to be 0–0.9 through wind tunnel measurements (Miklosovic et al. 2004). Adding this value to 0.003±0.001 (i.e. mean of the  $C_D$  prior), the simple drag term in the parenthesis is expected to range between 0.002 and 0.104 which overlaps with the individual drag term estimates we obtained here ( $C_D$  0.0022-0.0122).

### Comparison of simple and combined drag term models

The estimated body densities and their credible interval widths did not differ much between the models that used the simple drag term model compared to models that used the combined drag term model (Table 3-14). By substituting body mass and surface area estimated from body length for the  $C_D A m^{-1}$  term, drag coefficient  $C_D$  was back calculated from the  $C_D A m$  term of combined drag term model. The estimated  $C_D$  was consistent with that derived from the simple drag term (Table 3-14).

The 95% credible interval of both models tended to decrease with no. of glides for both models (Figure 3-39) as was found by Narazaki et al. (2018). However, contrary to our prediction, there was no consistent reduction in the 95% credible interval when the simple drag model (which used the measured dimension of each whale) was used (Figure 3-39). This indicates combined drag term models can estimate both unknown drag coefficient and induced drag even if the model doesn't know the body mass and surface area of animals.

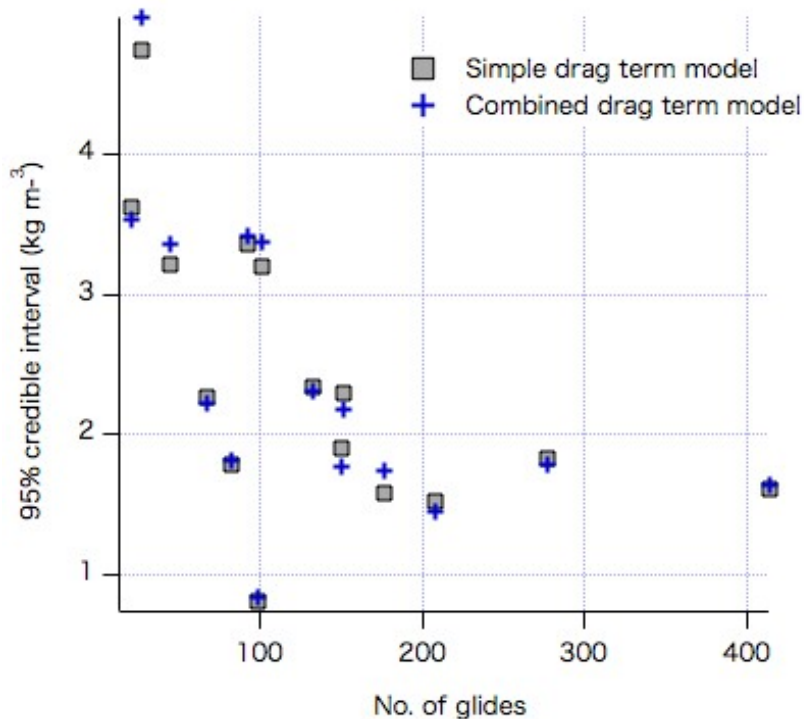


Figure 3-39. The 95% credible interval related with no. of glides. Gray squares show the credible interval values from the simple drag term model, while blue crosses show the values from the combined drag term model. Note there was no consistent difference in the values depending upon which drag term model was used.

## 4 CROSS-COMPARISON OF THREE BODY CONDITION INDICATORS

A central goal of RC-2337 was to compare and contrast the three different body condition indicators which were independently developed during the study (Section 3). To the extent possible given logistical constraints, we aimed to collect a consistent data sample each subject whale (Figure 4-1). Ultimately, this data-collection effort was successful with the easier-to-study humpback whales. While some biopsy samples were simultaneously collected during tagging of northern bottlenose whales off Jan Mayen, the sample was not sufficient for statistical contrast of body density versus cortisol concentrations in that species. Given the general inability to follow and re-sight northern bottlenose whales, we did not attempt to collect UAV drone images of tagged northern bottlenose whales.

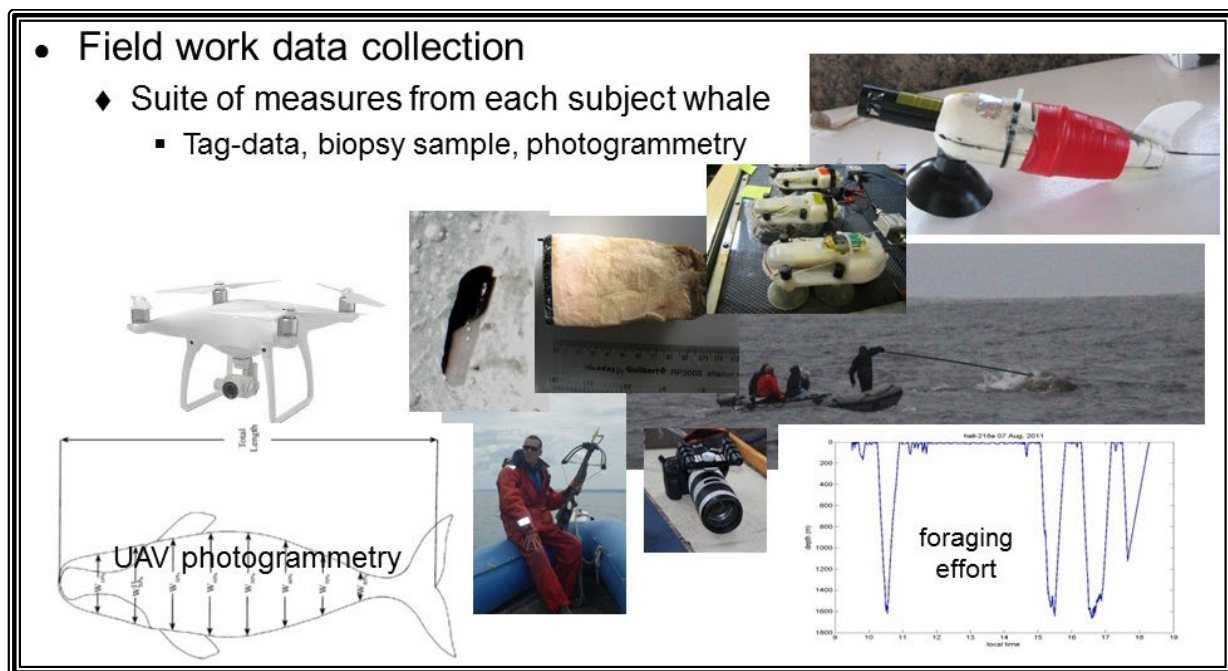


Figure 4-1. Illustration of the fieldwork efforts undertaken for RC-2337 to enable a contrast of three independent indicators of lipid-store body condition. From each subject whale found randomly in the study area, we sought to obtain three data samples: 1) tag-data using suction cup tags attached with poles (top-right), 2) biopsy samples of skin and external blubber layers collected using standard sample darts (center), and 3) photogrammetry images above whales using the UAV (lower-left). The three data samples were used to measure tissue density, cortisol concentration, and length-standardized surface area index (LSSAI) indicators of body condition, respectively.

For humpback whales, these samples were then used to calculate three candidate indicators of body condition based upon detailed evaluation of each method (section 3): tissue density, cortisol concentrations in blubber, and length-standardized surface area index (LSSAI).

In this section, we specifically contrast the three different body condition indicators developed in the study.

#### 4.1 Materials and methods

Data were collected from individual humpback whales to the extent feasible (Figure 4-1) and processed as detailed in section 3. Values for tissue density, cortisol concentration, and LSSAI were tabulated for each individual. The reproductive status of each whale was quantified based upon progesterone concentrations and observation of calf presence. We were not able to collect all three samples types from all whales, and in some cases samples that were obtained were not of sufficient quality to allow for derivation of the body condition indicator (i.e. due to too short a tag record). Therefore, separate statistical tests were run to assess the relationship between each pair of body condition indicators. This was done to make full use of all data where the two relevant body-condition indicators were available. A total of 33 whales had both body density and cortisol concentration estimates, 20 had both body density and LSSAI, and 25 had both cortisol concentration and LSSAI. Standard data plots showing the data encoded by reproductive status of each individual were prepared, with trends within each class of reproductive status shown for illustration of data patterns.

For statistical examination of the relationship between each of the pairs of body condition indicators, all data were correlated against each other using Pearson's product-moment correlation. A GLM approach was also used so that pregnancy could be included in the statistical model as an interaction (and therefore allow different correlation between females that were confirmed pregnant vs. other whales). Pregnancy is a particularly important reproductive state, in which females are expected to deposit large lipid stores to prepare for lactation demand, so was chosen a-priori as the key reproductive state to examine in these contrasts. Pregnancy was also useful to include in the models to account for any physical effects that a fetus could have on the shape or total body tissue density of the animal. The response variable was chosen arbitrarily for the three tests: body density ~ cortisol, body density ~ LSSAI, cortisol ~ LSSAI. Gamma distribution was assumed with an identity link function.

## 4.2 Results and discussion

### Cross-comparison of three body condition indicators – highlights

The strongest correspondence across the three pairs of indicators was between tissue density and LSSAI, for adult humpback whales with a statistically-significant relationship (Pearson's  $r^2=29.9\%$ ,  $p=0.019$ ,  $N=18$ ) in the predicted direction. Adult humpback whales that had measurably wider length-standardized surface areas had lower tissue density. This pattern was consistent across reproductive state, but measurements from two juvenile whales did not follow the trend observed for adult whales.

In contrast, cortisol concentration in blubber did not correlate strongly with either tissue density or LSSAI. Among pregnant females, whales with higher cortisol concentrations in their blubber tended to have lower body density.

These results indicate that tissue density and LSSAI correspond as effective indicators of body condition. Cortisol concentrations did relate to body condition in stranded specimens (section 3.1), but no clear relationship between cortisol concentration and the other body condition indicators was found here for free-ranging humpback whales.

#### 4.2.1 The relationship of tissue density with cortisol concentration

Pearson's production moment correlation estimate was  $r = 0.0$ ,  $N = 33$  (indicating no relationship body density to have higher cortisol concentrations in their blubber. Examination of the data indicated some variation across reproductive status classes (Figure 4-2).

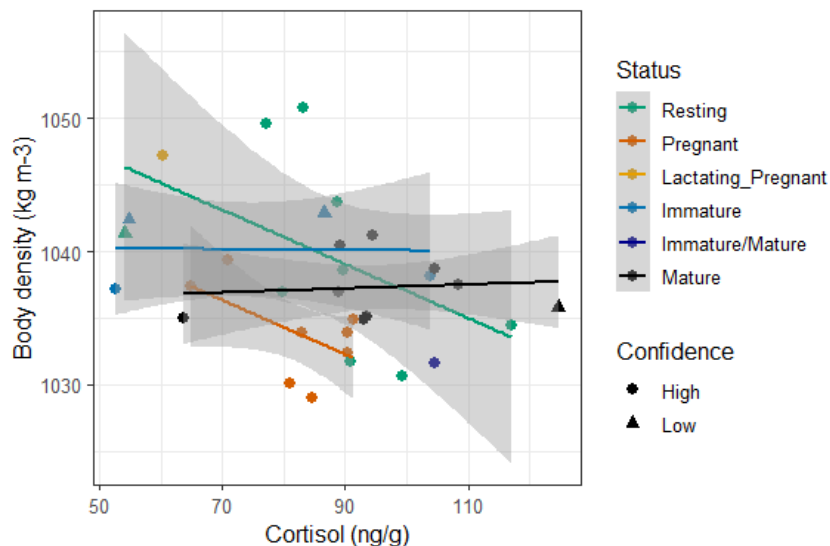


*Figure 4-2. Body density versus blubber cortisol concentration in humpback whales. Trend lines with confidence intervals are plotted for data from whales within each reproductive status class. Note the variation in trends across reproductive status.*

(Table 4-1). This indicates that pregnant humpback whales had a distinct negative correlation between body density and cortisol concentration compared to whales in other reproductive states. Pregnant humpback whales with high cortisol levels in their blubber tended to have lower body density (which should indicate greater overall lipid stores).

The GLM analysis indicated a statistically significant interaction term with pregnancy as a co-factor

Table 4-1. Analysis of deviance table for body density versus cortisol concentration. \*Significant.

Response: BD mean ~ Cortisol			
	LR Chisq	Df	Pr(>Chisq)
Cortisol	0.0954	1	0.7574
Pregnant	3.2201	1	0.07271
Cortisol:Pregnant	5.4404	1	0.01968 *

*The relationship of tissue density with LSSAI*

Examination of the data indicated the same negative trend observed for whales in all reproductive states, with only minor differences in negative slope (Figure 4-3). However, the values for immature humpback whales were clearly outside the distribution of values for adult humpback whales. We therefore here report the correlation for adult humpback whales, excluding the two immature data-points.

The Pearson’s production moment correlation estimate for adult humpback whales was  $r = -0.55$ , indicating a significant trend ( $p = 0.019$ ,  $r^2 = 0.299$ ,  $N = 18$ ) for animals with lower body density to have higher length-standardized surface area.

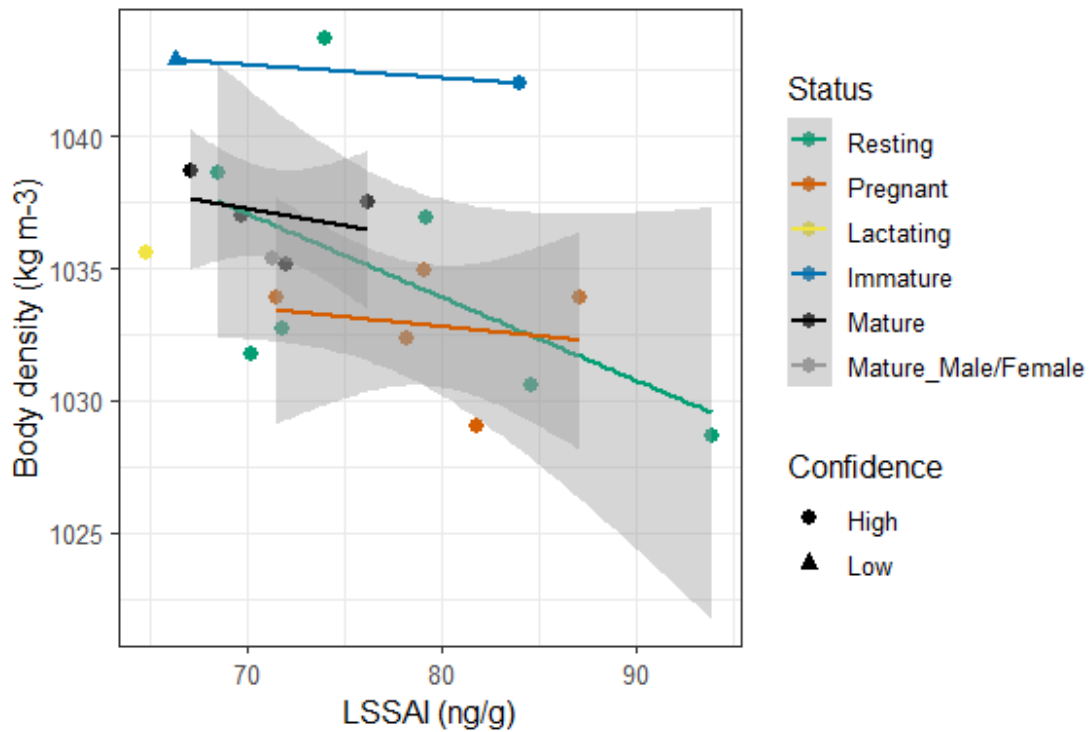


Figure 4-3 . Body density versus LSSAI in humpback whales. Trend lines with confidence intervals are plotted for data from whales within each reproductive status class. Note the consistent negative trend across reproductive status in the dataset, and the outlier status of immature animals.

The GLM analysis did not find a statistically significant interaction term with pregnancy, so the GLM model was evaluated without any interaction (Table 2). The statistically significant relationship indicates that whales with higher LSSAI values had statistically-significantly lower body density values. This relationship follows the predicted pattern that animals with greater lipid stores are predicted to have lower body density and higher surface area per unit length (LSSAI).

Table 4-2. Analysis of deviance table for body density versus LSSAI for adult humpback whales.  
 \*\* Significant

Response: BD_mean ~ LSSAI			
	LR Chisq	Df	Pr(>Chisq)
LSSAI	6.8515	1	0.008857 **

#### 4.2.1.1 The relationship of cortisol concentration with LSSAI

Pearson’s production moment correlation estimate was  $r = +0.17$ , indicating no significant relationship ( $p = 0.42$ ,  $R^2 = 0.03$ ,  $N = 33$ ) between LSSAI and cortisol concentrations indicators of body condition. Examination of the data indicated no strong relationship within any of the reproductive status classes investigated (Figure 4-4).

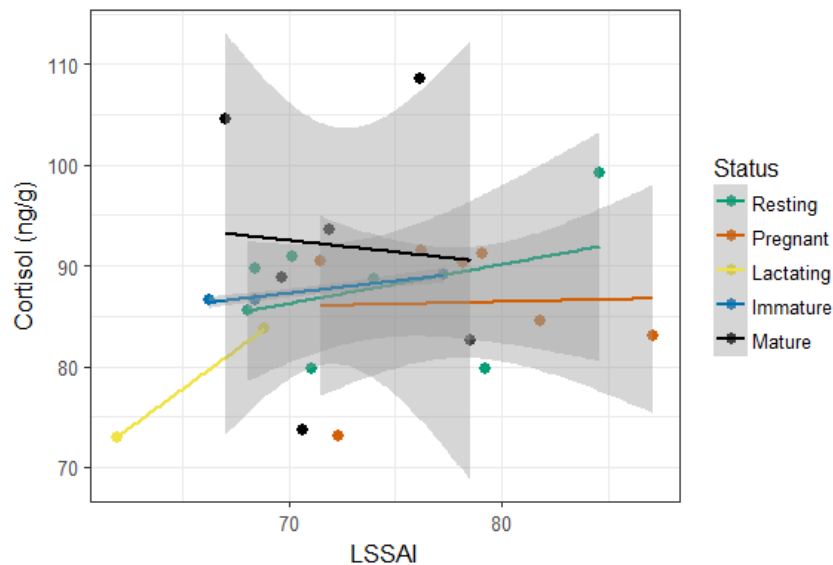


Figure 4-4. Blubber cortisol concentration versus LSSAI in humpback whales. Trend lines with confidence intervals are plotted for data from whales within each reproductive status class. Note the lack of clear trend for any reproductive status.

The GLM analysis did not find a statistically significant interaction term with pregnancy, so the GLM model was evaluated without any interaction (Table 4-3). This indicates no observed relationship between cortisol concentrations in blubber and length-standardized surface area (LSSAI) in humpback whales.

Table 4-3. Analysis of deviance table for cortisol concentration versus LSSAI.

Response: Cortisol ~ LSSAI			
	LR Chisq	Df	Pr(>Chisq)
LSSAI	0.70511	1	0.4011

## 5 PATTERNS OF BEHAVIOUR IN RELATION TO BODY CONDITION IN CETACEANS

### 5.1 Introduction

Most of the focus of RC-2337 has been on refining, and validating independent indicator of lipid-store body condition in free-ranging marine mammals as a tool to measure health of individual cetaceans at sea using minimally-invasive or non-invasive procedures. We typically consider that individual health, such as energy store status, is a consequence of behavioral patterns that affect energy balances. In this final data section, we use data from tags attached to whales using suction cups to evaluate if and how body condition may also be a driver of behavior patterns in cetaceans.

Theory and data both suggest that body condition should influence how individuals trade-off foraging and anti-predator behaviors (Hilton et al., 1999; Mcnamara and Houston, 1990), with poor condition foragers taking greater risks in order to increase foraging rates. This leads to the prediction that cetaceans should have some ability to adjust their foraging effort to recover their desired body condition, or to maintain “allostasis” (McEwen and Wingfield, 2003). Thus, individuals whose body condition is poor are predicted to have some capacity to compensate for those effects (Figure 5-1), though the effort of compensation could have its own costs, such as increased predation risk.

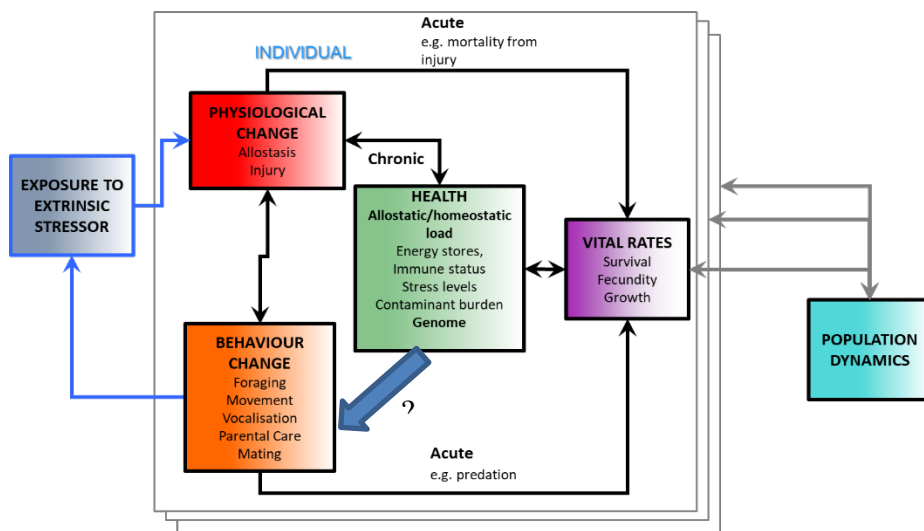


Figure 5-1. A conceptual framework to link responses to extrinsic stressors to vital rates of individuals and populations. ‘Health’ links the physiology of individuals to their ability to survive, grow, and reproduce. The focus of this chapter is how behavior patterns (focusing on foraging effort) might be driven by energy store body condition (blue arrow). Image adapted from NRC, 2016.

For animals like beaked whales that face predation risk from killer whales, behaviours that increase an animal's foraging efficiency often increase its risk of being predated upon (Lima, 1998b). Thus animals must balance the risk of predation against the risk of starvation (Houston et al., 1993; Lima and Dill, 1990; Mcnamara, 1990; Mcnamara and Houston, 1987; Sih, 1980). Body condition is central to the starvation-predation trade-off (Bednekoff and Houston, 1994; Houston et al., 1993; Pond, 1992). Animals in poorer condition are expected to take more predation risks in exchange for increased energy intake (Krebs and Davies, 1981), Lima 1998). Condition-dependent risk taking concepts have been long established (Anholt and Werner, 1995; Mcnamara and Houston, 1987; Sinclair and Arcese, 1995), yet the influence of body condition on the starvation-predation trade-off has been little explored in marine ecosystems (Heithaus et al., 2007b). Despite the starvation-predation trade-off influencing the Darwinian fitness of virtually all animals (Houston et al., 1993; Lima, 1998; Lima and Dill, 1990), little work has been done on this topic in among cetaceans (but see (MacLeod et al., 2007).

Humpback whales, one of the largest baleen whales, are a group of marine mammals that cycle fat stores on an annual basis, substantially changing their appearance, behaviour, and fitness (Kasuya, 1995). Adult humpback whale are not thought to face much predation risk from killer whales, though calves might be at greater risk (Jefferson et al., 1991; Pitman et al., 2015). Humpback whales are predicted to reduce feeding once they have stored enough body fat to achieve long migration efficiently. In this case, energy store status modifies behavior as the animal seeks to maintain "allostasis" (McEwen and Wingfield, 2003) and avoid the costs of becoming too fat.

Though the basis for the prediction differs among our two study species, we predict that both northern bottlenose and humpback whales should reduce their foraging effort with improved body condition. In subsection 5.2, we evaluate if and how body density might influence the starvation-predation tradeoff in bottlenose whales. In Subsection 5.4, we assess how humpback whale foraging effort changes as a function of body condition. For both studies, we used body density derived from animal-attached tag data as an index of body condition.

## 5.2 Northern bottlenose whale body condition and the starvation-predation trade-off

Condition-dependent risk taking has long been of interest to behavioural ecologists (Brodersen et al., 2008; Ekman and Hake, 1990; Godin and Sproul, 1988; Heithaus et al., 2007a; Houston and Mcnamara, 1993; Hughes, 2009; Mcnamara and Houston, 1987; Richards, 1983), yet few studies have explored the role of energy-store body condition on the starvation-predation trade-off of upper trophic marine animals (MacLeod et al., 2007). Heithaus et al. (2007a) revealed that green sea turtles in poor body condition took more risks, selecting habitats with higher shark predation risk but more profitable prey, whereas turtles in good body condition avoided high risk habitats at the cost of less efficient foraging (Heithaus et al., 2007a). This follows in-line with the starvation-predation trade-off theory (Lima, 1998a): animals of poorer condition accept more predation risks to forage and reduce starvation risk.

Despite being one of the least known mammalian families (Hooker and Baird, 1999a; Lacsamana et al., 2015; New et al., 2013b), beaked whales (*Ziphiidae*) are ideal for exploring how upper trophic marine animals manage the starvation-predation trade-off. Beaked whales are amongst the best studied in terms of how wild animals use echolocation to hunt (Madsen et al., 2014). A range of highly detailed foraging behaviours have been revealed (Arranz et al., 2011; Johnson et al.,

2008; Johnson et al., 2004; Johnson et al., 2006; Wahlberg et al., 2011). Terminal acoustic buzzes, i.e. fast echolocation click trains, with high pulse repetition rate and short pulse duration (Madsen et al., 2005), are routinely used as a proxy for beaked whale prey capture attempts (Arranz et al., 2011; Baumann-Pickering et al., 2015; Dunn, 2014; Dunn et al., 2013; Gassmann et al., 2015; Johnson et al., 2006; Madsen et al., 2014; Miller et al., 2015c; Stimpert et al., 2014; Tyack, 2015; Wahlberg et al., 2011; Zimmer et al., 2005). Several studies have revealed a range of possible beaked whale anti-predation behaviours by describing natural behavior patterns (Tyack et al., 2006; Zimmer and Tyack, 2007) and by experimentally exposing beaked whales to sonar (DeRuiter et al., 2013; Miller et al., 2015c; Stimpert et al., 2014; Tyack et al., 2011). Behaviours linked to reducing predation risk include: acoustic crypsis, prolonged long ascents from deep foraging dives and bounce dives (a series of relatively shallow silent dives in-between deep foraging dives) (Aguilar de Soto et al., 2012; Miller et al., 2015c; Tyack et al., 2006b; Zimmer and Tyack, 2007). Such behaviours are thought to avoid visual and acoustic detection from relatively shallow diving killer whales (Jefferson et al., 1991; Zimmer and Tyack, 2007), the main predator of *Ziphiidae* species (Allen et al., 2014; Jonsgård, 1968a, b; Notarbartolo-di-Sciara, 1987; Wellard et al., 2016).

This study aims to evaluate the starvation-predation trade-off in northern bottlenose whales by determining the relationship between body condition and the trade-off between foraging and anti-predation behaviours. The body condition of northern bottlenose whales will be estimated as body density using hydrodynamic models (Miller et al., 2016a). Foraging measures will be estimated from bio-logging tags deployed around Jan Mayen, revealing the behaviour of the little studied north-eastern Atlantic population (Whitehead and Hooker, 2012). A range of measures representing predation avoidance will be defined, based upon previously described candidates for anti-predation behaviour (Dunphy-Daly et al., 2010; Wirsing et al., 2011). As has been done for social behavioural studies (Sapolsky et al., 1997; Silk et al., 2003), multiple behavioural measures will be combined as composite indices.

In line with the starvation-predation trade-off (Houston et al., 1993), it is hypothesized that an increase in the foraging behaviour index will correlate with a decrease in the anti-predation behaviour index. Data from controlled sonar exposures provide an opportunity to explore how animals balance the starvation-predation trade-off when perceived risk is increased. Animals of worse condition are predicted to take more risks in exchange for the benefits of increased foraging (Heithaus et al., 2007; McNamara and Houston, 1990, 1987). Thus the ratio of the anti-predation and foraging indices is expected to decrease when tissue density is higher, i.e. energy store body condition is lower. Using tissue density as a proxy for body condition, this study provides the first insights into the influence of body condition on the starvation-predation trade-off for any beaked whale species.

### 5.2.1 Materials and Methods

Fieldwork took place off Jan Mayen, Norway, from the M/S *HU Sverdrup* in 2013, from the T/S *Prolific* in 2014 and the T/S *Donna Wood* in 2015 and 2016. Research protocols were approved by Norwegian Animal Research Authority, the University of St Andrews Animal Welfare and Ethics Committee and the Woods Hole Oceanographic Institution Animal Care and Use Committee. Animals were detected visually or acoustically via a towed hydrophone array. Tagging was attempted on any individual, except calves. Tags were deployed via a 5m hand pole or an

aerial rocket transmitting system (Kvadsheim et al., 2011) and attached via suction cups. Conductivity-temperature-depth (CTD) casts occurred in 2013 (Miller et al., 2016a) and 2016 (Miller et al., 2016b), alongside temperature-only casts in 2014 (Miller et al., 2016a).

The dataset comprises fifteen deployments of digital sound and movement recording tags (Johnson and Tyack, 2003) on northern bottlenose whales (Table 1). A combination of DTAG-2 (SOUNDTAG, 2017a), DTAG-3 (SOUNDTAG, 2017b) and Mixed-DTAGs (M-DTAG) were deployed (Table 1). M-DTAGs consist of a DTAG-3 core unit, a Fastloc-GPS logger and a SPOT transmitter. Tags sampled audio at 192-240 kHz and pressure, 3-axis acceleration ( $\pm 2g$ ) and 3-axis magnetism at 50Hz (DTAG-2) or 250Hz (DTAG-3 and M-DTAG). A 50Hz sampling frequency was used to include both DTAG-3 and DTAG-2 deployments.

Tag data was processed with MATLAB v. 2017b (The MathWorks Inc., Natick, Massachusetts, United States). Sensor data was calibrated and converted to whale-frame axis using the SOUNDTAG (2016) DTAG toolbox and established methods (Johnson and Tyack, 2003; Miller et al., 2004b). Acoustic audits identified focal-animal sounds via aural cues and spectrogram analysis (Pérez et al., 2016). For deployments including controlled exposures of sonar and / or killer whale sounds (Miller, 2013; Miller et al., 2015a; Miller et al., 2016b), only baseline data were analysed unless otherwise stated. To eliminate any potential influences of tagging, the first 20 minutes of deployments was excluded.

#### *Estimating body condition via tissue density*

Body tissue density was estimated as an indicator of lipid-store body condition via hydrodynamic models of drag and buoyancy under a Bayesian framework for 2015 and 2016 deployments as in Miller et al. (2016a). See section 3.3 for details of how tissue density is calculated. For 2013 and 2014 deployments, published tissue density estimates were used (Miller et al., 2016a).

#### *Estimating foraging effort*

Three measures of foraging behaviour were calculated: 1) buzz rate (buzzes/hour); 2) the percentage of time producing regular clicks; and 3) the percentage of time in long-deep foraging dives. Buzz rate is a proxy for foraging rate (Miller et al., 2009), with the number of buzzes divided by time representing individual patterns in beaked whale foraging behaviour (Arranz et al., 2011; Tyack et al., 2011). The percentage of time regularly clicking was measured as the total time spent regularly clicking divided by the deployment duration. The time between the first and last echolocation clicks of deep diving odontocetes represents time spent actively searching for prey (Watwood et al., 2006). Long-deep foraging dives were identified using k-means cluster analysis of dive duration, maximum depth, descent and ascent rates. Dives from the two deepest clusters in which echolocation signals were produced were labelled as long-deep foraging dives for this study.

#### 5.2.2 Estimating anti-predation parameters

Measures representing a range of possible beaked whale anti-predation behaviours were calculated (Table 5-1). Ascent pitch angle from long-deep dives represented the anti-predation tactic of long ascents. Low ascent pitch from deep dives increases both the time and horizontal displacement from when individuals stop vocalising to when they re-surface (Tyack et al., 2006b); thus increasing the uncertainty of the whale's position when it resurfaces (Aguilar de Soto et al., 2018).

Hence average pitch angle was estimated from the point in time at which silent ascents start until the time at which the animal reached the surface; with a steeper pitch angle representing higher predation risk. Ascents were defined as starting at the time at which regular echolocation clicks last ceased (Tyack et al., 2006b). If a long-deep dive did not contain regular echolocation clicks, the start of the ascent phase was defined as the last point in time that an animal's pitch was  $<0^\circ$  (Miller et al., 2004b). The number of long-deep dives without regular clicking was low ( $n = 83$ ) relative to the total number of long-deep dives across all deployments. For each deployment, the mean pitch angle ( $\pm$  the standard error of the mean) was estimated across ascents from all long-deep dives.

*Table 5-1. Candidate anti-predation behaviours and the measures representing each behaviour. Includes examples of where such behaviours have been linked to beaked whale anti-predator tactics. \*Measures with respect to ascents from long-deep dive types. References: 1 = Aguilar de Soto et al. (2018); 2 = Aguilar de Soto et al. (2012); 3 = Allen et al. (2014); 4 = Baird et al. (2008); 5 = DeRuiter et al. (2013); 6 = Hooker and Baird (1999); 7 = Martín López et al. (2015) 8 = Miller et al. (2015c); 9 = Tyack et al. (2006b); 10 = Zimmer and Tyack (2007).*

<b>Behaviour</b>	<b>Description</b>	<b>Measure</b>	<b>Species</b>
Long ascents	Prolonged ascents from deep foraging dives, with low pitch angle and vertical speed	Pitch angle*	<i>Hyperoodon ampullatus</i> <sup>6,8</sup> <i>Mesoplodon densirostris</i> <sup>1,2,3,7,9</sup> <i>Ziphius cavirostris</i> <sup>1,7,9</sup>
Acoustic crypsis	Acoustic inactivity at shallow depths and during ascents from deep foraging dives	% of surface time vocalising Depth silent ascents start*	<i>Hyperoodon ampullatus</i> <sup>8</sup> <i>Mesoplodon densirostris</i> <sup>2,3,9</sup> <i>Ziphius cavirostris</i> <sup>5,9</sup>
Horizontal displacement	Consistent heading during deep dive ascents, maximising horizontal distance from end of bottom phase to surfacing	Tortuosity index*	<i>Mesoplodon densirostris</i> <sup>9</sup> <i>Ziphius cavirostris</i> <sup>9</sup>
Bounce dives	Series of several relatively shallow dives (up to approximately 400m) in-between deep foraging dives	% of inter-foraging-dive-interval spent in silent dives	<i>Mesoplodon densirostris</i> <sup>4,9</sup> <i>Ziphius cavirostris</i> <sup>4,9,10</sup>

Acoustic crypsis was represented as the depth silent ascents start, and proportion of time at the surface spent vocalising (Table 5-1). Silent ascents may impede a near-surface predator from tracking and intercepting an individual (Tyack et al., 2006b). Terminating regular clicking at shallower depths after long-deep dives increases predation risk by broadcasting an individual's position at depths closer to those inhabited by killer whales (Baird et al., 1998). Thus silent ascent start time was defined as the time at which regular clicking last ceased (Tyack et al., 2006b) during a long-deep dive or start of ascent for dives with no clicking. Given silence at shallow depths may be the best option to avoid killer whale predation (Jefferson et al., 1991), the higher the proportion of the time spent vocalising at the surface, the greater the risk of being detected. The overall percentage of time at depths  $<20\text{m}$  spent vocalising was estimated for each deployment.

Tortuosity was estimated to represent horizontal displacement during ascents (Table 5-1). High horizontal displacement after animals cease clicking on the ascent from deep dives could impede near-surface predators from tracking beaked whales (Tyack et al., 2006b). The tortuosity index (TI) is the ratio of the horizontal distance covered (assuming a constant speed) to the horizontal distance that could have been covered given a constant heading and the same speed (Tyack et al., 2006b). Mean TI was estimated from the depth at which silent ascents from long-deep dives start until the time the animal surfaces. Ascent start time was defined as either the time at which regular echolocation ceased (Tyack et al., 2006b) or the start of ascent for long-deep dives that contained no regular clicking. A TI of 0 indicates straight-line movement, whereas a TI of 1 indicates extreme circular movement.

The proportion of time spent in silent dives was estimated to represent non-foraging 'bounce' dives (Table 5-1). Beaked whale 'bounce' dives are a series of silent dives that often occur between deep foraging dives (Cox et al., 2006; Tyack et al., 2006b). Thus the measure was defined as the percentage of the non-foraging dive time spent in silent dives. Non-foraging dive time was defined as the total inter-foraging-dive-interval (IFDI) duration (i.e. the time between long-deep dives that contained regular clicking). For this measure, a minimum depth threshold (70m) was used to ensure the silent dive measure included only dives occurring deeper than the depths at which predators are likely present: killer whales spend over 70% of their time in depths <20m (Baird et al., 1998) and 90% of their time at depths <40m (Miller et al., 2010).

### 5.2.3 Composite indices of foraging and anti-predation behavior

The measures of foraging and anti-predation behaviour were each combined into two composite indices. A composite behaviour index allows several behavioural measures to be combined into a single index (Silk et al., 2003). Composite behaviours indices are ideal for analysing several potentially correlated measures as it prevents having to analyse measures independently (Silk et al., 2003). Pearson's correlation coefficient was used to indicate correlation between foraging and anti-predation measures. Based on sociality indices estimated by Sapolsky et al. (1997) and Silk et al. (2003), a composite foraging index ( $CI_F$ ) and composite anti-predation index ( $CI_{AP}$ ) was estimated per deployment as:

$$CI = \frac{\sum_{i=1}^n \frac{x_i}{m_i}}{n}$$

where  $n$  is the number of behavioural measures,  $x_i$  is the tag deployment specific value for each behavioural measure, and  $m_i$  is the median value of each respective behavioural measure across all tag deployment records. Composite indices measure the deviation of an individual from the population average across all measures combined (Sapolsky et al., 1997; Silk et al., 2003).

All foraging measures positively correlated; however there was negative correlation between three of the anti-predation measures and the overall anti-predation behaviour index. Increased ascent pitch angles, TI and the percentage of surface time vocalising all indicate taking greater predation risk. Thus these anti-predation measures were inverted to ensure all measures positively correlated with their associated composite index  $CI_{AP}$  (Mazziotta and Pareto, 2013). A linear model was used

to estimate whether  $CI_{AP}$  varied as a function of  $CI_F$  to explore the possible trade-off between foraging and anti-predation behaviours.

#### *Comparing periods before and after the start of exposure to sonar*

To further explore the starvation-predation trade-off, behavioural indices were estimated for periods after controlled sonar exposures (Table 1). Sonar exposures might be perceived as a threat similar to predation risk (Isojunno et al., 2016), thus  $CI_{AP}$  was expected to increase and  $CI_F$  to decrease post-exposure in line with the starvation-predation trade-off (Lima and Dill, 1990b). Three deployments (ha13\_176a, ha15\_179b and ha16\_170a) contained controlled sonar exposures (Miller, 2013; Miller et al., 2015a; Miller et al., 2016b) and thus provided the opportunity to compare foraging and anti-predation behaviour during the baseline period to post-exposure periods (from the end of sonar exposures until the end of deployments). Deployment ha15\_171a also included controlled exposures to sonar and killer whale sounds; however no audio data was recorded post-exposure (Miller et al., 2015a) so this exposure was not included in the analysis.

The ratio of anti-predation to foraging index ( $CI_{AP}/CI_F$ ) was modelled as function of tissue density estimates. Models using  $\rho_{tissue}$  and combinations of the covariates (deployment duration, group size and an interaction with dominant stroke frequency DSF, i.e. a proxy for body size) were compared using AIC.

#### 5.2.4 Results and Discussion

##### **Bottlenose whale body condition and the starvation-predation trade-off – highlights**

Using hydrodynamic models, the tissue density of 15 northern bottlenose whales tagged with DTags around Jan Mayen was estimated. Measures of foraging and predator avoidance behaviours were combined as composite indices of foraging and anti-predation effort.

An increase in the composite foraging index corresponded to a significant reduction of the anti-predation index. In line with the starvation-predation trade-off, anti-predation effort increased when foraging effort decreased. Sonar exposures caused extreme reductions in foraging and increased anti-predation effort, as predicted under the risk-disturbance hypothesis.

Increased tissue density (i.e. a lower proportion of lipid) was statistically-significantly correlated with an increased ratio of anti-predation to foraging behavior, indicating animals with worse body condition took fewer risks and foraged less during the tag deployment period, contrary to condition-dependent risk-theory.

These results suggest that over the range observed, lipid store body condition was more likely a consequence than a driver of behavioral patterns in the animals tagged in this study. However, short tag durations and a small sample size of individuals weaken the strength of the conclusions.

As found for all of our analyses to date (Section 3), individual variation in tissue density was supported by model selection using DIC. Tissue density estimates ranged from 1028.4 to 1033.9 kg m<sup>-3</sup> (Table 5-2) with a mean density of 1030.8 kg m<sup>-3</sup> ( $\pm .4$ ). The global mean (i.e. the expected

mean of the population from which the tagged whales came from) was  $14.0 \times 10^{-6} \text{ m}^2 \text{ kg}^{-1}$  ( $\pm 2.5$ ) for the combined drag term  $[(C_d A)/m]$ ,  $0.39$  ( $\pm .004$ ) for tissue compressibility ( $r$ ) and  $29.2$  ( $\pm 3.0$ ) for diving gas volume ( $V_{air}$ ). As in Miller et al. (2016), the tissue densities of northern bottlenose whales fell within a narrow range compared to humpback whales (Narazaki et al., 2018) - (see section 3.3).

Composite foraging and anti-predation indices and the ratio between the two were estimated for each deployment (Table 5-2). Individuals deviated by a wider extent from the mean across all foraging measures ( $CI_F$  range:  $.5 - 1.5$ ) compared to anti-predation measures ( $CI_{AP}$  range:  $.7 - 1.2$ ). There was a significant negative relationship between  $CI_{AP}$  and  $CI_F$  ( $\beta = -.43$ ,  $t(13) = -3.66$ ,  $\rho < .01$ ), with an increase in  $CI_F$  correlating with decrease in  $CI_{AP}$  (Fig. 2). Deployment ha16\_173a had the lowest  $CI_F$  and highest  $CI_{AP}$  (.004 above the next highest deployment) resulting in the highest  $CI_{AP}/CI_F$  value (Table 5-2). If deployment ha16\_173a was excluded, the negative relationship between  $CI_{AP}$  and  $CI_F$  remained strongly supported, albeit with a slightly lower effect size ( $\beta = -.42$   $t(12) = -2.99$ ,  $\rho < .02$ ). This result demonstrates that whales did tradeoff foraging versus anti-predator effort in their behaviour patterns.

Relative to baseline of the three deployments with controlled sonar exposures there was a decrease (by  $.71 - 1.36$ ) in  $CI_F$  and an increase (by  $.01 - .43$ ) in  $CI_{AP}$  (triangles in Figure 5-2; Table 5-2). Bottlenose whales decreased foraging and increased anti-predator behaviors in response to an anthropogenic disturbance, supporting the hypothesis that they are perceived as a ‘risk’ factor with responses shaped by anti-predator response templates (Frid and Dill, 2002; Harris et al., 2016).

*Table 5-2. Deployment estimates including: number of 5s glide segments, estimated tissue density,  $\rho_{tissue}$  (mean  $\pm$  95% posterior credible interval in  $\text{kg m}^{-3}$ ); composite foraging index ( $CI_F$ ); composite anti-predation index ( $CI_{AP}$ ) and the ratio of composite anti-predation to foraging indices ( $CI_{AP} / CI_F$ ). Composite indices for post-exposure periods (from the end of the exposure to the end of the deployment) are parenthesised for deployments containing controlled sonar exposures. Group size at the time of tagging and estimated dominant stroke frequency (DSF), as an index of body size, are also shown.*

Deployment ID	# glides	$\rho_{tissue}$	$CI_{AP}$	$CI_F$	$CI_{AP} / CI_F$	Group size	DSF (Hz)
ha13_176a	273	$1030.2 \pm 0.1$	1.0(1.3)	.9 (.0)	1.2	6	.4
ha14_165a	74	$1032.6 \pm 0.3$	1.1	1.3	.9	2	.4
ha14_166a	164	$1031.6 \pm 0.1$	1.2	.7	1.8	3	.1
ha14_174a	87	$1031.6 \pm 0.2$	1.1	.8	1.3	3	.1
ha14_174b	152	$1030.0 \pm 0.1$	1.0	1.0	1.0	3	.4
ha14_175a	153	$1028.4 \pm 0.1$	1.0	1.0	1.0	4	.4
ha15_171a	115	$1029.3 \pm 0.1$	.7	1.2	.7	2	.1
ha15_173a	243	$1031.1 \pm 0.1$	.8	1.5	.5	4	.1
ha15_174a	23	$1031.8 \pm 0.5$	1.1	.6	1.9	8	.1
ha15_173b	389	$1029.5 \pm 0.0$	.8	1.1	.7	5	.5
ha15_174b	181	$1031.2 \pm 0.1$	.9	1.3	.6	3	.1
ha15_179b	282	$1030.2 \pm 0.1$	1.2(1.2)	1.0 (.29)	1.2	4	.5
ha16_169a	104	$1030.6 \pm 0.1$	.7	1.2	.6	8	.4
ha16_170a	154	$1029.9 \pm 0.0$	.8 (1.2)	1.4 (.0)	.6	4	.1
ha16_173a	206	$1033.9 \pm 0.3$	1.2	.5	2.2	3	.4

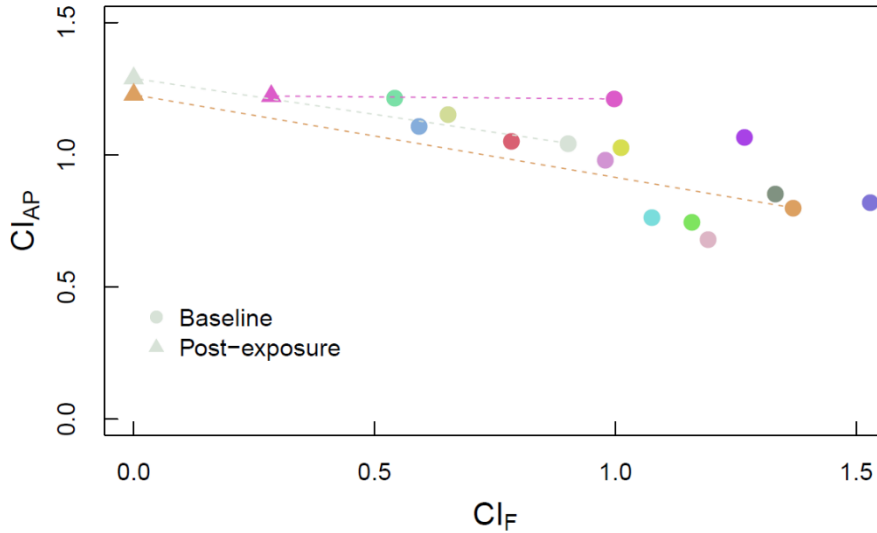
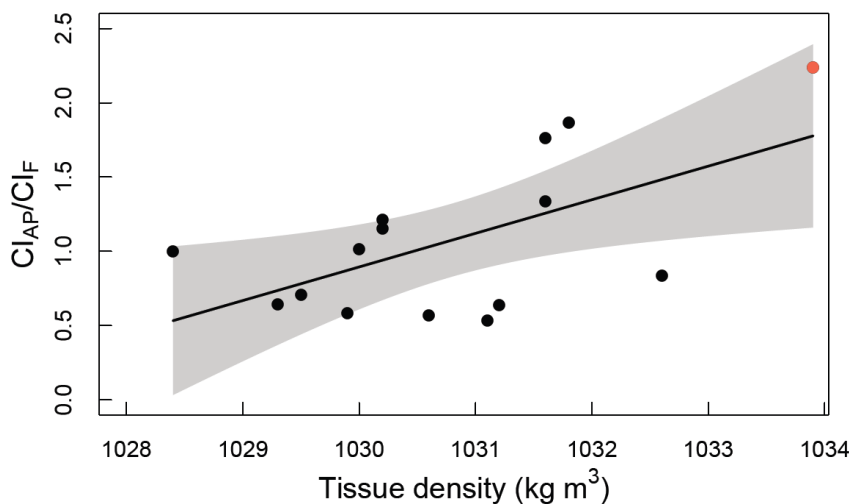


Figure 5-2. Composite anti-predation index ( $CI_{AP}$ ) as a function of composite foraging index ( $CI_F$ ), with values for post-exposure periods. Dashed lines relate post-exposure periods to baseline values of the same deployment. Colours are unique to each deployment.

### 5.2.5 Tissue density variation with anti-predation and foraging behaviour

The ratio of anti-predation to foraging index ( $CI_{AP}/CI_F$ ) was modelled as function of tissue density estimates. There was substantial support ( $\Delta AIC_c < 2$ ) for  $\rho_{tissue}$  as the sole predictor of  $CI_{AP}/CI_F$ . The model with  $\rho_{tissue}$  as the only predictor had an Akaike weight (i.e. the normalised relative likelihood)  $AIC_{cw} = .50$ , three times that of the next best fitting model (i.e. the model with tag record duration as the sole predictor,  $AIC_{cw} = .16$ ), suggesting a greater weight of evidence for tissue density as a predictor of  $CI_{AP}/CI_F$  given the models selected.

There was a significant relationship between  $CI_{AP}/CI_F$  and tissue density (Figure 5-3), with a  $1 \text{ kg m}^{-3}$  increase in  $\rho_{tissue}$  resulting in an average increase of .23 in  $CI_{AP}/CI_F$  ( $t(13) = 2.68, \rho < .02$ ). However, one tag record (ha16\_173a) appears to have had a strong influence on the outcome of the statistical analysis (red data point in Figure 5-3). This data-point had a Cook's distance of  $>.5$  (Cook, 1977), and removing ha16\_173a from the dataset, resulted in there being no significant



variation in  $CI_{AP}/CI_F$  with  $\rho_{tissue}$  ( $t(12) = 1.32, \rho = .21$ ).

Figure 5-3. Ratio of composite foraging to anti-predation indices ( $CI_{AP}/CI_F$ ) as a function of tissue density with the predicted linear model and the 95% confidence interval. Deployment ha16\_173a had a high Cook's index, so is highlighted in red.

The observed relationship was the opposite of that predicted: increasing tissue density (i.e. a lower proportion of fat) correlated with an increase in the ratio of the anti-predation to foraging behaviour (Figure 5-3). This indicates that worse condition animals had higher predator avoidance and reduced foraging behaviours. There are several potential reasons for the unexpected relationship between tissue density and the ratio of anti-predation to foraging behaviours. One simple explanation could simply be that lipid-store body condition (across the range of values observed in this study) is a consequence of behavioural patterns rather than a driver. Across animal taxa, individuals differ in average behaviour across a range of contexts, with behavioural traits persisting over time (Biro and Stamps, 2008; Dall et al., 2004; Réale et al., 2007; Sih et al., 2004). Such intrinsic ‘personality’ traits also influence how individuals balance foraging and anti-predation behaviours (Dammhahn and Almeling, 2012; Quinn et al., 2011; Van Oers et al., 2004). Animals with strategies (or personalities) that include taking more risks and foraging more can be expected to have better lipid store body condition than animals that use safer strategies. Such feedback loops, wherein personality traits (e.g. foraging boldness) have fitness consequences (e.g. increased energy reserves) have been developed theoretically (Sih et al., 2015) and proven empirically (Sinn et al., 2006).

Our method of observing free-ranging animals enables us to observe the benefit of increased foraging effort as improved lipid-store body condition. However, animals that take more risks are expected to incur the corresponding cost of a higher predation rate, which we cannot observe –our dataset is limited to only surviving individuals. The starvation-predation trade-off may become a stronger driver when animals are at extremes of body condition than we observed here: taking more risks when close to starvation or decreasing foraging when fat stores become excessive.

### 5.3 Foraging effort in relation to body in condition in humpback whales

Using both body density and body shape indicators, in project RC-2337, we confirmed the expectation that humpback whales should accumulate body fat over their summertime feeding season and to be fatter and buoyant in late feeding seasons (sections 3.2 and 3.3). Locomotion cost of marine divers increases with deviation from neutral buoyancy (Sato et al., 2013), particularly when animals move in the direction hindered by buoyancy (Miller et al., 2012). Such costs of carrying too much lipid should lead to reduced foraging effort. Therefore humpback whales are predicted to reduce feeding once they store enough body fat to achieve long migration efficiently.

In this subsection, we examine and report how humpback whale foraging effort varies in relation to body density as an indicator of lipid-store body condition.

#### 5.3.1 Materials and Methods

The data in this study, and body density estimates of subject whales, are the same as those used to explore how body density of humpback whales varied with season and reproductive status (section 3.3.2). Foraging dives were defined as any dive that contained a lunge feeding event. Lunges are characterized by a rapid acceleration in speed and (Fig. 4) energetic stroking (Ware et al., 2011, Simon et al. 2011 ). Using these characteristics, we identified lunge events from swimming speed obtained by flow noise (Simon et al. 2012, Sivle et al., 2015) for data from Dtag and swim speed

and/or stroking signals for data from Little Leonardo tags (Akiyama et al., in prep). Percentage of time feeding was calculated from the proportion of times individual whales were undertaking lunge feeding dives. We defined "resting dives" to meet two conditions (Miller et al. 2008): 1) the count of flywheel sensor is zero for more than 1 min and 2) No fluking for more than 1 min. (Miller et al. 2008). The end of resting bout was defined as continuous active state for more than 5 minutes after resting. We have applied this analysis to only Little Leonardo data loggers due to the lack of a speed sensor in the Dtag recordings. We have analyzed the time budget in feeding of 45 tagged animals in total: 14 animals in early season and 10 animals in late feeding season from Norway, and 17 tagged animals in early feeding season and 4 animals in middle feeding season from Canada.

We used generalized linear models (GLMs) with a binomial error distribution and a log link function to investigate percentage time spent in feeding in relation to the tissue body density and the life history traits (i.e. sex, age class and reproductive status, for details see Table 1 in section II.c.6). This statistical model included percentage time spent in feeding as a dependent factor and tissue body density, season and/or life history traits as fixed independent factors. The offset was set as tag duration. We used Akaike's Information Criterion (AIC) to assess the most parsimonious model.

### 5.3.2 Results and discussion

#### **Foraging effort in relation to body condition in humpback whales – highlights**

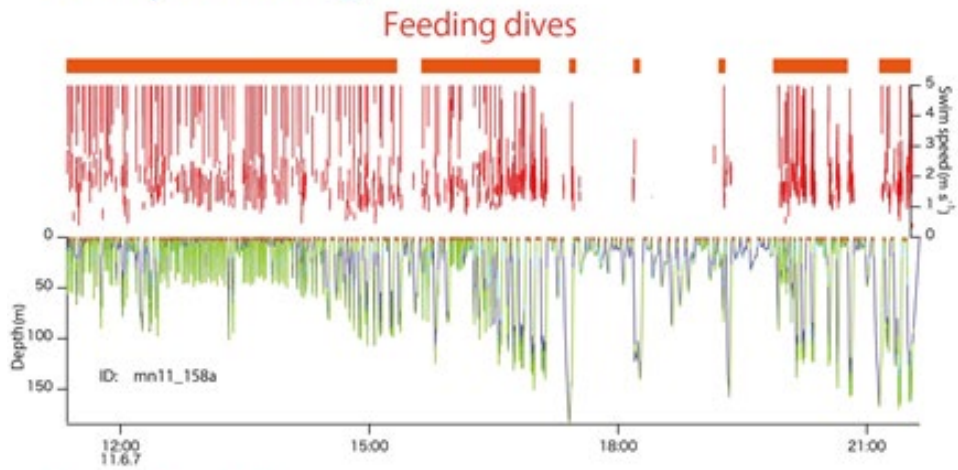
Foraging dives of humpback whales were identified using speed and acceleration characteristics of lunge feeding. The proportion of time spent feeding was related to the body condition (using tissue density) across whales.

Whales tagged in Norway spent a much lower proportion of time feeding than whales tagged in Canada. This result could be due to the fact that whales in Norway were tagged much later in the feeding season, though it is possible that differences in prey characteristics may have driven that difference.

Statistical modelling on this preliminary dataset indicate that body density appears to influence the proportion of time in feeding dives, with more feeding occurring when animals had lower lipid stores (higher body density), as predicted. Interestingly, other factors of age, sex, and reproductive status also seemed to be important predictors of foraging effort in humpback whales.

The time budget of whales tended to be different between the two study areas (Figure 5 4): tagged animals from Norway spent a relatively large proportion of time resting and a small proportion of time feeding compared with the animals tagged in Canada. The time spent resting by tagged animals in the late feeding season in Norway was more than 10% (range, 0-42%). The time spent in feeding by most animals (8 of 10 animals) was less than 30% (the range, 0-62%). In contrast, tagged animals from Canada spent most of their time feeding and rarely resting in both early and mid-seasons. The time spent resting by most of the animals (16 of 17 animals in the early feeding season and all animals in the middle feeding season) was 0%, with the remaining animal resting 12% of the time. The time spent feeding by most of the animals (15 of 17 animals in the early feeding season and 3 of 4 animals in the mid season) was more than 50% (range of early season, 17-92%; range of the mid season, 10-93%).

## Early feeding season



## Late feeding season

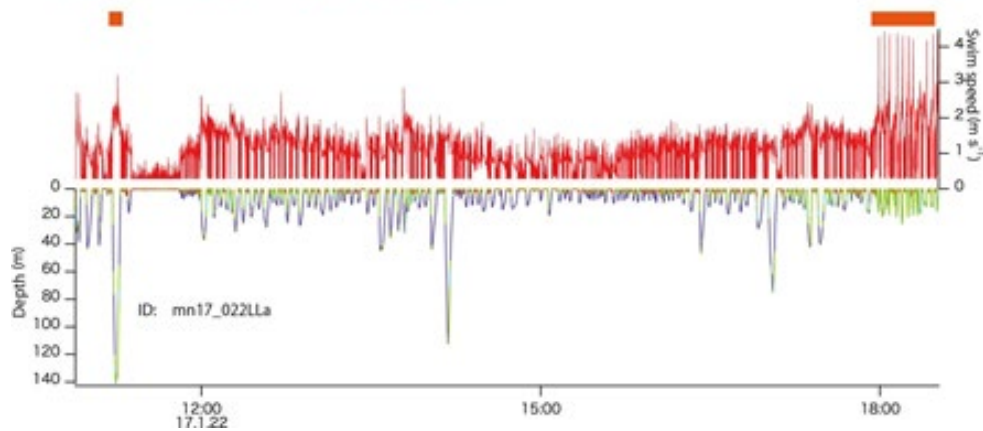


Figure 5-4. Examples of humpback whale tag records. Orange bars mark dives that contained lunge events. Note the clear peaks in swim speed associated with lunge dives.

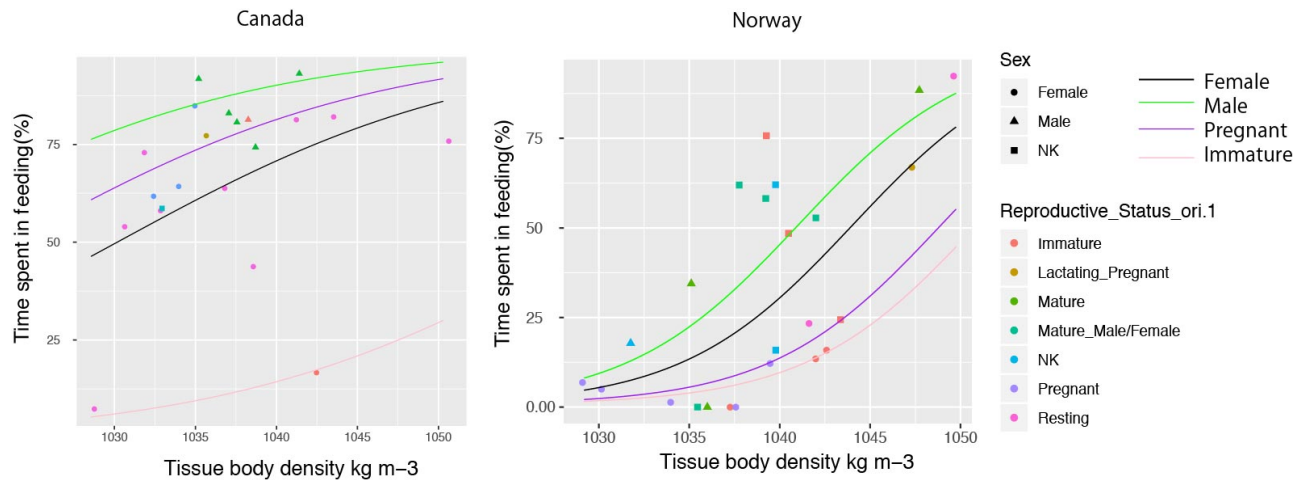


Figure 5-5. Time spent in feeding in relation to tissue body density in both Canada and Norway.

Our analysis of body density versus time in the feeding season indicated that body density decreased  $2.7 \text{ kg m}^{-3}$  per 90 days in Canada as well as Norway (section 3.3.6.2). Decreasing tissue body density involved a relatively lower proportion of time spent in feeding but the time spent in feeding was relatively higher in Canada than that of Norway especially for animals with relatively low tissue body density (Fig. 5-5). Tagged whales spent a relatively large amount of time in foraging in both the early ( $68 \pm 19\%$ , range, 17-92%,  $n = 17$  whales) and middle season ( $61 \pm 38\%$ , range, 7-93%,  $n = 4$  whales) in Canada. Tagged whales from Canada might be motivated to feed throughout the entire feeding season because of their relative short stay on those feeding grounds. Indeed, resting duration of the whales from Canada was shorter than the whales from Norway in late feeding season (Fig. 5-5).

Tissue body density was low (indicating high lipid stores) during the late feeding season in Norway (section 3.3.2). Tagged whales in Norway spent relatively little time foraging in the late season ( $18 \pm 24\%$ , range, 0-62%,  $n = 10$  whales) compared with the early season ( $42 \pm 31\%$ , range, 17-92%,  $n = 14$  whales). Indeed, time spent feeding substantially decreased with decreasing tissue body density. The result suggests lipid store body condition affects feeding behavior and that relatively fat humpback whales might be less motivated to feed.

The statistical model indicated that tissue density improved model fit (Fig. 5-5; Table 5-3). However, other factors in the model also had a strong influence. Although the data set was small, the statistical models detected differences of life-history traits (ie. sex, reproductive status and age class) in relation to time spent in feeding. Time spent in feeding by male whales was higher than that of females in both areas. Time spent feeding by immature animals was less than that of adults. Of course, we observed only snap shots of both tissue body density and behaviors, but our results indicates monitoring body condition is an important first step to understand the feeding strategy between life traits and/or geographic locations.

Table 5-3. Fit of general linear models to data of the proportion of time spent in feeding of tagged humpback whales by AIC. The lowest AIC model is highlighted.

Model	AIC	
	Canada	Norway
Time spent in feeding ~ 1	1197	563
Time spent in feeding ~ Tissue body density	747	522
Time spent in feeding ~ Tissue body density+Season	748	519
Time spent in feeding ~ Season	1041	557
Time spent in feeding ~ Tissue body density+Season+Sex	548	404
Time spent in feeding ~ Tissue body density+Season+Sex+Age_class	522	304
Time spent in feeding ~ Tissue body density+Season+Sex+Age_class+Sex:Age_class	507	273
Time spent in feeding ~ Tissue body density+Season+Sex+Age_class+Sex:Age_class+Reproductive status	497	256

## 6 CONCLUSIONS AND IMPLICATIONS FOR FUTURE RESEARCH / IMPLEMENTATION

The results presented in this report represent a successful outcome of study RC-2337, with all of the objectives effectively addressed. The overall goal of this study was to develop, validate and apply a novel, non-invasive tag-based technique to measure the body condition of free-ranging cetaceans. The inter-locking objectives of the project centered around development and application of a novel technique to measure body tissue density of cetaceans as a means to estimate their lipid-store body condition (Figure 6-1).

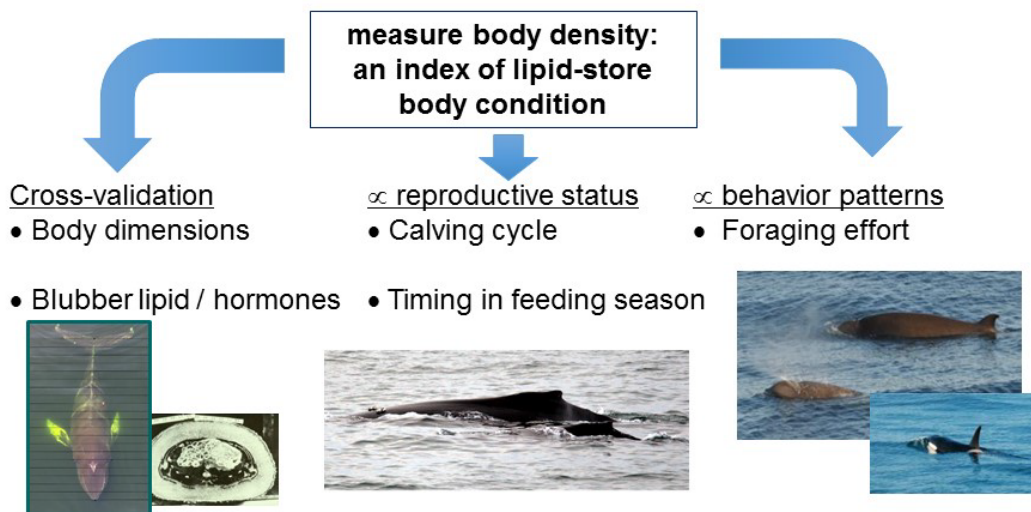


Figure 6-1. Interlocking objectives of RC-2337. Develop the body density index (top); validate it using two independent approaches (left); quantify how it varies with female reproductive status (middle) and relate foraging effort with body density (right).

In this section, we describe the study conclusions and recommend future research directions. We provide suggestions for DoD and other resource managers for how these new approaches might be used to assess the biological significance of disturbance from anthropogenic disturbance.

**Objective 1:** *Measure the body density of individual northern bottlenose and humpback whales through modelling the hydrodynamic performance of animals during glide patterns, obtained using temporarily deployed high resolution data-logging tags.*

Body tissue density was successfully measured in the two primary subject species: northern bottlenose whale (family *Ziphiidae*: *Hyperoodon ampullatus*) and humpback (family: *Balaenopteridae*: *Megaptera novaeangliae*) whales, and also in a third species via external collaboration, the long-finned pilot whale (family *Delphinidae*: *Globicephala melas*) an oceanic delphinid. Previous to this study, body density had only been measured in sperm whales (family *Physeteridae*: *Physeter microcephalus*; Miller et al., 2004). The approach of identifying gliding periods during ascent and descent phases of dives functioned for all species in the study, as gliding does appear to be a ubiquitous behavior among cetacea. The method was successful using data from either Dtags (Johnson and Tyack, 2003) or Little Leonardo 3MPD3GT loggers (Aoki et al., 2011) attached to whales using suction cups.

We particularly highlight the important advance that body density was measured for relatively shallow diving humpback whale, which dove to an average maximum recorded depth of just  $64.0 \pm 67.2\text{m}$  (section 3.3.1.3). This is a much shallower diving depth than the other species for which body density had previously been estimated, and indicates that the approach can be widely applicable among cetacea - as well as with shallower-diving pinnipeds (Aoki et al., 2011).

One of the key advantages of the body tissue density approach is that it provides a quantitative, numerical estimate of lipid-store body condition, along with estimates of other important physiological variables (Miller et al., 2016). The Bayesian statistical modelling procedure was effective at estimating a specific value for the tissue density parameter using the model of hydrodynamic performance (Equation 1, introduction) during glides. As predicted, statistical analyses for all three species indicated measurable individual-level variation in tissue density within the samples we obtained. Individual-level variation was also found for the combined drag-term  $CdAm^{-1}$ , which was expected given across-whale differences in body size, while dive-by-dive variation was found for diving gas volumes likely reflecting that cetaceans do not always dive on full inspiration. We found that including specific measures of body length (using UAV photogrammetry) to more accurately define surface area  $A$  and mass  $m$  of tagged whales prior to calculating body density neither improved the 95% CI precision of the tissue density estimate nor altered the tissue density estimate itself compared to when  $CdAm^{-1}$  was estimated from the data (section 3.3.3). This indicates that the glide method developed in this project can be effectively applied to animal-attached tag data even when no animal size measurements are available. However, we would still recommend collecting animal size data when feasible, as that information makes it possible to estimate the drag coefficient  $Cd$  itself, which is a physiological parameter of considerable importance to understand the energetic costs of swimming.

The numerical indicator of tissue density reflects the quantity of lipid stores because the density of lipids is much lower than the density of other animal tissues. Thus, body density correlates

strongly with total body lipid-store content in mammals (Fields et al., 2005)(Fields et al., 2005). However, conversion of a specific body tissue density to an accurate value for lipid-store content value is only possible if the precise density of lipids and non-lipid tissues is known (Biuw et al., 2003). Density measurements of body components of cetaceans would be useful to more effectively convert total body density to lipid store values, and we strongly recommend more research in that area.

The results of our study indicate that issue body density within a given species should provide a relative index of lipid-store body condition across individuals (and changes over longer time periods within the few individuals that were repeat sampled). Longitudinal tracking of changes in lipid stores using tags has been very effective in the study of resource acquisition and diving energetics of elephant seals (Biuw et al., 2003). Onboard implementation of the algorithm described in this work in a longer-duration telemetry tag could enable longitudinal tracking of body condition of individual whales over time. Use of a long-duration tag that reports body condition would be strongly recommended. Such studies could identify effective foraging areas for cetaceans, and quantify energy-store impacts of anthropogenic disturbance on the body condition status of individual cetaceans, which could be a critical tool for DoD to evaluate biological significance of impacts of sonar on cetaceans.

**Objective 2:** *Validate the body density metrics obtained using two independent approaches. These were based on measurement of body shape and the analysis of blubber from remote biopsy samples.*

A fundamental challenge of the project is that it is not possible to measure lipid-store body condition of free-ranging cetaceans using a ‘gold-standard’ method like isotope dilution. While not technically a ‘validation’, we instead separately tested and developed two independent approach to estimate body condition of cetaceans, using measurement of body shape and analysis of condition indicators or biomarkers in blubber. We then applied those methods to samples obtained during a single encounter with a whale – which required successful accomplishment of three advanced field procedures: tagging with a suction cup, imaging the whale using an AUV, and collection of remote blubber biopsy sample. Unfortunately, despite maximal efforts in the field, we were not able to collect all of these types of samples from northern bottlenose whales, so the cross-validation was only possible with the humpback whale.

For body-shape estimation (Section 3.2), we first evaluated use of a 3D scanning sonar to obtain length and girth estimates of individual whales. It was possible to use the scanning sonar at sea with free-ranging killer whales to obtain point-cloud data of reflections from the external body of the whales (Section 3.2.1). However, evaluation of the accuracy of the system to extract length and girth of killer whales measured in captivity was complicated by the need to define a set of parameters to obtain measurements using an automatic unbiased measurement method. For some parameter combinations, we were able to find an excellent match (<10% error) with the tape-measured length and girth of the captive killer whales, but for other combinations the errors were much larger. Further work is needed to specify what parameters to use, or to explore a less automated approach to measure whale dimensions.

After the start of our project, developments in unmanned-aerial vehicle (UAV) technology made it possible to take overhead photogrammetry images of whales, and one study measured body condition changes in humpback whales over the breeding season when they fast (Christiansen et al., 2016). We therefore made use of UAVs to take overhead photogrammetry images of humpback whales, focusing on whales already tagged with suction cups in our study. After extracting high-quality images taken from overhead target whales, we calculated the length-standardized surface area index (LSSAI) of body condition. LSSAI effectively quantifies width-length ratios over defined sections of each whale's body, which had previously been shown in right whales to vary with reproductive status (Miller et al., 2012). A key advantage of LSSAI is that it only requires the ratio of width to length, and does not require absolute measurements of the animal which are more complicated to obtain. Ultimately (see below), we found LSSAI to vary as expected across reproductive status and with time in the feeding season (Section 3.2.2). Supported by other work using width-length measurements from overhead photogrammetry to estimate body condition, we have high confidence that this method has promise as a tool to measure body condition of free-ranging cetaceans.

For the analysis of blubber tissue obtained in biopsy samples we first need to validate and optimise the laboratory methods for evaluating biomarkers. For this approach we used samples from freshly dead animals and found that blubber lipid content from remotely obtained, shallow biopsy samples provided little information about the body condition of the species sampled. Whilst animals that died of chronic diseases had less lipid in their blubber, there was no relationship between morphometric body condition measurements and blubber lipid content.

Other measurements that could be obtained from blubber samples included the metrics relating to the size and area of the fat cells (adipocytes), particularly focussing on adipocyte size. A pilot study found that there was a positive linear relationship between morphometric measures of condition and adipocyte area in a number of different cetacean species, suggesting that this approach may also have some promise in future. However, it was not possible to progress with this method due to the limited amount of tissue available from the free-living cetaceans sampled during the study.

Thus our investigation of additional blubber markers to estimate condition, concentrated on investigating the concentration of the glucocorticoid hormone cortisol, which is involved in fat metabolism and release. In addition we made a great deal of progress in determining the upregulation of other potentially useful protein markers in the blubber, identified using a shotgun proteomic approach (particularly investigating changes in the adipocytokines that are known to be related in energy store in terrestrial species).

Validation and optimisation studies from stranded species found that cortisol concentrations in the dorsal, outer blubber layer could be useful as a biomarker for condition as they significantly correlated with morphometric condition measures in both small and large cetaceans. Higher blubber cortisol are found when animals are metabolising and releasing fat (lipolysis) and this appears to be consistent in both fast adapted and non-fast adapted species. In addition, cortisol in blubber is not related to short term stress as we found no relationship with handling time. This has also recently been reported in bottlenose dolphins (*Tursiops truncatus*) (Galligan et al., 2018). Galligan et al. also reported the interconversion between cortisone and cortisol in this species, confirming our hypothesis that local production of cortisol is likely occurring in cetaceans during

times of high energy demand. Cortisol concentrations could therefore be used to determine the general physiological state of the animal (i.e. if it is undergoing lipolysis or lipogenesis) at the time of sampling.

The proteomic shotgun approach identified a wide range of proteins in the blubber of cetaceans and results indicate that further refinement of this method could lead to additional important condition markers or qualitative metabolic state indicators, particularly when combined with the hormone markers. However, this study has been limited by relatively small sample sizes and inability to account for all potential confounding factors.

We fully developed and tested the separate metrics of body condition (body density, LSSAI, cortisol concentration) before inspecting any correlation of their values from the same whale. It was challenging to collect multiple sample types during single encounters with whales, and not all data samples could be used to derive the associated metric (ie if tag duration was too short, we could not calculate body tissue density). Nonetheless, we obtained both body tissue density and cortisol concentrations from 25 whales, LSSAI and body tissue density from 16 whales, and LSSAI and blubber cortisol concentrations from 25 whales. We were able to obtain all three indices for 13 whales.

The result of the cross-correlation of the methods was clear. We found a strong statistical correlation between body density and LSSAI for adult humpback whales ( $p = 0.019$ ,  $r^2 = 0.299$ ,  $N=18$ ) in the expected direction. Whales with high tissue density values were visibly thinner per unit length in the photogrammetry images that whales with low tissue density values were notably wider per unit length. In contrast, cortisol concentrations in blubber did not correlate with either tissue density or LSSAI across the whale sample. A strong correlation was found between tissue density and cortisol concentrations in blubber for pregnant female humpback whales ( $N=9$ ), with higher cortisol concentrations being related to lower tissue density (indicating high lipid values of lipid stores).

In conclusion, the strong correlation of the tissue density from tag data with the LSSAI from overhead photogrammetry indicates that either or both of these methods can be used to monitor changes in lipid-store body condition of free-ranging cetaceans. However, more work is needed to understand the role of cortisol concentrations in blubber in relation to body condition and metabolic status at the time of sampling, as confirmed by Galligan et al. (2018). Overhead photogrammetry using UAVs is less invasive than tagging, and large numbers of whales can be photographed efficiently (Christiansen et al., 2016), which indicate it could be considered a state-of-the-art technique for cross-sectional sampling of body condition of cetaceans. The tag-based tissue density method can also be used in cross-sectional designs like those employed here, but sample sizes are likely to be more limited than what should be possible using UAV photogrammetry. As described above, the tag-based body density method may be most effective for longer-term longitudinal tracking of individual tagged whales. When possible, we recommend that research employ a combination of methods to measure body condition.

**Objective 3.** *Identify patterns of lipid store body condition for individuals based on their sex, reproductive status, location and time of year.*

In the initial stated goals of RC-2337, we proposed to evaluate patterns of only tissue density based upon sex, reproductive status, location, and time of year (timing in the feeding season for

humpback whales). However, we were also able to carry out this analysis for the other body condition metrics, as described in section 3.

For tissue density, we found a strong statistical pattern of seasonal change with humpback whales reducing their tissue density throughout the feeding season, as expected (3.3.2.2). A similar seasonal change was found for LSSAI with humpback whales growing visibly wider through the feeding season (3.2.2.3). For LSSAI, but not for body density, we also found important indications of variation across age-sex classes and with reproductive status. Adult females overall tended to have wider bodies per unit length, through lactating females were thinner per unit length than other females. These are the expected variations given that females need to store large lipid stores preparing for and during pregnancy, but the demands of lactation will cause depletion of those stores, leading to worse lipid-store body condition.

The patterns of variation of cortisol concentrations were less clear. Whilst there was no overall correlation between blubber cortisol and LSSAI or body density, there was a significant relationship between cortisol and body density among the pregnant females. This could be due to variations in density related to the size of the fetus at the time of sampling, the stage of gestation or the metabolic status of the tissue when the blubber sample was collected. Further work in this area is essential for further interpretation of the blubber hormones during complex physiological changes at key life-history stages.

Future research in this area should focus on obtaining body condition samples of known females within long-term studies of free-ranging populations. Body condition metrics should then be linked to growth, survival, and reproductive success of the individuals. Lipid-store body condition could thereby become a key indicator of ‘health’ which could be explicitly related to vital rates in the population, as has been demonstrated using visual indicators of health in right whales (Schick et al., 2013).

**Objective 4.** *Describe how individuals vary foraging effort in relation to body condition*

The same tag data used to calculate body density as an index of body condition records a rich data stream that enables evaluation of the function of underwater behavior, including specific indicators of foraging and anti-predator behaviors. We used these data to explore how body condition might influence foraging effort of our two study species. With humpback whales, we found the expected pattern that animals late in the feeding season, which tended to have low tissue density (indicating high lipid-stores) spend dramatically less time feeding than humpback whales earlier in the feeding season. In contrast, northern bottlenose whales showed the opposite tendency – whales with lower body density (and hence more stores) tended to forage more and undertake less anti-predator behaviour.

## 7 LITERATURE CITED

- Ackman, R.G., Hingley, J.H., Eaton, C.A., Logan, V.H., Odense, P.H., 1975a. Layering and tissue composition in the blubber of the northwest Atlantic sei whale (*Balaenoptera borealis*). Canadian Journal of Zoology 53, 1340-1344.
- Ackman, R.G., Hingley, J.H., Eaton, C.A., Sipos, J.C., Mitchell, E.D., 1975b. Blubber fat deposition in mysticeti whales. Canadian Journal of Zoology 53, 1332-1339.
- Adachi, T., Maresh, J.L., Robinson, P.W., Peterson, S.H., Costa, D.P., Naito, Y., Watanabe, Y.Y., Takahashi, A., 2014. The foraging benefits of being fat in a highly migratory marine mammal. Proceedings of the Royal Society B: Biological Sciences 281.
- Aguilar, A., Borrell, A., 1990. Patterns of Lipid Content and Stratification in the Blubber of Fin Whales (*Balaenoptera physalus*). Journal of Mammalogy 71, 544-554.
- Aguilar, A., Borrell, A., Gomez-Campos, E., 2007. The reliability of blubber thickness as a measure of body condition in large whales. 59th Annual Meeting of the Scientific Committee of the International Whaling Commission (SC/59/017)
- Aguilar de Soto, N., Madsen, P.T., Tyack, P., Arranz, P., Marrero, J., Fais, A., Revelli, E., Johnson, M., 2012. No shallow talk: Cryptic strategy in the vocal communication of Blainville's beaked whales. Marine Mammal Science 28, E75-E92.
- Aguilar de Soto, N., Visser, F., Madsen, P.T., Tyack, P., Ruxton, G., Alcazar, J., Arranz, P., Johnson, M., 2018. Beaked and killer whales show how collective prey behaviour foils acoustic predators. bioRxiv, 303743.
- Ahima, R.S., 2006. Adipose Tissue as an Endocrine Organ. Obesity 14, 242S-249S.
- Allen, A.N., Schanze, J.J., Solow, A.R., Tyack, P.L., 2014. Analysis of a Blainville's beaked whale's movement response to playback of killer whale vocalizations. Marine Mammal Science 30, 154-168.
- Andreasson, U., Perret-Liaudet, A., van Waalwijk van Doorn, L.J.C., Blennow, K., Chiasserini, D., Engelborghs, S., Fladby, T., Genc, S., Kruse, N., Kuiperij, H.B., Kulic, L., Lewczuk, P., Mollenhauer, B., Mroczko, B., Parnetti, L., Vanmechelen, E., Verbeek, M.M., Winblad, B., Zetterberg, H., Koel-Simmelink, M., Teunissen, C.E., 2015. A Practical Guide to Immunoassay Method Validation. Frontiers in Neurology 6, 179.
- Anholt, B.R., Werner, E.E., 1995. Interaction between Food Availability and Predation Mortality Mediated by Adaptive-Behavior. Ecology 76, 2230-2234.
- Aoki, K., Sato, K., Isojunno, S., Narazaki, T., Miller, P.J.O., 2017. High diving metabolic rate indicated by high-speed transit to depth in negatively buoyant long-finned pilot whales. Journal of Experimental Biology 220, 3802-3811.
- Aoki, K., Watanabe, Y.Y., Crocker, D.E., Robinson, P.W., Biuw, M., Costa, D.P., Miyazaki, N., Fedak, M.A., Miller, P.J., 2011a. Northern elephant seals adjust gliding and stroking patterns with changes in buoyancy: validation of at-sea metrics of body density. Journal of Experimental Biology 214, 2973-2987.
- Arranz, P., De Soto, N.A., Madsen, P.T., Brito, A., Bordes, F., Johnson, M.P., 2011. Following a foraging fish-finder: Diel habitat use of Blainville's beaked whales revealed by echolocation. PloS one 6, e28353.

- Bagge, L.E., Koopman, H.N., Rommel, S.A., McLellan, W.A., Pabst, D.A., 2012. Lipid class and depth-specific thermal properties in the blubber of the short-finned pilot whale and the pygmy sperm whale. *The Journal of Experimental Biology* 215, 4330-4339.
- Baird, R.W., Dill, L.M., Hanson, M.B., 1998. Diving behaviour of killer whales. In: *World Marine Mammal Science Conference*, Monaco.
- Baird, R.W., Webster, D.L., Schorr, G.S., McSweeney, D.J., Barlow, J., 2008. Diel variation in beaked whale diving behavior. *Marine Mammal Science* 24, 630-642.
- Banner, K.M., Higgs, M.D., 2017. Considerations for assessing model averaging of regression coefficients. *Ecological Applications* 27, 78-93.
- Barbieri, M.M., McLellan, W.A., Wells, R.S., Blum, J.E., Hofmann, S., Gannon, J., Pabst, D.A., 2010. Using infrared thermography to assess seasonal trends in dorsal fin surface temperatures of free-swimming bottlenose dolphins (*Tursiops truncatus*) in Sarasota Bay, Florida. *Marine Mammal Science* 26, 53-66.
- Barlow, J., Clapham, P.J., 1997. A new birth-interval approach to estimating demographic parameters of humpback whales. *Ecology* 78, 535-546.
- Baumann-Pickering, S., Hildebrand, J.A., Yack, T., Moore, J.E. 2015. Modeling of Habitat and Foraging Behavior of Beaked Whales in the Southern California Bight (Scripps Institution of Oceanography, University of California, San Diego La Jolla United States).
- Beale, C.M., Monaghan, P., 2004. Behavioural responses to human disturbance: a matter of choice? *Anim Behav* 68, 1065-1069.
- Beaulieu-McCoy, N.E., Sherman, K.K., Trego, M.L., Crocker, D.E., Kellar, N.M., 2017. Initial validation of blubber cortisol and progesterone as indicators of stress response and maturity in an otariid; the California sea lion (*Zalophus californianus*). *General and Comparative Endocrinology* 252, 1-11.
- Beck, G.G., Smith, T.G., Hammill, M.O., 1993. Evaluation of Body Condition in the Northwest Atlantic Harp Seal (*Phoca groenlandica*). *Canadian Journal of Fisheries and Aquatic Sciences* 50, 1372-1381.
- Bednekoff, P.A., Houston, A.I., 1994. Optimizing Fat Reserves over the Entire Winter - a Dynamic-Model. *Oikos* 71, 408-415.
- Bé langer, C., Luu-The, V., Dupont, P., Tchernof, A., 2002. Adipose Tissue Intracrinology: Potential Importance of Local Androgen/Estrogen Metabolism in the Regulation of Adiposity. *Horm Metab Res* 34, 737-745.
- Benjaminsen, T. 1972. On the biology of the bottlenose whale, *Hyperoodon ampullatus* (Forster). *Norwegian Journal of Zoology* 20: 233-241.
- Bennett, K.A., Moss, S.E.W., Pomeroy, P., Speakman, J.R., Fedak, M.A., 2012. Effects of handling regime and sex on changes in cortisol, thyroid hormones and body mass in fasting grey seal pups. *Comparative Biochemistry and Physiology Part A: Molecular & Integrative Physiology* 161, 69-76.
- Bergendahl, M., Vance, M.L., Iranmanesh, A., Thorner, M.O., Veldhuis, J.D., 1996. Fasting as a metabolic stress paradigm selectively amplifies cortisol secretory burst mass and delays the time of maximal nyctohemeral cortisol concentration in healthy men. *J. Clin. Endocrinol. Metab.* 81, 692-699.
- Biro, P.A., Stamps, J.A., 2008. Are animal personality traits linked to life-history productivity? *Trends in Ecology & Evolution* 23, 361-368.

- Biuw, M., McConnell, B., Bradshaw, C.J.A., Burton, H., Fedak, M., 2003. Blubber and buoyancy: monitoring the body condition of free-ranging seals using simple dive characteristics. *Journal of Experimental Biology* 206, 3405-3423.
- Bolker, B.M., Brooks, M.E., Clark, C.J., Geange, S.W., Poulsen, J.R., Stevens, M.H.H., White, J.-S.S., 2008. Generalized linear mixed models: a practical guide for ecology and evolution. *Trends in Ecology & Evolution* 24, 127-135.
- Boness, D.J., Clapham, P.J., Mesnick, S.L., 2002. Life History and Reproductive Strategies, In: Hoelzel, A.R. (Ed.) *Marine Mammal Biology: An Evolutionary Approach*. Blackwell Science Ltd., Oxford, UK.
- Bonier, F., Martin, P.R., Moore, I.T., Wingfield, J.C., 2009. Do baseline glucocorticoids predict fitness? *Trends in Ecology & Evolution* 24, 634-642.
- Bose, N.a.L., J. , 1989. Propulsion of a fin whale (*Balaenoptera physalus*): why the fin whale is a fast swimmer. . *Proc R Soc Lond B Biol Sci* 237, 175-200.
- Bradford, A.L., Weller, D.W., Punt, A.E., Ivashchenko, Y.V., Burdin, A.M., VanBlaricom, G.R., Brownell, R.L., 2012. Leaner leviathans: body condition variation in a critically endangered whale population. *Journal of Mammalogy* 93, 251-266.
- Brodersen, J., Nilsson, P.A., Hansson, L.-A., Skov, C., Brönmark, C., 2008. Condition-dependent individual decision-making determines cyprinid partial migration. *Ecology* 89, 1195-1200.
- Brooks, S.P.a.G., A., 1998. General Methods for Monitoring Convergence of Iterative Simulations. *Journal of Computational and Graphical Statistics* 7, 434\*455.
- Caon, G., Fialho, C.B., Danilewicz, D., 2007. Body Fat Condition in Franciscanas (*Pontoporia blainvillei*) in Rio Grande do Sul, Southern Brazil. *Journal of Mammalogy* 88, 1335-1341.
- Castellini, M.A., Rea, L.D., 1992. The biochemistry of natural fasting and its limits. *Experientia* 48, 575-582.
- Castrillon, J., Huston, W., Nash, S.B., 2017. The blubber adipocyte index: A nondestructive biomarker of adiposity in humpback whales (*Megaptera novaeangliae*). *Ecology and Evolution* 7, 5131-5139.
- Champagne, C.D., Houser, D.S., Costa, D.P., Crocker, D.E., 2012. The Effects of Handling and Anesthetic Agents on the Stress Response and Carbohydrate Metabolism in Northern Elephant Seals. *PLoS ONE* 7.
- Champagne, C.D., Houser, D.S., Crocker, D.E., 2006. Glucose metabolism during lactation in a fasting animal, the northern elephant seal. *American Journal of Physiology - Regulatory, Integrative and Comparative Physiology* 291, R1129-R1137.
- Champagne, C.D., Kellar, N.M., Crocker, D.E., Wasser, S.K., Booth, R.K., Trego, M.L., Houser, D.S., 2017. Blubber cortisol qualitatively reflects circulating cortisol concentrations in bottlenose dolphins. *Marine Mammal Science* 33, 134-153.
- Christiansen, F., Dujon, A.M., Sprogis, K.R., Arnould, J.P.Y., Bejder, L., 2016. Noninvasive unmanned aerial vehicle provides estimates of the energetic cost of reproduction in humpback whales. *Ecosphere* 7, e01468.
- Christiansen, F., Vikingsson, G.A., Rasmussen, M.H., Lusseau, D., 2013. Minke whales maximise energy storage on their feeding grounds. *The Journal of Experimental Biology* 216, 427-436.
- Christiansen, F., Vivier, F., Charlton, C., Ward, R., Amerson, A., Burnell, S., Bejder, L., 2018. Maternal body size and condition determine calf growth rates in southern right whales. *Marine Ecology Progress Series* 592, 267-281.

- Clapham, P.J., 2000. The humpback whale: seasonal feeding and breeding in a baleen whale, In: Mann, J., Connor, R.C., Tyack, P.L., Whitehead, H. (Eds.) Cetaceans societies: field studies of dolphins and whales. University of Chicago Press, Chicago, IL, pp. 173-196.
- Clark, C.T., Fleming, A.H., Calambokidis, J., Kellar, N.M., Allen, C.D., Catelani, K.N., Robbins, M., Beaulieu, N.E., Steel, D., Harvey, J.T., 2016. Heavy with child? Pregnancy status and stable isotope ratios as determined from biopsies of humpback whales. *Conservation Physiology* 4, cow050.
- Coleman, R.A., Lee, D.P., 2004. Enzymes of triacylglycerol synthesis and their regulation. *Progress in Lipid Research* 43, 134-176.
- Collins, S., Kuhn, C.M., Petro, A.E., Swick, A.G., Chrnyk, B.A., Surwit, R.S., 1996. Role of leptin in fat regulation. *Nature* 380, 677-677.
- Cox, T.M., Ragen, T., Read, A., Vos, E., Baird, R., Balcomb, K., Barlow, J., Caldwell, J., Cranford, T., Crum, L. 2006. Understanding the impacts of anthropogenic sound on beaked whales (DTIC Document).
- Dalebout, M.K., Hooker, S.K., Christensen, I., 2001. Genetic diversity and population structure among northern bottlenose whales, *Hyperoodon ampullatus*, in the western North Atlantic Ocean. *Canadian Journal of Zoology* 79, 478-484.
- Dall, S.R., Houston, A.I., McNamara, J.M., 2004. The behavioural ecology of personality: consistent individual differences from an adaptive perspective. *Ecology Letters* 7, 734-339
- Dammhahn, M., Almeling, L., 2012. Is risk taking during foraging a personality trait? A field test for cross-context consistency in boldness. *Animal Behaviour* 84, 1131-1139.
- Dunphy-Daly, M.M., Heithaus, M.R. Wirsing, A.J., Mardon, J.S., Burkholder D.A., 2010. Predation risk influences the diving behaviour of a marine mesopredator. *Open Ecology Journal* 3, 8-15.
- De Ruiter, S.L., Southall, B.L., Calambokidis, J., Zimmer, W.M.X., Sadykova, D., Falcone, E.A., Friedlaender, A.S., Joseph, J.E., Moretti, D., Schorr, G.S., Thomas, L., Tyack, P.L., De Ruiter, S.L., Southall, B.L., Calambokidis, J., Zimmer, W.M.X., Sadykova, D., Falcone, E.A., Friedlaender, A.S., Joseph, J.E., Moretti, D., Schorr, G.S., Thomas, L., Tyack, P.L., 2013. First direct measurements of behavioural responses by Cuvier's beaked whales to mid-frequency active sonar. *Biology Letters* 9, 1-5.
- Deslypere, J.P., Verdonck, L., Vermeulen, A., 1985. Fat Tissue: A Steroid Reservoir and Site of Steroid Metabolism. *The Journal of Clinical Endocrinology & Metabolism* 61, 564-570.
- Dinneen, S., Alzaid, A., Miles, J., Rizza, R., 1993. Metabolic effects of the nocturnal rise in cortisol on carbohydrate metabolism in normal humans. *Journal of Clinical Investigation* 92, 2283-2290.
- Divertie, G.D., Jensen, M.D., Miles, J.M., 1991. Stimulation of Lipolysis in Humans by Physiological Hypercortisolemia. *Diabetes* 40, 1228-1232.
- Djurhuus, C.B., Gravholt, C.H., Nielsen, S., Mengel, A., Christiansen, J.S., Schmitz, O.E., Møller, N., 2002. Effects of cortisol on lipolysis and regional interstitial glycerol levels in humans. *American Journal of Physiology-Endocrinology and Metabolism* 283, E172-E177.
- Djurhuus, C.B., Gravholt, C.H., Nielsen, S., Pedersen, S.B., Møller, N., Schmitz, O., 2004. Additive effects of cortisol and growth hormone on regional and systemic lipolysis in humans. *American Journal of Physiology - Endocrinology and Metabolism* 286, E488-E494.

- Dunkin, R.C., McLellan, W.A., Blum, J.E., Pabst, D.A., 2005. The ontogenetic changes in the thermal properties of blubber from Atlantic bottlenose dolphin *Tursiops truncatus*. *Journal of Experimental Biology* 208, 1469-1480.
- Dunn, C., 2014. Insights into Blainville's beaked whale (*Mesoplodon densirostris*) communication. University of St Andrews, St Andrews, UK.
- Dunn, C., Hickmott, L., Talbot, D., Boyd, I., Rendell, L., 2013. Mid-frequency broadband sounds of Blainville's beaked whales. *Bioacoustics* 22, 153-163.
- Durban, J.W., Fearnbach, H., Barrett-Lennard, L. G., Perryman, W. L., Leroi, D. J. , 2015. Photogrammetry of killer whales using a small hexacopter launched at sea. *J. Unmanned Veh. Syst.* 3, 1-5.
- Ekman, J.B., Hake, M.K., 1990. Monitoring starvation risk: adjustments of body reserves in greenfinches (*Carduelis chloris L.*) during periods of unpredictable foraging success. *Behavioral Ecology* 1, 62-67.
- Engelhard, G., Brasseur, S., Hall, A., Burton, H., Reijnders, P., 2002. Adrenocortical responsiveness in southern elephant seal mothers and pups during lactation and the effect of scientific handling. *J Comp Physiol B* 172, 315-328.
- Eraud, C., Duriez, O., Chastel, O., Faivre, B., 2005. The energetic cost of humoral immunity in the Collared Dove, *Streptopelia decaocto*: is the magnitude sufficient to force energy-based trade-offs? *Funct Ecol* 19, 110-118.
- Evans, K., Hindell, M.A., Thiele, D., 2003. Body fat and condition in sperm whales, *Physeter macrocephalus*, from southern Australian waters. *Comparative Biochemistry and Physiology Part A: Molecular & Integrative Physiology* 134, 847-862.
- Exton, J.H., Friedmann, N., Wong, E.H.-A., Brineaux, J.P., Corbin, J.D., Park, C.R., 1972. Interaction of Glucocorticoids with Glucagon and Epinephrine in the Control of Gluconeogenesis and Glycogenolysis in Liver and of Lipolysis in Adipose Tissue. *Journal of Biological Chemistry* 247, 3579-3588.
- Fearnbach, H., Durban, J.W., Ellifrit, D.K., Balcomb, K.C., 2011. Size and long-term growth trends of Endangered fish-eating killer whales. *Endangered Species Research* 13, 173-180.
- Fields, D.A., Higgins, P.B., Radley, D., 2005. Air-displacement plethysmography: here to stay. *Curr Opin Clin Nutr* 8, 624-629.
- Fish, F.E., 1993. Power output and propulsive efficiency of swimming bottlenose dolphins (*Tursiops truncatus*). *Journal of Experimental Biology* 185, 179-193.
- Fish, F.E., 1998. Comparative kinematics and hydrodynamics of odontocete cetaceans: morphological and ecological correlates with swimming performance. *Journal of Experimental Biology* 201, 2867-2877.
- Folch, J., Lees, M., Stanley, G.H.S., 1957. A simple method for the isolation and purification of total lipides from animal tissues. *J. Biol. Chem.* 226, 497-509.
- Frid, A., Dill, L., 2002. Human-caused disturbance stimuli as a form of predation risk. *Conserv Ecol* 6.
- Frühbeck, G., Gómez-Ambrosi, J., Muruzábal, F.J., Burrell, M.A., 2001. The adipocyte: a model for integration of endocrine and metabolic signaling in energy metabolism regulation. *American Journal of Physiology - Endocrinology And Metabolism* 280, E827-E847.
- Galatius, A., Jansen, O.E., Kinze, C.C., 2013. Parameters of growth and reproduction of white-beaked dolphins (*Lagenorhynchus albirostris*) from the North Sea. *Marine Mammal Science* 29, 348-355.

- Galic, S., Oakhill, J.S., Steinberg, G.R., 2010. Adipose tissue as an endocrine organ. *Molecular and Cellular Endocrinology* 316, 129-139.
- Gardiner, K.J., Hall, A.J., 1997. Diel and annual variation in plasma cortisol concentrations among wild and captive harbor seals (*Phoca vitulina*). *Canadian Journal of Zoology* 75, 1773-1780.
- Gassmann, M., Wiggins, S.M., Hildebrand, J.A., 2015. Three-dimensional tracking of Cuvier's beaked whales' echolocation sounds using nested hydrophone arrays. *The Journal of the Acoustical Society of America* 138, 2483-2494.
- Godin, J.-G.J., Sproul, C.D., 1988. Risk taking in parasitized sticklebacks under threat of predation: effects of energetic need and food availability. *Canadian Journal of Zoology* 66, 2360-2367.
- Gómez-Campos, E., Borrell, A., Aguilar, A., 2011. Assessment of nutritional condition indices across reproductive states in the striped dolphin (*Stenella coeruleoalba*). *Journal of Experimental Marine Biology and Ecology* 405, 18-24.
- Gomez-Campos, E., Borrell, A., Correas, J., Aguilar, A., 2015. Topographical variation in lipid content and morphological structure of the blubber in the striped dolphin. *Sci Mar* 79, 189-197.
- Gowans, S., Whitehead, H.A.L., Arch, J.K., Hooker, S.K., 2000. Population size and residency patterns of northern bottlenose whales (*Hyperoodon ampullatus*) using the gully, Nova Scotia. *Journal of Cetacean Research and Management* 2, 201-210.
- Guerre-Millo, M., 2004. Adipose tissue and adipokines: for better or worse. *Diabetes Metab* 30, 13-19.
- Guinet, C., Servera, N., Mangin, S., Georges, J.-Y., Lacroix, A., 2004. Change in plasma cortisol and metabolites during the attendance period ashore in fasting lactating subantarctic fur seals. *Comparative Biochemistry and Physiology Part A* 137, 523-531.
- Hall, A.J., McConnell, B.J., Barker, R.J., 2001. Factors affecting first-year survival in grey seals and their implications for life history strategy. *J Anim Ecol* 70, 138-149.
- Hansen, I.A., Mead, J.M., 1965. The fate of dietary wax esters in the rat. *Proc Soc Exp Biol Med* 120, 527-532.
- Harcourt, R., Turner, E., Hall, A., Waas, J., Hindell, M., 2010. Effects of capture stress on free-ranging, reproductively active male Weddell seals. *J Comp Physiol A* 196, 147-154.
- Harris, C.M., Thomas, L., Sadykova, D., DeRuiter, S.L., Tyack, P.L., Southall, B.L., Read, A.J., Miller, P.J.O., 2016. The challenges of analyzing behavioral response study data: an overview of the MOCHA (Multi-study ocean acoustics human effects analysis) project. In: Popper, A.N., Hawkins, A. (Eds.) *The Effects of Noise on Aquatic Life II*. Springer, pp. 399-407.
- Hauksson, E., Víkingsson, G.A., Halldórsson, S.D., Ólafsdóttir, D., Sigurjónsson, J., 2011. Preliminary report on biological parameters for NA minke whales in Icelandic waters. *International Whaling Commission Reports SC/63/O15*.
- Heithaus, M.R., Frid, A., Wirsing, A.J., Dill, L.M., Fourqurean, J.W., Burkholder, D., Thomson, J., Bejder, L., 2007a. State-dependent risk-taking by green sea turtles mediates top-down effects of tiger shark intimidation in a marine ecosystem. *J Anim Ecol* 76, 837-844.
- Heithaus, M.R., Wirsing, A.J., Frid, A., Dill, L.M., 2007b. Behavioral indicators in marine conservation: Lessons from a pristine seagrass ecosystem. *Isr J Ecol Evol* 53, 355-370.
- Heyning, J.E., 2002. Cuvier's Beaked Whale, In: Jefferson, T.A. (Ed.) *Encyclopedia of Marine Mammals*. Academic Press, pp. 305-207.

- Hilton, G.M., Ruxton, G.D., Cresswell, W., 1999. Choice of foraging area with respect to predation risk in redshanks: the effects of weather and predator activity. *Oikos* 87, 295-302.
- Hooker, S.K., Baird, R.W., 1999a. Deep-diving behaviour of the northern bottlenose whale, *Hyperoodon ampullatus* (Cetacea: Ziphiidae). *Proceedings of the Royal Society of London B: Biological Sciences* 266, 671-676.
- Hooker, S.K., Baird, R.W., 1999b. Observations of Sowerby's Beaked Whales, *Mesoplodon bidens*, in the Gully, Nova Scotia. *Canadian Field Naturalist* 113, 273-277.
- Hooker, S.K., Iverson, S.J., Ostrom, P., Smith, S.C., 2001. Diet of northern bottlenose whales inferred from fatty-acid and stable-isotope analyses of biopsy samples. *Canadian Journal of Zoology* 79, 1442-1454.
- Hooker, S.K., Whitehead, H., Gowans, S., Baird, R.W., 2002. Fluctuations in distribution and patterns of individual range use of northern bottlenose whales. *Marine Ecology Progress Series* 225, 287-297.
- Houston, A.I., McNamara, J.M., 1993. A theoretical investigation of the fat reserves and mortality levels of small birds in winter. *Ornis Scandinavica*, 205-219.
- Houston, A.I., Mcnamara, J.M., Hutchinson, J.M.C., 1993. General Results Concerning the Trade-Off between Gaining Energy and Avoiding Predation. *Philos T Roy Soc B* 341, 375-397.
- Hughes, K.A., Reynolds, R.M., Andrew, R., Critchley, H.O.D., Walker, B.R., 2010. Glucocorticoids Turn Over Slowly in Human Adipose Tissue in Vivo. *The Journal of Clinical Endocrinology & Metabolism* 95, 4696-4702.
- Hughes, R., 2009. *Diet selection: an interdisciplinary approach to foraging behaviour*. John Wiley & Sons.
- Hunt, K. E., Moore, M. J., Rolland, R. M., Kellar N. M., Hall, A. J., Kershaw, J. L., Raverty, S. A., Davis, C. E., Yeates, L. C., Fauquier, D. A., Rowles, T. K., Kraus, S. D. 2013. Overcoming the challenges of studying conservation physiology in large whales: a review of available methods. *Conservation Physiology* 1, <https://doi.org/10.1093/conphys/cot006>
- Isojunno, S., Curé, C., Kvasdheim, P.H., Lam, F.P.A., Tyack, P.L., Wensveen, P.J., Miller, P.J.O.M., 2016. Sperm whales reduce foraging effort during exposure to 1–2 kHz sonar and killer whale sounds. *Ecological Applications* 26, 77-93.
- Isojunno, S., Miller, P.J.O., 2015. Sperm whale response to tag boat presence: biologically informed hidden state models quantify lost feeding opportunities. *Ecosphere* 6.
- Iverson, S.J., 2009. Blubber, In: Perrin, W.F., Würsig, B., Thewissen, J.G.M. (Eds.) *Encyclopedia of Marine Mammal* (Second Edition). Academic Press.
- Jefferson, T.A., Stacey, P.J., Baird, R.W., 1991. A review of Killer Whale interactions with other marine mammals: predation to co-existence. *Mammal Review* 21, 151-180.
- Johnson, M., Hickmott, L., Soto, N.A., Madsen, P.T., 2008. Echolocation behaviour adapted to prey in foraging Blainville's beaked whale (*Mesoplodon densirostris*). *Proceedings of the Royal Society of London B: Biological Sciences* 275, 133-139.
- Johnson, M., Madsen, P.T., Zimmer, W.M.X., Aguilar de Soto, N., Tyack, P.L., 2004. Beaked whales echolocate on prey. *Proceedings of the Royal Society of London B: Biological Sciences* 271, S383-S386.
- Johnson, M., Madsen, P.T., Zimmer, W.M.X., de Soto, N.A., Tyack, P.L., 2006. Foraging Blainville's beaked whales (*Mesoplodon densirostris*) produce distinct click types matched to different phases of echolocation. *Journal of Experimental Biology* 209, 5038-5050.
- Johnson, M.P., Tyack, P.L., 2003. A digital acoustic recording tag for measuring the response of wild marine mammals to sound. *Oceanic Engineering, IEEE Journal of* 28, 3-12.

- Jonsgård, Å., 1968a. Another note on the attacking behaviour of killer whales (*Orcinus orca*). Norsk Hvalfangst-Tidende 57, 175-176.
- Jonsgård, Å., 1968b. A note on the attacking behaviour of the killer whale (*Orcinus orca*). Norsk Hvalfangst-Tidende 57, 84-85.
- Kellar, N.M., Keliher, J., Trego, M.L., Catelani, K.N., Hanns, C., George, J.C., Rosa, C., 2013. Variation of bowhead whale progesterone concentrations across demographic groups and sample matrices. *Endangered Species Research* 22, 61-72.
- Kellar, N.M., Trego, M.L., Marks, C.I., Dizon, A.E., 2006. Determining pregnancy from blubber in three species of delphinids. *Marine Mammal Science* 22, 1-16.
- Kershaw, E.E., Flier, J.S., 2004. Adipose Tissue as an Endocrine Organ. *Journal of Clinical Endocrinology & Metabolism* 89, 2548-2556.
- Kershaw, J.L., Hall, A.J., 2016. Seasonal variation in harbour seal (*Phoca vitulina*) blubber cortisol - A novel indicator of physiological state? *Scientific Reports* 6, 21889.
- Kershaw, J.L., Sherrill, M., Davison, N.J., Brownlow, A., Hall, A.J., 2017. Evaluating morphometric and metabolic markers of body condition in a small cetacean, the harbor porpoise (*Phocoena phocoena*). *Ecology and Evolution* 7, 3494-3506.
- Konishi, K., 2006. Characteristics of blubber distribution and body condition indicators for Antarctic minke whales (*Balaenoptera bonaerensis*). *Mammal Study* 31, 15-22.
- Koopman, H.N., 1998. Topographical distribution of the blubber of harbour porpoises. *Journal of Mammalogy* 79, 260-270.
- Koopman, H.N., 2007. Phylogenetic, ecological, and ontogenetic factors influencing the biochemical structure of the blubber of odontocetes. *Marine Biology* 151, 277-291.
- Koopman, H.N., Iverson, S.J., Gaskin, D.E., 1996. Stratification and age-related differences in blubber fatty acids of the male harbour porpoise (*Phocoena phocoena*). *J Comp Physiol B* 165, 628-639.
- Koopman, H.N., Pabst, D.A., McLellan, W.A., Dillaman, R.M., Read, A.J., 2002. Changes in blubber distribution and morphology associated with starvation in the harbour porpoise (*Phocoena phocoena*): Evidence for regional differences in blubber structure and function. *Physiological and Biochemical Zoology* 75, 498-512.
- Koopman, H.N., Westgate, A.J., 2012. Solubility of nitrogen in marine mammal blubber depends on its lipid composition. *The Journal of Experimental Biology* 215:3856-3863.
- Kooyman, G.L., 1989. *Diverse Divers. Physiology and behaviour*. Berlin: Springer-Verlag.
- Krahn, M.M., Herman, D.P., Ylitalo, G.M., Sloan, C.A., Burrows, D.G., Hobbs, R.C., Mahoney, B.A., Yanagida, G.K., Calambokidis, J., Moore, S.E., 2004. Stratification of lipids, fatty acids and organochlorine contaminants in blubber of white whales and killer whales. *J. Cetacean Res. Manage.* 6, 175-189.
- Krebs, J.J.R., Davies, N.B., 1981. *An introduction to behavioural ecology*. Blackwell Scientific Publications, Oxford, 292 p.
- Kuiken, T., Hartmann, M.G., 1991. Dissection techniques and tissue sampling. *Proceedings of the first European Cetacean Society workshop on cetacean pathology*. Leiden, The Netherlands. *European Cetacean Society Newsletter* No. 17 - Special issue., 39.
- Kvadsheim, P., Lam, F.P.A., Miller, P.J., Doksaeter, L., Visser, F., Kleivane, L., Ijsselmuide, S.V., Samarra, F., Wensveen, P.J., Curé, C., Hickmott, L., Dekeling, R. 2011. Behavioural response studies of cetaceans to naval sonar signals in Norwegian waters - 3S-2011 cruise report.

- Lacsamana, J.K.M., Ventolero, M.F.H., Blatchley, D., Santos, M.D., 2015. First record of a rare beaked whale *Mesoplodon hotaula* in the Philippines. *Marine Biodiversity Records* 8, 1.
- Lee, M.-J., Pramyothin, P., Karastergiou, K., Fried, S.K., 2014. Deconstructing the roles of glucocorticoids in adipose tissue biology and the development of central obesity. *Biochimica et Biophysica Acta (BBA) - Molecular Basis of Disease* 1842, 473-481.
- Lima, S.L., 1998a. Nonlethal effects in the ecology of predator-prey interactions. *Bioscience* 48, 25-34.
- Lima, S.L., 1998b. Stress and decision making under the risk of predation: Recent developments from behavioral, reproductive, and ecological perspectives. *Adv Stud Behav* 27, 215-290.
- Lima, S.L., Dill, L.M., 1990. Behavioral decisions made under the risk of predation: a review and prospectus. *Canadian Journal of Zoology* 68, 619-640.
- Litchfield, C., Greenberg, A.J., Caldwell, D.K., Caldwell, M.C., Sipos, J.C., Ackman, R.G., 1975. Comparative lipid patterns in acoustical and nonacoustical fatty tissues of dolphins, porpoises and toothed whales. *Comparative Biochemistry and Physiology Part B: Comparative Biochemistry* 50, 591-597.
- Litchfield, C., Greenberg, A.J., Mead, J.G., 1976. The distinctive character of Ziphiidae head and blubber fats. *Cetology* 23, 1-10.
- Lockyer, C., 1976. Body weights of some species of large whales. *J Du Conseil* 36, 259-273.
- Lockyer, C., 1986. Body Fat Condition in Northeast Atlantic Fin Whales, *Balaenoptera physalus*, and Its Relationship with Reproduction and Food Resource. *Canadian Journal of Fisheries and Aquatic Sciences* 43, 142-147.
- Lockyer, C.H., McConnell, L.C., Waters, T.D., 1984. The biochemical composition of fin whale blubber. *Canadian Journal of Zoology* 62, 2553-2562.
- Lockyer, C.H., McConnell, L.C., Waters, T.D., 1985. Body condition in terms of anatomical and biochemical assessment of body fat in North Atlantic fin and sei whales. *Canadian Journal of Zoology* 63, 2328-2338.
- Lonati, G.L., Westgate, A.J., Pabst, D.A., Koopman, H.N., 2015. Nitrogen solubility in odontocete blubber and mandibular fats in relation to lipid composition. *The Journal of Experimental Biology* 218, 2620-2630.
- Lunn, D., Jackson, C., Best, N., Thomas, A., Spiegelhalter, D., 2012. *The BUGS book: A Practical Introduction to Bayesian Analysis*. CRC press, Boca Raton, New York, US.
- MacLeod, C.D., 2018. Beaked Whales, Overview, In: Wursig, B., Thewissen, J.G.M., Kovacs, K. (Eds.) *Encyclopedia of Marine Mammals*, 3rd Edition. Academic Press.
- MacLeod, R., MacLeod, C., Learmonth, J., Jepson, P., Reid, R., Deaville, R., Pierce, G., 2007. Mass-dependent predation risk and lethal dolphin–porpoise interactions. *Proceedings of the Royal Society of London B: Biological Sciences* 274, 2587-2593.
- Madsen, P.T., Aguilar de Soto, N., Tyack, P.L., Johnson, M., 2014. Beaked whales. *Current Biology* 24, R728-R730.
- Madsen, P.T., Johnson, M., de Soto, N.A., Zimmer, W.M.X., Tyack, P., 2005. Biosonar performance of foraging beaked whales (*Mesoplodon densirostris*). *Journal of Experimental Biology* 208, 181-194.
- Mansour, A.H., McKay, D., Lien, J., Orr, J.C., Banoub, J.H., Oien, N., Stenson, G., 2002. Determination of pregnancy status from blubber samples in minke whales (*Balaenoptera acutorostrata*). *Marine Mammal Science* 18, 112-120.

- Masuzaki, H., Paterson, J., Shinyama, H., Morton, N.M., Mullins, J.J., Seckl, J.R., Flier, J.S., 2001. A Transgenic Model of Visceral Obesity and the Metabolic Syndrome. *Science* 294, 2166-2170.
- Mazziotta, M., Pareto, A., 2013. Methods for constructing composite indices: one for all or all for one. *Rivista Italiana di Economia Demografia e Statistica* 67, 67-80.
- McClelland, S.J., Gay, M., Pabst, D.A., Dillaman, R., Westgate, A.J., Koopman, H.N., 2012. Microvascular patterns in the blubber of shallow and deep diving odontocetes. *Journal of Morphology* 273, 932-942.
- McEwen, B.S., Wingfield, J.C., 2003. The concept of allostasis in biology and biomedicine. *Horm Behav* 43, 2-15.
- McKinney, M.A., Atwood, T., Dietz, R., Sonne, C., Iverson, S.J., Peacock, E., 2014. Validation of adipose lipid content as a body condition index for polar bears. *Ecology and Evolution* 4, 516-527.
- McMahon, C.R., Burton, H.R., Bester, M.N., 2000. Weaning mass and the future survival of juvenile southern elephant seals, *Mirounga leonina*, at Macquarie Island. *Antarctic Science* 12, 149-153.
- McMahon, M., Gerich, J., Rizza, R., 1988. Effects of glucocorticoids on carbohydrate metabolism. *Diabetes/Metabolism Reviews* 4, 17-30.
- Mcnamara, J.M., 1990. The Policy Which Maximizes Long-Term Survival of an Animal Faced with the Risks of Starvation and Predation. *Adv Appl Probab* 22, 295-308.
- Mcnamara, J.M., Houston, A.I., 1987. Starvation and Predation as Factors Limiting Population-Size. *Ecology* 68, 1515-1519.
- Mcnamara, J.M., Houston, A.I., 1990. The Value of Fat Reserves and the Tradeoff between Starvation and Predation. *Acta Biotheor* 38, 37-61.
- Mead, J.G., 1989. Beaked whales of the genus *Mesoplodon*., In: Ridgway, S.H., Harrison, R. (Eds.) *Handbook of Marine Mammals: River Dolphins and Toothed Whales*. Academic Press, San Diego, pp. 349-430.
- Meseguer, A., Puche, C., Cabero, A., 2002. Sex Steroid Biosynthesis in White Adipose Tissue. *Horm Metab Res* 34, 731-736.
- Miklosovic, D.S., Murray, M.M., Howle, L.E., Fish, F.E., 2004. Leading-edge tubercles delay stall on humpback whale (*Megaptera novaeangliae*) flippers. *Physics of Fluids* 16, L39-L42.
- Miller, C.A., Best, P.B., Perryman, W.L., Baumgartner, M.F., Moore, M.J., 2012a. Body shape changes associated with reproductive status, nutritive condition and growth in right whales *Eubalaena glacialis* and *E. australis*. *Marine Ecology Progress Series* 459, 135-156.
- Miller, C.A., Reeb, D., Best, P.B., Knowlton, A.R., Brown, M.W., Moore, M.J., 2011. Blubber thickness in right whales *Eubalaena glacialis* and *Eubalaena australis* related with reproduction, life history status and prey abundance. *Marine Ecology Progress Series* 438, 267-283.
- Miller, P. 2013. 3S (expn 2): Behavioral Response Studies of Cetaceans to Navy Sonar Signals in Norwegian Waters (DTIC Document).
- Miller, P., Narazaki, T., Isojunno, S., Aoki, K., Smout, S., Sato, K., 2016a. Body density and diving gas volume of the northern bottlenose whale (*Hyperoodon ampullatus*). *Journal of Experimental Biology* 219, 2458-2468.
- Miller, P.J., Narazaki, T., Isojunno, S., Hansen, R., Kershaw, J., Neves dos Reis, M., Kleivane, L. 2015a. Body Condition and 3S15 Projects: 2015 Jan Mayen Trial. In Sea Mammal Research Unit, Technical Report.

- Miller, P.J., Wensveen, P.J., Isojunno, S., Hansen, R., Siegal, E., Neves dos Reis, M., Visser, F., Kvadsheim, P., Kleivane, L. 2016b. Body Condition and ORBS Projects: 2016 Jan Mayen Trial Cruise Report. In SMRU Technical Report.
- Miller, P.J.O., Biuw, M., Watanabe, Y.Y., Thompson, D., Fedak, M.A., 2012b. Sink fast and swim harder! Round-trip cost-of-transport for buoyant divers. *The Journal of Experimental Biology* 215, 3622-3630.
- Miller, P.J.O., Johnson, M.P., Madsen, P.T., Biassoni, N., Quero, M., Tyack, P.L., 2009. Using at-sea experiments to study the effects of airguns on the foraging behavior of sperm whales in the Gulf of Mexico. *Deep-Sea Res Pt I* 56, 1168-1181.
- Miller, P.J.O., Johnson, M.P., Tyack, P.L., Terray, E.A., 2004a. Swimming gaits, passive drag and buoyancy of diving sperm whales (*Physeter macrocephalus*). *Journal of Experimental Biology* 207, 1953-1967.
- Miller, P.J.O., Johnson, M.P., Tyack, P.L., Terray, E.A., 2004b. Swimming gaits, passive drag and buoyancy of diving sperm whales *Physeter macrocephalus*. *Journal of Experimental Biology* 207, 1953-1967.
- Miller, P.J.O., Kvadsheim, P.H., Lam, F.P.A., Tyack, P.L., Cure, C., DeRuiter, S.L., Kleivane, L., Sivle, L.D., van IJsselmuide, S.P., Visser, F., Wensveen, P.J., von Benda-Beckmann, A.M., Lopez, L.M.M., Narazaki, T., Hooker, S.K., 2015b. First indications that northern bottlenose whales are sensitive to behavioural disturbance from anthropogenic noise. *Royal Society Open Science* 2.
- Miller, P.J.O., Kvadsheim, P.H., Lam, F.P.A., Wensveen, P.J., Antunes, R., Alves, A.C., Visser, F., Kleivane, L., Tyack, P.L., Sivle, L.D., 2012c. The Severity of Behavioral Changes Observed During Experimental Exposures of Killer (*Orcinus orca*), Long-Finned Pilot (*Globicephala melas*), and Sperm (*Physeter macrocephalus*) Whales to Naval Sonar. *Aquat Mamm* 38, 362-401.
- Miller, P.J.O., Narazaki, T., Isojunno, S., Aoki, K., Smout, S.C., Sato, K., 2016c. Body density and diving gas volume of the northern bottlenose whale (*Hyperoodon ampullatus*). *The Journal of Experimental Biology* 219, 2458-2468.
- Miller, P.J.O.M., Shapiro, A.D., Deecke, V.B., 2010. The diving behaviour of mammal-eating killer whales (*Orcinus orca*): variations with ecological not physiological factors. *Canadian Journal of Zoology* 88, 1103-1112.
- Millero, F.J., 2010. History of the equation of state of seawater. *Oceanography* 23, 18-33.
- Montie, E.W., Garvin, S.R., Fair, P.A., Bossart, G.D., Mitchum, G.B., McFee, W.E., Speakman, T., Starczak, V.R., Hahn, M.E., 2008. Blubber morphology in wild bottlenose dolphins (*Tursiops truncatus*) from the Southeastern United States: Influence of geographic location, age class, and reproductive state. *Journal of Morphology* 269, 496-511.
- Moya-Larano, J., Macias-Ordóñez, R., Blanckenhorn, W.U., Fernandez-Montraveta, C., 2008. Analysing body condition: mass, volume or density? *J Anim Ecol* 77, 1099-1108.
- Narazaki, T., Isojunno, S., Nowacek, D.P., Swift, R., Friedlaender, A.S., Ramp, C., Smout, S., Aoki, K., Deecke, V.B., Sato, K., Miller, P.J.O., 2018. Body density of humpback whales (*Megaptera novaengliae*) in feeding aggregations estimated from hydrodynamic gliding performance. *PLoS One* 13, e0200287.
- Nevenzel, J.C., 1970. Occurrence, function and biosynthesis of wax esters in marine organisms. *Lipids* 5, 308-319.
- New, L.F., Harwood, J., Thomas, L., Donovan, C., Clark, J.S., Hastie, G., Thompson, P.M., Cheney, B., Scott-Hayward, L., Lusseau, D., 2013a. Modelling the biological significance

- of behavioural change in coastal bottlenose dolphins in response to disturbance. *Funct Ecol* 27, 314-322.
- New, L.F., Moretti, D.J., Hooker, S.K., Costa, D.P., Simmons, S.E., 2013b. Using energetic models to investigate the survival and reproduction of beaked whales (family *Ziphiidae*). *PLoS ONE* 8, e68725.
- Newton, C.J., Samuel, D.L., James, V.H.T., 1986. Aromatase activity and concentrations of cortisol, progesterone and testosterone in breast and abdominal adipose tissue. *J. Steroid Biochem.* 24, 1033-1039.
- Nordøy, E.S., 1995. Do minke whales (*Balaenoptera acutorostrata*) digest wax esters. *Br J Nutr* 74, 717-722.
- Noren, P.D., Williams, M.T., Berry, P., Butler, E., 2009. Thermoregulation during swimming and diving in bottlenose dolphins, *Tursiops truncatus*. *J Comp Physiol B* 169, 93-99.
- Notarbartolo-di-Sciara, G., 1987. Killer whale, *Orcinus orca*, in the Mediterranean Sea. *Marine Mammal Science* 3, 356-360.
- Nowacek, D.P., Christiansen, F., Bejder, L., Goldbogen, J.A., Friedlaender, A.S., 2016. Studying cetacean behaviour: new technological approaches and conservation applications. *Anim Behav* 120, 235-244.
- NRC 2005. Marine Mammal Populations and Ocean Noise. Determining when noise causes biologically significant effects. (Washington DC, National Research Council).
- NRC 2016. Approached to understanding the cumulative effects of stressors on marine mammals. (Washington DC, National Research Council).
- Olsen, E., Grahl-Nielsen, O., 2003. Blubber fatty acids of minke whales: stratification, population identification and relation to diet. *Marine Biology* 142, 13-24.
- Ortiz, R.M., Houser, D.S., Wade, C.E., Ortiz, C.L., 2003. Hormonal changes associated with the transition between nursing and natural fasting in northern elephant seals (*Mirounga angustirostris*). *General and Comparative Endocrinology* 130, 78-83.
- Ortiz, R.M., Wade, C.E., Ortiz, C.L., 2001. Effects of prolonged fasting on plasma cortisol and TH in postweaned northern elephant seal pups. *American Journal of Physiology - Regulatory, Integrative and Comparative Physiology* 280, R790-R795.
- Pabst, D.A., Rommel, S., McLellan, W.A., 1999. Functional morphology of marine mammals, In: Reynolds, J.E., Rommel, S.A. (Eds.) *Biology of Marine Mammals*. Smithsonian Institution Press, Washington, pp. 15-72.
- Pallin, L.J., Baker, C.S., Steel, D., Kellar, N.M., Robbins, J., Johnston, D.W., Nowacek, D.P., Read, A.J., Friedlaender, A.S., 2018. High pregnancy rates in humpback whales (*Megaptera novaeangliae*) around the Western Antarctic Peninsula, evidence of a rapidly growing population. *Royal Society Open Science* 5.
- Peckett, A.J., Wright, D.C., Riddell, M.C., 2011. The effects of glucocorticoids on adipose tissue lipid metabolism. *Metabolism: clinical and experimental* 60, 1500-1510.
- Pérez, J.M., Jensen, F.H., Rojano-Doñate, L., Aguilar de Soto, N., 2016. Different modes of acoustic communication in deep-diving short-finned pilot whales (*Globicephala macrorhynchus*). *Marine Mammal Science*.
- Perez, S., Garcia-Lopez, A., De Stephanis, R., Gimenez, J., Garcia-Tiscar, S., Verborgh, P., Mancera, J.M., Martinez-Rodriguez, G., 2011. Use of blubber levels of progesterone to determine pregnancy in free-ranging live cetaceans. *Marine Biology* 158, 1677-1680.

- Perryman, W.C., Lynn, M.S., 2002. Evaluation of nutritive condition and reproductive status of migrating gray whales (*Eschrichtius robustus*) based on analysis of photogrammetric data, Vol 4.
- Pineda, M.H., 2003. Female Reproductive System : Ovarian Hormones. McDonald's Veterinary Endocrinology and Reproduction.
- Place, A.R., 1992. Comparative aspects of lipid digestion and absorption: physiological correlates of wax ester digestion. *Am J Physiol* 263.
- Plummer, M., Best, N., Cowles, K., Vines, K., Sarkar, D., Bates, D., Almond, R., Magnusson, A., Plummer, M.M. 2015. Package *coda* (Comprehensive R Archive Network).
- Pomeroy, P.P., Fedak, M.A., Rothery, P., Anderson, S., 1999. Consequences of maternal size for reproductive expenditure and pupping success of grey seals at North Rona, Scotland. *J Anim Ecol* 68, 235-253.
- Pond, C.M., 1992. An Evolutionary and Functional View of Mammalian Adipose-Tissue. *P Nutr Soc* 51, 367-377.
- Pond, C.M., 1998. The fats of life. Cambridge University Press, Cambridge.
- Quinn, J.L., Cole, E., Bates, J., Payne, R., Cresswell, W., 2011. Personality predicts individual responsiveness to the risks of starvation and predation. *Proceedings of the Royal Society of London B: Biological Sciences*, rspb20112227.
- Ramp, C., Berube, M., Palsboll, P., Hagen, W., Sears, R., 2010. Sex-specific survival in the humpback whale *Megaptera novaeangliae* in the Gulf of St. Lawrence, Canada. *Marine Ecology Progress Series* 400, 267-276.
- Ramp, C., Delarue, J., Palsboll, P.J., Sears, R., Hammond, P.S., 2015. Adapting to a warmer ocean-seasonal shift of baleen whale movements over three decades. *PLoS One* 10, e0121374.
- Rands, S.A., Pettifor, R.A., Rowcliffe, J.M., Cowlshaw, G., 2004. State-dependent foraging rules for social animals in selfish herds. *P Roy Soc B-Biol Sci* 271, 2613-2620.
- Read, A.J., 1990. Estimation of body condition in harbour porpoises, *Phocoena phocoena*. *Canadian Journal of Zoology* 68, 1962-1966.
- Réale, D., Reader, S.M., Sol, D., McDougall, P.T., Dingemanse, N.J., 2007. Integrating animal temperament within ecology and evolution. *Biological Reviews* 82, 291-318.
- Reilly, J.J., Fedak, M.A., 1990. Measurement of the body composition of living gray seals by hydrogen isotope dilution. *J. Appl. Physiol.* 69, 885-891.
- Richards, L.J., 1983. Hunger and the optimal diet. *The American Naturalist* 122, 326-334.
- Ridgway, S.H., Howard, R., 1979. Dolphin lung collapse and intramuscular circulation during free diving: evidence from nitrogen washout. *Science* 206, 1182-1183.
- Riviere, J.E., Engelhardt, F.R., Solomon, J., 1977. The relationship of Thyroxine and Cortisol in the Moulting of the Harbour Seal (*Phoca vitulina*). *General and Comparative Endocrinology* 31, 398-401.
- Rosel, P.E., 2003. PCR-based sex determination in Odontocete cetaceans. *Conservation Genetics* 4, 647-649.
- Ruchonnet, D., Boutoute, M., Guinet, C., Mayzaud, P., 2006. Fatty acid composition of Mediterranean fin whale *Balaenoptera physalus* blubber with respect to body heterogeneity and trophic interaction. *Marine Ecology Progress Series* 311, 165-174.
- Ryan, C., McHugh, B., O'Connor, I., Berrow, S., 2012. Lipid content of blubber biopsies is not representative of blubber in situ for fin whales (*Balaenoptera physalus*). *Marine Mammal Science* 00, 1-6.

- Samra, J.S., Clark, M.L., Humphreys, S.M., MacDonald, I.A., Bannister, P.A., Frayn, K.N., 1998. Effects of Physiological Hypercortisolemia on the Regulation of Lipolysis in Subcutaneous Adipose Tissue. *The Journal of Clinical Endocrinology & Metabolism* 83, 626-631.
- Samuel, A.M., Worthy, G.A.J., 2004. Variability in fatty acid composition of bottlenose dolphin (*Tursiops truncatus*) blubber as a function of body site, season, and reproductive state. *Canadian Journal of Zoology* 82, 1933-1942.
- Sapolsky, R.M., Alberts, S.C., Altmann, J., 1997. Hypercortisolism associated with social subordination or social isolation among wild baboons. *Archives of General Psychiatry* 54, 1137-1143.
- Saraswathy, N., Ramalingam, P., 2011. 11 - Two-dimensional gel electrophoresis of proteins, In: Saraswathy, N., Ramalingam, P. (Eds.) *Concepts and Techniques in Genomics and Proteomics*. Woodhead Publishing, pp. 159-170.
- Sargent, J.R., 1978. Marine wax esters. *Science Progress* 1933 (65), 437-458.
- Sargent, J.R., Gatten, R.R., McIntosh, R., 1977. Wax esters in the marine environment — their occurrence, formation, transformation and ultimate fates. *Marine Chemistry* 5, 573-584.
- Sato, K., Aoki, K., Watanabe, Y.Y., Miller, P.J.O., 2013. Neutral buoyancy is optimal to minimize the cost of transport in horizontally swimming seals. *Scientific Reports* 3, 2205.
- Sato, K., Mitani, Y., Cameron, M.F., Siniff, D.B., Naito, Y., 2003. Factors affecting stroking patterns and body angle in diving Weddell seals under natural conditions. *Journal of Experimental Biology* 206, 1461-1470.
- Schwacke, L.H., Smith, C.R., Townsend, F.I., Wells, R.S., Hart, L.B., Balmer, B.C., Collier, T.K., De Guise, S., Fry, M.M., Guillette, L.J., Lamb, S.V., Lane, S.M., McFee, W.E., Place, N.J., Tumlin, M.C., Ylitalo, G.M., Zolman, E.S., Rowles, T.K., 2014. Health of Common Bottlenose Dolphins (*Tursiops truncatus*) in Barataria Bay, Louisiana, Following the Deepwater Horizon Oil Spill. *Environmental Science & Technology* 48, 93-103.
- Seckl, J.R., Walker, B.R., 2001. Minireview: 11 $\beta$ -Hydroxysteroid Dehydrogenase Type 1— A Tissue-Specific Amplifier of Glucocorticoid Action. *Endocrinology* 142, 1371-1376.
- Shier, P.D., Schemmel, R., 1975. Effects of Diet, Age, Strain and Anatomical Site on Fat Depot Triglyceride and Fatty Acid Content in Rats. *Proceedings of the Society for Experimental Biology and Medicine* 149, 864-870.
- Sih, A., 1980. Optimal Behavior - Can Foragers Balance 2 Conflicting Demands. *Science* 210, 1041-1043.
- Sih, A., Bell, A., Johnson, J.C., 2004. Behavioral syndromes: an ecological and evolutionary overview. *Trends in Ecology & Evolution* 19, 372-378.
- Sih, A., Mathot, K.J., Moirón, M., Montiglio, P.O., Wolf, M., Dingemanse, N.J., 2015. Animal personality and state-behaviour feedbacks: a review and guide for empiricists. *Trends in Ecology & Evolution* 30, 50-60.
- Siiteri, P.K., 1987. Adipose tissue as a source of hormones. *Am. J. Clin. Nutr.* 45, 277-282.
- Silk, J.B., Alberts, S.C., Altmann, J., 2003. Social bonds of female baboons enhance infant survival. *Science* 302, 1231-1234.
- Sinclair, A.R.E., Arcese, P., 1995. Population Consequences of Predation-Sensitive Foraging - the Serengeti Wildebeest. *Ecology* 76, 882-891.
- Singleton, E.M., McLellan, W.A., Koopman, H.N., Pokorny, A., Scharf, F.S., Pabst, A.D., 2017. Lipid composition and thermal properties of the blubber of Gervais' beaked whale (*Mesoplodon europaeus*) across ontogeny. *Marine Mammal Science* 33, 695-705.

- Sinn, D., Apiolaza, L., Moltchanivskyj, N., 2006. Heritability and fitness-related consequences of squid personality traits. *Journal of Evolutionary Biology* 19, 1437-1447.
- Smith, H.R., Worthy, G.A.J., 2006. Stratification and intra- and inter-specific differences in fatty acid composition of common dolphin (*Delphinus sp.*) blubber: Implications for dietary analysis. *Comparative Biochemistry and Physiology Part B: Biochemistry and Molecular Biology* 143, 486-499.
- SOUNDTAG 2016. DTAG Accessed 19 October 2016. <http://soundtags.st-andrews.ac.uk/dtags/dtag-toolbox/>
- SOUNDTAG 2017a. DTAG-2 Accessed 16 August 2017. <https://www.soundtags.org/dtags/dtag-2/>
- SOUNDTAG 2017b. DTAG-3 Accessed 16 August 2017. <https://www.soundtags.org/dtags/dtag-3/>
- Southall, B.L., Nowacek, D.P., Miller, P.J.O., Tyack, P.L., 2016. Experimental field studies to measure behavioral responses of cetaceans to sonar. *Endangered Species Research* 31, 293-315.
- Steffen, P., Kwiatkowski, M., Robertson, W.D., Zarrine-Afsar, A., Deterra, D., Richter, V., Schlüter, H., 2016. Protein species as diagnostic markers. *Journal of Proteomics* 134, 5-18.
- Stevick, P.T., Allen, J., Clapham, P.J., Katona, S.K., Larsen, F., Lien, J., Mattila, D.K., Palsboll, P.J., Sears, R., Sigurjonsson, J., Smith, T.D., Vikingsson, G., Oien, N., Hammond, P.S., 2006. Population spatial structuring on the feeding grounds in North Atlantic humpback whales (*Megaptera novaeangliae*). *Journal of Zoology* 270, 244-255.
- Stimpert, A., DeRuiter, S.L., Southall, B., Moretti, D., Falcone, E., Goldbogen, J., Friedlaender, A., Schorr, G., Calambokidis, J., 2014. Acoustic and foraging behavior of a Baird's beaked whale, *Berardius bairdii*, exposed to simulated sonar. *Scientific Reports* 4.
- Stimson, R.H., Andersson, J., Andrew, R., Redhead, D.N., Karpe, F., Hayes, P.C., Olsson, T., Walker, B.R., 2009. Cortisol Release From Adipose Tissue by 11 $\beta$ -Hydroxysteroid Dehydrogenase Type 1 in Humans. *Diabetes*. 58, 46-53.
- Stirling, I., Thiemann, G.W., Richardson, E., 2008. Quantitative Support for a Subjective Fatness Index for Immobilized Polar Bears. *The Journal of Wildlife Management* 72, 568-574.
- Strack, A.M., Sebastien, R.J., Schwartz, M.W., Dallman, M.F., 1995. Glucocorticoids and insulin: reciprocal signals for energy balance. *American Journal of Physiology* 268, 142-149.
- Struntz, D.J., McLellan, W.A., Dillaman, R.M., Blum, J.E., Kucklick, J.R., Pabst, D.A., 2004. Blubber development in bottlenose dolphins (*Tursiops truncatus*). *Journal of Morphology* 259, 7-20.
- Stulnig, T.M., Waldhäusl, W., 2004. 11 $\beta$ -Hydroxysteroid dehydrogenase Type 1 in obesity and Type 2 diabetes. *Diabetologia* 47, 1-11.
- Su, Y.S., Yajima, M. 2012. Package *R2jags* (Comprehensive R Archive Network).
- Swaim, Z.T., Westgate, A.J., Koopman, H.N., Rolland, R.M., Kraus, S.D., 2009. Metabolism of ingested lipids by North Atlantic right whales. *Endangered Species Research* 6, 259-271.
- Tornero, V., Borrell, A., Forcada, J., Pubill, E., Aguilar, A., 2004. Retinoid and lipid patterns in the blubber of common dolphins (*Delphinus delphis*): implications for monitoring vitamin A status. *Comparative Biochemistry and Physiology Part B: Biochemistry and Molecular Biology* 137, 391-400.
- Trana, M.R., Roth, J.D., Tomy, G.T., Anderson, W.G., Ferguson, S.H., 2015. Influence of sample degradation and tissue depth on blubber cortisol in beluga whales. *Journal of Experimental Marine Biology and Ecology* 462, 8-13.

- Trayhurn, P., Wood, I.S., 2004. Adipokines: inflammation and the pleiotropic role of white adipose tissue. *British Journal of Nutrition* 92, 347-355.
- Trego, M.L., Kellar, N.M., Danil, K., 2013. Validation of Blubber Progesterone Concentrations for Pregnancy Determination in Three Dolphin Species and a Porpoise. *PLoS ONE* 8, e69709.
- Tyack, P.L. 2015. Comparing the Foraging Efficiency of Beaked Whales On and Off Naval Ranges (School of Biology, University of St Andrews Fife United Kingdom).
- Tyack, P.L., Johnson, M., Aguilar de Soto, N., Sturlese, A., Madsen, P.T., 2006. Extreme diving of beaked whales. *Journal of Experimental Biology* 209, 4238-4253.
- Tyack, P.L., Zimmer, W.M.X., Moretti, D., Southall, B.L., Claridge, D.E., Durban, J.W., Clark, C.W., D'Amico, A., DiMarzio, N., Jarvis, S., McCarthy, E., Morrissey, R., Ward, J., Boyd, I.L., 2011. Beaked Whales Respond to Simulated and Actual Navy Sonar. *PLoS ONE* 6, e17009.
- Van Oers, K., Drent, P.J., De Goede, P., Van Noordwijk, A.J., 2004. Realized heritability and repeatability of risk-taking behaviour in relation to avian personalities. *Proceedings of the Royal Society of London B: Biological Sciences* 271, 65-73.
- Vikingsson, G.A., 1995. Body condition of fin whales during summer off Iceland, In: Arnoldus Schytte Blix, L.W., Øyvind, U. (Eds.) *Developments in Marine Biology*. Elsevier Science, pp. 361-369.
- Wahlberg, M., Beedholm, K., Heerfordt, A., Møhl, B., 2011. Characteristics of biosonar signals from the northern bottlenose whale, *Hyperoodon ampullatus*. *The Journal of the Acoustical Society of America* 130, 3077-3084.
- Wang, Z., Chen, Z., Xu, S., Ren, W., Zhou, K., Yang, G., 2015. 'Obesity' is healthy for cetaceans? Evidence from pervasive positive selection in genes related to triacylglycerol metabolism. *Scientific Reports* 5, 14187.
- Watanabe, Y., Baranov, E.A., Sato, K., Naito, Y., Miyazaki, N., 2006. Body density affects stroke patterns in Baikal seals. *J Exp Biol* 209, 3269-3280.
- Watwood, S.L., Miller, P.J.O., Johnson, M., Madsen, P.T., Tyack, P.L., 2006. Deep-diving foraging behaviour of sperm whales (*Physeter macrocephalus*). *Journal of Animal Ecology* 75, 814-825.
- Wellard, R., Lightbody, K., Fouda, L., Blewitt, M., Riggs, D., Erbe, C., 2016. Killer Whale (*Orcinus orca*) Predation on Beaked Whales (*Mesoplodon* spp.) in the Bremer Sub-Basin, Western Australia. *PloS ONE* 11, e0166670.
- Whitehead, H., Wimmer, T., 2005. Heterogeneity and the mark-recapture assessment of the Scotian Shelf population of northern bottlenose whales (*Hyperoodon ampullatus*). *Canadian Journal of Fisheries and Aquatic Sciences* 62, 2573-2585.
- Whitehead, H.A.L., Gowans, S., Faucher, A., MacCarrey, S.W., 1997a. Status of the northern bottlenose whale, *Hyperoodon ampullatus* in the Gully, Nova Scotia. *Canadian Field Naturalist* 111, 287-292.
- Whitehead, H.A.L., Gowans, S., Faucher, A., MacCarrey, S.W., 1997b. Population analysis of Northern Bottlenose whales in the Gully, Nova Scotia. *Marine Mammal Science* 13, 173-185.
- Whitehead, H., Hooker, S.K., 2012. Uncertain status of northern bottlenose whale *Hyperoodon ampullatus*: population fragmentation, legacy of whaling and current threats. *Endangered Species Research* 19, 47-61.

- Williams, R., Vikingsson, G.A., Gislason, A., Lockyer, C., New, L., Thomas, L., Hammond, P.S., 2013. Evidence for density-dependent changes in body condition and pregnancy rate of North Atlantic fin whales over four decades of varying environmental conditions. *J Conseil* 70, 1273-1280.
- Williams, T.M., Davis, R.W., Fuiman, L.A., Francis, J., Le Boeuf, B.L., Horning, M., Calambokidis, J., Croll, D.A., 2000. Sink or swim: Strategies for cost-efficient diving by marine mammals. *Science* 288, 133-136.
- Williams, T.M., Kendall, T.L., Richter, B.P., Ribeiro-French, C.R., John, J.S., Odell, K.L., Losch, B.A., Feuerbach, D.A., Stamper, M.A., 2017. Swimming and diving energetics in dolphins: a stroke-by-stroke analysis for predicting the cost of flight responses in wild odontocetes. *Journal of Experimental Biology* 220, 1135-1145.
- Wimmer, T., Whitehead, H., 2004. Movements and distribution of northern bottlenose whales, *Hyperoodon ampullatus*, on the Scotian Slope and in adjacent waters. *Can J Zool* 82, 1782-1794.
- Wirsing, A.J., Heithaus, M.R., Dill, L.M., 2011. Predator-induced modifications to diving behavior varying with foraging mode. *Oikos* 120, 1005-1012.
- Woodward, B.L., Winn, J.P., Fish, F.E., 2006. Morphological specializations of baleen whales associated with hydrodynamic performance and ecological niche. *Journal of Morphology* 267, 1284-1294.
- Young, R.A., 1976. Fat, Energy and Mammalian Survival. *Amer. Zool.* 16, 699-710.
- Zimmer, W.M., Johnson, M.P., Madsen, P.T., Tyack, P.L., 2005. Echolocation clicks of free-ranging Cuvier's beaked whales (*Ziphius cavirostris*). *The Journal of the Acoustical Society of America* 117, 3919-3927.
- Zimmer, W.M., Tyack, P.L., 2007. Repetitive shallow dives pose decompression risk in deep-diving beaked whales. *Marine Mammal Science* 23, 888-925.
- Zuur, A.F., Ieno, E.N., Elphick, C.S., 2010. A protocol for data exploration to avoid common statistical problems. *Methods Ecol Evol* 1, 3-14.

## 8 APPENDICES

### Appendix A. Supporting Data – None

### Appendix B. List of Scientific / Technical Publications

#### Articles in peer-review journals:

Narazaki, T., Isojunno, S., Nowacek, D.P., Swift, R., Friedlaender, A.S., Ramp, C., Smout, S., Aoki, K., Deecke, V.B., Sato, K., Miller, P.J.O. (2018). Body density of humpback whales (*Megaptera novaeangliae*) in feeding aggregations estimated from hydrodynamic gliding performance. *PLoS ONE* 13(7): e0200287. <https://doi.org/10.1371/journal.pone.0200287>

Kershaw, J. L., Botting, C. H., Brownlow, A. Hall, A. J. (2018). Not just fat: investigating the proteome of cetacean blubber tissue. *Cons Phys.* 6(1).

Aoki, K., Sato, K., Isojunno, S., Narazaki, T., Miller, P. J. O. (2017). High diving metabolic rate indicated by high-speed transit to depth in negatively buoyant long-finned pilot whales. *J. Exp. Biol.* 220, 3812-3811. Featured in Inside JEB.

Kershaw, J. L., Sherrill, M., Davison, H. J., Brownlow, A., Hall, A. J. (2017). Evaluating morphometric and metabolic markers of condition in a small cetacean, the harbour porpoise (*Phocoena phocoena*). *Ecology and Evolution* 7 (10): 3494-3506.

Miller, P., Narazaki, T., Isojunno, S., Aoki, K., Smout, S., Sato, K. (2016). Body density and diving gas volume of the northern bottlenose whale (*Hyperoodon ampullatus*). *J. Exp. Biol.* 219, 2458-2468.

Kershaw, J. L. & Hall, A. J. (2016). Seasonal variation in harbour seal (*Phoca vitulina*) blubber cortisol - A novel indicator of physiological state? *Scientific Reports.* 6: 21889. DOI: 10.1038/srep21889

Kershaw, J.L., Brownlow, A., Ramp, C., Miler, P., Hall, A.J. (submitted) A trade-off between buoyancy and energy storage in deep diving cetaceans? Implications for body condition assessments of beaked whales. *Aquat. Cons. Mar. Freshw. Ecosys.*

#### Conference / Symposium abstracts

Patrick Miller et al., Diving lung volume of Cuvier's beaked whale (*Ziphius cavirostris*) and Northern bottlenose whale (*Hyperoodon ampullatus*) measured using biomechanical data. Society for Experimental Biology. Salzburgh 02 July, 2012.

Patrick Miller et al. Body-density and diving lung volume of northern bottlenose whales (*H. ampullatus*) derived from analysis of hydrodynamic performance during glides. *Biologging* 5, Strasburg, 08 Sept. 2014.

Patrick Miller et al. Geographic variation in the body density of the northern bottlenose whale (*Hyperoodon ampullatus*). The 21st Biennial Conference on the Biology of Marine Mammals. USA, December 13th-18th, 2015

Tomoko Narazaki et al. Body density of feeding aggregations of humpback whales (*Megaptera novaengliae*) in Antarctica and the Gulf of St Lawrence estimated from hydrodynamic gliding performance. The 21st Biennial Conference on the Biology of Marine Mammals. 2015.

Joanna Kershaw et al. The pleiotropic role of cetacean blubber. The 21st Biennial Conference on the Biology of Marine Mammals. 2015.

Kagari Aoki et al. Negative buoyancy and high metabolic rate of long-finned pilot whales: An estimation of body condition and drag coefficient of freely diving animals. The 21st Biennial Conference on the Biology of Marine Mammals. 2015.

Joanna Kershaw et al. The Bigger the Better : Measuring Body Condition in Large Cetaceans. SMRU NERC conference 2016.

Kershaw. The Pleiotropic Role of Cetacean Blubber. Annual Conference for the UK and Ireland Regional Student Chapter for the Society of Marine Mammology, St. Andrews January 2016.

Patrick Miller et al. The Bottlenose Whales of Jan Mayen. 22nd Biennial Conference on the Biology of Marine Mammals, Canada, 2017.

Kershaw. Beaked whale blubber: What's more important, energy or buoyancy? Biennial Conference for the Society of Marine Mammology, Halifax October 2017.

Kershaw. Not just fat: The proteome of cetacean blubber tissue. Annual Conference for the UK and Ireland Regional Student Chapter for the Society of Marine Mammology, St. Andrews January 2018.

Kershaw. Not just fat: The proteome of cetacean blubber tissue. Annual School of Biology Postgraduate Conference, St. Andrews January 2018.

## C. Other Supporting Materials

### BIOMARKER DEVELOPMENT SUPPLEMENTARY MATERIALS

#### Steroid Extraction: Quantification Quality Assurance-Quality Control

Quality assurance and quality control tests were performed to validate the use of these two commercially available ELISAs with northern bottlenose whale and humpback whale blubber extracts. Limitations and sources of error in the cortisol extraction method were also assessed so as to better interpret the results and adapt this method for remotely obtained biopsy samples.

##### 8.1 Inter-Assay CVs

The intra assay variation describes the variation of results within a data set obtained from one assay. It is expressed by intra assay coefficient of variation (intra assay CV) to monitor the deviation within the same assay. Each sample is measured several times, and then %CV is calculated for each sample. Finally, the average of the individual CVs is denoted as intra assay CV, and this should be < 10% (Andreasson et al., 2015). The inter assay variation describes the variation of results obtained from repeated assays. It is expressed by inter assay coefficient of variation (inter assay CV) to monitor the precision of results between different assays and to ensure replicability of results across the different assays. Inter-assay CV should be less than 20% (Andreasson et al., 2015). These criteria were met for the biopsy sample analysis for both study species.

*Table 1-1. Inter- and intra- assay CV values for the cortisol and progesterone ELISAs using both northern bottlenose whale and humpback whale samples.*

	Northern Bottlenose Whales	Humpback Whales
<b>Cortisol</b>	Inter-Assay CV 4.30% (2.53 – 6.45%) (n = 3)	10.45% (2.27 – 16.29%) (n = 3)
	Intra-Assay CV 2.26% (0.61 - 4.29%) (n = 3)	6.54% (4.20 - 10.49%) (n = 3)
<b>Progesterone</b>	Inter-Assay CV 11.47% (n = 1 : pregnant female assayed twice)	2.81% (0.83 – 6.30%) (n = 3)
	Intra-Assay CV 0.19% (0.13 - 0.31%) (n = 3)	0.02% (0.01% - 0.05%) (n = 3)

##### Parallelism Assays:

For the northern bottlenose whale and the humpback whale samples separately, three biopsy extracts were pooled and serially diluted either three or four times using the 0 ng/ml standards provided by the ELISA kits. The resulting curve of the detection metric (optical density of the

sample read at 450nm) as a function of the dilution state (1,  $\frac{1}{2}$ ,  $\frac{1}{4}$ ,  $\frac{1}{8}$ ,  $\frac{1}{16}$ ) was then compared to the standard curve for each species. In order to statistically assess parallelism, two linear regression models for dilution state against optical density, one with and one without an interaction with sample type (ELISA standard or blubber extract), were compared (ANCOVA function in statistical package R, version 3.1.3, R Core Development Team, 2015). If the regression lines for each model do not have significantly different slopes, then these data indicate that the standard curve and the extract dilution curve are parallel. Parallelism of these regression lines supports the assumption that the antigen binding characteristics allow the reliable determination of hormone levels in the diluted blubber extracts (Andreasson et al., 2015), and the ELISA kits are therefore reliably measuring both cortisol and progesterone in the tissue samples.

The comparison between the two linear regression models using the cortisol ELISA, one with and one without an interaction with sample type showed that removing the interaction did not significantly affect the fit of the model for the northern bottlenose or the humpback blubber extract dilutions (ANCOVA;  $F = 9.89$ ,  $p = 0.3$ , and  $F = 0.079$ ,  $p = 0.7$  for each species model comparison respectively). Similarly, there were no significant differences between either model for the progesterone ELISA either (ANCOVA;  $F=2.95$ ,  $p =0.1$ , and  $F=0.81$ ,  $p = 0.4$  for northern bottlenose whales and humpback whales respectively). Therefore, we can conclude that the effect on optical density with increasing sample dilutions is the same for the standard curve samples and the blubber extracts, and that the regression lines are parallel (Figure 1-1). These ELISA are therefore suitable for the quantification of northern bottlenose whale and humpback whale cortisol and progesterone.

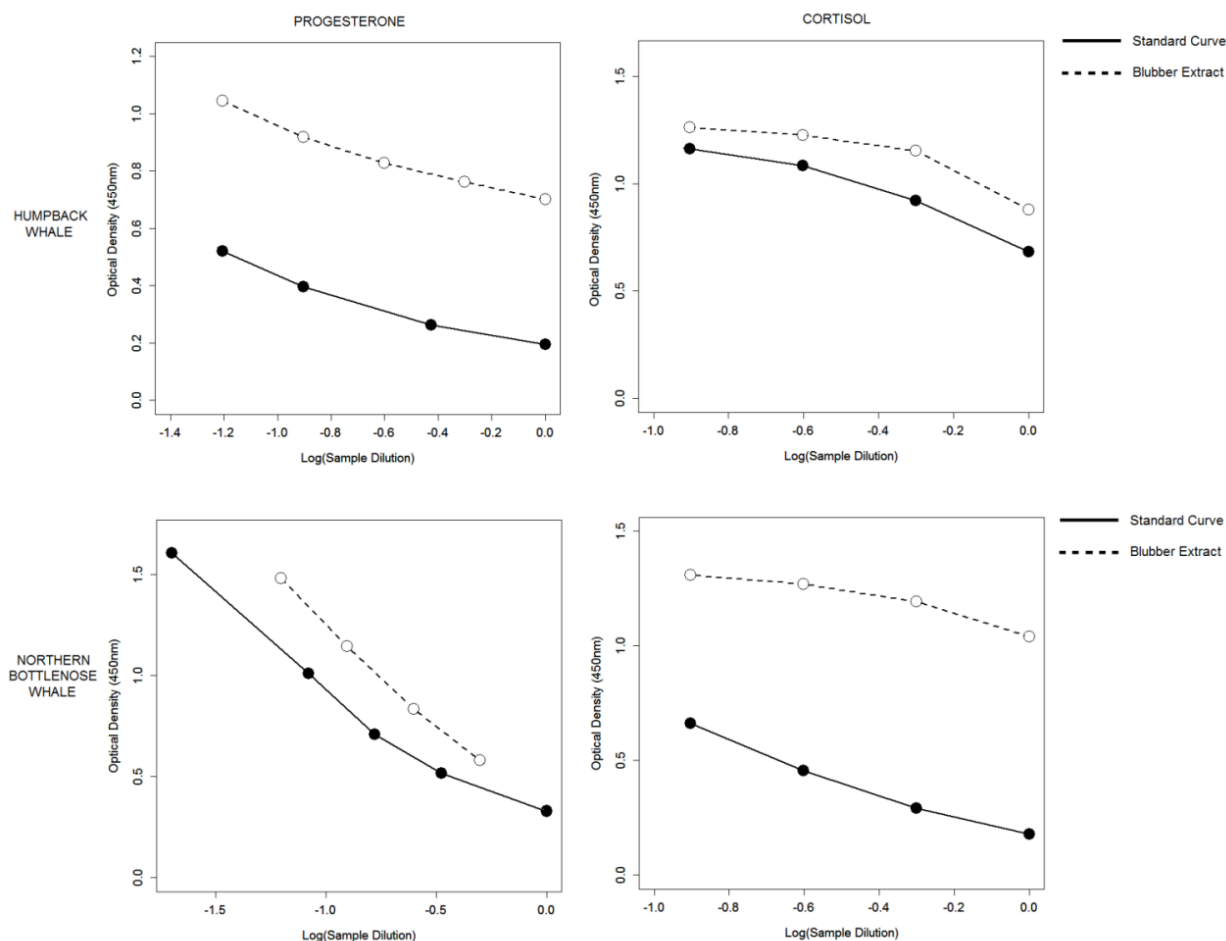
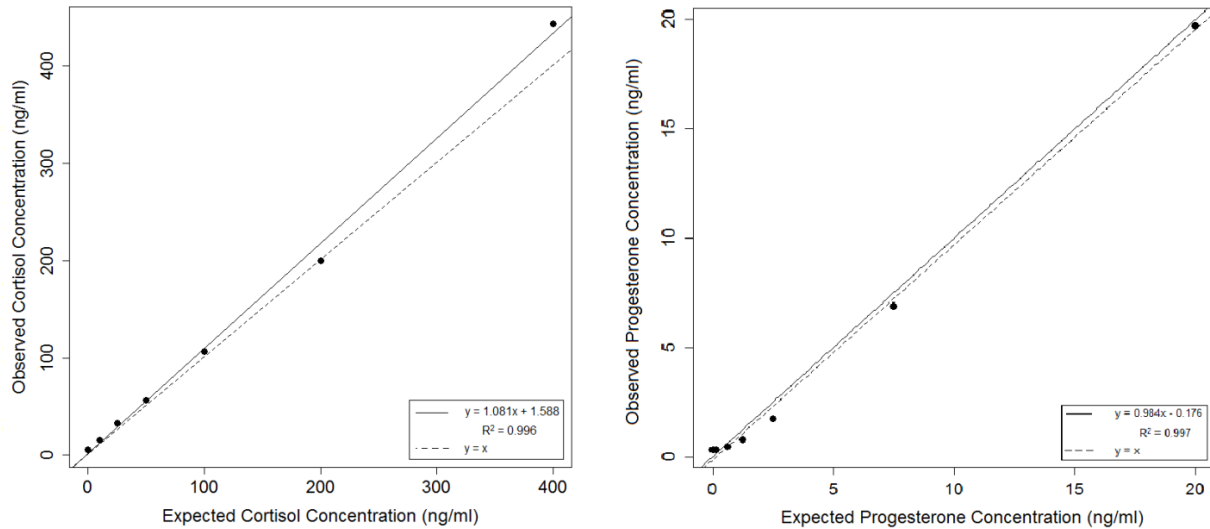


Figure 1-1. Linearity Assessment for the cortisol and progesterone ELISAs with northern bottlenose whale and humpback whale blubber tissue extracts. Serial dilutions of three pooled extracts for each species show parallelism with the ELISA standard curve.

### Matrix Effect Tests:

Successful immunologic assays require an optimal pH and ionic strength that promotes specific antibody–antigen complexes while reducing the nonspecific binding of other proteins in the samples that increase assay interference. As the ELISA kits used here were designed for use with serum or plasma samples, the compatibility of the kits with extracts resuspended in PBS was assessed. Equal volumes of each standard were spiked with PBS and assayed in tandem with the unspiked standard curve for each kit. The known and the apparent concentrations in the spiked samples should show a positive linear relationship with a slope of approximately 1.0 (Hunt et al., 2014). The matrix effect tests were successful with slope of 1.08 for the cortisol spiked samples, and 0.98 for the progesterone spiked samples (a slope of between 0.8-1.2 was considered acceptable Figure 1-2) . It was concluded that matrix effects are minimal and this sample diluent is therefore compatible with these immunoassays.



*Figure 1-2. Matrix Effect Test Validation. The linear regression lines for the expected against the observed concentrations are shown for the expected 1:1 relationship and the measured relationship from the assay results. The assay results show a positive linear relationship with a slope of 1.08 and 0.98 for the cortisol and the progesterone results respectively, thus confirming that PBS is an acceptable sample diluent compatible with these ELISA kits*

### **Extraction Efficiency:**

In order to assess the extraction efficiency of this method, cortisol recovery from spiked samples was measured. As blubber biopsies from live animals vary in size, it was necessary to determine the extraction efficiency of this method across tissue samples of different masses. Samples ranging between 0.1 and 0.3g, the typical range of sizes of biopsy samples obtained from free-ranging cetaceans, were used for analysis. One full depth blubber sample from a stranded harbour porpoise collected by the Scottish Marine Animal Stranding Scheme was divided into masses of 0.05g, 0.1g, 0.15g, 0.2g, 0.25g, and 0.3g (all  $\pm 0.025$ g), each one in triplicate, such that one sample of each mass was unspiked while the other two were spiked with 100ng of cortisol. Cortisol was then extracted and measured as discussed above, and the average percent recovery calculated for each sample.

The extraction efficiencies ranged from an average of 88.4% for the 0.05g samples, down to an average of 75.7% for the 0.3g samples. However, the relationship between the extraction efficiency and sample mass was not linear (Figure 1-3a). For this reason, a 4 parameter log-logistic model was fit to these data to model the effect of tissue mass on extraction efficiency (Figure 1-3a). This model was used to calculate the expected extraction efficiencies for all the blubber biopsy subsamples based on their mass. These extraction efficiencies were then used to adjust the measured cortisol concentrations in each sample. As cortisol and progesterone are very similar,

small, lipophilic steroid hormones, the same extraction efficiency ~ sample mass model was used to adjust the progesterone concentration data as well.

### **Minimum Sample Mass and Correction Factors:**

Remotely obtained blubber biopsy samples are often used for multiple analyses in order to maximize the potential information gained from the tissue. Subsampling remotely obtained biopsies for multiple analyses can therefore result in small amounts of tissue available for processing, and the minimum amount of tissue needed to obtain robust, replicable measurements of cortisol concentrations in the blubber samples needs to be established. Here, multiple extractions from the same piece of tissue of differing masses were assayed. Again, full depth, duplicate subsamples of different masses between 0.05-0.3g at 0.05g intervals were taken from the same blubber sample from the stranded harbour porpoise. Cortisol was extracted and measured in these samples in tandem, and the mean cortisol concentration calculated for each one.

As the sample mass increased, both the cortisol concentration measured and the variation between the duplicate subsamples decreased (Figure 1-3b). Only the 0.15g, 0.2g and 0.25g subsamples overlapped in their measured cortisol concentrations (Figure 1-3b). Thus, based on the decrease in extraction efficiency (Figure 1-3a) and increase in measurement variability (Figure 1-3b), it is recommended for maximum extraction efficiency and measurement replicability, that blubber samples for extraction should be between 0.15 and 0.2g. For this method to be applicable to remotely obtained biopsy samples that are sometimes smaller than this recommended 0.15-0.2g mass range, a 'correction factor' model was built using these data. The 'true' concentration was taken as the average concentration measured in the 0.15g sample and the 0.2g sample. The concentrations measured in the samples of other masses were divided by this 'true' concentration to give a correction factor. A 4 parameter log-logistic model was fit to these data to model the effect of tissue mass on correct factor (Figure 1-3c). As sample mass decreases from the recommended 0.15-0.2g, the correction factor increases, indicating that smaller sample masses give inflated cortisol concentration estimates (Figure 1-3c). This approach was used to correct cortisol and progesterone measurements in the biopsy samples based on the tissue mass. So the final hormone concentrations were therefore first measured using the ELISAs, then, adjusted for extraction efficiency using the 4-parameter log-logistic model based on sample mass, then a correction factor was applied based on the second 4-parameter log-logistic model based on sample mass to avoid overestimating hormone concentrations as an artefact of the small biopsy sample mass of some of the samples analysed.

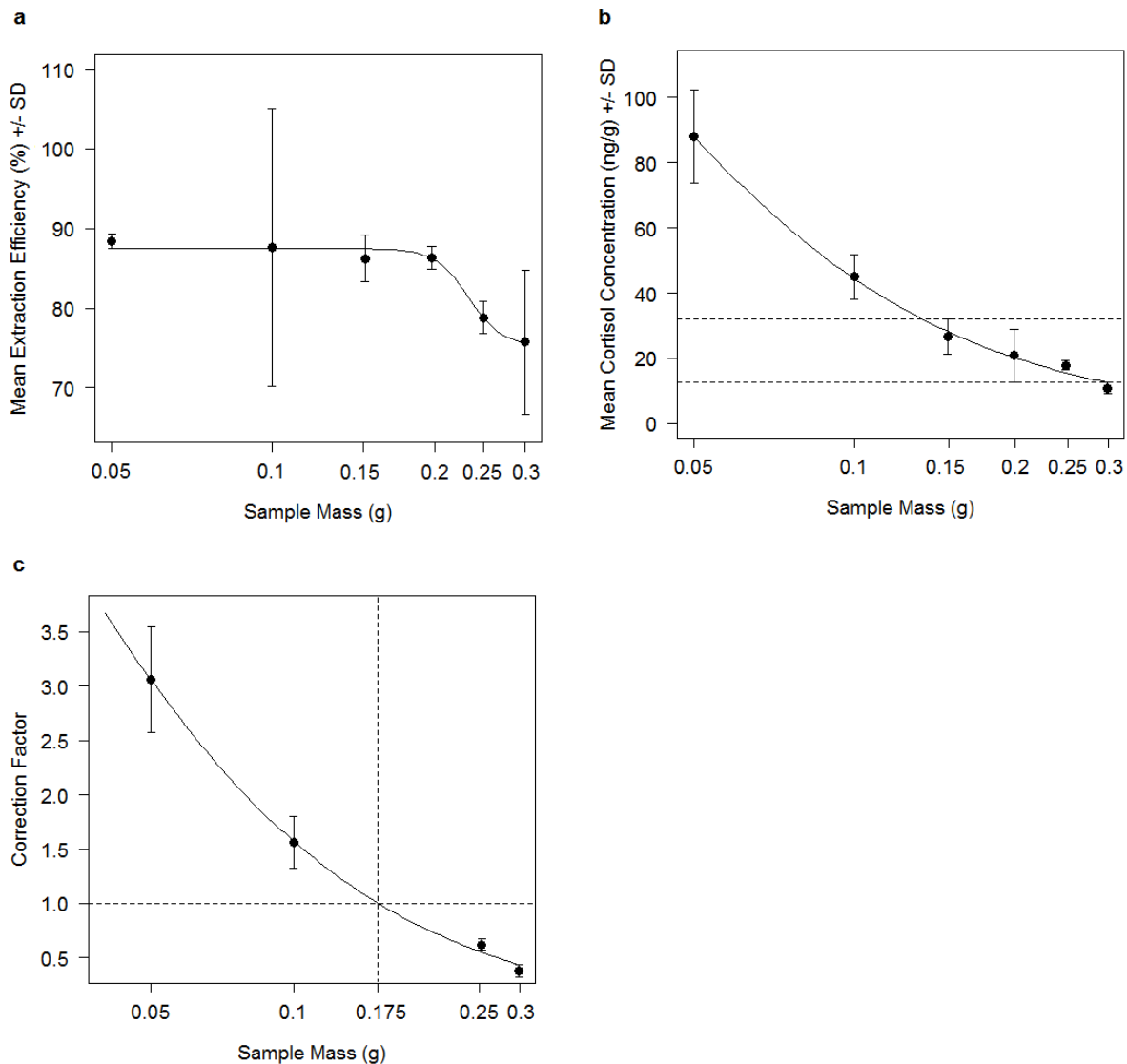


Figure 1-3. Steroid hormone extraction efficiency and quantification errors based on sample mass. a) Extraction efficiency decreases with increasing blubber sample mass in a non-linear fashion. b) Mean cortisol concentration in duplicate sub-samples increases with decreasing sample mass. Measured concentrations overlap in sample masses between 0.15g and 0.25g. c) A correction factor is applied to correct cortisol concentrations in samples smaller than the ideal sample mass between 0.15-0.2g

## 9 Total Protein Extraction Method Development

### 9.1 Sample Collection and Preparation

Full-depth skin, blubber, and underlying muscle samples were collected from dead harbour porpoises by the Scottish Marine Animal Strandings Scheme (SMASS) between 2013 and 2015. Only freshly dead animals, specifically those that either stranded alive or had recently died, and

thus showed no evidence of bloating and decomposition, were used in order to investigate blubber proteins that had not been subject to extensive degradation and metabolism after death. Samples showed no evidence of trauma or bruising as blood in the tissue would disproportionately represent proteins in circulation rather than proteins present in the blubber matrix itself. Samples were collected from the dorsal area immediately caudal to the dorsal fin. This site was chosen as this area is typically sampled through remote biopsy of free-ranging individuals and therefore has the most relevance for investigating the potential use of these total protein extraction methods on samples collected from live animals. A total of 24 samples were used from 21 individuals that were a mixture of both males ( $n = 10$ ) and females ( $n = 11$ ), and adults ( $n = 12$ ) and juveniles ( $n = 9$ ). The cause of death was determined following post-mortem examination, and individuals died as a result of acute trauma (entanglement in fishing gear, live standing, storm damage, dystocia and bottlenose dolphin or grey seal attacks) or chronic debilitation (starvation and infectious disease). Samples were collected and frozen in individual plastic vials at  $-20^{\circ}\text{C}$  prior to analysis. For the total protein extraction, sub-samples were taken on ice while the tissue was still frozen, and care was taken to remove all skin and muscle from the blubber. Full depth subsamples of each original sample were used for total protein extraction in order to investigate the proteins through all layers of the tissue.

#### 9.1.1 Total Protein Extraction Methods

Protein extraction from a tissue typically involves three stages: 1) tissue and cell disruption through homogenisation 2) precipitation of the protein fraction of the homogenate into a pellet form 3) re-suspension of the protein pellet into solution for quantification and downstream applications.

In a comparative study of different detergent-free protein extraction protocols using these three stages, the most suitable method for the extraction of white adipose tissue proteins from a wide range of cellular and structural compartments was a de-lipidation protocol based on the Bligh and Dyer method (Bligh and Dyer, 1959; Sajic et al., 2011). The optimal tissue and cell disruption part of the protocol described by Sajic and colleagues was replicated here using blubber samples collected from harbour porpoises. Then, two different protein precipitation methods were trialled. A protein precipitation method using a methanol-chloroform solution adapted by Friedman and colleagues (Friedman et al., 2009) for the recovery of proteins in dilute solution in the presence of detergents and lipids (Wessel and Flügge, 1984), was trialled first (method 1). A second protein precipitation method using a trichloroacetic acid (TCA)-acetone solution was also trialled which aggressively removes non-protein compounds (Wu et al., 2014) (method 2). TCA is often used for precipitation as it is effective at low concentrations (Wu et al., 2014). The sample volume therefore does not increase dramatically, and the protein concentration remains high which increases the efficiency of the precipitation (Wu et al., 2014).

Finally, a simpler extraction method using radio immunoprecipitation assay (RIPA) cell lysis and extraction buffer was trialled to assess if fewer sample processing stages, without the precipitation of protein into a pellet and resuspension into solution, results in a higher protein yield and less extraction variability (method 3). RIPA cell lysis buffer is highly effective for protein extraction from a variety of cell types because it contains three non-ionic and ionic detergents. One disadvantage, however, is that this detergent formulation is incompatible with certain downstream applications compared to other lysis reagents, and there is no possibility to suspend the extracted protein in a different buffer for further analysis. For a summary of the three sample processing methods (methods 1, 2 and 3) with their different stages see Figure 2-1.

### Method 1: Methanol-Chloroform Precipitation with Methanol Pellet Wash

Sixteen full depth blubber subsamples were accurately weighed (0.4 - 0.6g) and homogenised with 0.5mL of isolation medium (50mM Tris, 150mM NaCl, 0.2mM EDTA and 10ug/ml protease inhibitors), and 1.875mL of 1:2 chloroform/methanol. Samples were then placed on ice for 15 minutes with thorough mixing every three minutes. 625ul of chloroform and 625ul of deionised water were added to the sample. The sample was vortexed and centrifuged at 800g for 5 minutes at 4°C. This creates three layers, a lower lipid layer, an upper protein layer and a protein disc between the two. The upper protein phase and the protein disc were collected and transferred to a new tube.

Three volumes of water, four volumes of methanol and one volume of chloroform were added to the solution and vortexed vigorously for 5 min so that only one phase was visible in the tube. The mixture was centrifuged at 4700g at 4°C for 30 min. This forms two immiscible layers with the protein precipitate at the interface between the two. The water /methanol top layer was removed, and care was taken not to disturb the interface as often precipitated proteins do not form a visibly white surface. Another four times the volume of methanol was added to wash the precipitate, and the mixture was again vortexed vigorously for 5 min. The mixture was centrifuged at 4700g at 4°C for 45 min. This forms a protein pellet in the bottom of the tube. The supernatant was removed and the pellet was dried under N<sub>2</sub> at room temperature. Care was taken not to over dry the pellet causing it to become flaky and stick to the centrifuge tube which reduces the resuspension efficiency. Finally, the pellet was resuspended in 500ul of SDS/Tris (0.1% SDS in 40mM Tris).

### Method 2: TCA-Acetone Precipitation with Acetone Pellet Wash

Using another 16, different, full-depth blubber subsamples, the same protocol as previously described was followed up to the collection of the upper protein phase and the protein disc, and its transfer to a new tube. 10% TCA in acetone solution was added to the sample with a ratio of 1:3 of sample to TCA-acetone solution. The sample was frozen overnight at -20°C. The sample was allowed to warm to room temperature and then centrifuged at 4700g at 4°C for 45 minutes the following day. Proteins form a pellet in the bottom of the tube. The pellet was washed twice by adding 1ml of ice cold acetone which was then discarded. Any remaining acetone following the final wash was evaporated under nitrogen at room temperature. Care was taken not to over-dry the protein pellet, and the pellet was resuspended in 500µl of SDS/Tris. Of the two protein precipitation methods, using a TCA-acetone solution showed least total protein inter-assay variability. For this reason, alterations were made to improve this protocol in an attempt to firstly, further clean the extract, and secondly, to improve protein pellet resuspension by altering the pellet washing procedure.

#### Alteration 1: TCA-Acetone Precipitation with Butanol De-Lipidation and Acetone Pellet Wash

As cetacean blubber tissue has such a high lipid content, an extra butanol de-lipidation step was added before the precipitation of the protein pellet in an attempt to further 'clean' the extract (Zhao and Xu, 2010). Another 16 blubber subsamples were taken, as previously described, from the same individuals used for the TCA-acetone precipitation protocol. Following the collection of the upper protein phase and protein disc (after homogenisation and centrifugation), butanol was added in a

ratio of 1:3 sample to butanol. This was then centrifuged at 1750g at 10°C for 10 min and the upper phase containing any remaining lipids was removed and discarded. 10% TCA in acetone was added to the lower phase, and the precipitation and pellet wash continued as described above. The final protein pellet was resuspended in 500ul of SDS/Tris.

#### Alteration 2: TCA-Acetone Precipitation with Water Wash

Poor resuspension of the protein pellet in the SDS-Tris Buffer could result in under-estimates of total protein content if some pellets resuspend less efficiently than others. The effect of a different pellet wash was tested by using de-ionised water instead of acetone for the final wash stage. This was an attempt not to dehydrate the pellet, and therefore make its resuspension back into solution more efficient. As before, 16 blubber subsamples were taken from the same eight individuals used for the TCA-acetone precipitation protocol. Specifically, following the precipitation of the proteins in TCA-acetone, care was taken to discard all TCA-acetone solution, and the pellet was washed by adding 1ml of deionised water. It was vortexed briefly, and then centrifuged again for 5 min at 4700g at 4°C. The supernatant was again discarded, and the pellet washed a second time with deionized water. Care was taken not to disturb the washed pellet that was then re-suspended in 500µl of SDS/Tris.

#### Method 3 - RIPA Lysis and Extraction Buffer

Another 16, full depth blubber samples were used for analysis from 8 individuals. The subsamples were accurately weighed ( $0.1 \pm 0.01$ g). The frozen tissue was placed on ice in a 1.5ml low protein binding micro-centrifuge tube and 200µl RIPA lysis and extraction buffer (Thermo Fisher Scientific) with 2X concentration of protease inhibitors (Pierce Protease Inhibitor Mini Tablets) was added to the tissue. The samples were homogenised with a pestle designed for a 1.5ml tube for two minutes to give a cloudy white solution and small piece of connective tissue that could not be further homogenised. The samples were replaced on ice and then centrifuged at 4700g at 4°C for 15 minutes before being replaced on ice. The supernatant, the hardened lipid containing fraction, was pushed to one side, and the protein containing infranatant was removed and placed into a clean, low protein binding microcentrifuge tube. Care was taken not to disturb the insoluble/unhomogenised connective tissue pellet. The protein fraction was centrifuged, as before, as a second de-lipidation step, and replaced on ice. Again, the infranatant was removed and placed in a clean, low protein binding microcentrifuge tube taking care not to disturb any remaining lipid supernatant and insoluble pellet. This solution was used for further analysis.

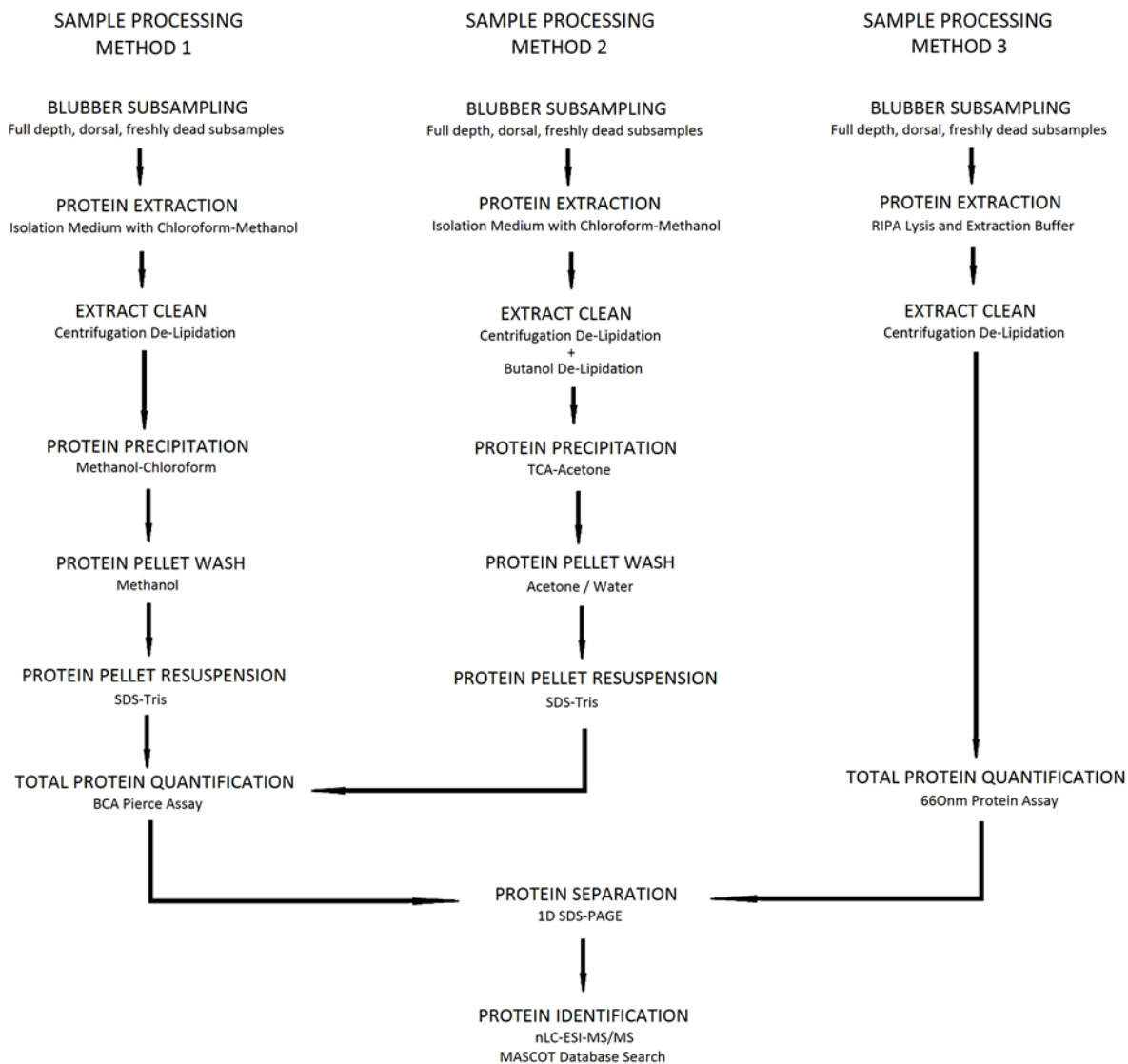


*Figure 2-1 Workflow showing the sample processing methods for protein extraction, quantification, separation and identification. Sample processing methods 1 and 2 involve various extract cleaning, protein precipitation and protein pellet wash stages. Sample processing method 3 involves fewer processing stages. The extracts using all three methods were used for downstream analyses; protein quantification, separation and identification*

### 9.1.2 Quality Assurance / Quality Control

Total protein extraction method comparison studies use various approaches to assess the protein extraction efficiencies for particular tissues including total protein yield, distribution of molecular weights of extracted proteins separated using 1D SDS-PAGE, reproducibility of protein bands with minimal streaking and background using 1D SDS-PAGE, presence of specific protein

markers from different cellular compartments using Western Blot techniques, presence / absence of individual protein spots using 2D SDS-PAGE, and reproducibility of protein spot patterns using 2D SDS-PAGE in both animal (Cilia et al., 2009; Jiang et al., 2007; Panchout et al., 2013; Sajic et al., 2011) and plant (Natarajan et al., 2005; Sheoran et al., 2009) studies. In keeping with such studies, here, the performance of the different extraction protocols in terms of their ability to efficiently and consistently extract protein from blubber tissue was assessed in four ways by (i) measuring total protein yield (ii) measuring extraction variability between duplicate extracts of the same sample extracted and assayed in tandem (iii) measuring assay variability in terms of the protein measured in the same sample over multiple assays (iv) visually inspecting the molecular weight distribution, the number and reproducibility of protein bands separated by 1D SDS-PAGE.

All statistical analyses were performed using the statistical package, R, version 3.1.3 (R Core Development Team, 2015). A one-way analysis of variance (ANOVA) was used to compare between the mean protein yields of all extracts processed using the five different method variations (method 1, three alterations of method 2, and method 3) (Figure 2-2). The extraction variability for each sample extracted in duplicate was calculated as a % coefficient of variation, and again, a one-way ANOVA was used to compare between the mean % extraction variability across the 5 method variations (Table 2-1). The inter-assay coefficients of variation for samples assayed multiple times across different plates were also assessed using a one-way ANOVA to determine differences in the repeatability of the measurements of the same extracts (Table 2-1). Finally, the 1D SDS-PAGE gels were assessed for the range of molecular weights of the bands that were separated, the number of protein bands separated and the consistency with which these bands appeared in multiple extracts and across multiple gels. For comparative example 1D gel images of extracts processed using the different methods, see Figure 2-3.

### **Identification on the most robust extraction method**

There was considerable variation seen in both the total protein yields, and the extraction variability between duplicate subsamples (Figure 2-2a and b). Of the two precipitation methods, the TCA-acetone precipitation method was chosen for further development. An extra butanol de-lipidation step and pellet wash with water were trialled in an attempt to further optimise the method in order to improve consistency. However, even with these changes, the total protein yield was still poor, and there were no statistically significant differences between the overall protein yield between the 4 precipitation methods (method 1 and the 3 variations of method 2) (ANOVA;  $df = 3$ ,  $F = 2.33$ ,  $p = 0.08$ ) (Figure 2-2a). The highest total protein yield, by at least an order of magnitude, was obtained using the third extraction method with RIPA cell lysis buffer which was significantly higher than all other extracts (ANOVA;  $df=4$ ,  $F = 280.1$ ,  $p < 0.0001$ ) (Figure 2-2b). The extraction variability was high and was not statistically different between methods (ANOVA;  $df = 4$ ,  $F = 1.13$ ,  $p = 0.36$ ), but extracts processed using method 3 had a lower mean extraction variability and a smaller range across duplicate samples (Table 2-1).

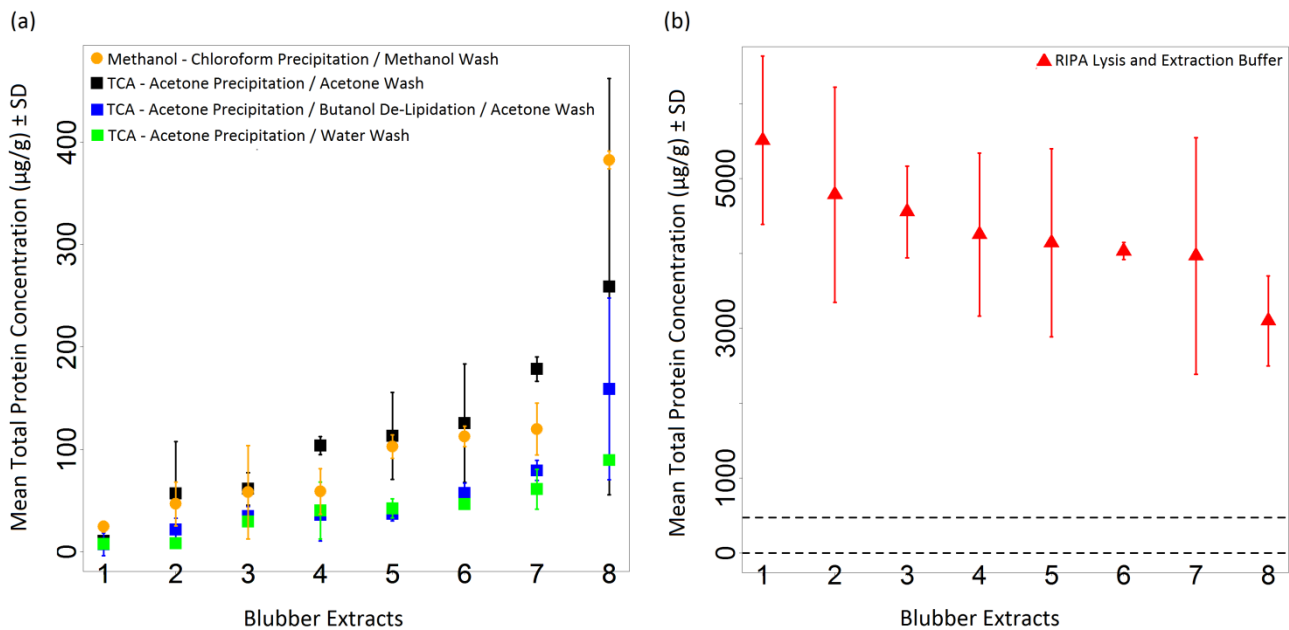


Figure 2-2. Total protein yield in blubber extracts using different sample processing methods 1, 2 and 3. a) Total protein concentrations measured in extracts processed using methods 1 and the three variations of method 2. b) Total protein concentrations measured in extracts processed using method 3. Overall, the total protein yield was an order of magnitude higher using this method although there was still high extraction variability. The horizontal dashed lines indicate the range of mean total protein concentrations measured using the other processing methods.

There was a wide range of inter-assay variability across all samples, particularly for methods 1 and 2, which were largely over the acceptable inter-assay % coefficient of variation threshold of 20%, based on general protocols for immunoassay validations (Grotjan and Keel, 1996) (Table 2-1). The extracts processed using method 1 had significantly higher inter-assay CVs than the other methods (ANOVA;  $df = 4$ ,  $F = 11.94$ ,  $p < 0.001$ ), while the others were not significantly different to each other. There were also consistent trends of higher or lower protein concentrations between assays for method 1 (data not shown), suggesting that there is some change in protein resuspension or protein loss between repeated freeze-thaw cycles of the extracts. Three of the five extraction protocols generally gave low average intra-assay % CVs below the 10% threshold that was considered acceptable for three extracts assayed twice on each plate (Grotjan and Keel, 1996) (Table 2-1). As the total protein standard curves were all almost identical between different plates (data not shown), the high between and within assay variation measured here for the Pierce BCA assay is likely indicative that measurement error or artefacts due to the assay reagents and the assay process were not the cause of the variability. Instead, resuspension of the protein in solution was likely a problem for reliable and consistent measurement of the precipitated proteins.

Table 2-1– Summary of the total protein assay results for the three different extraction methods and alterations. (CV: coefficient of variation. SD: standard deviation)

	Extraction Methods 1 and 2				Extraction Method 3
	Methanol-Chloroform Protein Precipitation	TCA-Acetone Protein Precipitation			RIPA Cell Lysis Buffer Extraction
		Original: Acetone Wash	Alteration 1: Butanol De-lipidation	Alteration 2: Water Wash	
<b>Total Protein Assay</b>	Pierce BCA	Pierce BCA	Pierce BCA	Pierce BCA	Pierce 660nm
<b>Minimum Protein Yield</b>	14.4 ug/g	3.8ug/g	7.3 ug/g	7.7ug/g	3101.8 ug/g
<b>Maximum Protein Yield</b>	361.6ug/g	918.0ug/g	158.8 ug/g	89.3ug/g	5512.7 ug/g
<b>Extraction CVs</b> ( <sup>SD</sup> / <sub>mean</sub> ) x 100 duplicate protein extracts	28.4% (2.3 - 78.7%)	42.0% (6.7 - 90.0%)	50.6% (12.5 - 151.0%)	31.8% (2.1 - 68.8%)	21.9% (2.8 - 39.8%)
<b>Inter-Assay CVs</b> ( <sup>SD</sup> / <sub>mean</sub> ) x 100 different total protein plates	86.5% (47.8 - 133.1%)	42.5% (0.5 - 141.4%)	31.6% (4.1 - 103.9%)	23.4% (3.31 - 69.5%)	15.8% (1.5 - 64.9%)
<b>Intra-Assay CVs</b> ( <sup>SD</sup> / <sub>mean</sub> ) x 100 same total protein plate	0.7% (0.1 - 1.3%)	2.0% (1.2 - 3.3%)	28.7% (4.7 - 100.0%)	19.3% (2.5 - 105.6%)	4.5% (3.6 - 5.5%)

Finally, visual inspection of the 1D SDS-PAGE gels showed that there was a wide range in molecular weights of the separated protein bands, with both more numerous and more consistent bands seen in the samples processed in RIPA cell lysis buffer (Figure 2-3) This further supports the conclusion that method 3 is the most appropriate for replicable protein extraction from blubber tissue.

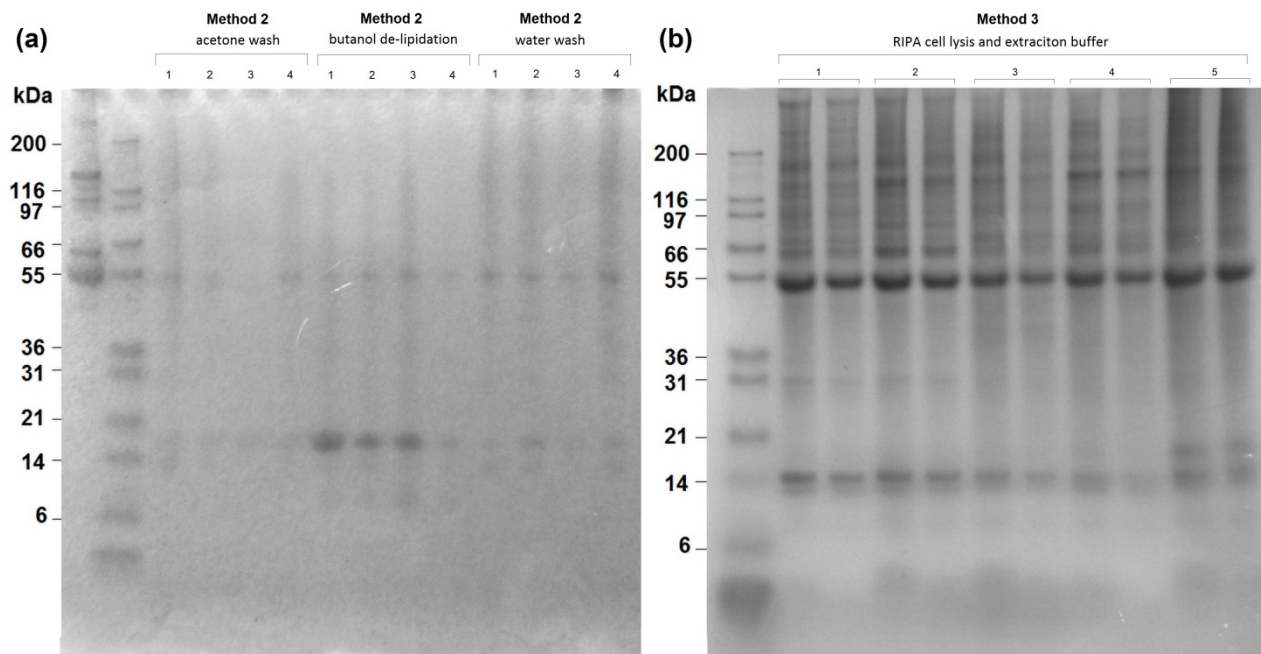


Figure 2-3. 1D SDS-PAGE analysis of harbour porpoise blubber tissue extracts on 4-12% Bis-Tris gels stained with Bio-Safe Coomassie brilliant blue. (a) Protein extracts labelled 1 - 4 were extracted using TCA-Acetone precipitation with an acetone wash, TCA-Acetone precipitation with butanol de-lipidation, and TCA-Acetone precipitation with a water wash. (b) Protein extracts labelled 1-5, extracted in RIPA cell lysis buffer, and each diluted  $\frac{1}{2}$  and  $\frac{1}{3}$ .

## 10 Adipocyte Metrics

### 10.1 Method Development using Stranded Animal Samples

The Scottish Marine Animal Stranding Scheme (SMASS) collected blubber tissue samples from freshly dead stranded harbour porpoises (n=16) minke whales (n=3), Risso's dolphins (n=3), long-finned pilot whales (n=2), white-beaked dolphins (n=5), short-beaked common dolphins (n=3) and striped dolphins (n=2, total sample size n=34) around the coast of Scotland (UK) between 2013 and 2015. Individuals were both male (n=19) and female (n=15), and grouped into adults (n=13) and juveniles (n=21) based on total body length (Olafsdottir et al., 2003). As mass was not available for all animals, girth/length ratio was used as an independent estimate of body condition (Bowen and Northridge, 2010).

### 10.2 Histological processing and measurements

Blubber samples were prepared following previously described methods (Berry et al., 2014). Having removed the epidermis, samples were cut to approximately 1cm x 1cm in size and soaked in sterile phosphate buffered saline (PBS) solution prior to processing. Samples were then dehydrated using an ascending series of ethanol (75%, 95%, and 100%), cleared using HistoClear (Fisher Scientific, Loughborough, UK) and embedded in a paraffin wax (Histoplast, Fisher Scientific) mold. Embedded samples were then sectioned using a rotating microtome, and stained with hematoxylin and eosin (H&E).

Two histological measurements, referred to as 'adipocyte metrics', were calculated for each image: adipocyte count, and adipocyte area. Images were analyzed using ImageJ Software (Version 1.5.8, (Schneider et al., 2012)). To estimate the number and size of adipocytes in each image, previous manual methods were followed (Montie et al., 2008a). A 1mm x 1mm box was positioned approximately in the center of each image, Figure 2-4. The number of adipocytes per image was calculated by counting the number of cells that intersected each diagonal line of the 1mm<sup>2</sup> grid, and the average of these two counts gave a mean adipocyte count per image. The size of the adipocytes (measured as the cross-sectional area of adipocyte cells) was measured using the area tool in Image J. Images were calibrated using scale bars of known length being included in each image. For each image, the first 15 cells that intersected the upper left diagonal line were measured. In images where there were less than 15 cells intersecting the left diagonal, the remaining measurements were taken from the upper right diagonal line.

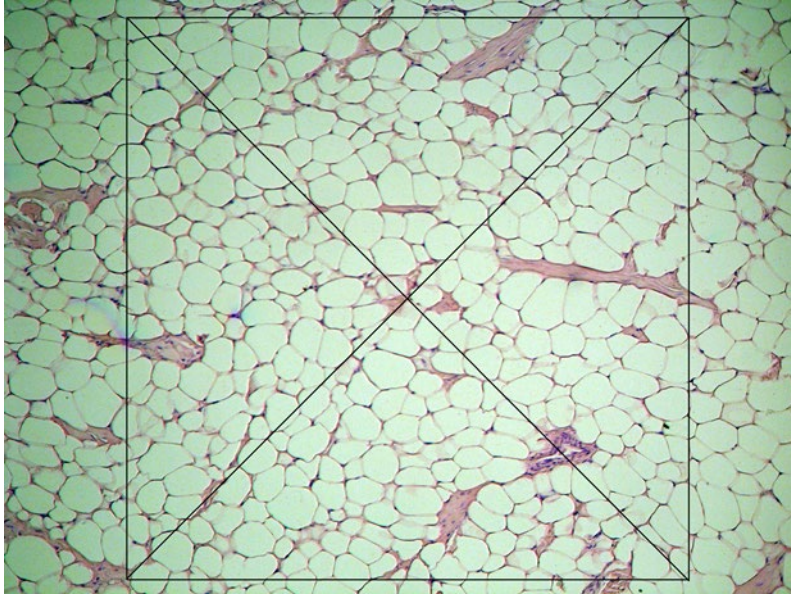


*Figure 3-1. Digital image of blubber adipocytes stained with H&E, enhanced using IrfanView. 1mm x 1mm box and diagonals used for histological analysis.*

### 10.3 Image and Statistical Analysis

Slides were viewed using a Zeiss Axiostar Plus microscope at 10x magnification. A Canon PowerShot G6 with an LA-DSC8DC 58mm conversion lens adapter was used to take color digital images of the adipocytes located in the middle blubber layer, identified as the region equidistant from the skin to the muscle layer, both structures being readily identifiable under magnification and included in each of the sections examined (Gomez-Campos et al., 2015). To increase the contrast between adipocyte cell walls and content, images were enhanced using the open source image analysis package, IrfanView (Version 4.44, 2017).

In order to investigate the relationship between adipocyte size and other measurements related to condition (blubber thickness and girth to length morphometric measurements), taking account of differences due to sex, age class and cetacean group (large delphinid, small delphinid, porpoise or mysticete), a generalized linear mixed modeling approach was used. The dependent variables, adipocyte area and count were continuous and normally distributed and were included as fixed effects. All statistical analyses were performed using the statistical package, R, version 3.1.2 (R Development Core Team, 2014). In the final models, the ability of the combination of adipocyte size metrics to predict condition (girth/length), again with the cetacean group as a random effect, was explored. Due to the skewed distribution of the girth/length as a dependent variable, a Gamma family was used in the models. Variable selection and model evaluation was carried out as outlined in the lipids section.

### 10.4 Relationship Between Different Adipocyte Metrics

There was a strong negative linear relationship between adipocyte count and area across all species ( $p < 0.0001$ , adjusted  $R^2 = 0.68$ , Figure 2-5).

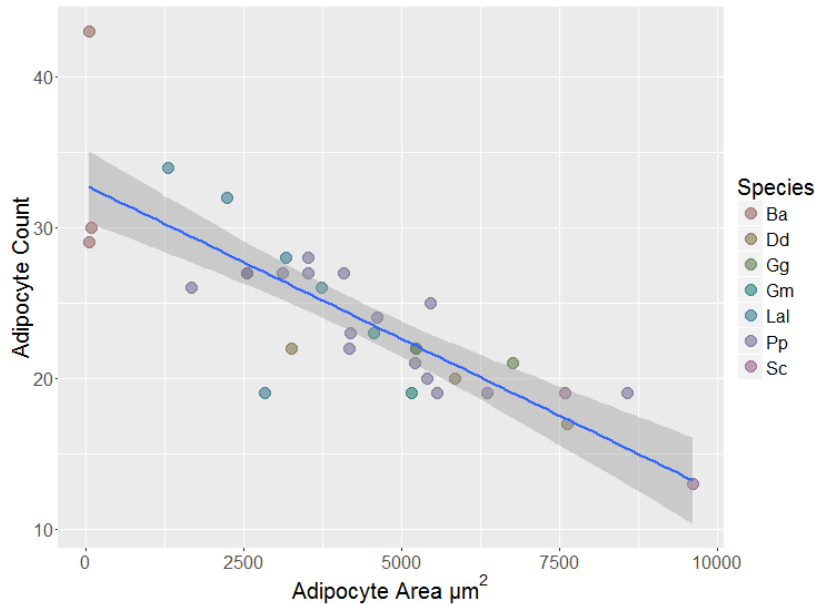


Figure 3-2. Relationship between adipocyte count and area across all species (Ba = minke whale, Dd = short-beaked common dolphin, Gg = Risso's dolphin, Gm = long-finned pilot whale, Lal = white beaked dolphin, Pp = harbor porpoise, Sc = striped dolphin).

Images therefore either contained fewer, larger adipocytes, or more, smaller adipocytes.

### 10.5 Relationship between Condition Index and Adipocyte size

#### Adipocyte Area

The seven species used in this analysis were grouped by cetacean class as large delphinids (Rissos' dolphin and long-finned pilot whale); small delphinids (white beaked dolphin, short beaked common dolphin and striped dolphin); porpoise (harbor porpoise) and mysticetes (minke whale), based on size and ecological niche. These were included in the generalised linear mixed models as random effects as the objective of the analysis was to determine general patterns of association between adipocyte area and condition measurements.

Following the method for determining which variables should be included in the model to avoid multicollinearity, girth/length was used as the independent morphometric condition measure as it was available for all the cetaceans, whereas mass was not. Figure 2-6 shows the basic relationship between girth/length against adipocyte area by cetacean group.

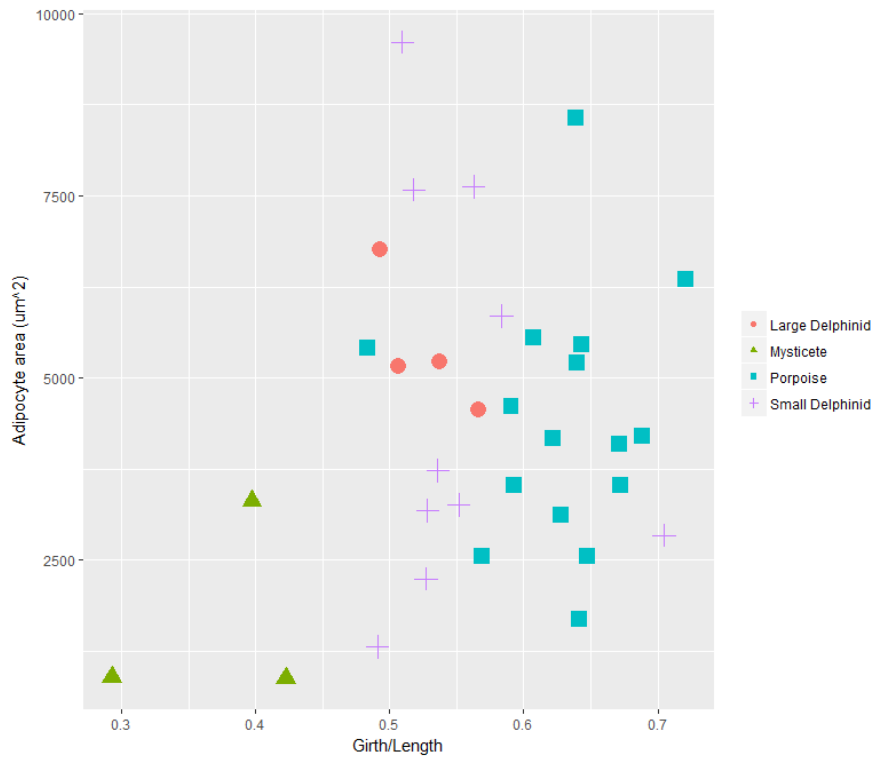


Figure 3-3. The relationship between girth/length and adipocyte area by cetacean group (not accounting for the other variables found to be important in the model).

The best model given the data, using AICc and the *dredge* function in R to determine the most parsimonious model, included girth/length, sex, age class and dorsal blubber thickness as fixed effects and cetacean group as a random effect (AICc weight 0.980, with the next best model that did not include blubber thickness having a weight of 0.017 and a delta AICc value of 8.12). The  $R^2$  values were 0.224 for the fixed effects and 0.564 for the fixed effects plus the random effects. The model coefficients suggest that dorsal blubber thickness increases with increased adipocyte area (thicker blubber is associated with larger fat cells), juveniles and females have smaller adipocytes than adults or males and that girth/length ratio is required as adipocyte area increased with increasing condition. The weighting given to this model was high, compared to the next best model (which dropped dorsal blubber thickness), suggesting that both were related to the size of the adipocytes.

### 10.6 Adipocyte Count

The relationship between girth/length and adipocyte count is shown in Figure 2-7. Using the same approach as for adipocyte area, adipocyte count was best model included three fixed effect; sex, age and girth/length (AICc weight 0.446). The  $R^2$  values were 0.322 for the fixed effects and 0.596 for the fixed effects plus the random effects. In this model blubber thickness was not a significant variable with most of the variability in count being explained by condition (higher girth/length is related to a smaller number of fat cells), taking account of sex and age (lower counts in adults and males).

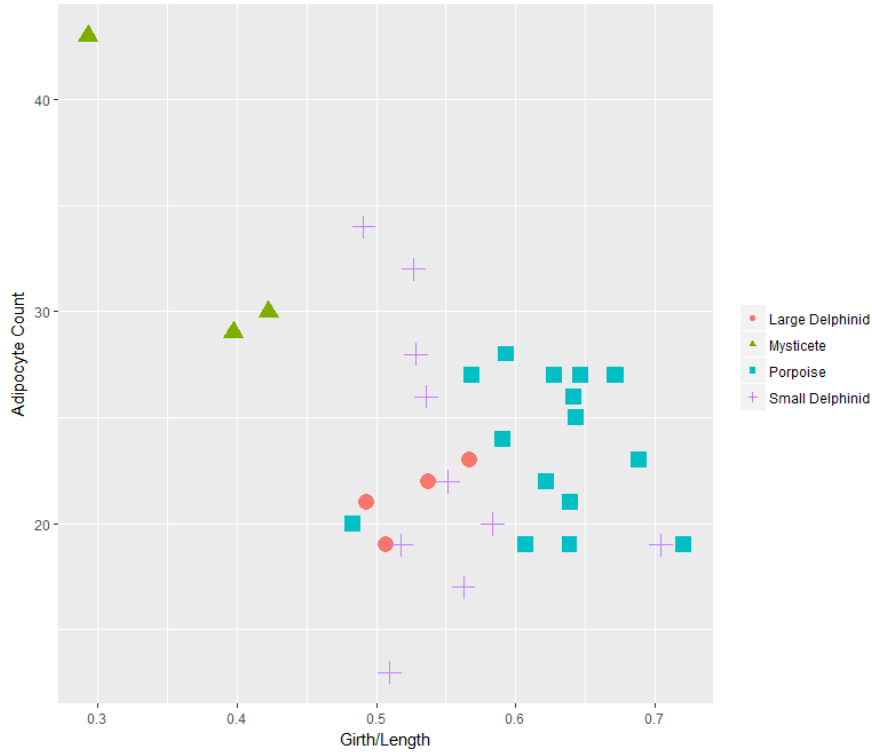
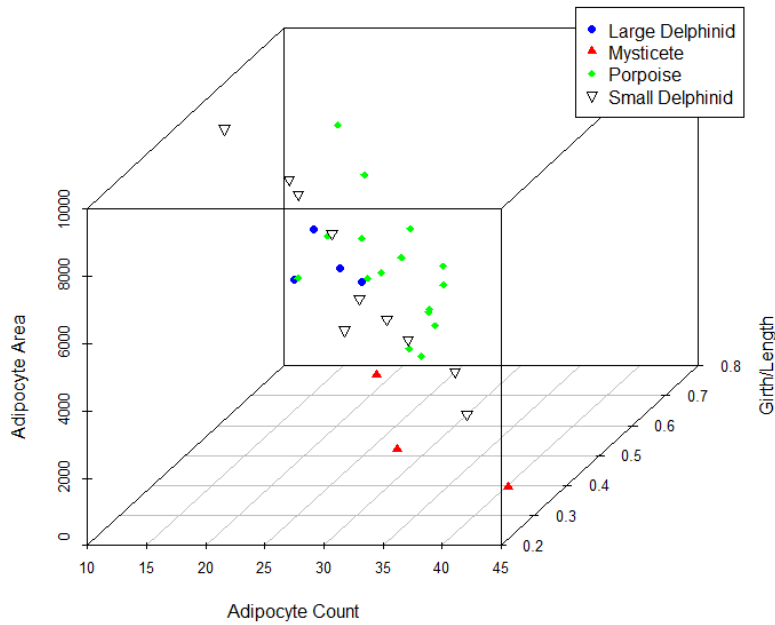


Figure 3-4. The relationship between girth/length and adipocyte count by cetacean group (not accounting for the other variables found to be important in the model).

### 10.7 Predicting Condition from Adipocyte Metrics

The final investigation of this biomarker included condition (girth/length) as the dependent variable in an effort to determine whether this was predictable using adipocyte metrics across cetacean groups. The best model included only adipocyte area and count as predictors (which both had variance inflation factors <2) but not sex or age (Figure 2-8). Both adipocyte variables were highly significant (Type II Wald Chi square tests; area  $p=0.0026$ , count  $p<0.00001$ ) with 79 % of the stochastic variation in the model being explained.



*Figure 3-5. Relationship between adipocyte area and count and girth/length condition index by cetacean group.*

Animals with a higher girth/length ratio had larger but fewer adipocytes. Again this would suggest that adipocyte size metrics would be useful in determining body condition. However, the small sample size for some species and age-class combinations, particularly the mysticetes, in this dataset would urge caution in generalising these results at this stage.

## 11 PROTEOMICS

### 11.1 Method Development using Stranded Animal Samples

**Harbour porpoises:** Full-depth skin, blubber, and underlying muscle samples were collected from 32 dead harbour porpoises by the SMASS between 2013 and 2015. Only freshly dead animals, specifically those that either stranded alive or had recently died. Samples showed no evidence of trauma or bruising as blood in the tissue would disproportionally represent proteins in circulation rather than proteins present in the blubber matrix itself. Samples were collected from the dorsal area immediately caudal to the dorsal fin from both males and females, and adults and juveniles. The cause of death was determined following post-mortem examination, and individuals died as a result of acute trauma (entanglement in fishing gear, live standing, storm damage, dystocia and bottlenose dolphin or grey seal attacks) or chronic debilitation (starvation and infectious disease).

**Balaenopterids:** Ten full depth blubber samples were also collected from stranded balaenopterid individuals. These were a mixture of minke whales (sampled by the SMASS and MICS), humpback whales and a fin whale (*Balaenoptera physalus*). Again, these were a mixture of males and females, and adults and juveniles with varying causes of death.

#### Application to Biopsies from Live Animals

**Minke whales:** Ten remotely obtained, shallow, biopsy samples collected from minke whales by the MICS in 2013, were used for comparative analyses. These animals were all females. Sub-samples of these biopsies were taken, and total protein was extracted using the most efficient method established using the SMASS samples.

**Humpback whales:** For the humpback whale biopsies that were large enough for multiple analyses following the steroid extraction, subsamples were used for total protein extraction following the determination of the most efficient method. Thus 59/73 biopsies were available for analysis (Table 4-1).

*Table 4-1. Summary of the 59 blubber biopsy samples from humpback whales for total protein extraction and separation using 1D SDS-PAGE. 31/43 (72%) of the samples from Coastal Norway were large enough for multiple analyses, and 28/30 (93%) of the samples collected after 2011 from Quebec were large enough (NB. Samples collected in 2011 in Quebec were processed in 2012, before the total protein / 1D SDS-PAGE work was started.)*

Area	Samples Analysed		
	Year	Total Protein	SDS-PAGE
Norway	2011	3	3
	2012	10	10
	2013	3	3
	2014	6	6
	2016	4	4
	2017	5	5
Canada	2011	0	0
	2012	1	1
	2013	1	1
	2016	7	7
	2017	19	19

## 11.2 Sample Analysis

### 11.2.1 Total Protein Extraction and quantification

Three different methods for total protein extraction were trialled to assess the most efficient method of total protein extraction with the highest total protein yield. A Pierce™ 660nm Protein Assay (22662, Thermo Scientific, Rockford, USA) is used to quantify the total protein in the blubber extracts. A series of dilutions of known concentrations of bovine serum albumin are used to generate a standard curve. A negative control of RIPA with 2X protease inhibitors is used as the zero standard on each plate, and the absorbance measured is used to correct the absorbance of the standard curve measurements which are then used to produce a 4 parameter log-logistic model and calculate the protein concentrations in the samples. The assay is performed following the microplate protocol and each extract is assayed in duplicate and total protein concentrations are reported as µg per wet weight of the sample.

### Total Protein Separation – SDS PAGE

1D SDS-PAGE (Sodium Dodecyl Sulfate - Polyacrylamide Gel Electrophoresis) is used to separate denatured proteins based on their molecular weight. The XCell SureLock® Mini-Cell (Life Technologies, UK) gel electrophoresis unit is used to run 4-12% NuPAGE Bis-Tris mini gels (8.0cm x 8.0cm x 1.0mm) (NP0321BOX, Thermo Fisher Scientific, Paisley, UK) with a wide protein separation range of 3.5 kDa to 160 kDa. A wide protein range ladder, Invitrogen™ Novex™ Mark 12™ Unstained Standard (LC5677, Fisher Scientific, USA) is run on each gel. In addition, 4 bovine serum albumin (BSA) standards of known concentration (125 µg/g, 25 µg/g,

12.5 µg/g and 6.25 µg/g in RIPA buffer) are included. The gels are stained in Bio-Safe Coomassie Stain (1610786, Bio-Rad, UK). Following destaining, gels are photographed on a white background using a BioDoc-It™ Imaging System (Ultra-Violet Products Ltd, Cambridge, UK).

### 1D SDS-PAGE Band Detection, Characterisation and Analysis

**Band Detection and Characterisation:** Gel images are analysed using ‘GelAnalyzer 2010’, a 1D gel electrophoresis image analysis software (Figure 2-9). The process of gel image analysis using the software is straightforward and covers automatic lane and band detection, background subtraction techniques, Rf calibration to correct for gel run distortions, and accurate quantity and molecular weight calculations with 4 different calibration curve types to choose from. Here, a combination of both automatic and manual band detection is used to assign band limits for the molecular weight markers, the BSA standards and the protein bands separated in each of the sample extracts. Log-linear models are fitted by the software to the molecular weight markers and the standards of known concentration in order to estimate, in an automated process, both the concentrations and the molecular weights of the bands identified in the sample extracts. Each band identified across all individuals and all gels is therefore assigned a molecular weight and a volume (concentration).

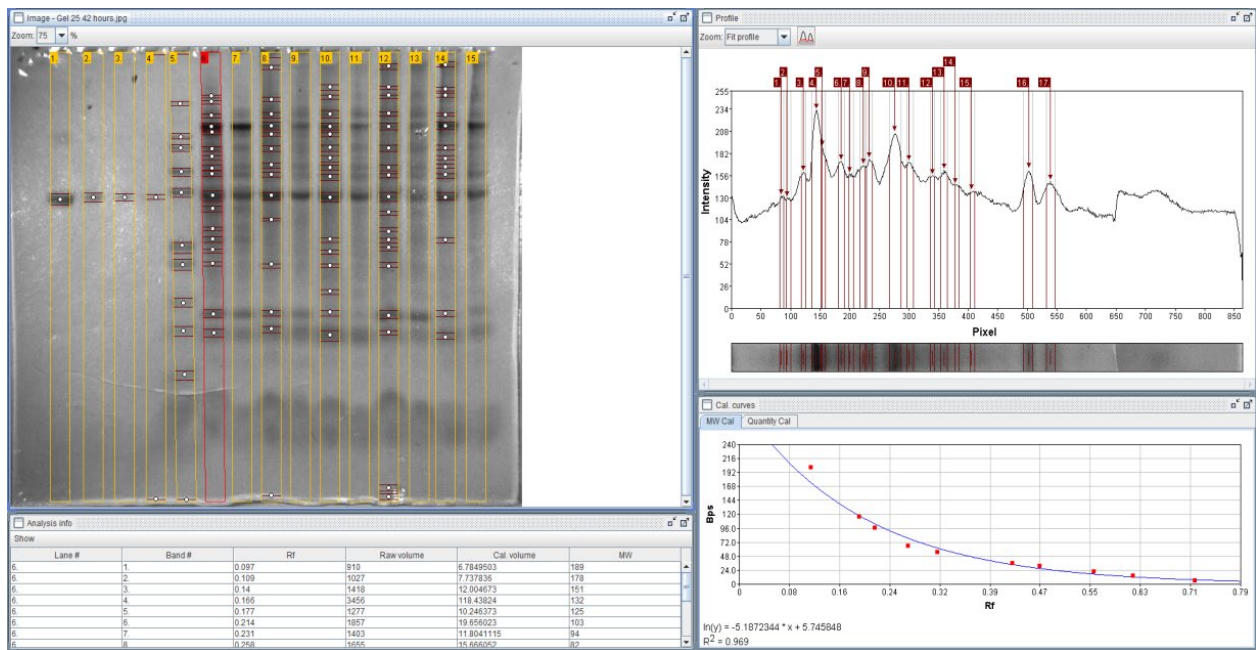


Figure 4-1. ‘GelAnalyzer’ software interface for the quantitative assessment of the protein band patterns of blubber extracts. Top left panel: Gel image with identified bands marked with points and bordered by red horizontal lines. Top right panel: Intensity of the bands of an individual lane representing one extract. Intensity is used to calculate the volume (concentration of proteins) of a band. Bottom left panel: Calculated values for the bands in the lane highlighted in the top right including Rf (distance from the sample loading well), calculated volume (concentration) and molecular weight (size of the proteins in that band). Bottom right panel: Model calibration curves fitted to the molecular weight markers and the BSA standards.

**Post-Image Analysis Band Processing:** As all gels ran slightly differently, the same band may appear as 17 kDa, 16 kDa or 15 kDa, on different gels for example, but this is the equivalent band separated across individuals. To overcome this problem, the bands were therefore separated into more manageable and meaningful units based on the maximum number of bands seen in any an individual, and the distribution of separated bands down the gels, whilst taking into account the fact that there was greater separation of smaller proteins than larger ones. This resulted in the separation of the bands data into 20 band groups shown in Figure 2-10 named Band Groups 1 – 20 with the smallest proteins in Band Group 1 and the largest proteins in Band Group 20. While Band Groups 18, 19 and 20 were all of proteins larger than the largest molecular weight marker at 200kDa, and the molecular weight of these bands has therefore been extrapolated and cannot be established with any certainty, the presence of these larger protein bands were retained for analysis as the presence and intensity of the bands was important for further interpretation rather than the accurate molecular weight.

In order to compare between individuals run on different gels, the relative band frequencies and band volumes (concentrations) were calculated for each individual:

Relative Frequency: The number of bands within a band group divided by the total number of bands detected for that individual

Relative Volume: The sum of the calculated volumes of the individual bands within a Band Group divided by the total sum of the volumes calculated for all the bands detected for an individual.

### 11.2.2 Protein Identification using nLC-ESI MS/MS

A total of 36 protein bands were excised from 5 harbour porpoise individuals run on 4 different 1D SDS-PAGE gels. A total of 11 protein bands were excised from 4 minke whale individuals run on the same 1D SDS-PAGE gel. The bands covered the full size range of separated proteins from the largest ones of more than 200kDa, down to the smallest bands visible at ~10kDa. In order to capture the full range of proteins that could be present in the tissue, bands from harbour porpoises were all of different molecular weights and were chosen from a mixture of males and females, and from adults and juveniles with varying causes of death. For the minke whale samples, in order to capture the full range in proteins present, bands from individuals sampled early in the feeding season (June) and late in the feeding season (September) were used for analysis. These were analysed using nanoflow Liquid Chromatography Electrospray Ionisation in tandem with Mass Spectrometry (nLC-ESI MS/MS) of in-gel trypsin digests.

The

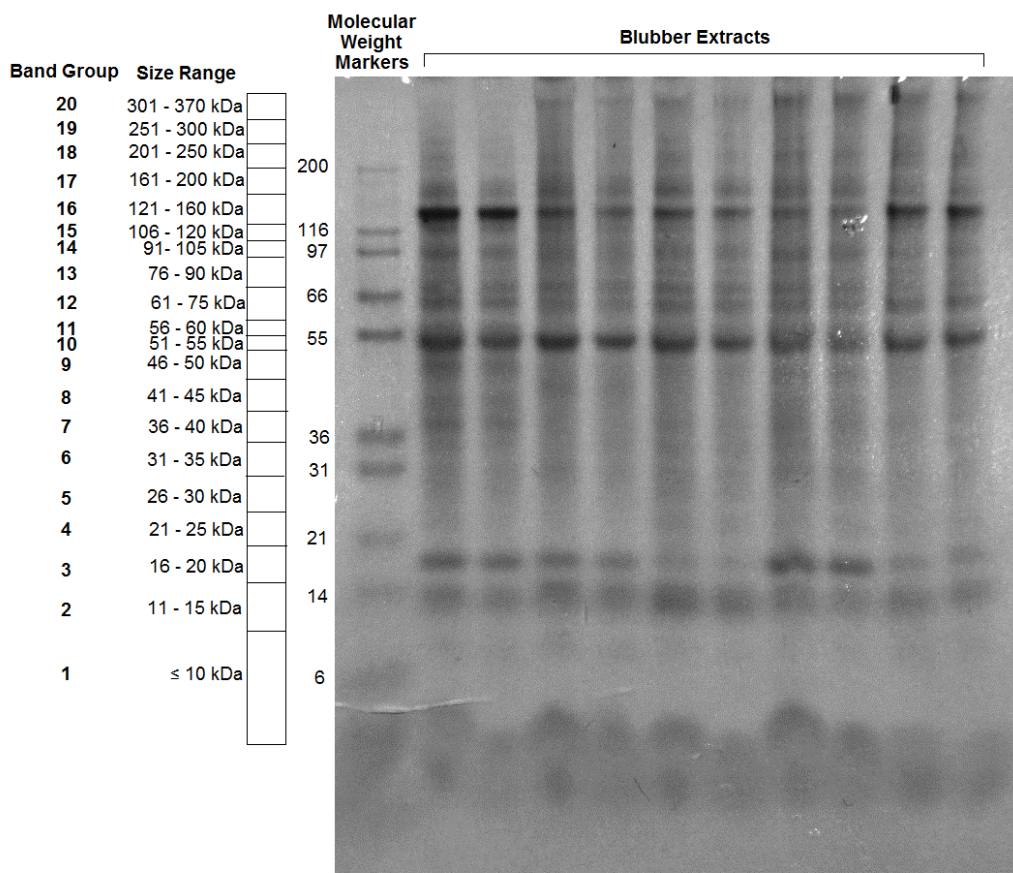


*Figure 4-2. Annotated image of a 1D SDS-PAGE gel showing the molecular weight markers in the lane on the left of the image, and the band groups of different molecular weights grouped together for analysis, named Band Groups 1-20, shown on the far left of the Figure.*

excised gel band was cut into 1mm cubes. These were then subjected to in-gel digestion, using a ProGest Investigator in-gel digestion robot (Genomic Solutions, Ann Arbor, MI) using standard

protocols (Shevchenko et al., 1996). A protein was accepted as identified if it had 2 or more peptides with Mascot Ion Scores above the Identity Threshold ( $p < 0.05$ ), and, for those proteins identified by only 2 peptides, the MSMS spectral assignments fulfil criteria previously described (Jonscher, 2005). The sequences matched to homologous vertebrate proteins. Identified proteins were grouped into functional classes and the frequency with which each protein was identified across different gel bands and individuals was also recorded in order to identify the kinds of proteins that appeared to be most abundant.

### 11.2.3 Statistical Analysis of SDS-PAGE Protein Bands Data

**Non-metric Multidimensional Scaling (NMDS):** The objective of Non-Metric Multidimensional Scaling (NMDS) is to group data points into clusters of similar points based on a few explanatory variables so that they can be visualized and interpreted. Here, we aimed to investigate whether there were clusters of individuals that grouped together based on the frequency and volumes of different protein bands measured in their SDS-PAGE profiles. Then, where clusters were observed, which of the qualitative variables listed in Table 2-3. Qualitative data used to investigate variation between individuals for both band relative frequency and relative band group volume data could explain the observed groupings, and which band frequencies or volumes specifically contributed to this clustering.

Here, the Bray-Curtis dissimilarity calculation was used in an NMDS framework to identify clusters of individuals based on both the frequency with which different bands were identified, and also the relative volumes of the identified bands. The Bray-Curtis calculation was used as it has a number of properties which make it suitable for this kind of data in that it is invariant to changes in units, it can recognize differences in total abundances when relative abundances are the same, and it is unaffected by zero-inflated data. The function ‘*metaMDS*’ from the ‘*vegan*’ package in R (version 3.1.3) was used to investigate the band frequency data, and then to investigate the band volume data for the four sample groups separately; stranded harbour porpoises, stranded balaenopterids, minke whale biopsies and humpback whale biopsies.

Any clustering observed in the data by the qualitative variables listed in Table 4-1 was then assessed visually to determine if any of the variation in the band frequency and band volume data can be explained using these variables of interest.

*Table 4-1. Qualitative data used to investigate variation between individuals for both band relative frequency and relative band group volume data.*

		Porpoises (n = 32)		Balaenopterids (n = 10)		Minke whales (n = 10)		Humpback whales (n = 42)	
		Band Freq.	Band Vol.	Band Freq.	Band Vol.	Band Freq.	Band Vol.	Band Freq.	Band Vol.
Qualitative Variables	Gel Number	✓						✓	
	Sex	✓		✓				✓	
	Age Class	✓		✓				✓	
	Rep.							✓	

	Status				
	Species		✓		
	COD	✓	✓		
	Area				✓
	Season			✓	✓

### 11.3 Blubber Protein Identification Initial Investigations Results and Discussion

#### 11.3.1 Blubber Proteins Identification Results

**Harbour porpoises:** A total of 295 proteins were identified across the 36 gel bands separated through 1D SDS-PAGE from 5 individuals. Many of the proteins, and protein fragments were identified across multiple bands from the same gel, and therefore did not show clear clustering around their expected molecular weight range. This was possibly due to protein degradation and / or some proteins being more abundant than others. The identified proteins were grouped into general subclasses firstly, based on their type, and secondly based broadly on their function using data from UniProt (<http://www.uniprot.org>) and a literature search. This resulted in the identification of proteins belonging to 5 main types: enzymes (proteins involved in the catalysis of various processes), immune proteins (proteins involved in the regulation of immune system function and activation as well as inflammation), carrier proteins (proteins that bind other factors for extracellular or intracellular transport), structural proteins (proteins responsible for the maintenance of cell shape and integrity as well as the extracellular matrix), and regulatory proteins (any other proteins involved in the regulation of other cellular processes) were grouped together.

Proteins were then grouped into functional classes which resulted in the identification of 8 main groups: amino acid metabolism, lipid metabolism, tissue structure, cell structure, glucose homeostasis, biomolecule transport, immune response and inflammation and overall cell function and metabolism. As an indicator of relative abundance, the frequency with which each protein was identified across different gel bands and individuals was also recorded in order to identify the kinds of proteins that appeared to be most abundant. Over half of all proteins identified were only seen once across all 36 gel samples analysed, while less than 5% of the proteins were seen more than 10 times. The top six proteins were haemoglobin, immunoglobins, serum albumin, fatty acid binding protein, myoglobin and annexins.

Proteins involved in amino acid metabolism, tissue structure, glucose homeostasis, biomolecule transport and cell structure were the least abundant of the protein functional groups, each making up less than 10% of all the identified proteins (Figure 4-3). Proteins involved in lipid metabolism made up approximately 10% of the identified proteins and these included one of the adipokines, adiponectin, regulatory proteins including fatty acid binding proteins and perilipin-1, as well as enzymes including 3-hydroxyacyl-CoA dehydrogenase and acetyl CoA synthetase for example (Figure 4-3).

The second largest functional group were immune proteins. These were of varying sizes and functions, and made up approximately 15% of all identified proteins (Figure 4-3). The immune proteins were dominated by two classes of immunoglobulin, IgA and IgG. Annexins and cyclophilins were also present, and are involved in the regulation of the inflammatory response (Bukrinsky, 2015; Sugimoto et al., 2016). Other proteins included transferrin, fibrinogen and

fibronectin that are involved in the acute phase response (Kilicarslan et al., 2013). Dermicidin has antimicrobial properties (Schitteck et al., 2001), and 4 complement proteins (C1, C3, C4 and C9) were identified that act as parts of the complement system which forms part of innate immunity (Nesargikar et al., 2012). B-cell antibody and galectins expressed by immune cells were also identified (Figure 4-3).

Finally, the largest functional group were proteins involved in general cell function and metabolism, and made up approximately 45% of the proteins identified. These were proteins involved in a range of different processes including protein degradation and modification, biosynthesis, metabolic pathways (e.g. glycolysis), redox proteins, heat shock proteins, signal transduction, vesicle trafficking, cell cycle regulation and protein chaperones, to name just a few (Figure 4-3).

**Minke whales:** Between the two species, a total to 409 different proteins were identified, and 258 proteins were identified across the 11 gel bands separated through 1D SDS-PAGE from the 4 minke whales. These were classified into the same 5 protein types as the harbour porpoises, and the same 8 functional classes, with the addition of two extra classes. These were the peripheral nervous system (peripherin), and vasodilation and circulation (eg. heparin and angiotensinogen). Across the two species groups, 55.8% of the proteins identified in the minke whale samples were also seen in harbour porpoise samples, so over 40% of the proteins were newly identified in the biopsy samples. Almost half (48.8%) of the proteins identified were only seen once, and just less than 20% were seen more than 5 times across the extracts. Similarly to the harbour porpoise data, the top six proteins were haemoglobin, fatty acid binding protein, apolipoprotein, immunoglobulins, serum albumin and perilipins.

Proteins involved in the peripheral nervous system, amino acid metabolism, glucose metabolism and vasodilation and circulation were the least abundant of the protein functional groups, each making up less than 5% of all the identified proteins (Figure 4-4). Proteins involved in tissue structure, biomolecule transport and lipid metabolism each made between 7 - 10% of the data. Cell structure proteins made up a larger proportion of the minke whale data than the harbour porpoise data, but immune response and inflammation proteins were again the second largest class for these data, making up approximately 14% of the identified proteins (Figure 4-4). Only one class of immunoglobulin was identified in these samples compared to the harbour porpoises, but 3 extra complement proteins we identified (Figure 4-4). Finally, the cell function and metabolism proteins were the largest protein functional group, making up over 40% of the data, and involved in a huge range of different cellular and metabolic processes (Figure 4-4). Thus, while we saw a huge number of new proteins, the overall patterns in terms of what proportion of the proteins were attributed to the different functional groups were generally the same between the two species.

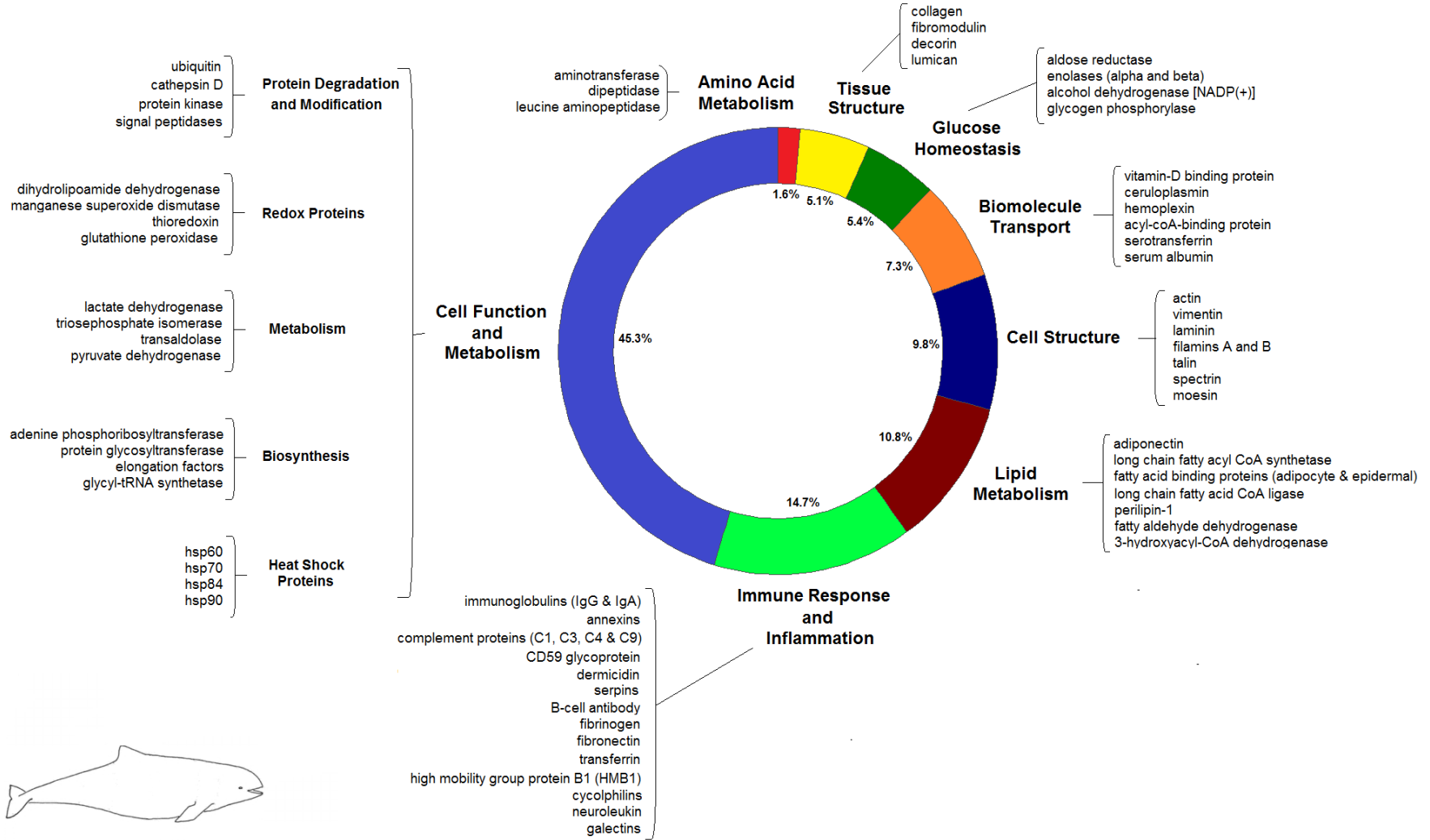


Figure 4-3. Protein components identified from the harbour porpoise blubber extracts. The proportion of each functional group is indicated as well as examples of some of the most abundant and the most well-studied proteins that were identified. The most abundant functional group was proteins involved in cell function and metabolism followed by the immune response and inflammation

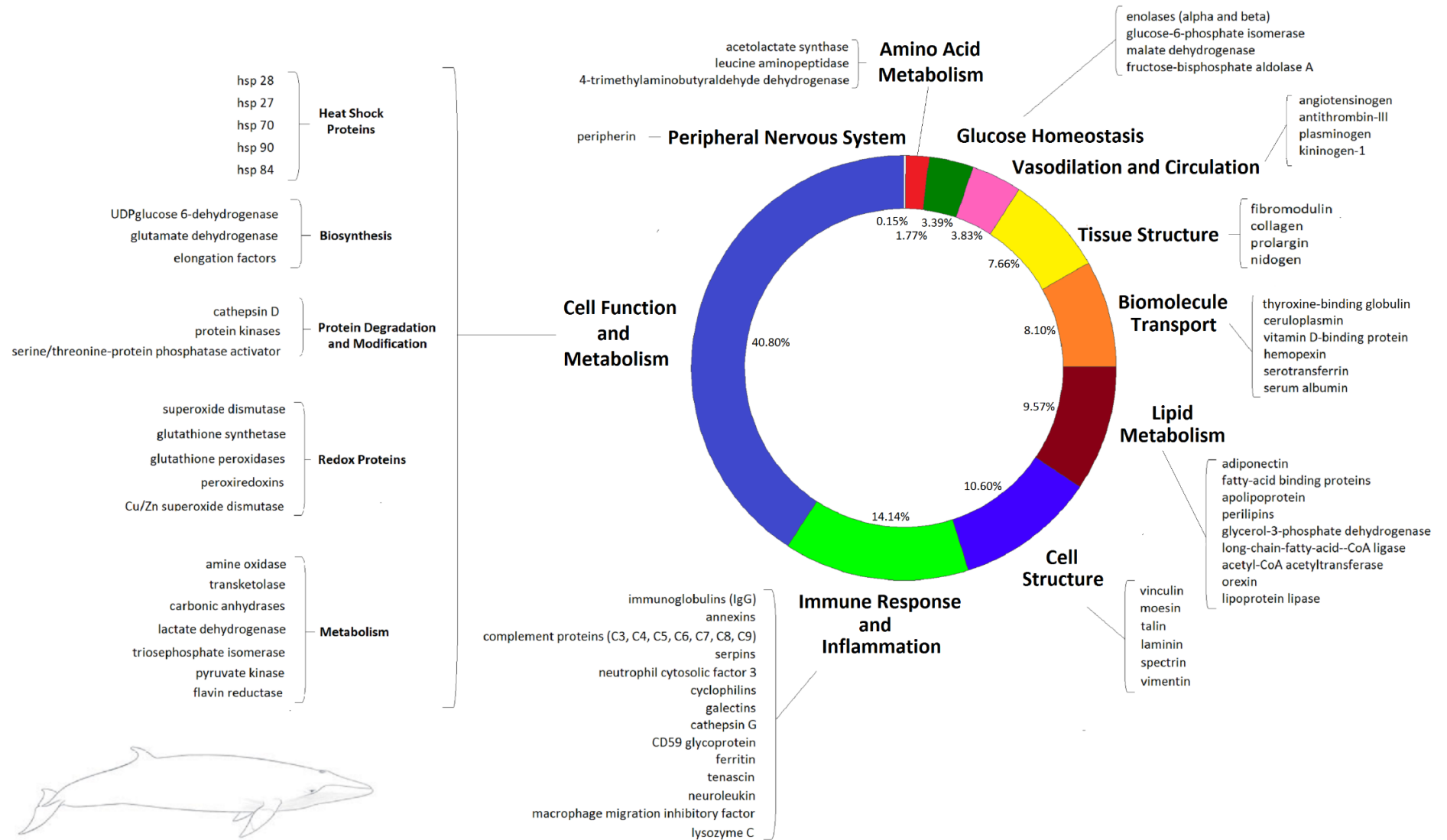


Figure 4-4. Protein components identified from minke whale blubber extracts. The proportion of each functional group is indicated as well as examples of some of the most abundant and the most well-studied proteins that were identified. The most abundant functional groups were the same as for the harbour porpoise data while two new groups were identified; the peripheral nervous system and vasodilation and circulation

## 11.4 Blubber Proteins as Potential Biomarkers Discussion

### 11.4.1 Proteins Identified

As the gel protein bands extracted from the harbour porpoise samples were all of different molecular weights, from all sex and age classes that had suffered various causes of death, we captured a wide variety of proteins present in the tissue. Similarly, while all biopsy samples from the minke whales were from adult female individuals, they were taken over a 4 month period of the summer feeding season, again with the aim to capture a wide variety of proteins in tissue. The largest functional group for both species were proteins involved in general cell function and metabolism. Within this group, the proteins were further classed into more specific functional roles including proteins involved in biosynthesis, antioxidant proteins, regulators of the cell cycle and signal transduction pathway proteins, to name just a few. The variety of the proteins in this group with a range of different metabolic functions is in keeping with a recent transcriptomic study of Northern elephant seal (*Mirounga angustirostris*) blubber tissue which showed that the most significantly enriched pathway in the blubber transcriptome, compared to the human proteome, was metabolism (Khudyakov et al., 2017). The identification of important metabolic factors could therefore provide insight into localised tissue function. For example, heat shock proteins were identified here in the blubber extracts, and changes in gene expression for the heat shock response were detected in the transcriptome of the elephant seals (Khudyakov et al., 2017). Heat shock proteins are key cellular defences against stress and play crucial roles in the folding and unfolding of proteins, the transport and sorting of proteins, as well as cell-cycle control and signalling (Li and Srivastava, 2001). In phocid seals, greater requirements for heat shock proteins and other antioxidants have been hypothesised at certain times during the life cycle as a result of rapid protein synthesis and high metabolic fuel availability (Bennett et al., 2014). Six different heat shock proteins were identified between the two species groups, and the expression of these proteins could provide insight into cellular and physiological stresses of individuals.

The second largest functional group for both species were proteins involved in the immune response and inflammation. Some of the immune, and acute-phase response proteins that were identified included haptoglobin, transferrin and eight members of the complement pathway. This is in-keeping with the recognition of the extensive and direct involvement of white adipocytes in inflammation and the acute-phase response in other mammals (Frühbeck et al., 2001). It has been shown that adipocytes synthesise all of the proteins involved in the alternative complement pathway, specifically, factor C3. However, further research is required to determine the primary functions and regulation of this pathway in adipose tissue (Frühbeck et al., 2001). Other proteins involved in immune system function were also identified including immunoglobulins (IgA and IgG) which, together, were the second most abundant proteins in the extracts from both species. These were likely either in the circulation or were secreted directly from B-cell infiltrates within the blubber itself. Annexins, cyclophilins and dermicidin were among the other proteins identified that are involved in the regulation of inflammation and the immune response. Annexin A1, for example, is an endogenous glucocorticoid-regulated protein involved in the regulation of the inflammatory response by reducing leukocyte infiltration and activating neutrophil apoptosis to avoid tissue damage caused by excess neutrophils at a site of inflammation (Sugimoto et al., 2016). Both innate and the adaptive components of the immune system were therefore present in the tissue. Given the current understanding of the involvement of adipose tissue in immune system function, it is possible that cetacean blubber could show a similar role, and the presence of such

proteins could provide information regarding immune system function and response in these animals.

As expected, there were also a range of factors identified that play key roles in lipid metabolism, and these made up the third largest functional group of identified proteins in the harbour porpoises and the fourth largest group in the minke whales. Fatty acid binding proteins are low molecular-weight cytoplasmic proteins, and were particularly abundant here in both species. The adipose-specific fatty acid-binding protein has been shown to be involved in intracellular trafficking and targeting of fatty acids (Frühbeck et al., 2001), and may modulate lipolytic rate. Apolipoproteins were particularly abundant in the minke whale samples, and are known to play important roles in both the synthesis and catabolism of plasma lipoproteins, in lipid transport, and in the activation of various enzymes involved in lipid and lipoprotein metabolism (Donma and Donma, 1989).

Enzymes involved in lipolysis, as well as regulatory proteins were identified, including the hormone adiponectin which was particularly abundant in the minke whale samples. Adiponectin is an adipokine produced by white adipose tissue and released into the circulation, and is important for whole body metabolic regulation by increasing adipogenesis and lipid storage in fat tissue, as well as increasing insulin sensitivity (Fu et al., 2005). Circulating adiponectin concentrations have been negatively correlated with total body fat stores in a number of terrestrial mammals (for a review see (Fain et al., 2004)), and, in marine mammals specifically, adiponectin is thought to be important in the development of blubber reserves in grey seal (*Halichoerus grypus*) pups (Bennett et al., 2015). Concentrations of this hormone in the blubber could therefore provide information on the physiological state of an individual in terms of current energy stores. Adiponectin signalling pathways were also identified in the transcriptomic study of Northern elephant seals when investigating the acute metabolic response to glucocorticoids (Khudyakov et al., 2017). Other differential gene expression was measured that promoted lipid catabolism and oxidation at the expense of lipid synthesis and storage (Khudyakov et al., 2017). The presence of factors involved in various stages of lipid metabolism could be used to assess whether the individual is undergoing a period of lipolysis or lipogenesis at the time of sampling. This is a good example of how the integration of proteomic and transcriptomic methods could result in a powerful assessment tool. Moving forward, the quantification of individual proteins could be coupled to the transcriptome so that transcription and translation can be linked.

Finally, for the harbour porpoises, although every attempt was made to obtain very fresh tissue samples, they were nevertheless collected from dead-stranded animals, so minor autolysis could have affected our findings. This would also complicate the functional interpretation of any proteins involved in *ante-* or *post-mortem* metabolic processes. Similarly, the remotely obtained biopsy samples from the minke whales were stored on ice immediately after collection, but a small amount of tissue degradation is possible as a result of the delay between sample collection and when the sample was frozen. Ideally, samples should be collected and snap frozen immediately using dry ice or liquid nitrogen. However, the wide range of proteins and peptides identified here across a variety of metabolic pathways and processes suggests that proteomics is a robust tool to investigate tissue function using this biopsy sampling approach.

#### 11.4.2 Tissue Specific and Circulatory Proteins

While a range of different molecular weight proteins were identified, there may be some size selective loss of protein species as well as some loss of the least abundant proteins through the

extraction procedure. There may also be some loss of more hydrophobic proteins that are more difficult to solubilise. Thus, if a protein was not identified following nLC-ESI MS/MS, this does not confirm its absence from the tissue, but this work does suggest that there are some proteins, and protein classes that are more abundant than others. Serum albumin and haemoglobin, from the circulation, were two of the most abundant proteins identified in both species, and likely affected the detection of other proteins by swamping the samples. Further efforts to remove the albumin from the extracts would likely be required to detect less abundant proteins of potential interest. This could be achieved by fractionation of the extract for example or, the use of 'Cibacron Blue', a commercially available resin to remove albumins from solution. Alternatively, antibody columns could be used to target specific proteins. Similarly, targeted mass spectrometry could be used to detect particular peptides from a particular protein of interest to therefore detect the presence of proteins at lower concentrations within the samples.

Proteins identified here probably do not originate solely from the blubber tissue itself, but are a mixture of blubber proteins together with plasma proteins. Attempts were made to limit any external blood on the samples by using visibly 'cleaner' parts of the harbour porpoise tissue samples. The presence of plasma proteins in the extracts were therefore likely largely a result of their presence *within* the tissue vasculature rather than *on* each piece of tissue from contaminating sources during the necropsy sampling. The vascularisation of marine mammal blubber tissue is still not well understood, but one study comparing the microvasculature of deep diving and shallow diving odontocetes saw that blubber tissue is more highly vascularised than adipose tissue in terrestrial mammals (McClelland et al., 2012). As such, blubber tissue sampling can provide information on both the proteins produced and metabolised *in situ* as well as those in circulation. Double sampling of freshly dead stranded animals before blood coagulation occurs would be useful here for further comparisons of proteins present in both the blood and blubber of the same individuals. This would be an important next step to identify those proteins present in both matrices, and those that are found more exclusively in the blubber itself. For example, the absence of some proteins identified in the minke whale samples compared to the harbour porpoise samples could reflect differences in the vascularisation of the outermost part of the tissue compared to the full blubber depth.

The range of proteins identified here across both species, and the presence of a huge number of proteins identified exclusively in the full depth harbour porpoise samples or exclusively in the superficial minke whale samples, clearly demonstrate the heterogeneity of blubber tissue. A comparison of the proteins present through the different blubber layers from the same individuals would help to establish if this heterogeneity results from longitudinal differences in metabolic activity of the tissue and / or different cell types through the blubber depth. While it has been well established that adipocytes express and secrete several endocrine hormones, many secreted proteins within the tissue are derived from the non-adipocyte fraction (Fain et al., 2004). For example, the innermost blubber layer has been shown to consist of a heterogeneous mix of white adipocytes, brown adipocytes and connective tissue as well as muscle and nerve fibres (Hashimoto et al., 2015). Therefore, as the full depth blubber layer was sampled in the harbour porpoises, proteins detected in these samples were most likely the result of differential gene expression in these different cell and tissue types which explains the presence of myoglobin, a muscle protein, across all samples. Thus, as well as the origin of certain proteins in terms of either the blubber or the circulatory system, an important next step would also be to establish the secreting cell types within the tissue. It would be possible to determine whether gene expression and protein secretion

occurs within the mature adipocytes, or in the other cells that make up the tissue, either histologically (through *in situ* hybridisation) or by separation of the adipocytes from the stromal vascular fraction by collagenase digestion (Trayhurn and Wood, 2004).

## 11.5 1D SDS-PAGE Exploratory Band Group Analysis Results and Discussion

### 11.5.1 Stranded Animal Samples Results and Discussion

Correlations between the band group frequencies and volumes with the morphometric condition of the animals was first investigated by plotting them against the body condition index for the harbour porpoises and the balaenopterids (Figure 4-5). While there was no obvious trend in the frequency or volume of certain band groups with increasing or decreasing condition, there appear to be differences in the two datasets in terms of the band groups that appeared more frequently and made up a larger proportion of the volume data than others (Figure 4-5). For example, the 24-50kDa band group made up a large proportion of the data in the harbour porpoises, but not in the balaenopterids (Figure 4-5).

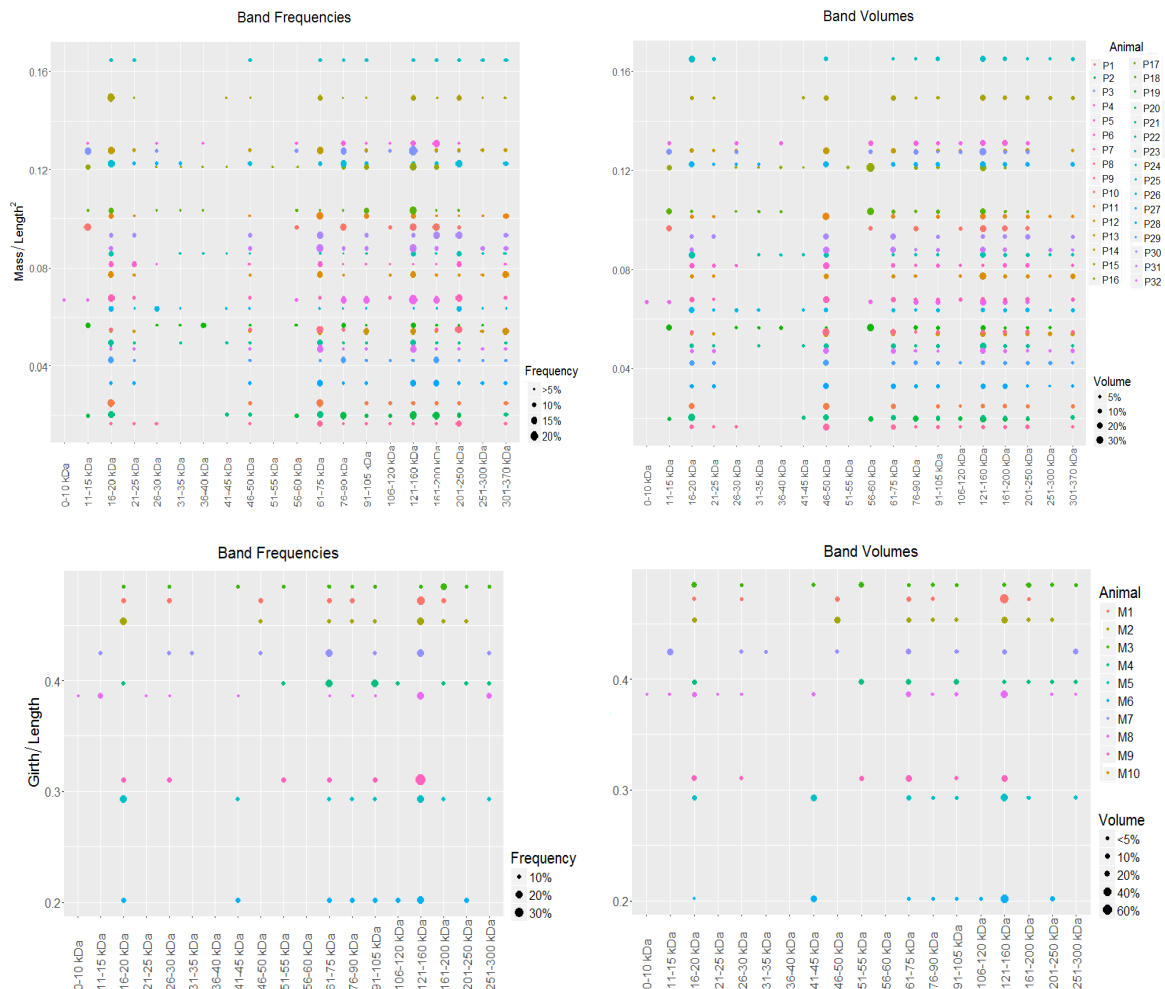


Figure 4-5. Band frequencies and volumes plotted against the body condition index for the harbour porpoises (top panel) and balaenopterids (bottom panel). Points are coloured by individual with the size of the points representing the relative frequency and volume for that individual

Results of the Non-Metric Multidimensional Scaling (NMDS) analysis for the harbour porpoise and the balaenopterid band group datasets showed that using 3 dimensions produced better fitting (lower stress values) models compared to using just 2 dimensional scaling.

**Harbour porpoises:** The harbour porpoise NMDS results data showed no clustering of individuals by sex, age class or cause of death, but did show some clustering of individuals based on the gel number (Figure 4-6a). Overall, there were differences between gels 1 and 4 that showed similar band group patterns across individuals, and gels 2, 3, 5 and 6 that shared similar band group characteristics (Figure 4-6a).

**Balaenopterids:** There was no clustering by sex, age class or COD for the balaenopterid data. There was limited clustering by species for the band group frequency data, whereby the minke whales were more similar (more tightly clustered) than the fin whale and humpback whale samples, although this was a small sample size (Figure 4-6a). As all samples were run on the same gel, there were no differences between different gel trials to be investigated.

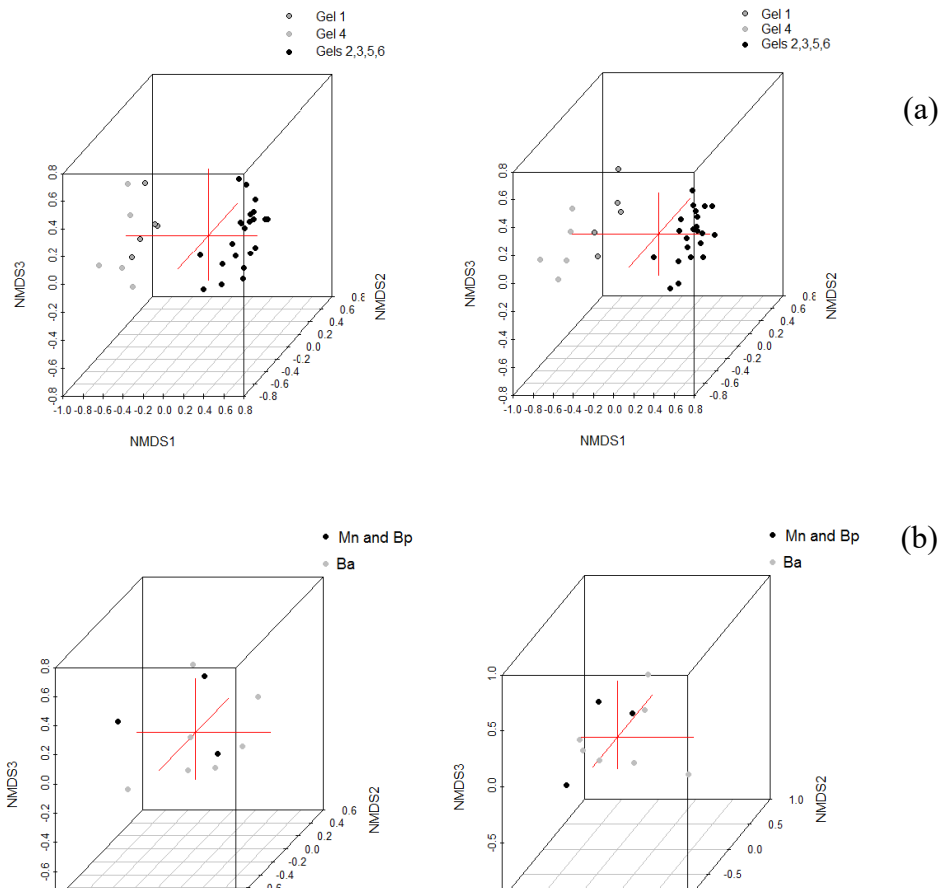
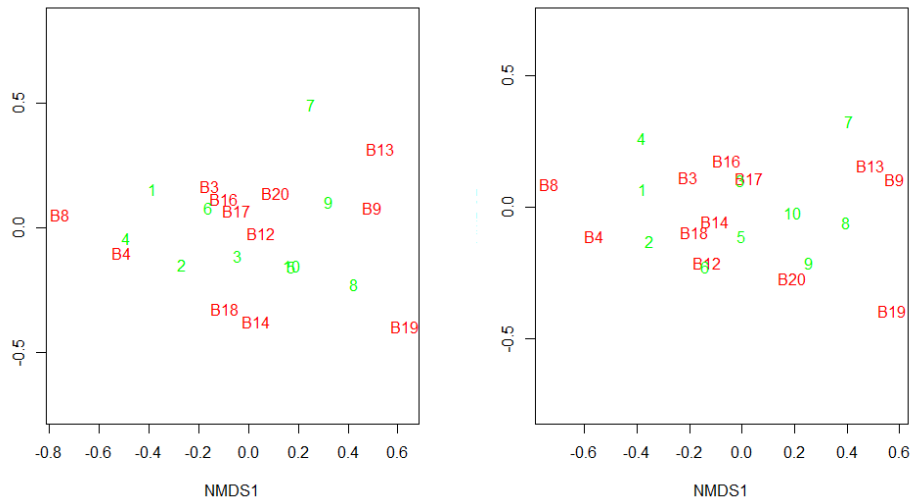


Figure 4-6. (a) 3D NMDS results for the harbour porpoise band group frequency (left) and volume data (right), showing clustering by gel number. Band groups did not cluster by any other variable investigated. (b) 3D NMDS results for the balaenopterid band group frequency (left) and volume data (right), showing limited clustering by species. Band groups did not cluster by any other variable investigated.

### 11.5.2 Biopsies from Live Animals Results and Discussion

**Minke whales:** Season was the only qualitative covariate to include in the analysis of minke whale biopsies from Canada, so 2D NMDS results are shown in Figure 4-7. There was some clustering of different band groups for the both the frequency and the volume data, but no apparent clustering of these 10 individuals that consisted of ‘early’ (June and July) or ‘late’ (August and September) feeding season samples (Figure 4-7).



*Figure 4-7. 2D NMDS results for the minke whale biopsy band group frequency (left) and volume data (right). In red are the band groups, showing limited clustering, and in green are the individual numbers (from 1 to 10) showing no clustering patterns.*

**Humpback whales:** Of the 59 biopsy samples that were large enough for total protein extraction and protein separation, the results from 42 of them were used for protein band group frequency and volume analysis. The 17 samples that were excluded from the analysis were from 2011 (n = 3), 2012 (n = 8), 2013 (n = 2) and 2014 (n = 4). These were excluded as they showed low total protein content (Figure 4-8), and poor protein separation and visualization. Thus, band group profiles in these samples likely represented the products of tissue degradation through storage rather than differences in the protein content of the tissue between individuals. NMDS results showed that, similarly to the harbour porpoise data, the clustering of band group frequencies and volumes in the humpback whale biopsy profiles was explained most strongly by the gel number on which the sample was separated (Figure 4-10), and not by any of the other variables investigated. This clustering was most apparent for the band group volumes data (Figure 4-10).

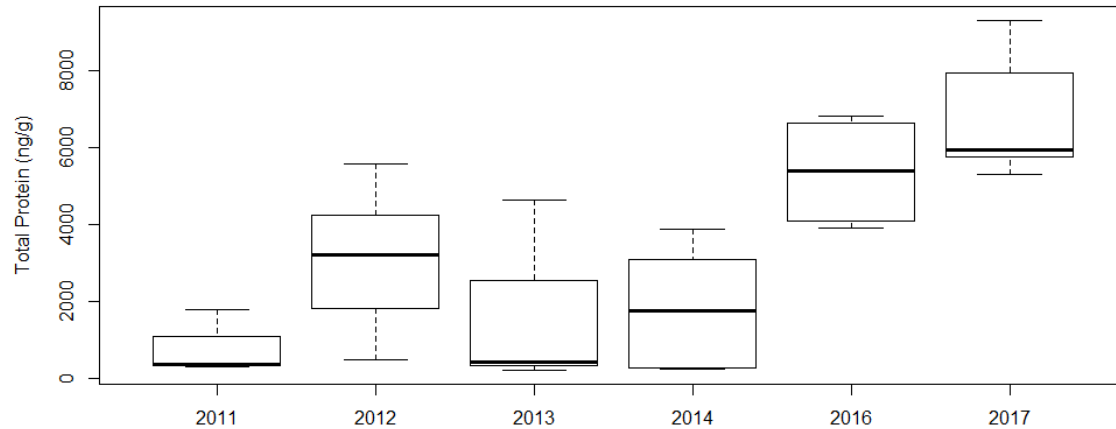


Figure 4-7. Boxplot of total protein content measured in the blubber biopsies collected between 2011 and 2017. The overall increase in total protein content from the oldest to the most recent samples indicates some protein degradation and loss from the samples with increased time in storage.

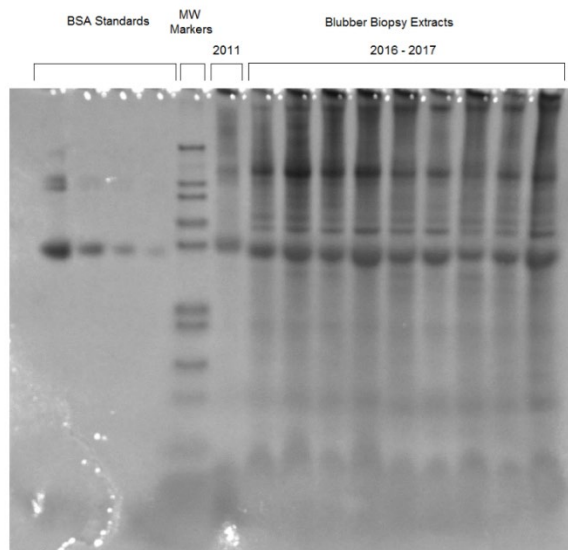
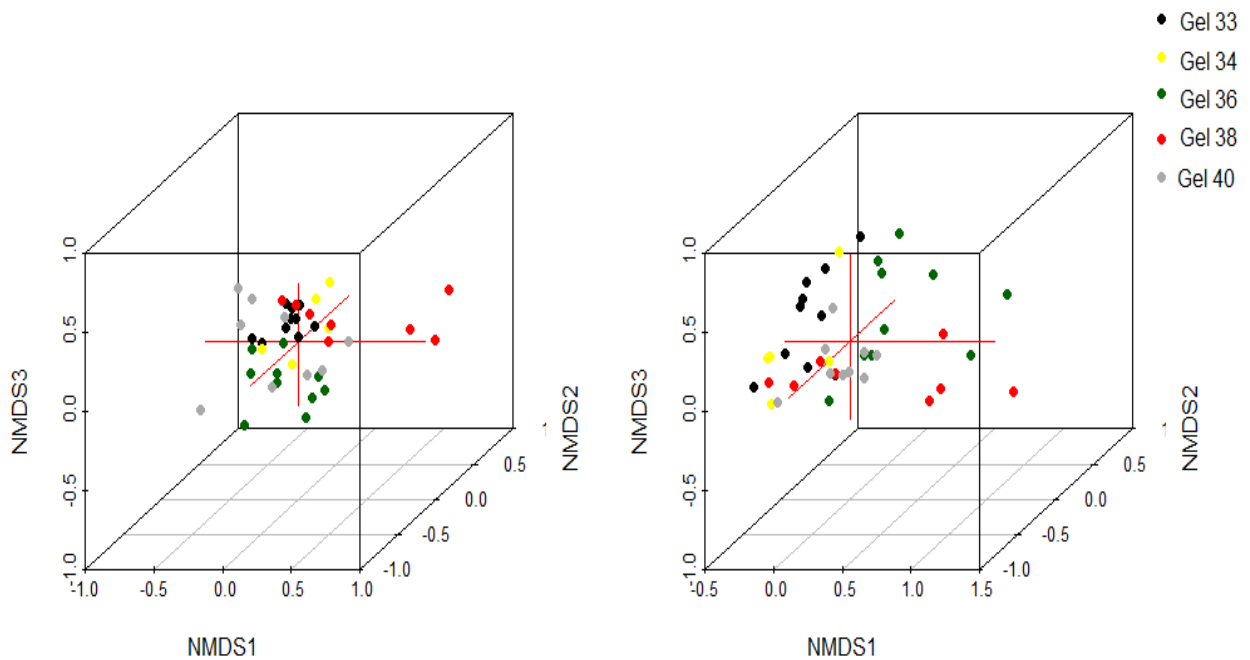


Figure 4-8. 1D-SDS PAGE image showing the difference between a total protein blubber extract from a biopsy collected in 2011, compared to extracts from biopsies collected in 2016 and 2017. The 2011 extract shows both lower protein content and poor separation and visualisation of extracted proteins indicative of sample degradation, likely as a result of long-term sample storage. \*BSA – Bovine Serum Albumin standards used for protein band volume quantification. \*MW – Molecular Weight Markers used to determine the molecular size of protein bands separated in the blubber extracts

Here, we have identified some method processing issues that affect the protein band group profiles. Firstly, time in storage impacts both the total amount of protein extracted from the samples and likely affects the protein band profiles separated using 1D SDS-PAGE. It is therefore recommended that for protein content investigations and analysis of blubber samples, biopsies should be processed as soon as possible because prolonged storage at  $-20^{\circ}\text{C}$  for more than two years results in measurement artefacts associated with tissue degradation. Secondly, there appears to be some measurement error associated with running 1D SDS-PAGE gels. The harbour porpoise and the humpback whale samples were run on multiple gels, and there was some clustering by gel number for both of these datasets. This suggests that while the processing of the samples and the running of the gels was as standardised as possible, there are potentially sources of variation in the process that account for patterns in the band groups seen across individuals. It therefore appears that there are sources of measurement variability inherent in this method which determine, to some extent, the band group profiles seen across individuals. With the larger sample size of humpback whale samples compared to the harbour porpoise samples however, these differences between the profiles on different gels were less pronounced. For further development of this method would be to assay the same samples multiple times on different gels in order to quantify the error associated with different trials.



*Figure 4-9. 3D NMDS results for the humpback whale band frequency (left) and volume data (right), showing clustering by gel number. Band groups did not cluster by any other variable investigated.*

## Literature cited in Appendix

- Andreasson, U., Perret-Liaudet, A., van Waalwijk van Doorn, L.J.C., Blennow, K., Chiasserini, D., Engelborghs, S., Fladby, T., Genc, S., Kruse, N., Kuiperij, H.B., Kulic, L., Lewczuk, P., Mollenhauer, B., Mroczko, B., Parnetti, L., Vanmechelen, E., Verbeek, M.M., Winblad, B., Zetterberg, H., Koel-Simmelink, M., Teunissen, C.E., 2015. A Practical Guide to Immunoassay Method Validation. *Frontiers in Neurology* 6, 179.
- Bligh, E.G., Dyer, W.J., 1959. A rapid method of total lipid extraction and purification. *Canadian Journal of Biochemistry and Physiology* 37, 911-917.
- Cilia, M., Fish, T., Yang, X., McLaughlin, M., Thannhauser, T.W., Gray, S., 2009. A Comparison of Protein Extraction Methods Suitable for Gel-Based Proteomic Studies of Aphid Proteins. *Journal of Biomolecular Techniques : JBT* 20, 201-215.
- Friedman, D.B., Hoving, S., Westermeier, R., 2009. Chapter 30 Isoelectric Focusing and Two-Dimensional Gel Electrophoresis, In: Richard, R.B., Murray, P.D. (Eds.) *Methods in Enzymology*. Academic Press, pp. 515-540.
- Galligan, T.M., Schwacke, L.H., McFee, W.E., Boggs, A.S., 2018. Evidence for cortisol–cortisone metabolism by marine mammal blubber. *Marine Biology* 165.
- Grotjan, H.E., Keel, B.A. 1996. Data Interpretation and Quality Control. In *Immunoassay*, Diamandis, E.P., Christopoulos, T.K., eds. (New York, NY, Academic Press), pp. 51-95.
- Hunt, K.E., Rolland, R.M., Kraus, S.D., 2014. Detection of steroid and thyroid hormones via immunoassay of North Atlantic right whale (*Eubalaena glacialis*) respiratory vapor. *Marine Mammal Science* 30, 796-809.
- Jiang, X., Ye, M., Jiang, X., Liu, G., Feng, S., Cui, L., Zou, H., 2007. Method Development of Efficient Protein Extraction in Bone Tissue for Proteome Analysis. *Journal of Proteome Research* 6, 2287-2294.
- Natarajan, S., Xu, C., Caperna, T.J., Garrett, W.M., 2005. Comparison of protein solubilization methods suitable for proteomic analysis of soybean seed proteins. *Analytical Biochemistry* 342, 214-220.
- Panchout, F., Letendre, J., Bultelle, F., Denier, X., Rocher, B., Chan, P., Vaudry, D., Durand, F., 2013. Comparison of Protein-Extraction Methods for Gills of the Shore Crab, *Carcinus maenas* (L.), and Application to 2DE. *Journal of Biomolecular Techniques : JBT* 24, 218-223.
- Sajic, T., Hopfgartner, G., Szanto, I., Varesio, E., 2011. Comparison of three detergent-free protein extraction protocols for white adipose tissue. *Analytical Biochemistry* 415, 215-217.
- Sheoran, I.S., Ross, A.R.S., Olson, D.J.H., Sawhney, V.K., 2009. Compatibility of plant protein extraction methods with mass spectrometry for proteome analysis. *Plant Science* 176, 99-104.
- Wessel, D., Flügge, U.I., 1984. A method for the quantitative recovery of protein in dilute solution in the presence of detergents and lipids. *Analytical Biochemistry* 138, 141-143.
- Wu, X., Xiong, E., Wang, W., Scali, M., Cresti, M., 2014. Universal sample preparation method integrating trichloroacetic acid/acetone precipitation with phenol extraction for crop proteomic analysis. *Nat. Protocols* 9, 362-374.
- Zhao, Z., Xu, Y., 2010. An extremely simple method for extraction of lysophospholipids and phospholipids from blood samples. *Journal of Lipid Research* 51, 652-659.

